IOWA STATE UNIVERSITY
Digital Repository

1999

Group 4 metalloporphyrin alkoxido, amido, hydrazido, and imido complexes: synthesis and reactivity

Joseph Lyndon Thorman
Iowa State University

Recommended Citation

INFORMATION TO USERS

Group 4 metalloporphyrin alkoxido, amido, hydrazido, and imido complexes:

synthesis and reactivity

by

Joseph Lyndon Thorman

A dissertation submitted to the graduate faculty

in partial fulfillment of the requirements for the degree of

DOCTOR OF PHILOSOPHY

Major: Inorganic Chemistry

Major Professor: L. Keith Woo

Iowa State University

Ames, Iowa

1999

UMI Number: 9940247

UMI

DEDICATION

To my sisters

Janessa, Jeana, Jessica, JoLene, Josie

iii

Graduate College
Iowa State University

This is to certify that the Doctoral dissertation of

Joseph Lyndon Thorman

has met the dissertation requirements of Iowa State University

Signature was redacted for privacy.

Major Professor

Signature was redacted for privacy.

For the Major Program

Signature was redacted for privacy.

For the Graduate College

TABLE OF CONTENTS

LIST OF ABBREVIATIONS

Ar^{iPr}	2,6-diisopropylphenyl
av	average
BM	Bohr magnetons
^{t}Bu	tertiary butyl
cal	calorie
Cp	cyclopentadienyl
Cp*	pentamethylcyclopentadienyl
Cy	cyclohexyl
DME	1,2-dimethoxyethane
eq	equation
GCMS	gas chromatography coupled to mass spectrometry
IR	infrared
TMP	*meso*-tetramesitylporphyrinato dianion
kcal	kilocalorie
Me	methyl
mg	milligram
MHz	megahertz
mL	milliliter
mmol	millimole
mol	mole

MS{EI}	mass spectrometry by electron impact
nm	nanometer
NMR	nuclear magnetic resonance
OAc	Acetate anion, $CH_3C(O)O^-$
Ph	phenyl
Por	general porphyrin dianion
ppm	parts per million
^iPr	isopropyl
py	pyridine
sol	donor solvent
THF	tetrahydrofuran
TMP	*meso*-tetramesitylporphyrinato dianion
tmtaa	dibenzotetramethyltetraaza[14]annulene
TMS	trimethylsilyl
tolyl	p-CH_3-C_6H_4
TPP	*meso*-tetraphenylporphyrinato dianion
TTP	*meso*-tetratolylporphyrinato dianion
μ_{eff}	magnetic moment
UV-vis	ultraviolet-visible

ABSTRACT

Group 4 metalloporphyrin alkoxido, amido, hydrazido, and imido complexes:

synthesis and reactivity

Joseph Lyndon Thorman

Major Professor: L. Keith Woo
Iowa State University

Previous examinations of group 4 coordination chemistry have predominately

involved cyclopentadienyl, alkoxido, and amido complexes. The systematic exploration of

the chemistry of group 4 metalloporphyrin complexes has recently been made possible by

facile routes to useful porphyrin starting materials. Of interest are complexes containing

hard π-donor ligands. From these, bonding characteristics and steric constraints of the

porphyrin periphery specific to the ligand can be studied.

The implementation of the group 4 metal halide complexes, $(TTP)MCl_2$, in

metathesis reactions has provided routes to amido, alkoxido, hydrazido, and imido

derivatives. These complexes have subsequently demonstrated unique reactivity properties.

It has been found that the formation of zirconium and hafnium imido metalloporphyrin

complexes is dependent on the steric bulk of the phenyl substituent of the lithiated amide.

Bis(amido) complexes are isolable when the *ortho* positions of phenyl amide are

unsubstituted. The presence of the sterically demanding methyl, *tert*-butyl, or isopropyl

groups at the *ortho* position of the phenyl amide effects an α-elimination of a primary aryl amine from the unstable secondary bis(amido) precursor to produce the imido derivative. These imido compounds were key starting materials for the production and investigation of a number of complexes containing M-O bonds. The zirconium and hafnium imido complexes, (TTP)M=NAr^{Pr}, couple two pinacolone molecules with concomitant loss of the amine H$_2$NAr^{Pr}. The hydrazido, (TTP)Ti=NNR$_2$ (R = Me, Ph), and imido, (TTP)Ti=N^{t}Pr, derivatives of titanium undergo novel nitrene group metathesis reactions with *p*-chlorobenzaldehyde and with nitrosobenzene, respectively.

Additional examples of atom and group transfer involving titanium(II) metalloporphyrins have been demonstrated. Utilization of a variety of donor molecules has facilitated the estimation of the double bond strength for complexes of the type (TTP)Ti=G (G = O, S, Se, NR). This dissertation focuses on the synthesis and reactivity of group 4 metalloporphyrin complexes containing hard π-donor ligands and on the properties of titanium(II) metalloporphyrin species.

GENERAL INTRODUCTION

Dissertation organization

The first chapter of this dissertation is a literature review on group 4 transition metal porphyrin complexes. The remaining chapters incorporate individual papers that have been published, submitted for publication, or are being prepared for submission. Approximately 50 percent of the work in chapter 2 was performed by Dr. Steven D. Gray.

Porphyrins as ligands

The distinct characteristics of porphyrins have been instrumental in the delineation of a variety of fundamental aspects of inorganic chemistry. The parent porphyrin is a planar, aromatic tetrapyrrole macrocycle that possesses four-fold symmetry. Aromaticity, according to the Hückel rule [4n + 2], is derived from the 22 π electrons, only 18 of which are used in any one continuous path. The β-pyrrole and *meso* positions can be functionalized to modify the electronic and steric properties of the metal and its coordination sphere. Such modifications are often utilized to facilitate solubility in common organic solvents. Two examples of commonly implemented synthetic porphyrins are shown in Figure 1.

In porphyrin complexes, the metal is coordinated to the four pyrrole nitrogens in the central cavity. The porphyrin hole, approximately 4 Å in diameter, and the size of the coordinated metal regulates the position of metal. Small metals will typically lie within the porphyrin cavity and larger metals will be displaced above the mean N_4 plane. However, some flexibility is possible. A revealing example is that of $(Por)Sn(Ph)_2$.[1] This six coordinate

metalloporphyrin complex can contain the phenyl ligands in either a *trans-* or *cis-*

configuration such that the metal is found within or above the porphyrin plane, respectively

(Figure 2). By discriminating preparative routes, both examples of this complex have been

observed. Upon descending the group 4 triad, a transformation from a *trans-* to *cis-*

configuration in the binding of two monodentate ligands is observed for metalloporphyrin

complexes.

meso-tetra-*p*-tolylporphyrin, H$_2$(TTP)   octaethylporphyrin, H$_2$(OEP)
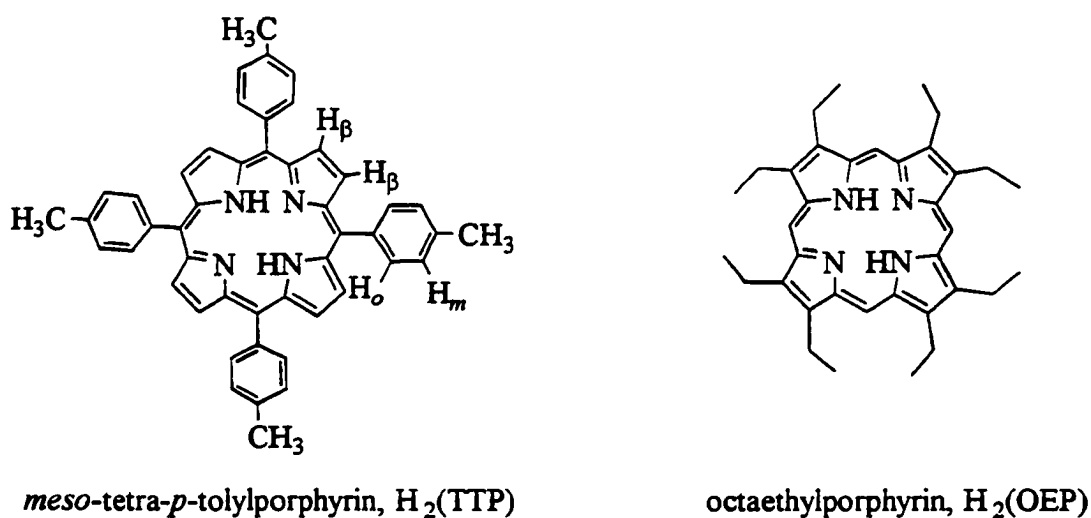
Figure 1. Common synthetic porphyrins.
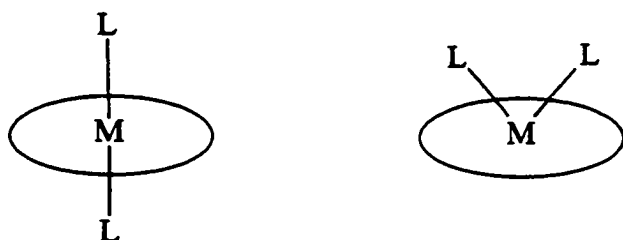
Figure 2. Arrangement of ligands in six-coordinate metalloporphyrin complexes

The porphyrin provides a robust platform for the binding of a metal. The chelation effect of the tetradentate porphyrin accounts for the rare occurrence of demetalation of early transition metal complexes. The structural rigidity originating from the aromatic porphyrin precludes excessive rearrangement upon change of the oxidation state or the number of bound ligands to the metal.

Porphyrins possess valuable spectroscopic properties. For diamagnetic metalloporphyrin complexes, the use of ^{1}H NMR spectroscopy often allows for unambiguous characterization of the coordination sphere of the metal. In the case of $(TTP)TiL_2$ complexes which possess D_{4h} symmetry, there are only four resonances observed in the ^{1}H NMR spectrum, assigned to the β-pyrrole, o-tolyl, m-tolyl, and tolyl-CH_3 protons. Cisoid complexes, such as $(TTP)ZrL_2$, have C_{2v} symmetry which results in 6 resonances, the β-pyrrole singlet, 2 o-tolyl doublets, 2 m-tolyl doublets, and one tolyl-CH_3 singlet. Also, the large ring current of the aromatic porphyrin strongly affects resonances of the metal bound ligands. Upfield shifts of 1 - 4 ppm are commonly observed in the ^{1}H NMR spectra. An additional characterization tool for metalloporphyrin complexes is their strong electronic absorption in the UV-vis spectrum.

Metalloporphyrin and related complexes

The chemistry of metalloporphyrin complexes in general has been reviewed in a series of monographs edited by Dolphin.[2] A general treatise of zirconium and hafnium organometallic compounds, predominately that of metallocene derivatives, is available.[3] Metal-ligand multiple bonding in metalloporphyrin complexes is primarily found in groups 4-

6 of the transition metals. Examples of oxo (M=O), sulfido (M=S), and selenido (M=Se)

moieties have been investigated. Fewer in number are examples of imido (M=NR), nitrido

(M≡N), and carbene (M=CR$_2$) derivatives. The greater number of terminal oxo derivatives

is a result of the strong multiple bond formed. Recent compilations have addressed the

synthesis, reactivity, and applications of such metal-ligand multiple bonds. A general

collection of the chemical aspects of metal-ligand multiple bonds can be found in a

monograph by Mayer and Nugent.[4] Also available is a specific examination of organoimido

complexes of the transition metals by Wigley.[5] A recent review article considers

metalloporphyrin derivatives of the early transition metals.[6]

CHAPTER 1: INTRODUCTION TO GROUP FOUR METAL TETRAAZA

MACROCYCLE-SUPPORTED COMPLEXES: A LITERATURE REVIEW

The chemistry of early transition metal porphyrin complexes has not been subject to

the intense research that the later transition metals have. This is largely due to their

oxophilic nature which results in the formation of inert complexes. Also crippling the

exploration of this class of compounds was the lack of efficient synthetic routes to useful

starting materials. This chapter will present a brief summary of developments in the

synthesis and reactivity of group 4 metal porphyrin complexes.

New ligand arrays continue to be of interest in an attempt to expand upon the rich

chemistry of the dichloro metallocene complexes, Cp_2MCl_2 (M = Ti, Zr, Hf). However, the

exploration of group 4 metalloporphyrin chemistry has been hindered by the lack of a

versatile metallation procedure. For the early transition metal complexes, this was overcome

by the development of alkali metal porphyrin complexes, $(POR)M_2(L)$ (M = Li, Na, K; L =

THF, DME).[7] These complexes are generated by treatment of the free base porphyrin,

$H_2(POR)$, with alkali metal amides in the presence of a donor molecule. The most

commonly used base is lithium silylamide, $LiN(SiMe_3)_2$, although for more sterically

demanding porphryins such as $H_2(TMP)$ the parent lithium amide, $LiNH_2$, is utilized. From

these alkali metallated porphyrins the insertion of early transition metals is significantly

simplified. High yield, large scale routes to these halogenated early transition

metalloporphyrin derivatives have become available (eq 1).[8] This class of molecules

provides a foundation from which to synthesize metalloporphyrin complexes with potential

for novel reactivity.

$$(POR)Li_2(sol)_2 \; + \; MCl_x(sol)_y \; \rightarrow \; (POR)MCl_{x-2} \; + \; 2\,LiCl \; + \; (y{+}2)\,sol \qquad (1)$$
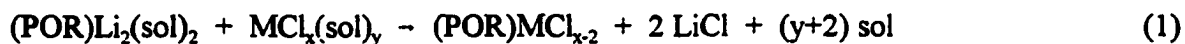
The chemistry of titanium metalloporphyrins before 1985 was largely limited to oxygen adducts. An important finding was the isolation of the first metalloporphyrin with a dioxygen moiety bound "side-on" to the metal, $(OEP)Ti(\eta^2\text{-}O_2)$.[9] Variable temperature ^{1}H NMR, X-ray crystal structure, and *ab initio* investigations show that the peroxo group eclipses two *trans* nitrogen atoms. This has been explained in terms of overlap of the oxygen π_g-orbital with the metal $3d_{xy}$-orbital. Likewise, the sulfur and selenium analogues, $(TTP)Ti(\eta^2\text{-}Ch_2)$ (Ch = S, Se), were found to adopt this same structure.[10] Although reactivity studies were frustrated by the inert $Ti{=}O^{2+}$ fragment, the oxotitanium(IV) porphyrins can be converted to the dihalogeno complexes $(POR)TiX_2$ under strongly acidic conditions involving the use of hydrogen halides HX (X = F, Cl, Br). Reduction of the these dihalogeno complexes with zinc amalgam produced a route into the mid-valent halotitanium(III) porphyrins. Treatment of (TTP)TiF with aryl Grignard reagents or alkyl and aryl thiolates generated Ti(III) organometallic or thiolato species.[11] Somewhat atypical of titanium chemistry, there were few reported alkoxido metalloporphyrin complexes. The titanium(III) methoxide, (TPP)Ti(OMe), was produced from the sequential treatment of (TPP)TiF with NaSMe and then HOMe.[12] The reaction of (TPP)Ti=O with catechol or 1,2-benzenedithiol produced the *cis*-coordinated titanium derivatives, $(TPP)Ti[1,2\text{-}(Ch)_2\text{-}C_6H_4]$ (Ch = O, S).[13]

Facile production of $(POR)TiCl_2$ from the lithiated porphyrin stimulated new work

with titanium metalloporphyrin complexes. Initial emphasis centered mainly on low valent

Ti(II) derivatives in the development of atom-transfer processes. In the presence of

coordinating ligands such as alkynes or THF, $(Por)TiCl_2$ is reduced by allylMgCl, $LiAlH_4$,

and $NaBEt_3H$ to $(Por)Ti(L)_2$.[14] These low valent species have proved effective in a variety

of atom-transfer processes.[15]

Zirconium and hafnium metalloporphyrin chemistry experienced similar

developmental problems as that of titanium. As a result of the difficulty in metalating the

porphyrin, investigations prior to 1992 dealt only with sandwich compounds, $(Por)_2M$.

Examination of porphyrin-porphyrin interactions and nonlinear optical properties of these

molecules continue to be of interest.[16] Utilization of the dichloro complex, $(Por)ZrCl_2$, first

prepared by Arnold,[17a] in metathesis reactions provided access to alkyl, aryl, alkoxide,

acetate, triflate, benzenedithiolato, carborane, and cyclooctane derivatives of zirconium.[17]

The novel insertions of CO_2 and acetone into the metal-alkyl bond of $(OEP)ZrMe_2$ have also

been studied. These form the respective bis(acetate), $(OEP)Zr(OAc)_2$, and bis(alkoxide),

$(OEP)Zr(O^tBu)_2$, complexes. The zirconium(IV) dialkyl, $(OEP)Zr(CH_2SiMe_3)_2$, acts as a

precatalyst for the catalytic hydrogenation of 1-alkenes by a putative zirconium hydride

intermediate.[17a] The significance of d^0 cationic group 4 complexes in alkene polymerization

prompted the synthesis of $[(OEP)M(CH_2SiMe_3)][BPh_4]$ (M = Zr, Hf) from the reaction of

$[HNMe_2Ph][BPh_4]$ with $(OEP)M(CH_2SiMe_3)_2$. However, this product was unreactive

towards ethylene.[18] As an indication of the high oxophilicity of the zirconium and hafnium

organometallic complexes, $(POR)MR_2$, attempts at producing X-ray diffraction quality

crystals instead resulted in the isolation of four dimeric oxo/hydroxy bridged complexes,

[(TPP)Zr(μ-OH)$_2$]$_2$,[19] [(TPP)Hf]$_2$(μ-OH)$_2$(μ-O),[20] [(TPP)Zr]$_2$(μ-OH)$_2$(μ-O),[21] [(OEP)Zr]$_2$(μ-OH)$_3$$^+$.[21] These examples of seven- and eight-coordinate zirconium and hafnium

metalloporphyrins have been structurally characterized by single-crystal X-ray diffraction.

Interestingly, all possess a M-O bond that eclipses a M-N$_{pyrrole}$ bond. Also common among

these complexes is the presence of eclipsed porphyrin rings. It has been suggested that these

conformations are stabilized by interactions between the oxygen p-orbitals and the metal d-

orbitals. The seven coordinate trimetaphosphate derivative, [NBu$_4$][(OEP)Hf(P$_3$O$_9$)], also

displays eclipsed M-O/M-N$_{pyrrole}$ bonds.[8c] Furthermore, the benzenedithiolato complex,

(TPP)Hf(1,2-S$_2$-C$_6$H$_4$) posseses eclipsed Hf-S and Hf-N$_{pyrrole}$ bonds. Examples of zirconium

and hafnium dimers bridged by two perchalcogenido linkages, [(TTP)M]$_2$(μ-η^2-Ch$_2$)$_2$, have

been synthesized from the metal halide complex, (TPP)MCl$_2$, and Li$_2$Ch$_2$ (Ch = S, Se). The

single-crystal X-ray diffraction study of the zirconium disulfido complex reveals that the two

porphyrin rings are eclipsed but the Zr-S bonds do not eclipse Zr-N bonds.[22]

Another catalytic application of group 4 metalloporphyrins is the ethylalumination of

1-heptyne.[23] Treatment of (TPP)ZrX$_2$ (X = Cl, O$_2$CMe, O$_2$C^{t}Bu, 1,2-(O$_2$C)$_2$-C$_6$H$_4$) with

Et$_3$Al in the presence of 1-heptyne, with subsequent work up in acidic media, produced

alkenes with high regio- and stereoselectivity. Superior conversion is found for the

porphyrin system over that of the metallocene homologue, Cp$_2$ZrCl$_2$.

The diacetate complex, (POR)M(OAc)$_2$ (M = Zr, Hf), was examined as an alternate

starting material for the synthesis of additional organometallic and inorganic complexes due

to its air and moisture stability, in contrast to the porphyrin dichlorides.[24] Unfortunately, the

diacetate species is limited to the preparation of alkyl complexes upon treatment with the appropriate organolithium reagent. The single crystal X-ray diffraction study reveals that the Zr-O bonds in (Por)M(OAc)$_2$ do not eclipse Zr-N$_{pyrrole}$ bonds.

Analogous to titanium, there are now examples of well characterized tri- and di-valent zirconium(III) and zirconium(II) metalloporphyrins.[25] Reduction of the metal is accomplished by the reaction of (TPP)ZrCl$_2$ with TlCp in the presence of Na/Hg to yield (TPP)Zr(Cp). The formation of (OEP)Zr(η^2-PhC≡CPh) was found from the reaction between equimolar amounts of magnesium, (OEP)ZrCl$_2$, and diphenylacetylene in THF. This alkyne complex is described as a zirconium(II) metal stabilized by an η^2 four-electron π-donor ligand, similar to the titanium complex analogue. This species is of potential importance in atom and group transfer reactions.

As an indication of the robust metal binding platform provided by the porphyrin, demetalation of group 4 metalloporphyrin complexes has been documented in only two cases. Refluxing (OEP)ZrR$_2$ (R = Cl, alkyl, alkoxide, acetate, Por, etc.) with KF in acetic acid returns the free base porphyrin in quantitative yield, apparently facilitated by formation of strong Zr-F bonds.[7b] Demetalation has also been claimed in the treatment of (TPP)Zr(OEt$_2$)$_2$ with water.[24a]

Other than the titanium oxo complexes, there are a limited number of studies of group 4 species containing metal-ligand multiple bonds. The first group 4 imido metalloporphyrin was produced from treatment of (TTP)TiCl$_2$ with 2 eq of LiNHR (R = Ph, tolyl, Cy).[26] Another synthetic route was found by the direct insertion of the preformed metal-imido moiety, Ti(=N^{t}Bu)Cl$_2$(py)$_3$, into the lithiated porphyrin, (TTP)Li$_2$(THF)$_2$.[27] The

terminal chalcogenido complexes, (TTP)Ti=S and (TTP)Ti=Se, were synthesized by atom

transfer from $Ph_3P=Ch$ to $(TTP)Ti(\eta^2\text{-}PhC\equiv CPh)$. Other than hydrolysis, the only example

of metal-ligand multiple bond reactivity is found in the treatment of the terminal sulfido

complex with elemental sulfur which yields the persulfido species, $(TTP)Ti(\eta^2\text{-}S_2)$.[14b] The

selenium analogue behaves similarly (eq 3).

$$(2)$$

$$(3)$$
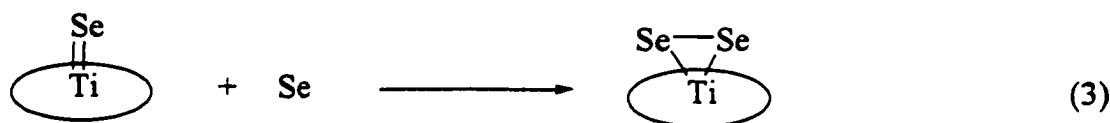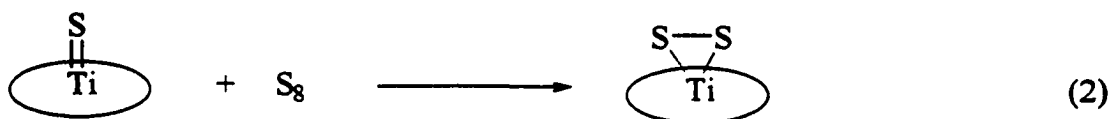
References

1. Dawson, D. Y.; Sangalang, J. C.; Arnold, J. *J. Am. Chem. Soc.* **1996**, *118*, 6082.

2. Dolphin, D.; *The Porphyrins*: Academic: New York, 1978: Vols. 1-4. (b) *Porphyrins and Metalloporphyrins*; Smith, K. M., Ed.; Elsevier: New York, 1975.

3. Cardin, D. J.; Lappert, M. F.; Raston, C. L. *Chemistry of Organo-Zirconium and Organo-Hafnium Compounds*; John Wiley: New York, 1986.

4. Nugent, W. A.; Mayer, J. M. Metal-Ligand Multiple Bonds; Wiley-Interscience, New York, 1988.

5. Wigley, D. E. *Progress in Inorganic Chemistry* **1994**, *42*, 239.

6. Brand, H.; Arnold, J. *Coord. Chem. Rev.* **1995**, *140*, 137.

7. (a) Arnold, J. *J. Chem. Soc., Chem. Commun.* **1990**, 976. (b) Arnold, J.; Dawson, D. Y.; Hoffman, C. G. *J. Am. Chem. Soc.* **1993**, *115*, 2707. (c) Brand, H.; Capriotto, J. A.; Arnold, J. *Inorg. Chem.* **1994**, *33*, 4334.

8. (a) Berreau, L. M.; Hays, J. A.; Young, V. G., Jr.; Woo, L. K. *Inorg. Chem.* **1994**, *33*, 105. (b) Kim, H.; Whang, D.; Kim, K.; Do, Y. *Inorg. Chem.* **1993**, *32*, 360. (c) Ryu, S.; Whang, D.; Kim, J.; Yeo, W.; Kim, K. *J. Chem. Soc., Dalton Trans.* **1993**, 205. (d) Buchler, J. W.; Eberle, M. *Chem. Ber.* **1995**, *128*, 1131.

9. (a) Guilard, R.; Fontesse, M.; Fournari, P.; Lecomte, C.; Protas, J. *J. Chem. Soc., Chem. Commun.* **1976**, 161. (b) Guilard, R.; Lecomte, C. *Coord. Chem. Rev.* **1985**, *65*, 87.

10. Guilard, R.; Ratti, C.; Tabard, A.; Richard, P.; Dubois, D.; Kadish, K. M. *Inorg. Chem.* **1990**, *29*, 2532.

11. (a) Latour, J. M.; Boreham, C. J.; Marchon, J. C. *J. Organomet. Chem.* **1980**, *190*, C61. (b) Marchon, J. C.; Latour, J. M.; Boreham, C. J.; *J. Mol. Catal.* **1980**, *7*, 227.

12. Boreham, C. J.; Buisson, G.; Duee, E.; Jordanov, J.; Latour, J.-M.: Marchon, J.-C. *Inorg. Chim. Acta* **1983**, *70*, 77.

13. (a) Deronzier, A.; Latour, J. M. *Nouv. J. Chim.* **1984**, *8*, 393. (b) Marchon, J.-C.; Latour, J.-M.; Grand, A.; Belakhovsky, M.; Loos, M.; Goulon, J. *Inorg. Chem.* **1990**, *29*, 57.

14. (a) Woo, L. K.; Hays, J. A; Jacobson, R. A.; Day, C. L. *Organometallics* **1991**, *10*, 2102. (b) Woo, L. K.; Hays, J. A; Young, V. G., Jr.; Day, C. L.; Caron, C. D'Souza, F.; Kadish, K. M. *Inorg. Chem.* **1993**, *32*, 4186. (c) Wang, X.; Gray, S. D.; Chen, J.; Woo, L. K. *Inorg. Chem.* **1998**, *37*, 5.

15. (a) Gray, S. D.; Thorman, J. L.; Adamian, V. A.; Kadish, K. M.; Woo, L. K. *Inorg. Chem.* **1998**, *37*, 1. (b) Wang, X.; Woo, L. K. *J. Org. Chem.* **1998**, *63*, 356.

16. (a) Martin, P. C.; Arnold, J.; Bocian, D. F. *J. Phys. Chem.* **1993**, *97*, 1332. (b) Collman, J. P.; Kendall, J. L.; Chen, J. L. Eberspacher, T. A.; Moylan, C. R. *Inorg. Chem.* **1997**, *36*, 5603.

17. (a) Brand, H.; Arnold, J. *J. Am. Chem. Soc.* **1992**, *114*, 2266. (b) Arnold, J.; Johnson, S. E.; Knobler, C. B.; Hawthorne, M. F.; *J. Am. Chem. Soc.* **1992**, *114*, 3996. (c) Brand, H.; Arnold, J. *Organometallics* **1993**, *12*, 3655. (d) Ryu, S.; Kim, J.; Yeo, H.; Kim, K. *Inorg. Chim. Acta* **1994**, *221*, 51.

18. Brand, H.; Capriotti, J. A.; Arnold, J. *Organometallics* **1994**, *13*, 4469.

19. Huhmann, J. L.; Corey, J. Y.; Rath, N. P.; Campana, C. F. *J. Organomet. Chem.* **1996**, *513*, 17.

20. Ryu, S.; Kim, J.; Yeo, H.; Kim, K. *Inorg. Chim. Acta* **1995**, *228*, 233.

21. Kim, H.-J.; Whang, Y.; Do, Y.; Kim, K. *Chem. Lett.* **1993**, 807.

22. Ryu, S.; Whang, D.; Kim, H. J.; Kim, K; Yoshida, M.; Hashimoto, K.; Tatsumi, K. *Inorg. Chem.* **1997**, *36*, 4607.

23. Shibata, K.; Aida, T.; Inoue, S. *Tetrahedron. Lett.* **1992**, *33*, 1077.

24. (a) Shibata, K.; Aida, T.; Inoue, S. *Chem. Lett.* **1992**, 1173. (b) Huhmann, J. L.; Corey, J. Y.; Rath, N. P. *Acta Cryst.* C **1995**, 195.

25. Kim, H. J.; Jung, S.; Jeon, Y. M.; Kim, K. *J. Chem. Soc. Chem. Comm.* **1997**, 2201.

26. Berreau, L. M.; Young, V. G., Jr.; Woo, L. K *Inorg. Chem.* **1995**, *34*, 527.

27. Swallow, D.; McInnes, J.; Mountford, P. *J. Chem. Soc., Dalton Trans.* **1998**, 2253.

CHAPTER 2: ALKOXIDO, AMIDO, AND IMIDO DERIVATIVES OF

TITANIUM(IV) TETRATOLYLPHORPHYRIN

Steven D. Gray, Joseph L. Thorman, Lisa M. Berreau, and L. Keith Woo[*2]

Abstract

Treatment of (TTP)TiCl$_2$ (1) [TTP = $meso$-5,10,15,20-tetra-p-tolylporphyrinato dianion] with excess NaOR (R = Ph, Me, ^{t}Bu) affords the (bis)alkoxide derivatives, (TTP)Ti(OR)$_2$ [R = Ph (2), Me (3), ^{t}Bu (4)] in moderate yield. The corresponding amido derivative, (TTP)Ti(NPh$_2$)$_2$ (5) is prepared in an analogous fashion employing LiNPh$_2$. The (bis)substituted complexes 2, 3, and 5, react cleanly with (TTP)TiCl$_2$ to afford the ligand exchange products, (TTP)Ti(OR)Cl [R = Ph (6), Me (7)] and (TTP)Ti(NPh$_2$)Cl (8), respectively. The monosubstituted complexes, 6–8, are also obtained by treatment of 1 with one equiv of the appropriate NaOR or LiNPh$_2$ reagent. Treatment of 5 with excess phenol produces the (bis)phenoxide derivative (2) and 2 equiv of HNPh$_2$. The imido derivatives, (TTP)Ti(=NR) [R = t-Bu (9), Ph (10), C$_6$H$_4$-p-Me (11)] are prepared by the treatment of 1 with excess LiNHR. The t-butyl derivative (9) is also obtained by reaction of 1 with excess H$_2$N-t-Bu at elevated temperatures. The phenyl imido complex (10) may be produced by the reaction of 0.5 equiv of PhN=NPh with (TTP)Ti(η^2-EtC≡CEt) in refluxing toluene. Finally, (TTP)Ti(=NTMS) (12) is obtained by oxidation of (TTP)Ti(η^2-EtC≡CEt) with N$_3$TMS.

Introduction

The highly reactive nature of the metal-nitrogen bond in many group 4 imido complexes has lead to a rapidly growing area of research.[3] For example, group 4 imido complexes can engage in aliphatic and aromatic C-H bond activation processes[4] as well as numerous 2 + 2 cycloaddition reactions with unsaturated organic substrates.[3d] Additionally, group 4 imido complexes have found use in the catalytic hydroamination[3d] of alkynes and the synthesis of various nitrogen heterocycles.[5]

Recently we reported the synthesis of a variety of imido-titanium *meso*-tetratolylporphyrinato complexes of the type (TTP)Ti(=NR) (R = Ph, tolyl, cyclohexyl).[6] Our interest in these systems stems from our observation that isoelectronic (POR)Ti=O complexes undergo facile intermetal oxygen atom transfer.[7] In addition, (POR)Ti=O complexes serve as precatalysts for the epoxidation of alkenes.[8] In this report, we summarize the preparation and properties of a variety of imido-titanium-porphyrin complexes and discuss their reactivity. Additionally, we report the synthesis and reactivity of new alkoxide and amide derivatives of titanium-porphyrin. These new complexes extend the class of group 4 porphyrin complexes possessing hard π-donor ligands.[9]

Experimental

General. All manipulations were performed under an inert atmosphere of nitrogen using a Vacuum Atmospheres glovebox equipped with a Model MO40–1 Dri-Train gas purifier. The glovebox atmosphere was continuously monitored with an Illinois Instrument Model 2550 trace oxygen analyzer. The concentration of O_2 in the glovebox was kept at

less than 5 ppm at all times. All solvents were rigorously degassed and dried prior to use.

Benzene-d_6, toluene, and hexane were freshly distilled from purple solutions of sodium

benzophenone and brought into the drybox without exposure to air. (TTP)TiCl$_2$ (1) was

prepared according to published procedures[10] and recrystallized from CH$_2$Cl$_2$/hexane prior to

use. Phenol was purchased from Aldrich and used as received. Methanol was purchased

from Fisher, dried with CaH$_2$, and vacuum transferred prior to use. NaOR (R = Ph, Me,

^{t}Bu) reagents were prepared by treating the appropriate alcohol with sodium in hexanes.

Diphenylamine was purchased from Fisher and was recrystallized from hexanes prior to use.

LiNPh$_2$ was prepared by reaction of the free amine with n-butyl lithium in hexanes. The

lithium amide salts, LiNHPh, LiNHC$_6$H$_4$-p-Me, and LiNHC$_6$H$_{11}$ were prepared as previously

described.[5] LiNH-t-Bu was prepared by the reaction of H$_2$N-t-Bu with n-butylithium in

hexanes and was recrystallized from hexanes at -20 °C. All amines used above were

purchased from Aldrich and were purified by literature methods.[11] N$_3$TMS was purchased

from Aldrich and used as received.

^{1}H NMR data were recorded at 20.0 °C on either a Varian VXR (300 MHz) or

Bruker DXR (400 MHz) spectrometer. Chemical shifts are referenced to proton solvent

impurities (δ 7.15, C$_6$D$_5$H). UV-vis data were recorded on a HP8452A diode array

spectrophotometer. Elemental analyses (C, H, N) were performed by Atlantic Microlab of

Norcross, Georgia. All samples were handled under nitrogen and WO$_3$ was used as a

combustion aid. MS-CI studies were performed on a Finnigan TSQ 700 at 70 eV in the

negative ion mode using ammonia as the ionization gas.

(TTP)Ti(OPh)₂ (2). (TTP)TiCl₂ (200 mg, 0.254 mmol) and NaOPh (62 mg,

0.53 mmol) were stirred in toluene (ca. 10 mL) to afford a light brown solution which

became an opaque deep brown color after several minutes. After 4 hours, the solution was

filtered. Removal of solvent from the filtrate under reduced pressure afforded

(TTP)Ti(OPh)₂ (123 mg, 0.137 mmol, 54% yield) as a semicrystalline, analytically pure,

deep blue solid. UV-vis (toluene): 330, 338, 382, 424 (Soret), 484, 488, 608, 654 nm.

^{1}H NMR (C₆D₆, 300 MHz): 9.02 (s, 8H, β-H), 8.01 (d, 8H, $^3J_{H-H}$ = 7.8 Hz, –C₆H_4Me), 7.26

(d, 8H, $^3J_{H-H}$ = 7.8 Hz, –C₆H_4Me), 2.38 (s, 12H, –C₆H₄Me), 5.83 (overlapping d&t, 6H, *m*-

p-C₆H₅), 2.67 (m, 2H, *o*-C₆H₅). Anal. Calcd for C₆₀H₄₅N₄O₂Ti: C, 79.81; H, 5.13; N, 6.20.

Found: C, 80.58; H, 5.44; N, 6.06.

(TTP)Ti(OMe)₂ (3). (TTP)TiCl₂ (158 mg, 0.20 mmol) and NaOMe (122,

2.25 mmol) were slurried in toluene and the resultant brown solution was rapidly stirred.

After 5 h, the solution was filtered and the solvent was removed from the dark brown filtrate

to afford blue (TTP)Ti(OMe)₂ (100 mg, 0.129 mmol, 66% yield). Despite numerous efforts

to obtain analytically pure compound, **3** consistently contains a trace (ca. 5%) of (TTP)Ti=O

impurity which precluded elemental analysis. UV-vis (toluene): 426 (Soret), 552 nm.

^{1}H NMR (C₆D₆, 300 MHz): 9.07 (s, 8H, β-H), 8.07 (d, 8H, $^3J_{H-H}$ = 7.8 Hz, –C₆H_4Me), 7.26

(d, 8H, $^3J_{H-H}$ = 7.8 Hz, –C₆H_4Me), 2.39 (s, 12H, –C₆H₄Me), –0.83 (s, 6H, OCH_3). MS (CI)

Calcd. (found) m/e: [M⁺] 778 (778).

(TTP)Ti(OᵗBu)₂ (4). (TTP)TiCl₂ (44 mg, 0.056 mmol) and NaOᵗBu (26 mg,

0.28 mmol) were slurried in toluene and the resultant brown solution was rapidly stirred at

ambient temperature. After 5 h, the solution was filtered and the solvent was removed from

the dark brown filtrate to afford blue (TTP)Ti(O^{t}Bu)$_2$ (32 mg, 0.037 mmol, 67% yield).

Despite numerous efforts to obtain analytically pure compound, **4** consistently contained

traces (ca. 5%) of impurities which precluded elemental analysis. UV-vis (toluene): 450

(Soret), 584, 622 nm. ^{1}H NMR (C$_6$D$_6$, 300 MHz): 9.05 (s, 8H, β-H), 8.23 (d, 8H, $^3J_{H-H}$ =

7.8 Hz, –C$_6H_4$Me), 7.31 (d, 8H, $^3J_{H-H}$ = 7.8 Hz, –C$_6H_4$Me), 2.40 (s, 12H, –C$_6$H$_4$*Me*), –2.18

(s, 18H, O^{t}Bu).

(TTP)Ti(NPh$_2$)$_2$ (5). (TTP)TiCl$_2$ (326 mg, 0.413 mmol) and LiNPh$_2$ (150 mg,

0.0859 mmol) were slurried in hexanes (ca. 20 mL). The solution slowly changed from light

brown to chocolate brown. After 5 h, the solution was filtered to collect a dark brown solid.

This solid was placed on a clean fritted filter and extracted with CH$_2$Cl$_2$ (3 x 3 mL).

Removal of solvent from the resultant filtrate afforded (TTP)Ti(NPh$_2$)$_2$ (251 mg,

0.238 mmol, 58% yield) as a semicrystalline, blue solid. UV-vis (toluene): 426 (Soret),

552 nm. ^{1}H NMR (C$_6$D$_6$, 400 MHz): 8.83 (s, 8H, β-H), 8.09 (d, 8H, $^3J_{H-H}$ = 7.6 Hz,

–C$_6H_4$Me), 7.37 (d, 8H, $^3J_{H-H}$ = 7.6 Hz, –C$_6H_4$Me), 6.17 (d, 2H, $^3J_{H-H}$ = 7.2 Hz, C$_6H_5$), 6.05

(d, 4H, $^3J_{H-H}$ = 7.2 Hz, C$_6H_5$), 2.86 (d, 4H, $^3J_{H-H}$ = 7.2 Hz, C$_6H_5$), 2.44 (s, 12H, –C$_6$H$_4$*Me*).

Anal. Calcd for C$_{72}$H$_{56}$N$_6$Ti: C, 82.11; H, 5.36; N, 7.98. Found: C, 81.58; H, 5.98; N,

7.56.

(TTP)Ti(OPh)Cl (6). (TTP)TiCl$_2$ (45 mg, 0.058 mmol) and LiOPh (6 mg,

0.06 mmol) were stirred in toluene (ca. 10 mL). The initial dark brown color of the solution

progressively darkens to a nearly black color. After 15 h, the solution was filtered and solids

on the frit were extracted with toluene. The solvent was removed from the combined

filtrates under reduced pressure to yield (TTP)Ti(OPh)Cl (31 mg, 0.37 mmol, 64% yield) as

a deep blue solid. UV-vis (toluene): 352, 404, 426 (Soret), 552 nm. ^{1}H NMR (C_6D_6,

400 MHz): 9.04 (s, 8H, β-H), 7.94 (d, 8H, $^3J_{H-H}$ = 7.6 Hz, $-C_6H_4Me$), 7.24 (m, 8H,

$-C_6H_4Me$), 5.77 (t, 1H, $^3J_{H-H}$ = 7.2 Hz, $-OC_6H_5$), 5.69 (t, 2H, $^3J_{H-H}$ = 7.2 Hz, $-OC_6H_5$), 2.72

(d, 2H, $^3J_{H-H}$ = 8.0 Hz, $-OC_6H_5$), 2.37 (s, 12H, $-C_6H_4Me$). MS (CI) Calcd (found) m/e:

[(TTP)TiOPh$^-$] 767 (767); [(TTP)TiCl$^-$] 751 (751).

(TTP)Ti(OMe)Cl (7). (TTP)TiCl$_2$ (56 mg, 0.72 mmol) and LiOMe (3 mg,

0.08 mmol) were dissolved in toluene (ca. 10 mL) to give a deep brown solution. After 4 h,

the nearly black solution was filtered. The solid left on the frit was extracted with toluene

and CH_2Cl_2. Removal of the solvent from the resultant filtrate under reduced pressure

afforded (TTP)Ti(OMe)Cl (20 mg, 36% yield) as a deep blue, microcrystalline solid which is

slightly contaminated with (TTP)TiCl$_2$ (ca. 5%) presumably due to stoichiometry

deficiencies. UV-vis (toluene): 376, 426 (Soret), 502 nm. ^{1}H NMR (C_6D_6, 300 MHz):

9.08 (s, 8H, β-H), 8.07 (d, 4H, $^3J_{H-H}$ = 7.8, $-C_6H_4Me$), 7.90 (d, 4H, $^3J_{H-H}$ = 7.8, $-C_6H_4Me$),

7.26 (d, 4H, $^3J_{H-H}$ = 8.1, $-C_6H_4Me$), 7.21 (d, 4H, $^3J_{H-H}$ = 8.1, $-C_6H_4Me$), 2.38 (s, 12H,

$-C_6H_4Me$), -0.79 (s, 3H, $-OMe$). MS(CI) Calcd (found) m/e: [(TTP)TiClO$^-$], 767 (767);

[(TTP)TiCl$^-$], 751 (751).

Reaction of (TTP)TiCl$_2$ with ^{t}BuOH. An anaerobic C_6D_6 (0.7 mL) solution of

(TTP)TiCl$_2$ (20 mg, 0.026 mmol), ^{t}BuOH (14 μL, 0.15 mmol), was sealed in an NMR tube

under N$_2$. The mixture was monitored by ^{1}H NMR until no further reaction was observed.

The only new species observed in solution were (TTP)Ti(O^{t}Bu)Cl (80%) and (TTP)Ti=O

(7%). Unreacted (TTP)TiCl$_2$ (13%) and ^{t}BuOH were also present. ^{1}H NMR signals for

(TTP)Ti(O^{t}Bu)Cl (300 MHz): 9.06 (s, 8H), 8.13 (d, 4H, $^3J_{H-H}$ = 7.8 Hz, $-C_6H_4Me$), 7.92 (d,

4H, $^3J_{H-H}$ = 7.8 Hz, $-C_6H_4$Me), 7.29 (m, 8H, $-C_6H_4$Me), 2.38 (s, 12H, $-C_6H_4Me$), -2.25 (s,

9H, ^{t}Bu).

(TTP)Ti(NPh₂)Cl (8). In a general procedure, approximately one equiv of LiNPh₂

was added to (TTP)TiCl₂. For example, (TTP)TiCl₂ (53 mg, 0.067 mmol) and LiNPh₂

(13 mg, 0.073 mmol) were stirred in hexanes (ca. 10 mL). The initial light brown solution

gradually darkened to deep brown solution. After 4 h, the solution was filtered and the

solvent was removed from the filtrate under reduced pressure to afford (TTP)Ti(NPh₂)Cl

(27 mg, 0.029 mmol, 43% yield) as a deep blue solid. Due to minor differences in

stoichiometry, compound **8** is consistently contaminated with (TTP)TiCl₂ or (TTP)Ti(NPh₂)₂

(ca. 5%). Even with several recrystallizations, these impurities could not be removed and

hence preclude elemental analysis. UV-vis (toluene): 372, 428 (Soret), 554 nm. ^{1}H NMR

(C₆D₆, 300 MHz): 8.98 (s, 8H, β-H), 8.05 (d, 4H, $^3J_{H-H}$ = 7.8, $-C_6H_4$Me), 7.88 (d, 4H,

$^3J_{H-H}$ = 7.8, $-C_6H_4$Me), 7.44 (m, 8H, $-C_6H_4$Me), 2.41 (s, 12H, $-C_6H_4$Me), 6.12 (t, 2H,

$^3J_{H-H}$ = 7.2, p-H), 5.96 (t, 4H, $^3J_{H-H}$ = 7.2, m-H), 2.83 (d, 4H, $^3J_{H-H}$ = 7.2, o-H). MS (CI)

Calcd (found) m/e: [(TTP)TiCl⁻], 751 (751); [(TTP)Ti(NPh₂)Cl–H⁻], 918 (918).

(TTP)Ti(=N-t-Bu) (9). (TTP)TiCl₂ (101 mg, 0.13 mmol) and LiNH-t-Bu (21 mg,

0.27 mmol) were dissolved in toluene (ca. 10 mL) to afford a deep red solution. After

5 min, the solution was filtered and the resultant deep red filtrate was taken to dryness under

reduced pressure to afford (TTP)Ti(=N-t-Bu) (95 mg, 0.12 mmol, 94% yield) as a

semicrystalline, purple solid. Analytically pure samples could be obtained by recrystallization

from toluene/hexane solution at -20 °C. UV-vis (toluene): 424 (Soret), 548 nm. ^{1}H NMR

(C₆D₆, 300 MHz): 9.24 (s, 8H, β-H), 8.32 (d, $^3J_{H-H}$ = 7.65 Hz, 4H, $-C_6H_4$Me), 8.04 (d,

$^3J_{H-H}$ = 7.05 Hz, 4H, $-C_6H_4$Me), 7.34 (d, J = 5.70 Hz, $-C_6H_4$Me), 7.30 (d, J = 5.70 Hz,

$-C_6H_4$Me), 2.42 (s, 12H, $-C_6H_4-CH_3$), -1.58 (s, 9H, ${}^tBu$). Anal. Calcd for $C_{52}H_{45}N_5Ti$: C,

79.28; H, 5.76; N, 8.89. Found: C, 79.34; H, 5.76; N, 8.75.

(TTP)Ti(=NPh) (10). (TTP)TiCl$_2$ (104 mg, 0.132 mmol) and LiNHPh (50 mg,

0.51 mmol) were dissolved in toluene (ca. 15 mL). The solution gradually turned a deep red

color. After 30 min, the solution was filtered to remove a black solid and the resultant ruby

filtrate was taken to dryness under reduced pressure. This afforded (TTP)Ti(=NPh) (94 mg,

0.12 mmol, 88% yield) as a purple solid. Analytically pure samples could be obtained by

recrystallization from toluene/hexanes at -20 °C. UV-vis (toluene): 426 (Soret), 548 nm.

^1H NMR (C_6D_6, 300 MHz): 9.21 (s, 8H, β-H), 8.14 (d, 4H, $-C_6H_4CH_3$), 8.03 (d, 4H,

$-C_6H_4CH_3$), 7.30 (d, 8H, $-C_6H_4CH_3$), 5.72 (m, 3H, m-, p-H), 3.85 (d, 2H, o-H), 2.41 (s,

12H, $-C_6H_4CH_3$). MS{EI} Calcd (found) (m/e): 806 (807), [M]$^-$. Anal. Calcd for

$C_{54}H_{41}N_5Ti$: C, 80.29; H, 5.12; N, 8.67. Found: C, 79.26; H, 5.48; N, 8.28.

(TTP)Ti(=NC$_6$H$_4$-p-Me) (11). (TTP)TiCl$_2$ (82 mg, 0.104 mmol) and LiNHC$_6$H$_4$Me

(45 mg, 0.40 mmol) were dissolved in toluene (ca. 15 mL) to produce a red solution. After

4 h, the solution was filtered and the resultant deep red filtrate was taken to dryness under

reduced pressure to afford (TTP)Ti(=NC$_6$H$_4$-p-Me) (74 mg, 0.09 mmol, 87% yield) as a

purple-red solid. Analytically pure samples could be obtained by recrystallization from

toluene/hexanes at -20 °C. UV-vis (toluene): 426 (Soret), 548 nm. ^1H NMR (C_6D_6,

300 MHz): 9.21 (s, 8H, β-H), 8.15 (d, 4H, $-C_6H_4CH_3$), 8.04 (d, 4H, $-C_6H_4CH_3$), 7.30 (d,

8H, $-C_6H_4CH_3$), 5.53 (d, 2H, m-H), 3.81 (d, 2H, o-H), 2.41 (s, 12H, $-C_6H_4CH_3$), 1.29 (s,

3H, -CH_3). Anal Calcd for C$_{55}$H$_{43}$N$_5$Ti: C, 80.36; H, 5.28; N, 8.52. Found: C, 80.29; H, 5.47; N, 8.20.

(TTP)Ti(=NTMS) (12). (TTP)Ti(η^2-EtC≡CEt) (105 mg, 0.132 mmol) was dissolved in toluene (ca. 10 mL) and neat N$_3$TMS (ca. 0.5 mL, ca. 4.0 mmol) was added to the rapidly stirred solution. Evolution of gas was observed and after 16 h, the solution was taken to dryness under reduced pressure to afford a dark oil. The oil was dissolved in a minimum of toluene (ca. 2 mL) and the solution was layered with hexanes (ca. 6 mL). After cooling the solution at -20 °C for 14 h, deep purple crystals formed. The crystals were collected by filtration and dried in vacuo to afford analytically pure (TTP)Ti(=NTMS) (40 mg, 0.050 mmol, 38% yield). UV-vis (toluene): 428 (Soret), 550 nm. ^{1}H NMR (C$_6$D$_6$, 300 MHz): 9.25 (s, 8H, β-H), 8.31 (d, $^3J_{H-H}$ = 9.0 Hz, 4H, -C$_6$H$_4$Me), 8.00 (d, $^3J_{H-H}$ = 9.0 Hz, 4H, -C$_6$H$_4$Me), 7.32 (m, 8H, -C$_6$H$_4$Me), 2.42 (s, 12H, -C$_6$H$_4$-CH_3), -2.04 (s, 9H, SiCH_3). Anal. Calcd for: C$_{51}$H$_{45}$N$_5$SiTi: C, 76.20; H, 5.64; N, 8.71. Found: C, 76.04; H, 5.99; N, 8.04.

Results

Synthesis and Properties of Bis(Alkoxide) Complexes. The titanium(IV) tetratolylporphyrinato complex (TTP)TiCl$_2$ (**1**) reacts readily with sodium phenoxide in toluene to afford the blue, bis(phenoxide) complex, (TTP)Ti(OPh)$_2$ (**2**) in moderate yield (eq 1). The (bis)alkoxide complexes, (TTP)Ti(OMe)$_2$ (**3**) and (TTP)Ti(O^{t}Bu)$_2$ (**4**), are obtained in an analogous fashion. Complexes **2** and **3** have also been prepared by the reaction of **1** with 2 equiv of the free alcohols in the presence of piperidine, which serves to

$$(TTP)TiCl_2 + 2\ NaOR \rightarrow (TTP)Ti(OR)_2 + 2\ NaCl \qquad (1)$$

$$[R = Ph\ (2),\ Me\ (3),\ ^tBu\ (4)]$$

scavenge the HCl byproduct. The ^1H NMR spectra of these complexes are consistent with

the alkoxide ligands being arranged in a trans geometry. In particular, the H_o and H_m

protons of the tolyl groups of the $[TTP]^{2-}$ ligand appear as two sharp sets of doublets.

These data indicate that the molecule possesses a mirror plane through the center of the

porphyrin and an approximate D_{4h} symmetry. In the ambient temperature ^1H NMR spectrum

of 2 in C_6D_6, the protons of the phenoxide ligands appear at 2.67 ppm (H_o) and 5.83 ppm

$(H_m$ and $H_p)$. The large upfield shift of these protons is representative of ligands above the

porphyrin plane. Similarly, a strong upfield shift is observed for the Me groups of the

methoxide ligands in 3.

In the solid state, complex 2 is inert and remains unchanged for more than four

months in air. The bis phenoxide is also stable to hydrolysis in solution with excess water

for more than one week. In contrast, exposure of a solution of the bis methoxide to air

results in instantaneous and quantitative conversion to the oxo complex (TTP)Ti=O.

Treatment of (TTP)Ti(OR)$_2$ (R = Me, ^tBu) with excess phenol cleanly produces

(TTP)Ti(OPh)$_2$ and ROH. In general, the spontaneous reaction involves the most basic

ligand becoming protonated. Thus, treatment of (TTP)Ti(OPh)$_2$ with 7.6 equiv MeOH

produces only 0.3 equiv of (TTP)Ti(OPh)(OMe) and 0.1 equiv of (TTP)Ti(OMe)$_2$.

In solution 2 has been found to engage readily in intermetal ligand exchange

reactions. Thus, treatment of 2 with one equiv of (TTP)TiCl$_2$ in toluene rapidly (ca. 10 min)

and quantitatively affords a new product, 6, in high yield. The ^{1}H NMR spectrum of 6

displays an aa'mm' pattern for the porphyrin tolyl protons. Thus, the porphyrin plane does

not serve as a mirror plane of symmetry in this new molecule. In addition, the porphyrin

tolyl ligands are not freely rotating about the C_{meso}-C_{ipso} bond on the NMR timescale.

Accordingly, this new complex is formulated as (TTP)Ti(OPh)Cl (6) (eq 2). Complex 6 is

also prepared by the reaction of (TTP)TiCl$_2$ with 1 equiv of NaOPh in toluene. The

monomethoxide complex, (TTP)Ti(OMe)Cl has also been synthesized by both these routes.

Interestingly the intermetal ligand redistribution reaction described in eq 2, unlike previously

reported exchanges for (TTP)Ti(IV) complexes, appears to be driven to completion. The

reverse process, disproportionation of (TTP)Ti(OPh)Cl (6) to (TTP)TiCl$_2$ and

(TTP)Ti(OPh)$_2$, has not been observed by either variable temperature ^{1}H NMR experiments

or UV-vis studies.

Alcohols are not sufficiently basic to displace both chloro ligands in (TTP)TiCl$_2$.

Instead an equilibrium is established for monoalkoxide formation as represented in eq 3.

$$(TTP)TiCl_2 + (TTP)Ti(OPh)_2 \rightarrow 2\ (TTP)Ti(OPh)Cl \tag{2}$$

$$(TTP)TiCl_2 + 2\ HOR \rightleftharpoons (TTP)Ti(OR)Cl + [H_2OR]^+ + Cl^- \tag{3}$$

In a mixture of 2.7 PhOH and (TTP)TiCl$_2$ in C$_6$D$_6$, the equilibrium lies far to the left. No

monophenoxide complex is detected by ^{1}H NMR. When 6.7 equiv of MeOH are added to

(TTP)TiCl$_2$ in C$_6$D$_6$, the equilibrium ratio of (TTP)Ti(OMe)Cl to (TTP)TiCl$_2$ is 0.37:1. With

the more basic *t*-butanol (5.8 equiv), the resulting ratio of (TTP)Ti(O^{t}Bu)Cl to (TTP)TiCl$_2$ is

6.2:1. Addition of an exogenous base drives the reaction completely to bisalkoxide

formation. Thus, injection of 3 equiv of piperidine into an equilibrated NMR tube containing

(TTP)TiCl$_2$ and *t*-butanol in C$_6$D$_6$ resulted in quantitative formation of (TTP)Ti(O^{t}Bu)$_2$.

Preparation of Bis(Amido) Complexes. Treatment of freshly prepared (TTP)TiCl$_2$

with ≥ 2 equiv of LiNPh$_2$ in hexanes results in the formation of the bis(amido) complex,

(TTP)Ti(NPh$_2$)$_2$ (5) in modest yield (eq 4). This reaction is very sensitive to solvent choice.

In our hands, 5 *could not be produced in pure fashion* employing toluene, benzene, THF or

$$(TTP)TiCl_2 + 2 \ LiNPh_2 \ \text{--} \ (TTP)Ti(NPh_2)_2 \ (5) + 2 \ LiCl \qquad (4)$$

CH$_2$Cl$_2$ as solvent. In these solvents, intractable paramagnetic (presumably Ti(III)) species

are formed. Another difficulty in preparing 5 is its extreme moisture-sensitivity. Complex 5

decomposes instantaneously in air to afford (TTP)Ti=O and free HNPh$_2$. Our attempts to

prepare other (bis)amido complexes have met with no success. Thus, the reaction of 1 with

LiNEt$_2$, LiNTMS$_2$, LiN(C$_6$H$_{11}$)$_2$, TMSNEt$_2$, or lithium tetrahydroquinolide, under similar

conditions employed to produce 5, lead only to intractable, paramagnetic products. Finally,

treatment of 5 with other secondary amines, such as HNEt$_2$, piperidine, *t*-BuNH$_2$, or 1,2,3,4-

tetrahydroquinoline, did not result in the production of any new (bis)amido transamination

products. These observations parallel those described for the alkoxide/alcohol system. The

equilibrium favors the complex bound to the least basic secondary amide.

Analogous to the bis(alkoxide) complexes discussed above, the diphenylamido

ligands in 5 are disposed in a trans fashion. Thus, 5 displays pseudo D_{4h} symmetry in the

ambient

temperature ^{1}H NMR spectrum. In C_6D_6, the resonances for phenyl groups of the NPh_2^-

ligands are shifted upfield [δ 6.17 (H_p), δ 6.05 (H_m) and δ 2.86 (H_o)] relative to the free

amine, again due to their proximity to the porphyrin ring current.

Like the bis(alkoxide) derivatives, the bis(amido) complex undergoes rapid ligand

redistribution upon treatment with 1 equiv of (TTP)TiCl$_2$ to afford the mono(amido)

complex, (TTP)Ti(NPh$_2$)Cl (8) (eq 5). Again, this reaction appears to be entirely

irreversible. Complex 8 can be prepared independently from treatment of 1 with 1 equiv of

LiNPh$_2$.

$$(TTP)Ti(NPh_2)_2 + (TTP)TiCl_2 \rightarrow 2\ (TTP)Ti(NPh_2)Cl \tag{5}$$

As is typical for early transition metal amido complexes, 5 undergoes rapid

alcoholysis with phenol to afford (TTP)Ti(OPh)$_2$ (2) (eq 6). Not surprisingly, this reaction is

irreversible. Complex 2 does not react with HNPh$_2$ to any observable extent. This behavior

is attributed to the acidity of phenol relative to diphenylamine. Correspondingly, water

rapidly converts (TTP)Ti(NPh$_2$)$_2$ to the oxo complex, (TTP)Ti=O.

$$(TTP)Ti(NPh_2)_2 + 2\ HOPh \rightarrow (TTP)Ti(OPh)_2 + 2\ HNPh_2 \tag{6}$$

Preparation of Imido Complexes. From Ti(IV) Species via α-Hydrogen

Abstraction. Treatment of (TTP)TiCl$_2$ with 2 equiv of LiNH-t-Bu in toluene results in the

formation of the imido derivative (TTP)Ti(=N-t-Bu) (9) (eq 7). This reaction is *extremely*

clean and proceeds quantitatively in C$_6$D$_6$ to afford 9 along with 1 equiv of t-butyl amine

(^{1}H NMR, Ph$_3$CH internal standard). The ^{1}H NMR spectrum (C$_6$D$_6$) of 9 reveals four

doublets assignable to the H$_o$, H$_o'$, H$_m$, and H$_m'$ resonances of the [TTP]$^{2-}$ ligand, indicating

the expected lack of a mirror plane of symmetry coincidental with the porphyrin plane. The

protons of the t-butyl group are shifted strongly upfield (δ -1.54 ppm), which as discussed

above, is diagnostic for axially bound ligands in porphyrin systems. Analogous preparations

have been employed to synthesize the series (TTP)Ti(=NR) [R = Ph (10), p-tolyl (11)] all of

which are obtained in high yield (eq 7). Attempts to prepare the parent imido complex by

treatment of 1 with LiNH$_2$ have, thus far, proved unsuccessful.

$$(TTP)TiCl_2 + 2\ LiNHR\ -\ (TTP)Ti(=NR) + H_2NR + 2\ LiCl \qquad (7)$$

$$[R = t\text{-Bu }(9),\ Ph\ (10),\ p\text{-tolyl }(11)]$$
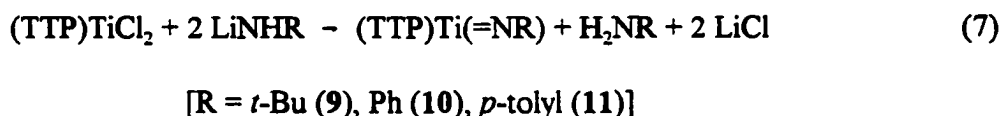
As noted above, with the secondary lithium amide, LiNPh$_2$, we can prepare the

monosubstituted amido complex, (TTP)Ti(NPh$_2$)Cl. However, with primary lithium amides

this is not possible. For example, treatment of 1 with one equiv of LiNH-t-Bu failed to

produce any (TTP)Ti(NH-t-Bu)Cl. Instead, this reaction led to the formation of a half equiv

of (TTP)Ti(=N-t-Bu) (9) and left an equimolar amount of unreacted 1 (eq 8). The reaction

of (TTP)Ti(NPh$_2$)Cl, a model complex for (TTP)Ti(NHR)Cl, with one equiv of LiNH-t-Bu

did not allow the isolation or observation of the mixed amido complex (TTP)Ti(NPh$_2$)(NH-

t-Bu). Instead, the only spectroscopically observable products at early times (~10 min) were

(TTP)Ti(=N-*t*-Bu), the bis(amido) complex (TTP)Ti(NPh$_2$)$_2$, formed in an approximate one-

to-one ratio along with free H$_2$N-*t*-Bu (eq 9). The bis(amido) complex apparently forms

from displaced NPh$_2$⁻ which undergoes metathesis with unreacted (TTP)Ti(NPh$_2$)Cl. After

long reaction times (> 10 h), the final products were (TTP)Ti=N-*t*-Bu and free HNPh$_2$ from

the subsequent reaction between (TTP)Ti(NPh$_2$)$_2$ and H$_2$N-*t*-Bu. This latter process was

confirmed independently. Treatment of (TTP)Ti(NPh$_2$)$_2$ with excess H$_2$N-*t*-Bu

quantitatively produced (TTP)Ti=N-*t*-Bu and HNPh$_2$ (eq 10).

$$\text{(TTP)TiCl}_2 + 1 \text{ LiNH-}t\text{-Bu} \ \rightarrow$$

$$\tfrac{1}{2} \text{(TTP)Ti(=N-}t\text{-Bu)} + \tfrac{1}{2} \text{(TTP)TiCl}_2 + \tfrac{1}{2} \text{H}_2\text{N-}t\text{-Bu} + \text{LiCl} \tag{8}$$

$$\text{(TTP)Ti(NPh}_2\text{)Cl} + 1 \text{ LiNH-}t\text{-Bu} \ \rightarrow$$

$$\text{(TTP)Ti(=N-}t\text{-Bu)} + \text{(TTP)Ti(NPh}_2\text{)}_2 + \text{H}_2\text{N-}t\text{-Bu} + \text{LiCl} \tag{9}$$

$$\text{(TTP)Ti(NPh}_2\text{)}_2 + \text{H}_2\text{N-}t\text{-Bu} \ \rightarrow \ \text{(TTP)Ti=N-}t\text{-Bu} + 2 \text{ NHPh}_2 \tag{10}$$
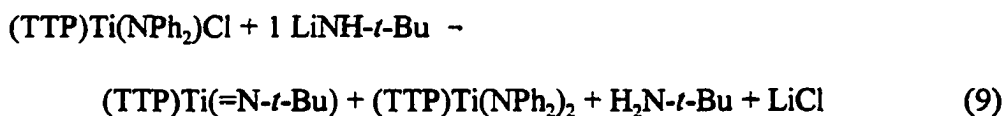
It has been previously reported that treatment of (TTP)TiCl$_2$ with excess aniline *does*

not produce the imido derivative, (TTP)Ti(=NPh) (10).[12] In accord with this earlier report,

we have confirmed that the arylimido complexes cannot be synthesized in this manner.

Thus, under similar conditions, 1 is unreactive towards *p*-toluidine. We have found,

however, that heating toluene solutions of 1 with excess t-butylamine produces

(TTP)Ti(=N-t-Bu) (9) in high yield along with [H_3N-t-Bu]Cl byproduct.

Imido Complexes Via Disproportionation of Ti(III). We have also found that

Ti(IV)-imido complexes can be produced from Ti(III)-precursor complexes. For example,

toluene solutions of (TTP)TiCl react instantaneously with LiNH-t-Bu in the presence of

PhC≡CPh to provide (TTP)Ti(=N-t-Bu) (9) and the known alkyne adduct,

(TTP)Ti(η^2-PhC≡CPh)[13a] in a one-to-one ratio (eq 11). Similarly, reaction of (TTP)TiCl

with 1 equiv of LiNH-t-Bu followed by the addition of excess pyridine affords 0.5 equiv of

the imido complex, 9, along with 0.5 equiv of (TTP)Ti(py)$_2$[12b] (eq 12). These

disproportionation reactions underscore the strong thermodynamic driving force for the

formation of these robust Ti(IV)-imido complexes.

(TTP)TiCl + LiNH-t-Bu + xs PhC≡CPh →

$\frac{1}{2}$ (TTP)Ti(=N-t-Bu) + $\frac{1}{2}$ (TTP)Ti(η^2-PhC≡CPh) + $\frac{1}{2}$ H_2N-t-Bu + LiCl   (11)

2 (TTP)TiCl + LiNH-t-Bu + xs py →

$\frac{1}{2}$ (TTP)Ti(=N-t-Bu) + $\frac{1}{2}$ (TTP)Ti(py)$_2$ + $\frac{1}{2}$ H_2N-t-Bu + LiCl   (12)
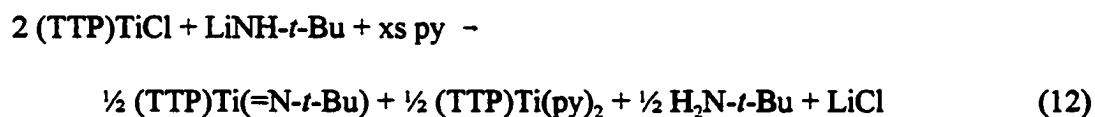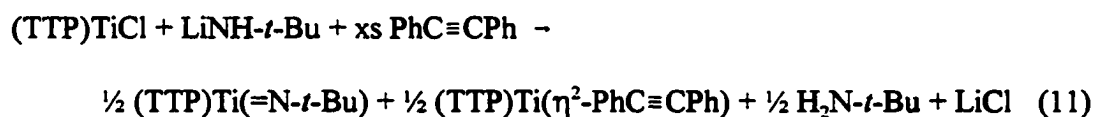
Imido Complexes Via Oxidation of Ti(II) Complexes. Imido complexes are

available from the oxidation of Ti(II) complexes with [NR]$^{2-}$ sources. For example, the

Ti(II) alkyne complex, (TTP)Ti(η^2-EtC≡CEt) reacts instantaneously with excess N_3TMS in

toluene to provide the imido complex (TTP)Ti(=NTMS) (12) and one equiv of free

EtC≡CEt (eq 13). Additionally, treatment of (TTP)Ti(η²-EtC≡CEt) with 0.5 equiv

PhN=NPh in refluxing toluene provides (TTP)Ti(=NPh) (10) as the sole porphyrin product

(eq 14).[14] Details of this reaction will be reported elsewhere.[15]

$$(TTP)Ti(\eta^2\text{-EtC≡CEt}) + xs\ N_3TMS \rightarrow (TTP)Ti(=NTMS) + EtC≡CEt + N_2 \qquad (13)$$

$$(TTP)Ti(\eta^2\text{-EtC≡CEt}) + 0.5\ PhN=NPh \rightarrow (TTP)Ti(=NPh) + EtC≡CEt \qquad (14)$$
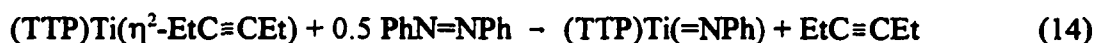
Reactivity of Ti-Imido Complexes. The imido complexes described above show

only limited reactivity. As expected, treatment of (TTP)Ti(=NR) complexes with alcohols

such as phenol and methanol results in the clean formation the (bis)alkoxide complexes, 2

and 3 respectively along with free amine. Unlike previously reported Ti-imido complexes,[16]

(TTP)Ti(=NR) complexes do not undergo exchange with primary amines. Thus treatment

of (TTP)Ti(=N-t-Bu) with aniline *does not* afford (TTP)Ti(=NPh) and free t-butyl amine.

The reverse reaction of (TTP)Ti(=NPh) with excess t-butyl amine also does not proceed to

any observable extent. We have previously shown that the oxo analogue, (TTP)Ti(=O)

rapidly undergoes incomplete oxygen atom transfer with (TTP)Ti(II) species to afford the

bridging Ti(III)-oxo dimer, [(TTP)Ti]₂(μ-O). In contrast, the imido complexes described

above do not react with (TTP)Ti(η²-EtC≡CEt) to afford the Ti(III) dimer, [(TTP)Ti]₂(μ-

NPh). This difference may be due to the steric problems presented by the imido substituents.

Discussion

The (TTP)Ti-fragment serves as a useful template for the study of a wide range of

metal-ligand multiple bonds. The series (TTP)Ti(=X) (X = O, S, Se, NR) is now firmly

established.[12] In the future, we hope to extend this interesting class of complexes to include

other metal-ligand multiply bonded species such as alkylidenes and phosphinidines. In order

to design rational syntheses of these complexes, we have attempted to elucidate the

mechanism by which the imido ligands are introduced via lithium amides. The formation of

imido complexes from 1 and LiNHR must involve α-hydrogen abstraction. Two possible

mechanisms are shown in Scheme 1. A concerted intramolecular elimination from the
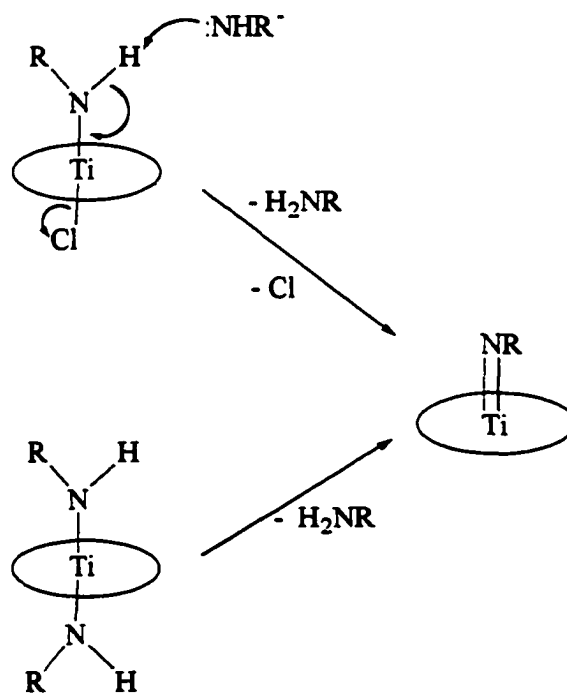
Scheme 1.

(bis)amido complex is unlikely given the known trans disposition of the amido ligands in

(TTP)Ti(NPh$_2$)$_2$ (5). A concerted bimolecular pathway in which 2 equiv of H$_2$NR are

simultaneously eliminated from two mol of (TTP)Ti(NHR)$_2$ is also implausible due to the

steric nature of the porphyrin ligands. Intermolecular deprotonation of an imido ligand by a

second equivalent of LiNHR is a reasonable alternative. Moreover, the strong π-donor

character of the amide ligand may facilitate the dissociation of the trans chloride and/or

increase the acidity of the α-proton (Scheme 2). This hypothesis is supported by reaction 8
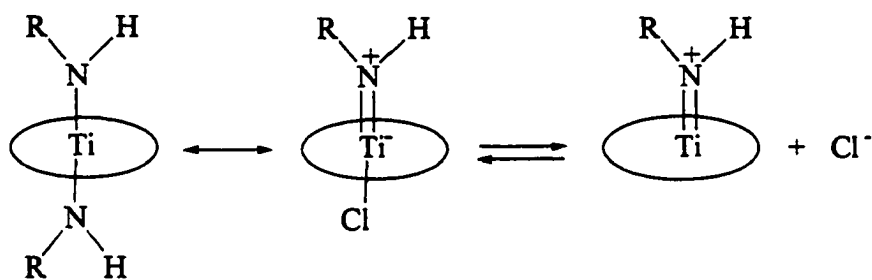
Scheme 2.

in which only (TTP)Ti(=N-t-Bu) was formed and no monoamido complex, (TTP)Ti(NH-t-

Bu)Cl, was observed on treating 1 with 1 equiv of LiNH-t-Bu. Additionally, since other

amide reagents (e.g. LiNEt$_2$) lead only to reduction of Ti(IV) to Ti(III), deprotonation of a

primary amide ligand appears to compete effectively with reduction processes. Moreover,

our inability to isolate or observe a primary amido complex is consistent with the high acidity

of the N–H proton of the complexed amido ligand.

The strong π-donor ability of the amido ligand also provides a rationale for reactions

5 and 8. In the ligand disproportionation (eq 5), the amido ligand prefers to be trans to a

weaker chloro ligand than trans to a second strong π-donor amido ligand. Correspondingly, treatment of (TTP)Ti(NPh$_2$)Cl with LiNH-t-Bu (eq 9) is likely to produce transiently the mixed amido complex (TTP)Ti(NPh$_2$)(NH-t-Bu). Competing π-donation serves to labilize both ligands. The loss of the primary amide is nonproductive. However, dissociation of NPh$_2^-$ produces [(TTP)Ti(NH-t-Bu)]$^+$ having an acidic α-hydrogen which is rapidly deprotonated to produce (TTP)Ti(=N-t-Bu).

To the best of our knowledge, the production of imido complexes from Ti(III) sources (reactions 11 and 12) is unprecedented. There are several scenarios one could envision to account for these reactions. It is important to note that (TTP)TiCl does not react with either diphenylacetylene or pyridine to produce (TTP)TiCl$_2$ and (TTP)Ti(η^2-Ph–C$\equiv$C–Ph) or (TTP)Ti(py)$_2$. Thus, (TTP)TiCl does not readily disproportionate. If the reaction of (TTP)TiCl with LiNH-t-Bu affords initially (TTP)Ti(NH-t-Bu), this species could undergo electron transfer (either in an inner or outer sphere sense) with a second Ti(III)-species to afford either (TTP)Ti(NH-t-Bu)X (X = NH-t-Bu or Cl) or [(TTP)Ti(NH-t-Bu)]$^-$ along with a Ti(II) complex (Scheme 3). The former complex could be deprotonated by an additional equiv of Li-amide to afford the imido complex while the latter complex is readily trapped by pyridine or diphenylacetylene. However, it is not clear why (TTP)Ti–NH-t-Bu would be more prone to disproportionation than (TTP)TiCl. However, based on the observations above, it appears that α-hydrogen abstraction occurs much more rapidly than reduction for Ti porphyrin complexes. Thus, we propose that any (TTP)Ti(NH-t-Bu) formed in the reaction is rapidly deprotonated to afford the transient Ti(III)-imido complex anion, [(TTP)Ti(=N-t-Bu)]$^-$. Due to its anionic charge,

Cl
|
Ti   + 2 LiNHR $\xrightarrow{\text{Ph-C≡C-Ph}}$ NR‖Ti   +   Ph—≡—Ph / Ti   + LiCl
                  toluene

                                    ↑ -H⁺   ↑ + PhC≡CPh
                                                       - Cl⁻

R\ /H   R\ /H ⁺
 N   Cl   N   Cl ⁻
 | | | |
 Ti   +   Ti   ⇌   Ti^IV   +   Ti^II
(inner or outer sphere electron transfer)
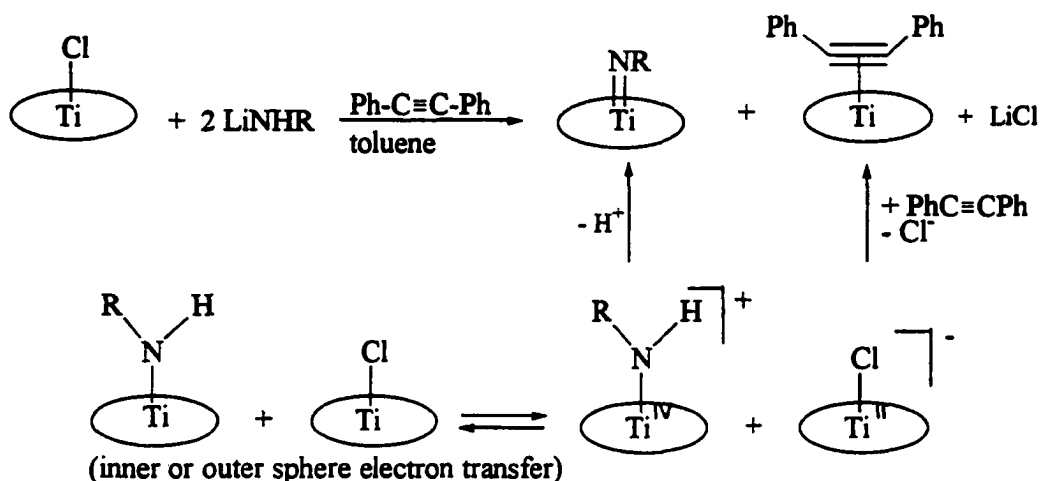
Scheme 3.

this Ti(III)-imido complex presumably is more capable of reducing (TTP)TiCl to Ti(II), which is subsequently trapped by either pyridine or diphenylacteylene.

Conclusion

In this work we have demonstrated that $(TTP)TiCl_2$, which is readily prepared from the reaction of $TiCl_4(THF)_2$ with $Li_2(THF)_2TTP$, serves as a useful precursor for the synthesis of a variety of Ti-porphyrin complexes possessing hard π-donor ligands. Prior to this work, the only reported complexes of this class of compounds are $(TPP)Ti(OMe)$,[17] and the η^2-catecolate, $(TTP)Ti(O_2C_6H_4)$.[18] We have shown that the Ti(IV)-(bis)alkoxides can be readily produced. Perhaps surprisingly, given the immense number of Ti-amido complexes known,[19] we have found the only isolable (bis)amido-porphyrin complex is $(TTP)Ti(NPh_2)_2$. The imido complexes, given the reactivity displayed by the oxo analogue (*vide supra*), are

perhaps of the greatest interest. Of particular interest, is the fact that (TTP)Ti(=NR) complexes may be isolated starting from Ti-porphyrin complexes in various oxidation states.

References

1. Reprinted with permission from *Inorganic Chemistry* **1997**, *36*, 278. Copyright 1997 American Chemical Society.

2. Presidential Young Investigator (1990–1995) and Camille and Henry Dreyfus Teacher–Scholar (1993–1998).

3. For a comprehensive review of transition metal imido complexes, see: Wigley, D. E., *Prog. Inorg. Chem.* **1994**, *42*, 239.

4. For examples in Ti-chemistry, see: (a) Cummins, C. C.; Schaller, C. P.; Van Duyne, G. D.; Wolczanski, P. T.; Chan, A. W. E.; Hoffmann, R. *J. Am. Chem. Soc.* **1991**, *113*, 2985. (b) Bennett, J. L.; Wolczanski, P. T. *J. Am. Chem. Soc.* **1994**, *116*, 2179. For examples in Zr chemistry, see: (c) Walsh, P. J.; Hollander, F. J.; Bergman, R. G. *J. Am. Chem. Soc.* **1988**, *110*, 8729. (d) Walsh, P. J.; Baranger, A. M.; Bergman, R. G. *J. Am. Chem. Soc.* **1992**, *114*, 1708. (e) Walsh, P. J.; Hollander, F. J.; Bergman, R. G. *Organometallics* **1993**, *12*, 3705. (f) Cummins, C. C.; Baxter, S. M.; Wolczanski, P. T. *J. Am. Chem. Soc.* **1988**, *110*, 8731.

5. (a) McGrane, P. L.; Livinghouse, T. *J. Org. Chem.* **1992**, *57*, 1323. (b) McGrane, P. L.; Jensen, M.; Livinghouse, T. *J. Am. Chem. Soc.* **1992**, *114*, 5459. (c) McGrane, P. L.; Livinghouse, T. *J. Am. Chem. Soc.* **1993**, *115*, 11485.

6. Berreau, L. M.; Young, V. G., Jr.; Woo, L. K. *Inorg. Chem.* **1995**, *34*, 527-529.

7. Woo, L. K.; Hayes, J. A.; Goll, J. G. *J. Inorg. Chem.* **1990**, *29*, 3916.

8. Ledon, H. J.; Varescan, F. *Inorg. Chem.* **1984**, *23*, 2735.

9. For examples of Zr-porphyrin-complexes with hard π-donors, see: (a) Brand, H.; Arnold, J. *J. Am. Chem. Soc.* **1992**, *114*, 2266. (b) Brand, H.; Arnold, J. *Organometallics* **1993**, *12*, 3655. For a review of recent advances in early transition metal porphyrin chemistry, see: Brand, H.; Arnold, J. *Coordination Chemistry Reviews* **1995**, *140*, 137 and references therein.

10. Berreau, L. M.; Hays, J. A.; Young, V. G., Jr.; Woo, L. K. *Inorg. Chem.* **1994**, *33*, 105-108.

11. Perrin, D. D.; Armagego, W. L. F.; Perrin, D. R. *Purification of Laboratory Chemicals*, *2nd Ed.*; Pergamon: New York, 1980.

12. Buchler, J. W.; Pfeifer, S. *Z. Naturforsch. B: Chem. Sci.* **1985**, *40B*, 1362.

13. (a) Woo, L. K.; Hays, J. A.; Jacobson, R. A.; Day, C. L. *Organometallics* **1991**, *10*, 2102. (b) Woo, L. K.; Hays, J. A.; Young, V. G., Jr.; Day, C. L.; Caron, C.; D'Souza, F.; Kadish, K. M. *Inorg. Chem.* **1993**, *32*, 4186.

14. For other examples of azobenzene cleavage leading to imido complexes in Ti-chemistry, see: (a) Hill, J. E.; Profilet, R. D.; Fanwick, P. E.; Rothwell, I. P. *Angew. Chem. Int. Ed. Engl.* **1990**, *29*, 664. (b) Duchateau, R.; Williams, A. J.; Gambarotta, S.; Chiang, M. Y. *Inorg. Chem.* **1991**, *30*, 4863.

15. Gray, S. D.; Woo, L. K. Unpublished results.

16. Collier, P. E.; Dunn, S. C.; Mountford, P.; Shishkin, O. V.; Swallow, D. *J. Chem. Soc., Dalton Trans.* **1995**, 3743.

17. Boreham, C. J.; Buisson, G.; Duee, E.; Jordanov, J.; Latour, J.-M.; Marchon, J.-C. *Inorg. Chim. Acta* **1983**, *70*, 77-82.

18. Marchon, J.-C.; Latour, J.-M.; Grand, A.; Belakhovsky, M.; Loos, M.; Goulon, J. *Inorg. Chem.* **1990**, *29*, 57-67.

19. Lappert, M. F.; Power, P. P.; Sanger, A. R.; Srivastava, R. C. *Metal and Metalloid Amides: Synthesis, Structures, and Physical and Chemical Properties*, John Wiley and Sons: New York, **1980**, Chap. 8, pp. 472-477.

CHAPTER 3: SYNTHESIS AND REACTIVITY OF HYDRAZIDO(2-)

DERIVATIVES OF TITANIUM(IV) TETRATOLYLPORPHYRIN

A paper to be submitted to Inorganic Chemistry

Joseph L. Thorman and L. Keith Woo*

Abstract

Titanium porphyrin hydrazido complexes $(TTP)Ti=NNR_2$ [TTP = *meso*-tetra-*p*-tolylporphyrinato dianion, R = Me, **1**; Ph, **2**] were synthesized by treatment of $(TTP)TiCl_2$ with 1,1-disubstituted hydrazines H_2NNR_2 (R = Me, Ph) in the presence of piperidine. The nucleophilic character of the hydrazido moiety is demonstrated in the reaction of complexes **1** and **2** with *p*-chlorobenzaldehyde which yield the titanium oxo complex $(TTP)Ti=O$ and the respective hydrazones. Protonation of complexes **1** and **2** with phenol or water produced the 1,1-disubstituted hydrazine along with $(TTP)Ti(OPh)_2$ or $(TTP)Ti=O$, respectively. Similar reactivity of *p*-chlorobenzaldehyde and phenol with $(TTP)Ti=N^iPr$, **3**, was observed. The reaction of complex **3** with nitrosobenzene cleanly forms the diazene compound, $^iPrN=NPh$, and the terminal oxo complex, $(TTP)Ti=O$.

Introduction

Research dedicated to early transition metal complexes possessing ligand-metal multiple bonds continues to develop. A substantial body of investigation concerning group

4 metals in this area has focused on the relatively electron-rich metallocene derivatives.[1,2]

From these studies, imido complexes have shown potential as aziridination, hydroamination, and heterocyclization catalysts. In comparison, the reactivity exhibited by the titanium imido functional group in porphyrin analogues is limited.[3] This lower reactivity is presumably due, in part, to steric factors involving the porphyrin ligand and the imido substituent.

Although the chemistry of imido complexes is now well established for groups 4-7, investigation of the isolobal hydrazido moiety has been confined mainly to groups 5-7.[4] Examples of group 4 hydrazido(2-) complexes are limited to a dimeric species [CpClTi=NNR$_2$]$_2$[5] and two monomeric complexes, Cp$_2$Ti=NN(TMS)$_2$[6] and (TMTAA)Ti=NNPh$_2$.[7] Titanium metalloporphyrin hydrazido(2-) complexes, (TTP)Ti=NNR$_2$, may offer an additional assessment of the reactivity of the Ti=N moiety, aided by the decreased steric bulk at the N$_\alpha$. As part of a continuing study of group 4 metalloporphyrin complexes containing terminal metal-nitrogen bonds, we report the synthesis of new examples of titanium hydrazido(2-) complexes.

Experimental

General. All manipulations were performed under an atmosphere of nitrogen using a Vacuum Atmospheres glovebox equipped with a Model MO40-1 Dri-Train gas purifier. All solvents were rigorously degassed and dried prior to use. Benzene-d_6, toluene, and hexane were freshly distilled from purple solutions of sodium benzophenone and brought into the drybox without exposure to air. Methylene chloride was dried by passage through a column of activated neutral alumina. Literature procedures were used to prepare

(TTP)Ti=N^{i}Pr,[8] 3, and (TTP)TiCl$_2$.[9] The latter compound was recrystallized from

CH$_2$Cl$_2$/hexane prior to use. 1,1-Dimethylhydrazine was purchased from Aldrich and dried

by passage over a column of activated neutral alumina. 1,1-Diphenylhydrazonium

hydrochloride was used as received from Aldrich . ^{1}H NMR data were recorded on either a

Varian VXR (300 MHz, 20 °C) or a Bruker DRX (400 MHz, 25 °C) spectrometer.

Chemical shifts were referenced to proton solvent impurities (δ 7.15, C$_6$D$_5$H). UV-vis data

were recorded on a HP8452A diode array spectrophotometer and reported as λ_{max} in nm

(log ϵ). Elemental analyses (C, H, N) were performed by Iowa State University Instrument

Services. MS-CI studies were performed on a Finnigan TSQ 700 at 70 eV in the negative

ion mode using ammonia as the ionization gas. GCMS studies were performed on a Varian

gas chromatograph coupled to an ITS 40 ion trap mass spectrometer (capillary column DB-

5MS).

(TTP)Ti=NNMe$_2$, 1. To a hexanes (ca. 20 mL) slurry of (TTP)TiCl$_2$ (257 mg,

0.326 mmol) was added piperidine (132 μL, 1.33 mmol) and H$_2$N$_2$Me$_2$ (30 μL, 0.388 mmol).

The blue solution was filtered after stirring 12 h at ambient temperature and the solid was

washed with hexanes (ca. 4 mL). This purple solid was divided into 3 approximately equal

portions and each placed on a clean fritted filter and washed with 2 mL of benzene. The

combined filtrates yielded dark blue (TTP)Ti=NNMe$_2$ (118 mg, 47 % yield) and a trace of

(TTP)Ti=O. ^{1}H NMR (C$_6$D$_6$, 300MHz): 9.16 (s, 8H, β-H), 8.20 (d, 4H, $^3J_{H-H}$ = 8 Hz, *meso-*

C$_6$*H*$_4$CH$_3$), 8.04 (d, 4H, $^3J_{H-H}$ = 8 Hz, *meso-*C$_6$*H*$_4$CH$_3$), 7.31 (t, 8H, $^3J_{H-H}$ = 8 Hz, *meso-*

C$_6$*H*$_4$CH$_3$), 2.42 (s, 12H, *meso-*C$_6$H$_4$C*H*$_3$), -0.28 (s, 6H, NN(C*H*$_3$)$_2$). UV/vis (toluene): 426

(5.65), 548 (4.64). The hydrolytic sensitivity of 1 precluded satisfactory elemental analysis.

(TTP)Ti=NNPh₂, 2. A mixture of $H_2N_2Ph_2\cdot HCl$ (234 mg, 1.06 mmol), piperidine

(173 μL, 1.75 mmol), and 4Å molecular sieves were stirred in hexanes (ca. 15 mL) overnight.

This mixture was filtered over a pad of activated neutral alumina and the filtrate added to

(TTP)TiCl₂ (154 mg, 0.196 mmol) and piperidine (ca. 2 mmol). This solution slowly turned

from red/brown in color to dark red over 13 h, at which time it was filtered and the solid

washed with hexanes (3 x 6 mL). The dark blue solid was placed on a clean fritted filter and

washed through with 2 mL benzene. The benzene was removed *in vacuo* to afford

analytically pure (TTP)Ti=NNPh₂ (40 mg, 23% yield). ^1H NMR (C_6D_6, 300MHz): 9.13 (s,

8H, β-H), 8.05 (d, 8H, $^3J_{H\text{-}H}$ = 8 Hz, *meso*-$C_6H_4CH_3$), 7.28 (d, 8H, $^3J_{H\text{-}H}$ = 8 Hz, *meso*-

$C_6H_4CH_3$), 6.31 (m, 6H, *m*-, *p*-NN(C_6H_5)₂, 4.34 (d, 4H, $^3J_{H\text{-}H}$ = 8 Hz, *o*-NN(C_6H_5)₂), 2.41(s,

12H, *meso*-$C_6H_4CH_3$). MS Calcd (found): [M⁺] 898.95 (898.3) m/z. Anal. Calcd (found)

for $C_{60}H_{46}N_6Ti$: C, 80.17 (79.97); H, 5.16 (5.24); N, 9.35 (8.49). UV/vis (toluene): 426

(5.61), 547 (4.69).

Reaction (TTP)Ti=NNMe₂ with *p*-chlorobenzaldehyde. An NMR tube was

charged with complex 1 (12.8 mg, 9.90 μmol), *p*-chlorobenzaldehyde stock solution (7.0

μL, 1.726 M, 12.1 μmol), Ph₃CH (89.0 μL, 0.1814 M, 16.14 μmol) as an internal standard,

and CD₂Cl₂ (ca. 0.5 mL). After allowing the mixture to stand overnight at ambient

temperature, (TTP)Ti=O (9.43 μmol, 95%) and the hydrazone[10] (7.74 μmol, 82%) were

detected. GCMS (*p*-chlorobenzaldehyde N,N-dimethylhydrazone): Calcd (found): [M⁺]

182.65 (182) m/z.

Reaction (TTP)Ti=NNPh₂ with *p*-chlorobenzaldehyde. An NMR tube was

charged with complex 2 (4.95mg, 5.51μmol), *p*-chlorobenzaldehyde stock solution (4.2 μL,

1.726 M, 7.25 μmol), Ph₃CH (92.6 μL, 0.1814 M, 16.78 μmol) as an internal standard, and

C₆D₆ (ca. 0.6 mL). The mixture was allowed to stand at ambient temperature for 180 h at

which time (TTP)Ti=O (5.23 μmol, 95%) was observed. The hydrazone[11] could not be

quantified due to the interfering internal standard and porphyrin signals. GCMS of p-

chlorobenzaldehyde N,N-diphenylhydrazone Calcd. (found): [M⁺] 306.79 (307) m/z.

Reaction (TTP)Ti=N'Pr with p-chlorobenzaldehyde. An NMR tube was charged

with complex 3, (TTP)Ti=N'Pr, (6.8 mg, 8.76 μmol), p-chlorobenzaldehyde (3.8 mg, 27

μmol), Ph₃CH (93.5 μL, 0.1743 M, 16.30 μmol) as an internal standard, and CDCl₃ (ca. 0.6

mL). Allowing the tube to stand at ambient temperature for 20 h produced (TTP)Ti=O

(8.94 μmol, 102 %) and the 'PrN=CH(C₆H₄-p-Cl) (8.98 μmol, 103 %). GCMS of p-

chlorobenzylidene isopropylamine Calcd (found): [M⁺] 181.66 (182) m/z. ¹H NMR

(CDCl₃): 8.25 (s, 1H, N*H*), 7.65 (d, 2H, ClC₆*H₄*), 7.36 (d, 2H, ClC₆*H₄*), 3.54 (m, 1H,

NC*H*(Me)₂), 1.26 (d, 6H, NCH(*Me*)₂).

Reaction (TTP)Ti=NNMe₂ with phenol. An NMR tube was charged with complex

1 (7.3 mg, 9.43 μmol), phenol (16 μL, 1.23 M, 19.68 μmol), Ph₃CH (96.0 μL, 0.1743 M,

16.73 μmol) as an internal standard, and C₆D₆ (ca. 0.6mL). Complex 1 was consumed

within approximately five minutes to produce (TTP)Ti(OPh)₂ (9.48 μmol, 101%) and 1,1-

dimethylhydrazine (9.83 μmol, 104%).

Reaction (TTP)Ti=NNPh₂ with phenol. An NMR tube was charged with complex

2 (6.63 mg, 7.37 μmol), PhOH (16.2 μL, 1.23 M, 19.9 μmol), Ph₃CH (92.0 μL, 0.1743 M,

16.04 μmol) as an internal standard, and C₆D₆ (ca. 0.6 mL). Complex 2 was consumed

within approximately five minutes to produce (TTP)Ti(OPh)₂ (7.11 μmol, 96%) and 1,1-

diphenylhydrazine (7.82 μmol, 106%).

Reaction (TTP)Ti=N^{i}Pr with phenol. An NMR tube was charged with imido

complex **3** (1.4 mg, 1.81 μmol), PhOH (3.6 μL, 1.23 M, 4.43 μmol), Ph₃CH (89.0 μL,

0.1448 M, 12.89 μmol) as an internal standard, and C₆D₆ (ca. 0.6 mL). Allowing the

solution to stand at ambient temperature for 21 h produced (TTP)Ti(OPh)₂ (1.68 μmol, 93

%).

Reaction (TTP)Ti=NNMe₂ with water. An NMR tube was charged with complex

1 (2.61 mg, 3.37 μmol), H₂O (0.4 μL, 22 μmol), Ph₃CH (54.0 μL, 0.1743 M, 9.41 μmol) as

an internal standard, and C₆D₆ (ca. 0.6 mL). Complex **1** was consumed within

approximately five minutes to produce (TTP)Ti=O (3.48 μmol, 103%) and 1,1-

dimethylhydrazine (3.34 μmol, 99%).

Reaction (TTP)Ti=NNPh₂ with water. An NMR tube was charged with complex

2 (8.54 mg, 9.50 μmol), H₂O (0.4 μL, 22 μmol), Ph₃CH (50.0 μL, 0.1743 M, 8.72 μmol) as

an internal standard, and C₆D₆ (ca. 0.6 mL). After allowing the tube to stand at ambient

temperature for 44 h (TTP)Ti=O (9.44 μmol, 99%) was detected by ¹H NMR. The free

hydrazine was not quantified due to decomposition.

Reaction of (TTP)Ti=N^{i}Pr with nitrosobenzene. An NMR tube was charged with

(TTP)Ti=N^{i}Pr (4.61 mg, 5.96 μmol), PhNO (0.8 mg, 7.47 mmol), Ph₃CH (91.0 μL, 0.1448

M, 13.18 μmol) as an internal standard, and C₆D₆ (ca. 0.6 mL). After approximately five

minutes at ambient temperature quantitative production of (TTP)Ti=O and PhN=N^{i}Pr[12] was

observed. GCMS of PhN=N^{i}Pr Calcd. (found): [M⁺] 148.21(149) m/z. ¹H NMR PhN=N^{i}Pr

(CDCl₃): 7.35 (t, 2H, *m-Ph*NN^{i}Pr), 7.19 (t, 1H, *p-Ph*NN^{i}Pr), 6.68 (d, 1H, *o-Ph*NN^{i}Pr), 3.88

(spt, 1H, PhNN^{i}Pr), 1.24 (d, 6H, PhNN^{i}Pr).

Results and Discussion

Synthesis and properties of hydrazido(2-) complexes. Treatment of the dichloro

complex, (TTP)TiCl$_2$, with a 1,1-disubstituted hydrazine in hexanes in the presence of a base

affords the hydrazido complexes (TTP)Ti=NNR$_2$ (R = Me, **1**; Ph, **2**) (eq 1). In the absence

$$\begin{array}{c}
\text{Cl} \\
| \\
\boxed{\text{Ti}} \\
| \\
\text{Cl}
\end{array}
+
\begin{array}{c}
\text{R} \quad \text{R} \\
\diagdown \text{N} \diagup \\
| \\
\text{N} \\
\diagup \diagdown \\
\text{H} \quad \text{H}
\end{array}
+ \; 2 \text{ piperidine} \quad \longrightarrow \quad
\begin{array}{c}
\text{NNR}_2 \\
\| \\
\boxed{\text{Ti}}
\end{array}
+ \; 2 \text{ piperidine} \bullet \text{HCl} \quad (1)$$
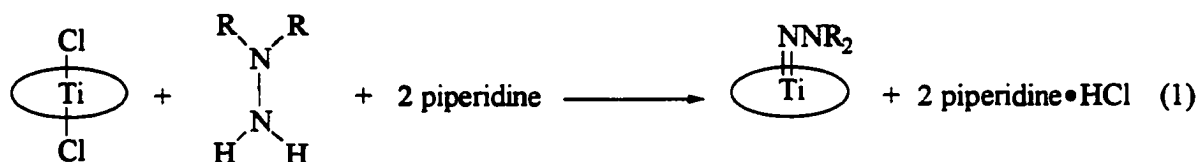
of a base, a 1:1 ratio of the hydrazido complex, **1**, and the 1,1-dimethylhydrazonium salt is

observed in the ^{1}H NMR spectrum of the reaction mixture. It was not possible to cleanly

separate the two products in large scale reactions. When bases such as triethylamine,

picoline, pyridine, 1,2,3,4-tetrahydroquinoline, and 2,2,6,6-tetramethylpiperidine were used,

the solubilities of the hydrazido complexes and the ammonium salts were similar and

impeded purification. Piperidine was found to be an adequate, but not ideal base as

separating the piperidinium salt from the product still proved difficult and resulted in modest

isolated yields (20-50 %) of the hydrazido complexes. Alternate routes, such as the use of

LiNHNR$_2$ or H$_2$N$_2$R$_2$ in the presence of Li^{n}Bu as well as other reaction solvents, led only to

intractable, paramagnetic products. Attempted synthesis of a diazenoid species from 1,2-

diphenylhydrazine in the presence of piperidine also led to intractable paramagnetic

products. Although complex **2** is robust in solution at elevated temperatures (ca. 350 K),

complex **1** is not and decomposed to paramagnetic species, as indicated by ^{1}H NMR

spectroscopy.

Due to the large ring current of the porphyrin macrocycle, the ^{1}H NMR resonances

associated with the substituents on the bound hydrazido ligand are significantly shifted

upfield relative to the hydrazine. For complex 1, the methyl resonance is shifted upfield

approximately 2.5 ppm from that of the free hydrazine. The phenyl signals for complex 2 are

similarly shifted upfield. For example, the o-NNPh_2 proton doublet found for 2 (4.34 ppm)

is shifted upfield from the free hydrazine (7.11 ppm). The ^{1}H NMR spectra show that the

substituents on the hydrazido(2-) moiety are equivalent on the NMR time scale (223-300 K).

This observation supports the formulation of the hydrazido(2-) unit as an η^1-bound ligand.

In the presence of water or phenol, both complexes 1 and 2 undergo metathesis to

form (TTP)Ti=O or (TTP)Ti(OPh)$_2$, respectively, and the appropriate 1,1-disubstituted

hydrazine (eq 2, 3).[13] As is generally the case for hydrazido complexes, N-N bond

$$
\underset{\text{R = Me, Ph}}{\overset{\text{NNR}_2}{\underset{\text{Ti}}{\bigcirc\!\!\!\!\parallel}}} \quad + \quad 2\,H_2O \quad \longrightarrow \quad \overset{O}{\underset{\text{Ti}}{\bigcirc\!\!\!\!\parallel}} \quad + \quad H_2N_2R_2 \tag{2}
$$

R = Me, Ph

$$
\underset{\text{R = Me, Ph}}{\overset{\text{NNR}_2}{\underset{\text{Ti}}{\bigcirc\!\!\!\!\parallel}}} \quad + \quad 2\,HOPh \quad \longrightarrow \quad \underset{\text{OPh}}{\overset{\text{OPh}}{\underset{\text{Ti}}{\bigcirc}}} \quad + \quad H_2N_2R_2 \tag{3}
$$
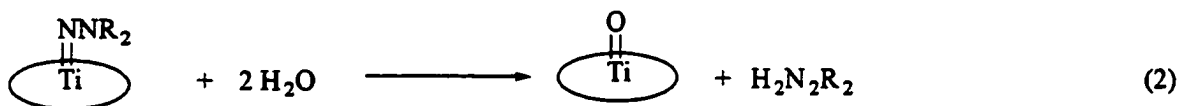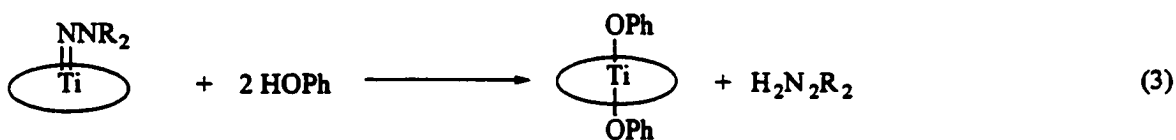
R = Me, Ph

cleavage was not observed in these hydrolysis reactions.[14] The extreme hydrolytic

susceptibility of complex 1 precluded a satisfactory elemental analysis while complex 3 was

found to be somewhat more inert. In the presence of approximately one equivalent of

phenol, a 1:1 mixture of the bis(phenoxide), $(TTP)Ti(OPh)_2$, and unreacted hydrazido, complex 2, were present. This finding may be attributed to the basic behavior of the hydrazido(1-) moiety, $NHNPh_2^-$, or a trans influence of the phenoxide as has been exhibited before with mixed alkoxido complexes, $(TTP)Ti(OR)(OR')$.[13b]

Exchange of the NNR_2 group was not observed upon treatment of $(TTP)Ti=NNR_2$ with free hydrazine $H_2N_2R'_2$ (R = Me, R' = Ph; R = Ph, R' = Me). In accord with acid/base considerations, the protonation of complexes 1 and 2 was not detected in the presence of excess $HNPh_2$ or H_2NPh. The potentially direct route to complexes 1 and 2 by treatment of the imido compound, 3, with the respective hydrazine was unproductive. The hydrazido and imido complexes were only minor components in an otherwise intractable mixture of products.

Treatment of complexes 1 or 2 with approximately 1 equivalent of p-chlorobenzaldehyde slowly produced the hydrazone, p-Cl-C_6H_4C(NNR_2)H (R = Me, Ph), and $(TTP)Ti=O$ in nearly quantitative yield as monitored by ^1H NMR spectroscopy (eq 4).

(4)
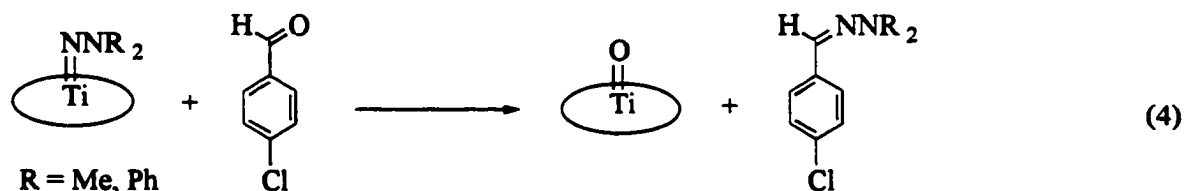
Reactions with a larger ratio of the aldehyde to hydrazido complex proceed to completion over a shorter period of time. The reaction rate of the diphenylhydrazido complex 2 with aldehyde is qualitatively slower than that of the dimethyl analogue 1. This is consistent with a less nucleophilic N_α of the hydrazido moiety in complex 2.

Reactivity of (TTP)Ti=N^{i}Pr. Although (TTP)Ti=N^{i}Pr, **3**, did not undergo nitrene

transfer in the presence of a variety of substrates such as OPR$_3$, OAsPh$_3$, RNCNR, and

R$_2$CO, it will undergo nitrene metathesis reactions with nitroso compounds. Facile and

quantitative production of the unsymmetric diazene compound PhN=N^{i}Pr results from

reaction of complex **3** with nitrosobenzene (eq 5). Low-valent titanium complexes have

$$\underset{Ti}{\overset{N^iPr}{\|}} \quad + \quad PhNO \quad \longrightarrow \quad \underset{Ti}{\overset{O}{\|}} \quad + \quad PhN=N^iPr \tag{5}$$
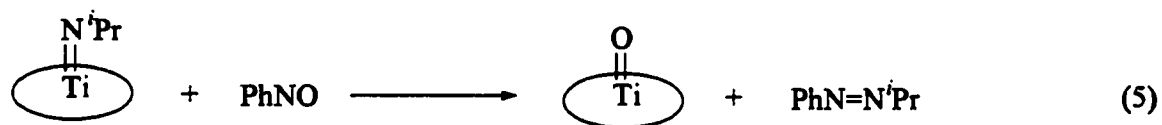
been found to mediate the coupling of nitrene groups derived from nitroso compounds.[15,16]

It was proposed that these reactions progressed through two different bimetallic

intermediates in order to explain the presence of azo- and azoxy-coupling products. In the

case presented here we conclude that the diazene product is the result of a monomeric

intermediate in which the nitrosobenzene is bound to the titanium *cis* to the imido group.

The nucleophilic character of nitrene groups has often been displayed by reaction with

aldehydes.[17] Likewise, reaction of complex **3** with excess *p*-chlorobenzaldehyde at 20°C

produced (TTP)Ti=O and *p*-chlorobenzylidene isopropylamine in 20 hours. In the presence

of only one equivalent of aldehyde, complete consumption of the imido complex required

approximately four weeks.

Conclusion

The (TTP)Ti=NNR$_2$ complexes have been investigated in an effort to further

elucidate the reactivity of the titanium-nitrogen double bond found in metalloporphyrin

complexes. The hydrazido complexes exhibited similar behavior to that of the imido species

(TTP)Ti=N'Pr in the presence of protic reagents. Nitrene group transfer from the titanium

imido complex, (TTP)Ti=N'Pr, is facilitated by treatment with p-chlorobenzaldehyde or

nitrosobenzene to yield the respective imine or diazene. The hydrazido derivatives also

undergo reaction with p-chlorobenzaldehyde to form the subsequent hydrazone. These

results show that by reducing the steric constraint at the N_α of the nitrene group, the

metalloporphyrin Ti=N moiety exhibits moderate nucleophilic reactivity.

References

1.   Leading references concerning terminal chalcogenido complexes: (a) Trnka, T. M.; Parkin, G. *Polyhedron*, **1997**, *16*, 1031. (b) Nugent, W. A.; Mayer, J. M. *Metal-Ligand Multiple Bonds*. Wiley-Interscience, New York, 1988.

2.   (a) Housemekerides, C. H.; Ramage, D. L.; Kretz, C. M.; Shontz, J. T.; Pilato, R. S.; Geoffroy, G .L; Rheingold, A. L.; Haggerty, B. S. *Inorg. Chem.* **1992**, *31*, 4453. (b) Doxsee, K. M.; Farah, J. B.; Hope, H. *J. Am. Chem. Soc.* **1991**, *113*, 8889.

3.   (a) Gray, S. D.; Thorman, J. L.; Adamian, V.; Kadish, K. M.; Woo, L. K. *Inorg. Chem.* **1998**, *37*, 1. (b) Berreau, L. M.; Young, V. G., Jr.; Woo, L. K. *Inorg. Chem.* **1995**, *34*, 527.

4.   (a) Kahlal, S. Saillard, J. Y.; Hamon, J. R.; Manzur, C.; Carrillo, D. *J. Chem. Soc., Dalton Trans.* **1998**, 1229. (b) Green, M. L. H.; James, J. T.; Chernega, A. N. *J. Chem. Soc., Dalton Trans.* **1997**, 1719. (c) For a review of organometallic diazo compounds: Sutton, D. *Chem. Rev.* **1993**, *93*, 995.

5.   Hughes, D. L.; Latham, I. A.; Leigh, G. J. *J. Chem. Soc., Dalton Trans.* **1986**, 393.

6.   N. Wiberg, Haring, H. W., Huttner, G., Friedrich, P. *Chem. Ber.* **1978**, *111*, 2708.

7.   Blake, A. J.; McInnes, J. M.; Mountford, P.; Nikonov, G. I.; Swallow, D.; Watkin, D. J. *J. Chem. Soc., Dalton Trans.* **1999**, 379.

8.   Thorman, J. L.; Young, V. G., Jr.; Woo, L. K. Manuscript in preparation.

9. Berreau, L. M.; Hays, J. A.; Young, V. G., Jr.; Woo, L. K. *Inorg. Chem.* **1994**, *33*, 105.

10. ^{1}H NMR of an authentic sample of *p*-chlorobenzaldehyde N,N-dimethylhydrazone: (CD$_2$Cl$_2$, 300 MHz): 7.48 (d, 2H, p-ClC$_6$$H_4$C(H)NNMe$_2$), 7.28 (d, 2H, p-ClC$_6$$H_4$C(H)NNMe$_2$), 7.15 (s, 1H, p-ClC$_6H_4$C(*H*)NNMe$_2$), 2.95 (s, 6H, p-ClC$_6H_4$C(H)NN*Me*$_2$): Wiley, R. H.; Slaymaker, S. C.; Kraus, H. *J. Org. Chem.* **1957**, *22*, 204.

11. Kamitori, Y.; Hojo, M.; Masuda, R.; Fujitani, T.; Ohara, S.; Yokoyama, T. *J. Org. Chem.* **1988**, *53*, 129.

12. Seyhan, N. E.; Sharp, R.R. *J. Chem. Soc. B* **1971**, 2014.

13. (a) Fournari, C.; Guilard, R.; Fontesse, M.; Latour, J.-M.; Marchon, J.-C. *J. Organomet. Chem.* **1976**, *110*, 205. (b) Gray, S. D.; Thorman, J. L.; Berreau, L. M.; Woo, L. K. *Inorg. Chem.* **1997**, *36*, 278.

14. For exceptions see Niemoth-Anderson, J. D.; Debord, J. R. D.; George, T. A.; Ross, C. R.; Stezowski, J. J. *Polyhedron* **1996**, *15*, 4031. and reference therein.

15. The chemistry of nitrosobenzene has been reveiwed: Zuman, P.; Shah, B. *Chem Rev.* **1994**, *94*, 1621.

16. Fochi, G.; Floriani, C. *J. Chem. Soc., Dalton Trans.* **1984**, 2577.

17. Arndtsen, B. A.; Sleiman, H. F.; Chang, A. K.; McElwee-White, L. *J. Am. Chem. Soc.* **1991**, *113*, 4871 and references therein.

CHAPTER 4: ATOM TRANSFER REACTIONS OF (TTP)Ti(η^2-3-HEXYNE):

SYNTHESIS AND MOLECULAR STRUCTURE OF *TRANS*-(TTP)Ti[OP(Oct)₃]₂

A paper to be submitted to Inorganic Chemistry

Joseph L. Thorman, Victor G. Young, Jr.[‡] and L. Keith Woo[*]

Abstract

Atom and group transfer reactions were found to occur between heterocumulenes and (TTP)Ti(η^2-3-hexyne), 1, (TTP = *meso*-5,10,15,20-tetra-*p*-tolylporphyrinato dianion). The imido derivatives (TTP)Ti=NR (R = ^{i}Pr, 2; ^{t}Bu, 3) were produced upon treatment of complex 1 with ^{i}PrN=C=N^{i}Pr, ^{i}PrNCO, or ^{t}BuNCO. Reaction between complex 1 and CS₂, ^{t}BuNCS, or ^{t}BuNCSe afforded the chalcogenido complexes, (TTP)Ti=Ch (Ch = Se, 4; S, 5). Treatment of complex 1 with 2 equivalents of PEt₃ yielded the bis(phosphine) complex, (TTP)Ti(PEt₃)₂, 6. Although (TTP)Ti(η^2-3-hexyne) readily abstracts oxygen from epoxides and sulfoxides, the reaction between 1 and O=P(Oct)₃ did not result in oxygen atom transfer. Instead, the paramagnetic titanium(II) derivative (TTP)Ti[OP(Oct)₃]₂, 7, was formed. The molecular structure of complex 7 was determined by single-crystal X-ray diffraction: Ti-O distance 2.080(2) Å, Ti-O-P angle of 138.43(10)°. Estimates of Ti=O, Ti=S, Ti=Se, and Ti=NR bond strengths are discussed.

Introduction

New insight concerning atom transfer reactions have emerged in the past few years. However, relatively few systematic studies involving transfer of multivalent atoms or groups to transition metal compounds have been conducted due to the lack of suitable, well-behaved low-valent metal acceptor complexes. An exemplary case was reported by Mayer involving oxidative addition and group transfer reactions with $WCl_2(PMePh_2)_4$.[1] From this study the W=O bond strength was estimated to be $\geq$ 138 kcal/mol. Similarly, rhenium-oxygen bond strengths have also been addressed.[2] In related group 4 transition metal complexes the large free energy barrier to oxygen atom abstraction from titanium(IV) oxo complexes is well known.[3] Consequently Ti^{2+} is an effective reducing agent and atom transfer acceptor. This was recently demonstrated in a previous study of Ti(II), where $(TTP)Ti(\eta^2\text{-3-hexyne})$, 1, was able to abstract oxygen and sulfur from a number of substrates.[4] This reactivity is unique and has not been reported for other divalent titanium compounds.[5] In this report, further chemistry of Ti(II) is described. Using new atom transfer reactions, estimates for the Ti=X multiple bond strengths are derived.

Experimental

General Procedures. All manipulations were performed under an inert atmosphere of nitrogen using a Vacuum Atmospheres glovebox equipped with a Model MO-40M Dri-Train gas purifier. Benzene-d_6, toluene, and hexane were freshly distilled from purple solutions of sodium benzophenone and brought into the glovebox without exposure to air. $(TTP)Ti(\eta^2\text{-3-hexyne})^{5c}$ and $^tBuNCSe^6$ were prepared according to published procedures.

Compounds ⁱBuNCO and ⁱBuNCS were purchased from Aldrich, vacuum distilled, and dried

by passage through a column of activated, neutral alumina. CS_2 was purchased from Fisher

Scientific, vacuum distilled, and dried over molecular sieves. The magnetization of **2** was

measured at a field of 3 Tesla over the range 6 - 296 K on a Quantum Design MPMS

SQUID magnetometer. Corrections for the diamagnetic molar susceptibility were

implemented for the porphyrin (-731 x 10^{-6} cgs/mol)[7] and O=P(Oct)₃ (-302.7 x 10^{-6}

cgs/mol).[8] ¹H NMR data were recorded on either a Varian VXR (300 MHz, 20°C) or

Bruker DRX (400 MHz, 25°C) spectrometer. Chemical shifts were referenced to proton

solvent impurities (δ 7.15 ppm, C_6D_5H). UV-vis data were recorded on a HP8452A diode

array spectrophotometer and reported as λ_{max} in nm (log ε). Elemental analyses were

performed by Iowa State University Instrument Services.

(TTP)Ti=NⁱPr, 2. Method A. Isopropylisocyanate (44 μL, 0.448 mmol) was

added to a stirred solution of **1** (304 mg, 0.380 mmol) in toluene (ca. 10 mL). After 1 h at

ambient temperature the dark blue solution was filtered and the filtrate reduced to dryness *in*

vacuo. Recrystallization at -25°C for one day from a toluene solution (8 mL) layered with

heptane (4 mL) afforded analytically pure product (128 mg, 44% yield). UV/vis (toluene):

549 (4.53), 424 (5.57), 399 (shoulder, 4.70). ¹H NMR (C_6D_6, 400 MHz): 9.24 (s, 12H, *β*-

pyrrole), 8.27 (d, 4H, *meso*-C₆H_4CH₃), 8.05 (d, 4H, *meso*-C₆H_4CH₃), 7.31 (t, 8H, *meso*-

C₆H_4CH₃), 2.42 (s, 12H, *meso*-C₆H₄CH_3), -0.45 (m, 1H, -NCHMe₂), -1.66 (d, 6H, -

NCHMe_2). Anal. Calcd. for $C_{51}H_{43}N_5Ti$: C, 79.16; H, 5.60; N, 9.05. Found: C, 78.72 ; H,

5.67 ; N, 8.73. **Method B.** An NMR tube equipped with a teflon stopcock was charged

with complex **1** (14.3 mg, 17.8 μmol), Ph₃CH (89.5 μL of 0.1455 M in C_6D_6, 13.0 μmol),

^{i}PrN=C=N^{i}Pr (3.2 µL, 20.4 µmol), and C$_6$D$_6$ (ca. 0.6 mL). The solution immediately

darkened and the imido complex (TTP)Ti=N^{i}Pr (14.2 µmol, 79% yield) had formed over 12

h at ambient temperature. ^{1}H NMR (C$_6$D$_6$, 300MHz): ^{i}PrNC: 2.84 (spt, 1H), 0.65 (d, 6H).

The ^{1}H NMR spectrum of (TTP)Ti=N^{i}Pr was identical to that reported in Method A.

Reaction of complex 1 with ^{i}PrNCO. An NMR tube equipped with a teflon

stopcock was charged with complex 1 (13.1 mg, 16.4 µmol), Ph$_3$CH (92.0 µL, 0.146 M,

13.4 µmol), ^{i}PrNCO (2.60 µL, 26.5 µmol), and C$_6$D$_6$ (ca. 0.6 mL). Within 5 minutes

(TTP)Ti=N^{i}Pr (16.6 µmol, 100 % yield) was produced. ^{1}H NMR (C$_6$D$_6$, 300MHz):

(TTP)Ti=N^{i}Pr: 9.24 (s, 12H, β-pyrrole), 8.27 (d, 4H, *meso*-C$_6$H$_4$CH$_3$), 8.05 (d, 4H, *meso*-

C$_6$H$_4$CH$_3$), 7.31 (t, 8H, *meso*-C$_6$H$_4$CH$_3$), 2.42 (s, 12H, *meso*-C$_6$H$_4$CH$_3$), -0.45 (m, 1H, -

NCHMe$_2$), -1.66 (d, 6H, -NCHMe$_2$).

Reaction of complex 1 with ^{t}BuNCO. An NMR tube equipped with a teflon

stopcock was charged with complex 1 (5.93 mg, 7.43 µmol), Ph$_3$CH (84.0 µL, 0.181 M,

15.2 µmol), ^{t}BuNCO (1.2 µL, 10.5 µmol), and C$_6$D$_6$ (ca. 0.6 mL). Within 5 minutes

(TTP)Ti=N^{t}Bu was produced in 48% yield. Allowing the solution to stand at 25°C for 16 h

produced (TTP)Ti=N^{t}Bu (7.39 µmol, 99% yield) as the only observable diamagnetic

porphyrin species. The ^{1}H NMR is identical to the literature spectrum for (TTP)Ti=N^{t}Bu:[9]

9.24 (s, 12H, β-pyrrole), 8.32 (d, 4H, *meso*-C$_6$H$_4$CH$_3$), 8.04 (d, 4H, *meso*-C$_6$H$_4$CH$_3$), 7.34

(d, 4H, *meso*-C$_6$H$_4$CH$_3$), 7.30 (d, 4H, *meso*-C$_6$H$_4$CH$_3$), 2.42 (s, 12H, *meso*-C$_6$H$_4$CH$_3$), -1.58

(s, 9H, -N^{t}Bu). CO was detected in a separate experiment with a Kratos MS50TC. Calc.

27.99491 m/z, found 27.99491 ± 0.0028 m/z.

Reaction of complex 1 with CS$_2$. An NMR tube equipped with a teflon stopcock was charged with complex 1 (12.2 mg, 15.3 μmol), Ph$_3$CH (85.0 μL, 0.181 M, 15.4 μmol), CS$_2$ (1.2 μL, 20.0 μmol), and C$_6$D$_6$ (ca. 0.6 mL). Heating the solution at 80°C for 112 h produced (TTP)Ti=S (12.5 μmol, 82% yield). ^{1}H NMR (C$_6$D$_6$, 300 MHz) (TTP)Ti=S:[4a] 9.29 (s, 8H, β-H), 8.14 (d, 4H, meso-C$_6$H$_4$CH$_3$), 7.95 (d, 4H, meso-C$_6$H$_4$CH$_3$), 7.30 (m, 8H, meso-C$_6$H$_4$CH$_3$), 2.41 (s, 12H, meso-C$_6$H$_4$CH$_3$).

Reaction of complex 1 with (MeO)$_2$SO. An NMR tube equipped with a teflon stopcock was charged with complex 1 (6.3 mg, 7.7 μmol), Ph$_3$CH (90.5 μL, 0.145 M, 13.1 μmol), (MeO)$_2$SO (1.7 μL, 20.0 μmol), and C$_6$D$_6$ (ca. 0.6 mL). Within 5 minutes all of the 3-hexyne had been displaced and a small amount of (TTP)Ti=O was present. Allowing the solution to stand at 25°C for 96 h produced (TTP)Ti=O in 43 % yield. ^{1}H NMR (C$_6$D$_6$, 300 MHz): (TTP)Ti=O:[10] 9.24 (s, 12H, β-pyrrole), 8.00 (d, 8H, meso-C$_6$H$_4$CH$_3$), 7.28 (d, 8H, meso-C$_6$H$_4$CH$_3$), 2.42 (s, 12H, meso-C$_6$H$_4$CH$_3$).

Reaction of 1 with 'BuNCS. An NMR tube equipped with a teflon stopcock was charged with 1 (10.65 mg, 13.33 μmol), Ph$_3$CH (92.5 μL, 0.146 M, 13.46 μmol), 'BuNCS (2.8 μL, 22.07 μmol), and C$_6$D$_6$ (ca. 0.6 mL). Upon allowing the solution to stand at 25°C for 13 h (TTP)Ti=S (12.94 μmol, 97% yield) was produced. ^{1}H NMR (C$_6$D$_6$, 300 MHz): 'BuNC: 0.86 (s, 9H); (TTP)Ti=S:[4a] 9.29 (s, 12H, β-pyrrole), 8.14 (d, 4H, meso-C$_6$H$_4$CH$_3$), 7.95 (d, 4H, meso-C$_6$H$_4$CH$_3$), 7.30 (m, 8H, meso-C$_6$H$_4$CH$_3$), 2.41 (s, 12H, meso-C$_6$H$_4$CH$_3$).

Reaction of 1 with 'BuNCSe. An NMR tube equipped with a teflon stopcock was charged with 1 (12.27 mg, 15.36 μmol), Ph$_3$CH (95.0 μL, 0.146 M, 13.82 μmol), 'BuNCSe

(5.4 mg, 33.3 µmol), and C_6D_6 (ca. 0.6 mL). The solution was allowed to stand at 25°C for

4 h at which time 'BuNC (14.73 µmol) and (TTP)Ti=Se (15.20 µmol, 99% yield) were

observed. Further monitoring of the sample revealed that after all the (TTP)Ti=Se was

formed, (TTP)Ti(η^2-Se$_2$) was being produced by the reaction between (TTP)Ti=Se and

excess 'BuNCSe. ^{1}H NMR (C_6D_6, 300 MHz): (TTP)Ti=Se:[44] 9.31 (s, 8H, β-H), 8.18 (d,

4H, meso-C_6H_4CH$_3$), 7.95 (d, 4H, meso-C_6H_4CH$_3$), 7.28 (m, 8H, meso-C_6H_4CH$_3$), 2.41 (s,

12H, meso-C_6H_4CH_3). 'BuNC: 0.86 (s, 9H). (TTP)Ti(η^2-Se$_2$): 9.08 (s, 8H, β-H), 8.15 (d,

4H, meso-C_6H_4CH$_3$), 7.89 (d, 4H, meso-C_6H_4CH$_3$), 7.26 (m, 8H, meso-C_6H_4CH$_3$), 2.39 (s,

12H, meso-C_6H_4CH_3). At early times an intermediate was observed: ^{1}H NMR (C_6D_6, 300

MHz) [(TTP)Ti(η^2-'BuNCSe)]: 9.01 (s, 8H, β-H), 8.43 (d, 4H, meso-C_6H_4CH$_3$), 7.96 (d,

4H, meso-C_6H_4CH$_3$), 7.29 (dd, 8H, meso-C_6H_4CH$_3$), 2.39 (s, 12H, meso-C_6H_4CH_3), -0.52 (s,

9H, η^2-'BuNCSe).

Reaction of 1 with Cy$_3$P=S. An NMR tube equipped with a teflon stopcock was

charged with 1 (8.9 mg, 11.12 µmol), Ph$_3$CH (92.5 µL, 0.146 M, 13.46 µmol), Cy$_3$P=S (4.0

mg, 12.8 µmol), and C_6D_6 (ca. 0.6 mL). After ≈ 5 minutes (TTP)Ti=S (1.47 µmol, 13%

yield) and 1 (6.96 µmol) were present. ^{1}H NMR (C_6D_6, 300 MHz): (TTP)Ti=S:[44] 9.29 (s,

12H, β-pyrrole), 8.14 (d, 4H, meso-C_6H_4CH$_3$), 7.95 (d, 4H, meso-C_6H_4CH$_3$), 7.30 (m, 8H,

meso-C_6H_4CH$_3$), 2.41 (s, 12H, meso-C_6H_4CH_3).

(TTP)Ti(PEt$_3$)$_2$, 6. A stirred solution of complex 1 (230 mg, 0.287 mmol) in

toluene (ca. 10 mL) was treated with PEt$_3$ (120 µL, 0.812 mmol). After stirring for 1.5

hours at ambient temperature, the solution was filtered and the filtrate reduced to dryness *in*

vacuo. The residue was recyrstallized from a toluene/hexanes (2:1) solution that was

allowed to stand at -25°C for one day which produced analytically pure black crystals of

complex **6** in two crops (145 mg, 53 % yield). UV/vis (toluene): 553(4.45), 426 (5.53), 406

(shoulder, 2.61). ^{1}H NMR (C$_6$D$_6$, 400MHz): 11.50 (bd, 12H, J = 7 Hz, P(C*H$_2$*CH$_3$)$_3$, 7.22

(bs, 18H, P(CH$_2$C*H$_3$*)$_3$), 6.14 (d, 8H, J = 8 Hz, *meso-*C$_6$*H$_4$*CH$_3$), 4.82 (d, 8H, J = 8 Hz,

*meso-*C$_6$*H$_4$*CH$_3$), 1.47 (s, 12H, *meso-*C$_6$H$_4$C*H$_3$*), -5.92 (bs, 8H, β-pyrrole). Anal. Calcd. for

C$_{60}$H$_{66}$N$_4$P$_2$Ti: C, 75.62; H, 6.98; N, 5.88. Found: C, 75.75; H, 7.35; N, 5.80.

(TTP)Ti[OP(Oct)$_3$]$_2$, 7. A round bottom flask was charged with complex **1** (364

mg, 0.455 mmol) and O=P(Oct)$_3$ (362 mg, 0.935 mmol). Upon addition of toluene (ca. 15

mL), the stirred solution became dark blue. The solution was concentrated *in vacuo* after

2.5 h to a black oil (ca. 1 mL). This oil was redissolved in hexanes (ca. 24 mL) and then

reduced in vacuo to 4 mL and cooled to -25°C for one day which produced analytically pure

black crystals of complex **7** (355 mg, 52% yield). UV/vis (hexane): 550 (2.14), 422 (5.69),

403 (shoulder, 2.98). ^{1}H NMR (C$_6$D$_6$, 300MHz): 12.11 (bs, 12H, 2-C*H$_2$*), 10.27 (bs, 12H,

3-C*H$_2$*), 8.72 (d, 8H, *meso-*C$_6$*H$_4$*CH$_3$), 4.65 (bs, 12H, 4-C*H$_2$*), 4.55 (s, 12H, *meso-*C$_6$H$_4$C*H$_3$*),

3.03 (bs, 12H, 5-C*H$_2$*), 2.02 (bs, 12H, 6-C*H$_2$*), 1.33 (bs, 12H, 7-C*H$_2$*), 1.18 (bs, 18H, 8-

C*H$_3$*), -0.43 (d, 8H, *meso-*C$_6$*H$_4$*CH$_3$), -33.0 (bs, 8H, β-pyrrole). ^{31}P NMR (C$_6$D$_6$, 200 MHz):

83.5 ppm, referenced to internal H$_3$PO$_4$ (0.00 ppm). (Free O=P(Oct)$_3$, -31.8 ppm) Anal.

Calcd. for C$_{96}$H$_{138}$N$_4$O$_2$P$_2$Ti: C, 77.39; H, 9.34; N, 3.76. Found: C, 76.89; H, 9.06; N, 3.08.

Structure Determination of (TTP)Ti(PEt$_3$)$_2$, 6 and (TTP)Ti[OP(Oct)$_3$]$_2$, 7.

Crystallographic data for complexes **6** and **7** are found in Appendix A. A crystal of complex

7 was attached to a glass fiber and mounted on a Siemens SMART system for data

collection at 173(2) K. Final cell constants were calculated from a set of 8192 strong

the actual data collection. The space group P2₁/n was determined from systematic absences and intensity statistics.[11] A successful direct-methods solution was calculated which provided most non-hydrogen atoms from the E-map. Several full-matrix least squares/difference Fourier cycles were performed which located the remainder of the non-hydrogen atoms. All non-hydrogen atoms were refined with anisotropic displacement parameters. All hydrogen atoms were placed in ideal positions and refined as riding atoms with relative isotropic displacement parameters. Complex **6** was treated in an analogous manner. A crystal of complex **6** was attached to a glass fiber and mounted on a Bruker CCD-1000 diffractometer for data collection at 173(2) K. A total of 28087 data were harvested by collecting four sets of frames with 0.3° scans in ω with an exposure time of 90 sec per frame. These highly reduntant datasets were corrected for Lorentz and polarization effects. The absorption correction was based on fitting a function to the empirical transmission surface as sampled by multiple equivalent measurements.[12] Final cell constants were calculated from a set of 6649 strong reflections from the actual data collection. The space group P$\bar{1}$ was determined from systematic absences and intensity statistics.[13] A successful direct-methods solution was calculated which provided most non-hydrogen atoms from the E-map. Several full-matrix least squares/difference Fourier cycles were performed which located the remainder of the non-hydrogen atoms. Due to poor quality of the diffraction data all atoms were refined with isotropic displacement coefficients. All hydrogen atoms were included in the structure factor calculation at idealized positions and were allowed to ride on the neighboring atoms with relative isotropic displacement

coefficients. There are two symmetry independent half molecules of complex **6** in the

asymmetric unit. These half molecules occupy crystallographic inversion centers.

Results

Reactivity of (TTP)Ti(η²-3-hexyne) with ⁱPrNCO, ᵗBuNCO, and ⁱPrN=C=NⁱPr.

Quantitative nitrene group transfer, as monitored by ¹H NMR spectroscopy, resulted from

treatment of (TTP)Ti(η^2-3-hexyne), **1**, with ⁱPrNCO or ᵗBuNCO. This occurred within 5

minutes by facile displacement of 3-hexyne and production of the imido complex

(TTP)Ti=NR (R = ⁱPr, **2**, ᵗBu, **3**) (eq 1). The formation of CO was confirmed by high-

$$\text{(TTP)Ti=NⁱPr} \xleftarrow[\substack{-\,ⁱPrNC \\ -\,3\text{-hexyne}}]{ⁱPrN=C=NⁱPr} \text{(TTP)Ti}(\eta^2\text{-3-hexyne}) \xrightarrow[\substack{-\,CO \\ -\,3\text{-hexyne}}]{ᵗBuNCO} \text{(TTP)Ti=NᵗBu} \qquad (1)$$
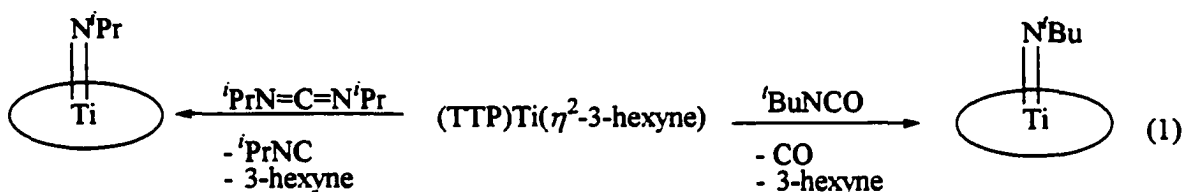
resolution mass spectrometry (found: 27.99491 ± 0.0028 m/z; calcd.: 27.99491). Over the

course of these reactions, intermediate substitution products were not observed. Due to

mechanical losses, complex **2** was isolated in 44% yield. The isopropyl imido complex **2**

could also be prepared by treatment of **1** with 1,3-diisopropylcarbodiimide although mass

balance was not realized during spectroscopic monitoring. In this case the yield of imido

complex (TTP)Ti=NⁱPr, **2**, was only 79 % as measured by ¹H NMR. The isocyanide side

product, ⁱPrNC, can also displace the alkyne from (TTP)Ti(η^2-3-hexyne) to form a

paramagnetic, ¹H NMR silent bis(isocyanide) complex, (TTP)Ti(ⁱPrNC)₂. However,

treatment of the sample with excess pyridine in an attempt to convert any NMR silent

porphyrin species to the NMR active complex $(TTP)Ti(py)_2$, did not reveal additional Ti complexes.

Despite the reduced steric bulk of the isopropyl group, the imido is quite air- and water-stable in comparison to previous titanium metalloporphyrin derivatives. For example, $(TTP)Ti=N^tBu$, **3**, was hydrolized within minutes on exposure to moisture to form free amine and $(TTP)Ti=O$. In contrast, the isopropyl complex, **2**, required hours to undergo complete hydrolysis.

Reactivity of $(TTP)Ti(\eta^2$-3-hexyne) with ^tBuNCSe, ^tBuNCS, and CS_2.

Quantitative displacement of the 3-hexyne was observed by ^1H NMR within minutes upon addition of ^tBuNCSe to $(TTP)Ti(\eta^2$-3-hexyne). In addition to the appearance of the terminal selenido complex, $(TTP)Ti=Se$, **4**, an additional set of sharp porphyrin signals was detected at early times (eq 2). The ratio of complex **4** to the new intermediate was 1:9 after

$$(2)$$
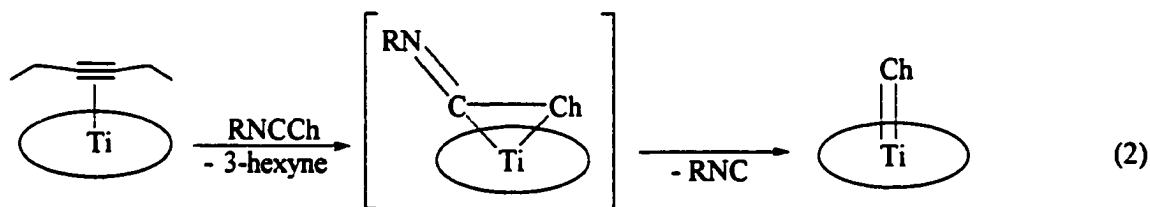
approximately 5 minutes. Associated with this new transient complex was a 9-proton singlet at -0.52 ppm. This signal is downfield from the ^tBu resonance of the imido species, $(TTP)Ti=N^tBu$, by over 1 ppm. An η^2-C,Se bound isoselenocyanate, $(TTP)Ti(\eta^2$-$^tBuCNSe)$ is the most reasonable formulation for this intermediate. At 20°C the intermediate is slowly converted over 4 hours to complex **4** (99% NMR yield) and ^tBuNC. Treatment of the hexyne complex **1** with ^tBuNCS proceeded somewhat faster to form the terminal

chalcogenido (TTP)Ti=S (95% NMR yield after ≈ 15 min). An additional set of broad,

transient NMR signals ($\Delta v_{\frac{1}{2}}$ = 16 Hz) was detected which had experimentally similar

chemical shifts to that for (TTP)Ti(η^2-'BuCNSe). This species was therefore assigned as an

η^2-C,S adduct, (TTP)Ti(η^2-'BuNCS).

Heating a benzene-d_6 solution of 1 in the presence of ≈ 1.25 eq CS_2 at 80°C for

112 h produced (TTP)Ti=S, 5, in 87 % yield by NMR. This reaction proceeds with the

formation of at least 5 intermediate titanium porphyrin species, indicated by the number of β-

pyrrole signals in the ^{1}H NMR spectrum.

Synthesis of (TTP)Ti(PEt$_3$)$_2$, 6. Although no reaction was observed between

(TTP)Ti(η^2-3-hexyne) and NEt$_3$, N(Oct)$_3$ or P(Oct)$_3$, treatment with PEt$_3$ rapidly afforded

the bis(phosphine) adduct (TTP)Ti(PEt$_3$)$_2$, 6, in 53 % isolated yield (eq 3). This reaction is

(3)
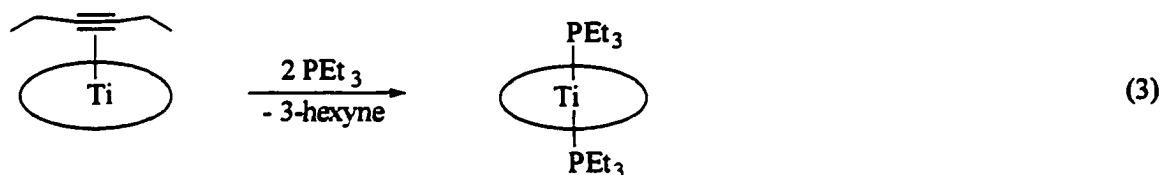
quantitative by NMR. Although 6 is paramagnetic, its ^{1}H NMR signals are relatively sharp

and integrations are sufficient for determining the metal:ligand stoichiometry. For example,

the β-pyrrole resonance integration is 8 protons relative to the 18-H methyl signals for the

two PEt$_3$ ligands. The coordination environment of titanium was found to contain *trans*-

PEt$_3$ groups by X-ray diffraction despite poorly diffracting crystals.[14] Phosphorus signals for

the PEt$_3$ groups were not observed in the ^{31}P NMR spectrum.

Synthesis and Structure of (TTP)Ti[OP(Oct)$_3$]$_2$, 7. Trioctylphosphine oxide

readily displaced 3-hexyne from complex 1 within 5 minutes to produce the bis(phosphine

oxide) adduct, $(TTP)Ti[OP(Oct)_3]_2$, 7 (eq 4). The significant solubility of this compound in hexane prevented isolated yields higher than 52 %. However, this reaction proceeded nearly quantitatively (93 %) in an NMR tube experiment with an internal standard. Assignment of this complex as a bis(phosphine oxide) adduct was facilitated by ^1H NMR spectroscopy.

$$\text{Ti} \xrightarrow[\text{- 3-hexyne}]{\text{2 OPOct}_3} \text{Ti} \tag{4}$$
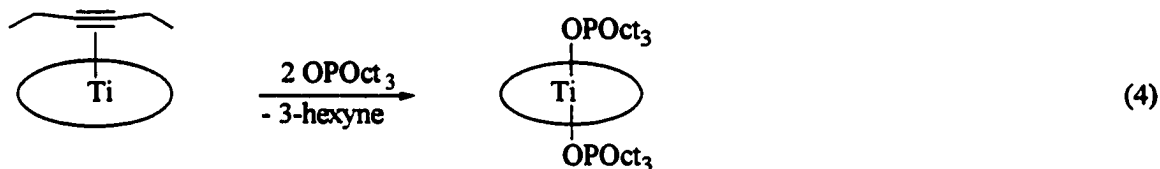
The β-carbon methylene resonance (12.11 ppm) integrates as 12 protons for two $OP(Oct)_3$ groups relative the 12 proton methyl resonance (4.55 ppm) of the porphyrin tolyl groups. The ^{31}P chemical shift for complex 7 is significantly deshielded relative to free $OPOct_3$. Similar behavior has been observed in other phosphine oxide adducts, although to a lesser extent.[15]

Complex 7 was found to crystallize in the highly symmetric space group $P2_1/n$. Consequently, the titanium resides in an octahedral coordination environment with the pyrrole nitrogens in the equatorial plane and the $OP(Oct)_3$ ligands occupying the axial positions (Figure 2). A number of Ti(IV) complexes containing O-bound phosphine oxide ligands have been crystallographically characterized,[15] but there appears to be only one Ti(II) compound containing Ti-O bonds. The Ti-O bond distances in complex 7 (2.080(2) Å) are significantly longer than the Ti-O single bond distances observed for $Ti(OPh)_2(1,2-$bis(dimethylphosphino)ethane)$_2$ (1.891(6), 1.930(6) Å).[16] The tetravalent imido complex, $TiCl_2(=N^tBu)(OPPh_3)_2$, possesses Ti-O bonds of 2.008(6) and 2.047(6) Å and Ti-O-P angles
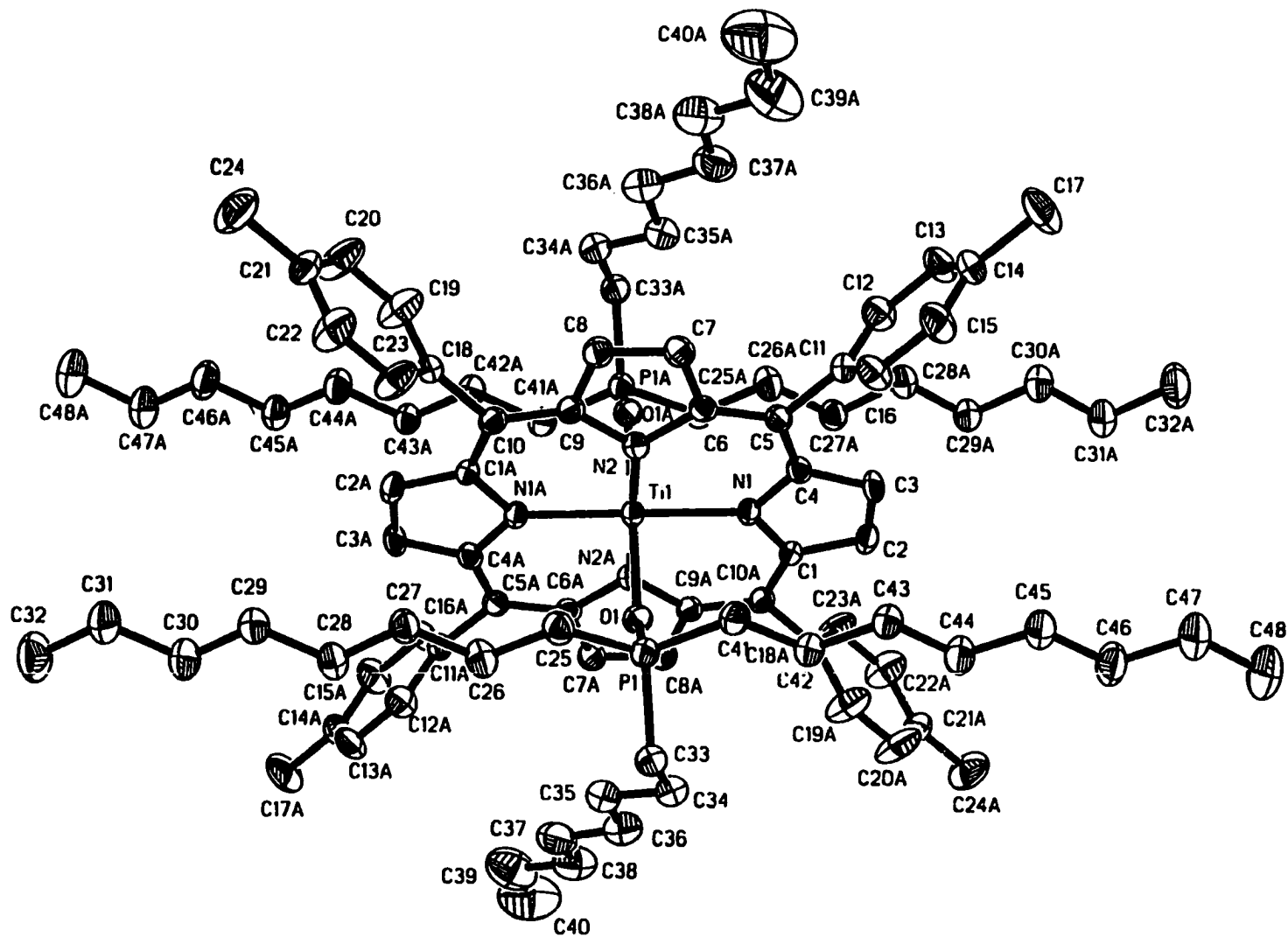
Figure 1. ORTEP representation of (TTP)Ti(OPOct₃)₂. Thermal ellipsoids drawn at the 50% probability level.

of 159.2(4)° and 154.6(4)°.[15a] The Ti-O-P angle of 138.43(10)° in complex 7 is surprisingly

acute in light of the expected steric interaction between the octyl groups and the porphyrin

macrocycle. This appears to be the most acute M-O-P bond angle observed for a

monodentate phosphine oxide-transition metal complex.[17,18] Although there are

crystallographically characterized transition metal analogues in a variety of oxidations states

and coordination environments, there is no clear trend with M-O-P bond angles.[18] The Ti-O

vector in complex 7 is canted with respect to the normal of the N_4 plane by 6° which results

in a Ti-P distance of 3.365 Å. This is well outside of an η^2-bonding interaction.[19,20] The O-

P bond distance in 7 (1.513(2) Å) is comparable to those of free phosphine oxides (1.490-

1.498 Å).[21] The OP(Oct)$_3$ moiety in 7 is perhaps best described by the limiting phosphonium

representation, $R_3\overset{+}{P}\text{-}\bar{O}$.[22] A waving distortion[23] is observed in the deviations from the mean

plane containing the 24-atom porphyrin core and titanium [Ti (3), N1 (3), N2 (-15), C1(-3),

C2 (-4), C3 (2), C4 (6), C5 (7), C6 (-5), C7 (0), C8 (1), C9 (-4), C10 (10 pm)]. Although

there are no short intermolecular contacts, the waving distortion and relatively small Ti-O-P

angle may result from the bulky OP(Oct)$_3$ groups. Two of the octyl groups extend linearly

and lie in a coplanar manner to the porphyrin. The third octyl group achieves similar spacing

relative to the porphyrin by rotation around the C33-C34 bond. Presumably, a more linear

Ti-O-P angle would disrupt this efficient packing arrangement. The pyrrole nitrogen, N2,

which is eclipsed by the Ti-O-P unit, follows the canting of the Ti-O vector and is above the

porphyrin plane by 0.15 Å.

The variable temperature magnetic behavior found for complex 7 is displayed in

Figure 2. At 296 K the magnetic moment is 1.60 μ_B and falls smoothly to 0.66 μ_B at 51 K.
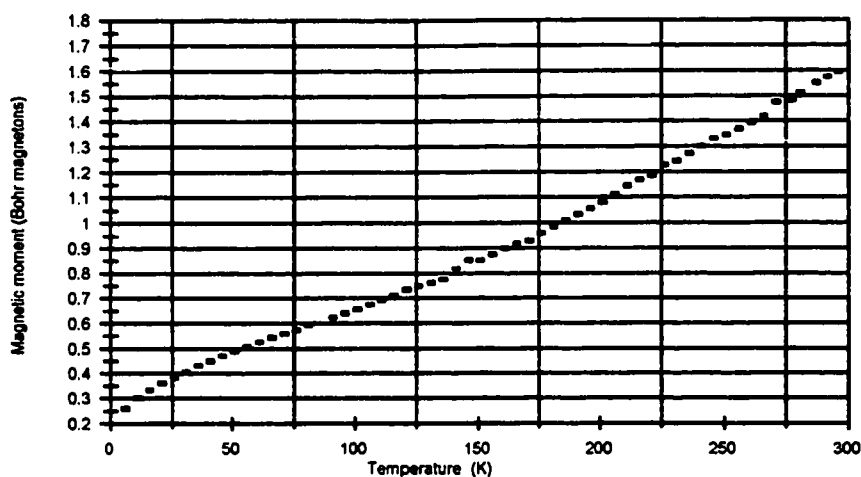
Figure 2. Magnetic moment vs. temperature plot for complex 7.

This behavior is analogous to that of $(TTP)Ti(4\text{-picoline})_2$.[4a] These values are much lower than the spin-only value of 2.83 μ_B for two unpaired electrons.

Discussion

Group and Atom Transfer Reactions. The porphyrin macrocycle serves as a robust framework for studying group and atom transfer reactions of transition metal complexes.[24] This is particularly true in cases where multi-electron redox processes are involved. The porphyrin ligand prevents severe structural reorganizations that typically accompany large changes in the formal metal oxidation states. Our development of low-valent Ti porphyrin complexes, $(TTP)Ti(\eta^2\text{-alkyne})$, has been very useful in this regard. The Ti(II) complex is an extremely potent reductant and a versatile atom acceptor reagent. In an extension of our previous atom transfer work, we have examined the chemistry of $(TTP)Ti(\eta^2\text{-3-hexyne})$ with heterocumulenes. These new reactions provide alternate

synthetic methods for preparing Ti(IV) complexes in addition to providing a means of

estimating Ti–X multiple bond strengths. It should be noted that the atom/group transfer

reactions here were not inhibited by the presence of added 3-hexyne.

Attempts at establishing absolute values for the Ti-alkyne bond strengths by

monitoring thermal ligand dissociation in solution ^{1}H NMR spectroscopy were unsuccessful.

For (TTP)Ti(η^2-3-hexyne) and (TTP)Ti(η^2-PhC$\equiv$CPh), no dissociation was observed up to

373 K. Thus, a lower estimate of the Ti-alkyne bond energy is $\geq$ 12 kcal/mol as no

dissociation was observed.[25] Using this Ti-alkyne bond strength and tabulated bond

strengths for small molecules (Table 1),[26] estimates of the (TTP)Ti=X bond strengths were

determined for (TTP)Ti=X (X = O, S, Se, NR). Cleavage of the sulfur-oxygen double bond

in dimethyl sulfite requires 116 kcal/mol. With the estimated bond energy of the Ti-alkyne

fragment, a Ti=O bond strength of $\geq$ 128 kcal/mol is obtained. In comparison, theoretically

and calorimetrically derived Ti=O bond strengths are 143 kcal/mol[27] and 147 kcal/mol.[28]

Furthermore, Ti-O single bond energies have been found to range from 89-115 kcal/ mol.[29]

Based on the sulfur atom abstraction between 1 and Cy$_3$P=S, a Ti=S bond strength of 110

kcal/mol is calculated. Selenium atom transfer between Ph$_3$P=Se and 1 provides a lower

limit to the Ti=Se bond of 79 kcal/mol. Similarly, nitrene group transfer from RNCO to 1

involves cleavage of the nitrogen-carbon double bond which requires approximately 88

kcal/mol. Thus the titanium-nitrogen bond energy in (TTP)Ti=NR is $\geq$ 100 kcal/mol.

Although similar atom and group transfer reactions were found with compounds 6

and 7, these reactions required heating. For example, formation of (TTP)Ti=N(SiMe$_3$) from

treatment of complex 7 with N$_3$(SiMe$_3$) required heating the reaction mixture to 60°C. In

Table 1. Atom and group transfer reactions utilizing (TTP)Ti(η^2-3-hexyne).

Reagent	Bond Cleavage by 1 [a]	Bond Strength (kcal/mol)
$(CH_3)_2S{=}O$ [b]	✓	87 [c]
$Ph_2S{=}O$ [b]	✓	89 [c]
$(MeO)_2S{=}O$ [d]	✓	116 [c]
$(tolyl)_2OS{=}O$ [b]		113 [c]
$Ph_3P{=}O$ [d]		128 [e]
$^tBuNC{=}O$ [d]		109 (MeNCO) [f]
$^tBuN{=}CO$ [d]	✓	
$Ph_3As{=}O$ [d]		103 [g]
$^tBuNC{=}S$ [d]	✓	71 (MeNCS) [c]
$Ph_3P{=}S$ [h]	✓	88 [i]
$Cy_3P{=}S$ [d]	✓	98 [i]
$SC{=}S$ [d]	✓	103 [c]
$^tBuNC{=}Se$ [d]	✓	
$Ph_3P{=}Se$ [h]	✓	67 [g]
$(TMS)N{-}N_2$ [j]	✓	40 ($^tBuN_3$) [k]
$^iPrNC{=}N^iPr$ [d]	✓	

a) Reactions were performed at 20°C in C_6D_6 and monitored by ^1H NMR unless otherwise indicated. b) Ref. [4b]. c) Ref. [26f]. d) This work. e) Ref. [26c]. f) Ref. [26d]. g) Ref. [26e]. h) Ref. [4a]. i) Ref [26a]. j) Ref. [9]. k) Ref. [26b].

contrast, the facile reaction between the alkyne adduct, 1, and $N_3(SiMe_3)$ occurred at ambient temperature. Heating a solution of the bis(phosphine) species, 6, in the presence of dimethyl sulfite produced (TTP)Ti(OMe)$_2$,[10] (TTP)Ti=O, and $Et_3P{=}S$.

Attempts at oxygen atom abstraction from CO_2, $(PhO)_3PO$, $(Et_2N)_3PO$, and Ph_3PO were unsuccessful despite the ability of low valent Ti(II) complexes to break such strong bonds.[30] The reverse reaction, oxygen atom transfer from (TTP)Ti=O to ^tBuNC, $POct_3$, PPh_3, or $P(OPh)_3$ was also not observed. Use of diphenylacetylene or pyridine to trap the

Ti(II) intermediate also failed to promote atom transfer. Thus, a kinetic barrier must exist in the down-hill direction.

Ligand Exchange Reactions. The reported ligand exchange reactions of titanocene and bis(pentadienyl) titanium(II) derivatives have dealt largely with CO and phosphines.[31] The system in this work has made use of a wide variety of axial donor ligands. The metalloporphyrin fragment (TTP)Ti(II) has a preference for strong σ-donors, exhibited by displacement of THF with picoline. The triethylphosphine ligands in complex **6** are rapidly displaced by pyridine and OP(Oct)$_3$. Treatment of complex **6** with excess diphenylacetylene produces an equilibrium mixture of the diamagnetic monoacetylene complex, (TTP)Ti(η^2-PhC≡CPh), and complex **6** (K ≈ 0.2). Further variable temperature analysis of this equilibrium was prevented by decomposition of the Ti(II) complexes to uncharacterized, NMR-silent products. In the presence of excess pyridine, the trioctylphosphine oxide ligands in complex **7** are only partially displaced to form a mixed species, (TTP)Ti[OP(Oct)$_3$](py).

There is a contrasting ability to displace 3-hexyne from complex **1** with OP(Ph)$_3$ compared to the phosphate, OP(OPh)$_3$. The phosphine oxide results in complete displacement of the alkyne within minutes. Whereas treatment of compound **1** with the phosphate, which is less nucleophilic and less bulky,[32] results in no displacement even at 80°C.

Atom Transfer Intermediates. The binding of heterocumulenes to mid- and late-transition metals has been well established.[33] However, isolable examples of early transition metal-heterocumulene complexes are rare. Known low valent metal complexes include

examples of η^1-CO_2, η^2-CO_2, η^2-CS_2, and η^2-RNCNR.[34] The reaction between 1 and

$^tBuNC=Ch$ (Ch = S, Se) yields a diamagnetic, short-lived species observed by NMR. This

transient compound possesses a 9-proton singlet at -0.52 ppm which is assigned as a ^tBu

group of a coordinated ligand. Since the chalcogenido complexes, (TTP)Ti=Ch, do not bind

additional donor ligands, it does not seem likely that this intermediate is a terminal

chalcogenido compound with a bound isocyanide or isocyanate. Moreover, (TTP)Ti=Ch,

free ^tBuNC, and $^tBuNC=Ch$ are quantitatively accounted for in the ^1H NMR. Likewise, the

3-hexyne is accounted for as either bound (-0.12 (q), -0.87 (t)) or free (2.05 (q), 1.00 (t)).

Thus, it is reasonable to assign this intermediate as a titanium complex containing only one

bound $^tBuNC=Ch$, structure A, B, or C (Figure 3). Given the diamagnetism of the

intermediate and the production of terminal sulfido and selenido products, the η^2-bound
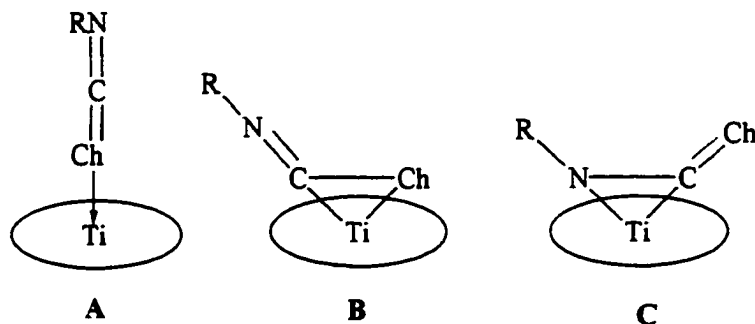
Figure 3. Bonding modes of isocyanates.

form B may be the most likely formulation. The formation of terminal chalcogenido

complexes, (TTP)Ti=Ch, from RNCS and RNCSe rather than imido production can be

traced to weaker C=Ch bonds relative to the C=N bond.

In the reaction of RNCO with 1, feasible intermediates are either η^1-O or η^2-

$O,C/\eta^2$-C,N configurations. In light of the imido complex produced from 'BuNCO, form C

is most likely, which sterically drives the relatively fast production of products. Steric

interaction between the porphyrin macrocycle and the coordinated RNCO ligand would be

displayed most readily by changing the size of the R group. However, for isocyanates,

increasing the steric bulk from 'BuNCO to 2,6-diisopropylphenyl isocyanate did not

qualitatively change the rate of formation of the imido complex.[35]

Based on steric considerations, it was postulated that interaction of CS_2 with the

tetraazaporphyrinato manganese(II) compound, [Mn(oespz)], resulted in an unstable η^1-S

intermediate.[36] The reaction of (TTP)Ti(II) with carbon disulfide also includes transient

intermediates. The diamagnetic species were readily observed by ^{1}H NMR. Specifically, in

benzene-d_6 at 20°C, within minutes after addition of CS_2 there is a single β-pyrrole signal at

8.78 ppm. This species represents 67 % of the starting metalloporphyrin complex. The

other 33 % of the starting reagent is not observed and is unaccounted for. Nonetheless, all

of the 3-hexyne has been displaced and is accounted for quantitatively. Allowing the mixture

to stand at ambient temperature for ~ 14 hours resulted in the formation of (TTP)Ti=S (9.29

ppm, β-pyrrole, 2% yield by NMR) and a decrease in the intensity of the signal at 8.78 ppm.

However, this is not directly related to the amount of the sulfido formed as two other broad

signals have appeared in the porphyrin β-pyrrole region, 9.09 ppm and 8.72 ppm. Heating

this solution for 1.5 hours at 80°C sharpens these two signals and produces an additional

resonance at 8.65 ppm. Continued heating for another 23 hours results in the loss of the

peak at 8.78 ppm, concomitant with the increase in the amount of (TTP)Ti=S formed

(46.5% yield). In addition, the peaks at 9.09, 8.72, and 8.65 ppm also increased in intensity.

This reaction sequence is not easily interpreted as the disappearance of intermediates are not directly related to the formation of (TTP)Ti=S. The peaks at 9.09 and 8.65 seem to be related as they are found throughout in a 1:1 ratio. After heating at 80°C for 126 hours the only β-pyrrole signals present are those located at 9.29 ((TTP)Ti=S, 78% yield) and 8.72 ppm in a ratio of 6.7:1. Addition of a large excess of CS_2 does not eliminate the peak at 8.72 ppm, nor does extended heating. A control experiment showed no reaction of (TTP)Ti=S with CS_2, even at 80°C. None of the ^1H NMR signals of the observed intermediates correspond to those of (TTP)Ti(η^2-S_2). A dimeric compound is suggested by the treatment of 1 with $\approx$ 0.50 equiv of CS_2, which results in quantitative disappearance of starting material and production of the intermediate possessing a β-pyrrole signal at 8.78 ppm. Although this species converts slowly to (TTP)Ti=S at ambient temperature, its solubility characteristics precluded isolation in a pure form.

Magnetic behavior of complex 7. Insight into the electronic structure of complex 7, which appears to be at the limit of atom transfer ability of titanium(II) metalloporphyrins, was facilitated by an investigation of the variable-temperature magnetic behavior. Notwithstanding the paucity of Ti(II) derivatives, parallel magnetic behavior is observed with $Cp_2Ti(bipy)$.[58] In this work by Stucky, et al., molecular orbital calculations suggest the occurrence of π-back donation into relevant bipyridyl MO's. This partial reduction of the bipyridyl ligand explains the lower than expected magnetic moment which was lower than the spin-only value. Although the presence of back-donation may explain the behavior of (TTP)Ti(4-picoline)$_2$, analogous behavior of complex 7 appears to be precluded by the full p-orbitals of oxygen. The magnetic behavior of complex 7 can not be the result of metal-

metal interaction due to the steric bulk of the porphyrin and the *trans* ligands. The magnetic

behavior of complex 7 is most likely the result of a spin equilibrium involving a low lying

excited state which is occupied at relatively high temperatures.

Conclusion

The Ti(II) complex, (TTP)Ti(η^2-3-hexyne), 1, is a potent reductant and a versatile

inner sphere acceptor reagent. Treatment of complex 1 with a variety of heterocumulenes

such as RN=CO, ^{i}PrN=CN^{i}Pr, CS_2, ^{t}BuNC=S, and ^{t}BuNC=Se results in group or atom

transfer and formation of the multiply-bonded species (TTP)Ti=NR, (TTP)Ti=S, or

(TTP)Ti=Se. In addition, complex 1 abstracts an oxygen from $(MeO)_2S=O$ to produce

(TTP)Ti=O. These reactions were useful in determining estimates for Ti=O, Ti=S, and

Ti=Se bond strengths. Notably, complex 1 does not abstract oxygen from $O=P(Oct)_3$.

Instead, simple substitution occurs to produce the bis-ligand adduct $(TTP)Ti[OP(Oct)_3]_2$, 7.

References

‡   University of Minnesota, X-ray Crystallographic Laboratory.

1.   Bryan, J. C.; Mayer, J. M. *J. Am. Chem. Soc.* **1990**, *112*, 2298.

2.   (a) Conry, R. R.; Mayer, J. M. *Inorg. Chem.* **1990**, *29*, 4862. (b) Gable, K. P.;
       Juliette, J. J. J.; Li, C.; Nolan, S. P. *Organometallics* **1996**, *15*, 5250.

3.   Holm, R. H. *Chem. Rev.* **1987**, *87*, 1401.

4.   (a) Woo, L. K.; Hays, J. A.; Young, V. G., Jr.; Day, C. L.; Caron, C.; D'souza, F.;
       Kadish, K. M. *Inorg. Chem.* **1993**, *32*, 4186. (b) Wang, X.; Woo, L. K. *J. Org. Chem.*
       1998, *63*, 356. (c) Wang, X.; Gray, S. D.; Chen, J.; Woo, L. K. *Inorg. Chem.* **1998**,
       37, 5.

5. (a) Peulecke, N.; Baumann, W.; Kempe, R.; Burlakov, V. V.; Rosenthal, U. *Eur. J. Inorg. Chem.* **1998**, 419. (b) Varga, V.; Mach, K.; Polasek, M.; Sedmera, P.; Hiller, J.; Thewalt, U.; Troyanov, S. I. *J. Organomet. Chem.* **1996**, *506*, 241. (c) Hill, J. E.; Profilet, R. D.; Fanwick, P. E.; Rothwell, I. P. *Angew. Chem. Int. Ed. Engl.* **1990**, *29*, 664. (d) Fochi, G.; Florine, C.; Bart, J. C. J.; Giuunchi, J. *J. Chem. Soc., Dalton Trans.* **1983**, 1515. (e) Stahl, L.; Ernst, R. D. *J. Am. Chem. Soc.* **1987**, *109*, 5673. (f) Stahl, L.; Trakampruk, W.; Freeman, J. W.; Arif, A. M.; Ernst, R. D. *Inorg. Chem.* **1995**, *34*, 1810. (g) McPherson, A. M.; Fieselmann, B. F.; Lichtenberger, D. L. McPherson, G. L.; Stucky, G. D. *J. Am. Chem. Soc.* **1979**, *101*, 3425. (h) Cohen, S. A.; Auburn,; P. R.; Bercaw, J. E. *J. Am. Chem. Soc.* **1983**, *105*, 1136. (i) Gahan, L. R.; O'Connor, M. J. *J. Chem. Soc. Chem. Comm.* **1974**, 66. (j) Fachinetti, G.; Floriani, C. *J. Chem. Soc., Dalton Trans.* **1974**, 2433. (k) Fachinetti, G.; Floriani, C.; Stoeckli-Evans, H. *J. Chem. Soc., Dalton Trans.* **1977**, 2297. (l) Fachinetti, G.; Biran, C.; Floriani, C.; Chiesi Villa, A.; Guastini, C. *J. Chem. Soc., Dalton Trans.* **1979**, 792. (m) Bottomley, F.; Chin, T. T.; Egharevba, G. O.; Kane, L. M.; Pataki, D. A.; White, P. S. *Organometallics* **1988**, *7*, 1214.

6. Sonoda, N.; Yamamot, G.; Tsutsum, S. *Bull. Chem. Soc. Japan* **1972**, *45*, 2937.

7. Sutter, T. P. G.; Hambright, P.; Thorpe, A. N.; Quoc, N. *Inorganica Chim. Acta* **1992**, *195*, 131.

8. Lister, M. W.; Marson, R. *Can. J. Chem.* **1964**, *42*, 1817.

9. Gray, S. D.; Thorman, J. L.; Berreau, L. M.; Woo, L. K. *Inorg. Chem.* **1997**, *36*, 278.

10. Fournari, C.; Guilard, R.; Fontesse, M.; Latour, J.-M.; Marchon, J.-C. *J. Organomet. Chem.* **1976**, *110*, 205.

11. SHELXTL-Plus V5.0, Siemens Industrial Automation, Inc., Madison, WI.

12. Blessing, R. H. *Acta Cryst.* **1995**, *A51*, 33.

13. All software and sources of the scattering factors are contained in the SHELXTL V5.1 program library, G. Sheldrick, Bruker Analytical X-ray Systems, Madison, WI.

14. A representation of 6 is contained in Appendix A, R = 0.127.

15. (a) Winter, C. H.; Sheridan, P. H.; Lewkebandara, T. S.; Heeg, M. J.; Proscia, J. W. *J. Am. Chem. Soc.* **1992**, *114*, 1095. (b) McKarns, P. J.; Yap, G. P. A.; Rheingold, A. L.; Winter, C. H. *Inorg. Chem.* **1996**, *35*, 5968. (c) Mimoun, H.; Postel, M.; Casabianca, F.; Fischer, J.; Mitschler, A. *Inorg. Chem.* **1982**, *21*, 1303. (d) Postel, M.; Casabianca, F.; Gauffreteau, Y.; Fischer, J. *Inorg. Chim. Acta.* **1986**, *113*, 173. (e) Winter, C. H.; Lewkebandara, T. S.; Proscia, J. W.; Rheingold, A. L. *Inorg. Chem.* **1994**, *33*, 1227.

16. Morris, R. J.; Girolami, G. S. *Inorg. Chem.* **1990**, *29*, 4167.

17. Leading reference for coordination chemistry of phosphine chalcogenides: The Chemistry of Organophosphorus Compounds, Chpt. 8, Hartley, F. R., 1992, John Wiley & Sons Ltd.

18. (a) Burford, N.; Royan, B. W.; Spence, R. E. v. H.; Cameron, T. S.; Linden, A.; Rogers, R. D. *J. Chem. Soc. Dalton Trans.* **1990**, 1521. (b) Burford, N.; Royan, B. W.; Spence, R. E. v. H.; Rogers, R. D. *J. Chem. Soc. Dalton Trans.* **1990**, 2111.

19. The sum of the covalent radii of Ti and O (1.98-2.05 Å), Ti and P (2.38 Å): (a) Porterfield, W. W. *Inorganic Chemistry*, 2nd ed.; Academic Press: San Deigo, CA, 1998; p 214. (b) Jolly, W. L. *Modern Inorganic Chemistry*; McGraw-Hill: New York, 1984; p 52.

20. For a theoretical treatment of diatomic ligand coordination modes to transition metals: (a) Hoffmann, R.; Chen, M. M. L.; Thorn, D. L. *Inorg. Chem.* **1977**, *16*, 503. (b) Mealli, C.; Hoffmann, R.; Stockis, A. *Inorg. Chem.* **1984**, *23*, 56.

21. (a) $O=P(C_6H_{11})_3$, 1.490(2) Å; Davies, J. A.; Dutremez, S.; Pinkerton, A. A. *Inorg. Chem.* **1991**, *30*, 2380. (b) $O=P(CH_3)_3$, 1.489(6) Å; Engelhardt, L. M.; Raston, C. L.; Whitaker, C. R.; White, A. H. *Aust. J. Chem.* **1986**, *39*, 2151. (c) $O=P(CH_2CH_2CN)_3$, 1.498(3) Å; Cotton, F. A.; Darensbourg, D. J.; Fredrich, M. F.; Ilsley, W. H., Troup, J. M. *Inorg. Chem.* **1981**, *20*, 1869.

22. Chesnut, D. B.; Savin, A. *J. Am. Chem. Soc.* **1999**, *121*, 2335 and references therein.

23. Jentzen, W.; Simpson, M. C.; Hobbs, J. D.; Song, X.; Ema, T.; Nelson, N. Y.; Medforth, C. J.; Smith, K. M.; Veyrat, M.; Mazzanti, M.; Ramasseul, R.; Marchon, J.-C.; Takeuchi, T.; Goddard, W. A., III.; Shelnutt, J. A. *J. Am. Chem. Soc.* **1995**, *117*, 11085.

24. Woo, L. K. *Chem. Rev.* **1993**, *93*, 1125.

25. This estimate is rather low based on the barrier to rotation of four electron donor alkyne ligands. Alt, H. G.; Engelhardt, H. E. *Z. Naturforsch., B: Anorg. Chem., Org. Chem.* **1985**, *40B(9)*, 1134 and references therein.

26. (a) Capps, K. B.; Wixmerten, B.; Bauer, A.; Hoff, C. D. *Inorg. Chem.* **1998**, *37*, 2861. (b) Claydon, A. P.; Fowell, P. A.; Mortimer, C. T. *J. Chem. Soc.* **1960**, 3284. (c) Hudson, R. F. *Structure and Mechanism in Organo-Phosphorus Chemistry*; Academic Press: London, 1965. (d) Stull, D. R.; Westrum, E. F., Jr.; Sinke, G. C. *The Chemical Thermodynamics of Organic Compounds*; Wiley: New York, 1969. (e) Barnes, D. S.; Burkinshaw, P. M.; Mortimer, C. T. *Thermochim. Acta* **1988**, *131*, 107. (f) Benson, S. W. *Chem. Rev.* **1978**, *78*, 23.

27. Fisher, J. M. Piers, W. E.; Ziegler, T. ; MacGillivray, L. R.; Zaworotka, M. J.; *Chem. Eur. J.* **1996**, *2*, 1221.

28. Glidewell, C. *Inorg. Chim. Acta* **1977**, *24*, 149.

29. (a) Lappert, M. F.; Patil, D. S.; Pedley, J .B. *J. Chem. Soc., Chem. Commun.* **1975**, 830. (b) Ziegler, T.; Tschinka, V.; Versluis, L.; Baerends, E. J.; Ravenek, W. *Polydedron* **1988**, *7*, 1625. (c) Dias, A. R.; Martinho Simoes, J. A. *Polyhedron* **1988**, *7*, 1531.

30. (a) Fachinetti, G.; Floriani, C.; Chiesta-Villa, A.; Guastini, C. *J. Am. Chem. Soc.* **1979**, *101*, 1767. (b) Mathey, F.; Maillet, R. *Tetrahedron Lett.* **1980**, *21*, 2525.

31. Fryzuk, M. D.; Haddad, T. S.; Berg, D. J.; *Coord. Chem. Rev.* **1990**, *99*, 137.

32. Dias, P. B.; Minas de Piedade, M. E.; Martinho Simoes, J. A. *Coord. Chem. Rev.* **1994**, *135*, 737.

33. (a) Rosi, M.; Sgamellotti, A. Tarantelli, F.; Floriani, C. *Inorg. Chem.* **1987**, *26*, 3805 and references therein. (b) Gibson, J. A. E.; Cowie, M. *Organometallics* **1984**, *3*, 984.

34. (a) Jegat, C.; Fouassier, M.; Tranquille, M.; Mascetti, J.; *Inorg. Chem.* **1991**, *30*, 1529. (b) Baird, M. C.; Hartwell, G.; Wilkinson, G. *J. Chem. Soc. A* **1967**, 2037. (c) Pasquali, M.; Gambarotta, S.; Floriani, C.; Chiesa-Villa, A.; Guastini, C. *Inorg. Chem.* **1981**, *20*, 165. (d) Gambarotta, S.; Floriani, C.; Chiesi-Villa, A.; Guastini, G. *J. Am. Chem. Soc.* **1985**, *107*, 2985. (e) Carmona, E.; Munoz, M. A.; Peraz, P. J.; Poveda, M. L. *Organometallics* **1990**, *9*, 1337. (f) Bristow, G. S.; Hitchcock, P. B.; Lappert, M. F.; *J. Chem. Soc. Chem. Commun.* **1981**, 1145. (g) Cenini, S.; La Monica, G. *Inorganica Chim. Acta* **1976**, *18*, 279. (h) Gambarotta, S.; Fiallo, M. L.; Floriani, C.; Chiesa-Villa, A.; Guastini, C. *Inorg. Chem.* **1984**, *23*, 3532. (i) Fachinetti, G.; Biran, C.; Floriani, C.; Chiesa-Villa, A. Guastini, C. *Inorg. Chem.* **1978**, *11*, 2995. (j) Antinolo, A.; Carillo-Hermosilla, F.; Otero, A.; Fajardo, M.; Garces, A.; Gomez-Sal, P.; Lopez-Mardomingo, C.; Martin, A.; Miranda, C. *J. Chem. Soc., Dalton Trans.* **1998**, 59.

35. Thorman, J. L., Woo, L. K. Unpublished results. All 3-hexyne displaced in less than 5 minutes and quantitative formation of concomitant imido compound observed.

36. Ricciardi, G.; Bencini, A.; Belviso, S.; Bavoso, A.; Lelj, F. *J. Chem. Soc., Dalton Trans.* **1998**, 1985.

APPENDIX A

Table I. Crystal data and structure refinement for compound **6**, (TTP)Ti(PEt$_3$)$_2$.

Empirical formula	C$_{60}$H$_{66}$N$_4$P$_2$Ti
Formula weight	953.01
Temperature	173(2) K
Wavelength	0.71073 Å
Crystal system	Triclinic
Space group	P$\bar{1}$
Unit cell dimensions	a = 10.9163(6) Å $\quad$ α = 83.747(1)°
	b = 11.5404(6) Å $\quad$ β = 78.928(1)°
	c = 20.7951(11) Å $\quad$ γ = 85.252(1)°
Volume	2550.5(2) Å^3
Z	2
Density (calculated)	1.241 Mg/m^3
Absorption coefficient	0.274 mm^{-1}
F(000)	1012
Crystal size	0.38 x 0.21 x 0.08 mm^3
Theta range for data collection	1.00 to 23.25°.
Index ranges	-11 ≤ h ≤ 12, -12 ≤ k ≤ 12, 0 ≤ l ≤ 23
Reflections collected	28087
Independent reflections	7015 [R(int) = 0.1083]
Completeness to theta = 23.25°	96.0 %
Absorption correction	Empirical with SADABS
Max. and min. transmission	0.9784 and 0.9032
Refinement method	Full-matrix least-squares on F^2
Data / restraints / parameters	7015 / 0 / 267
Goodness-of-fit on F^2	1.088
Final R indices [I>2σ(I)]	R1 = 0.1262, wR2 = 0.3514
R indices (all data)	R1 = 0.1766, wR2 = 0.3795
Largest diff. peak and hole	2.033 and -1.557 eÅ^{-3}
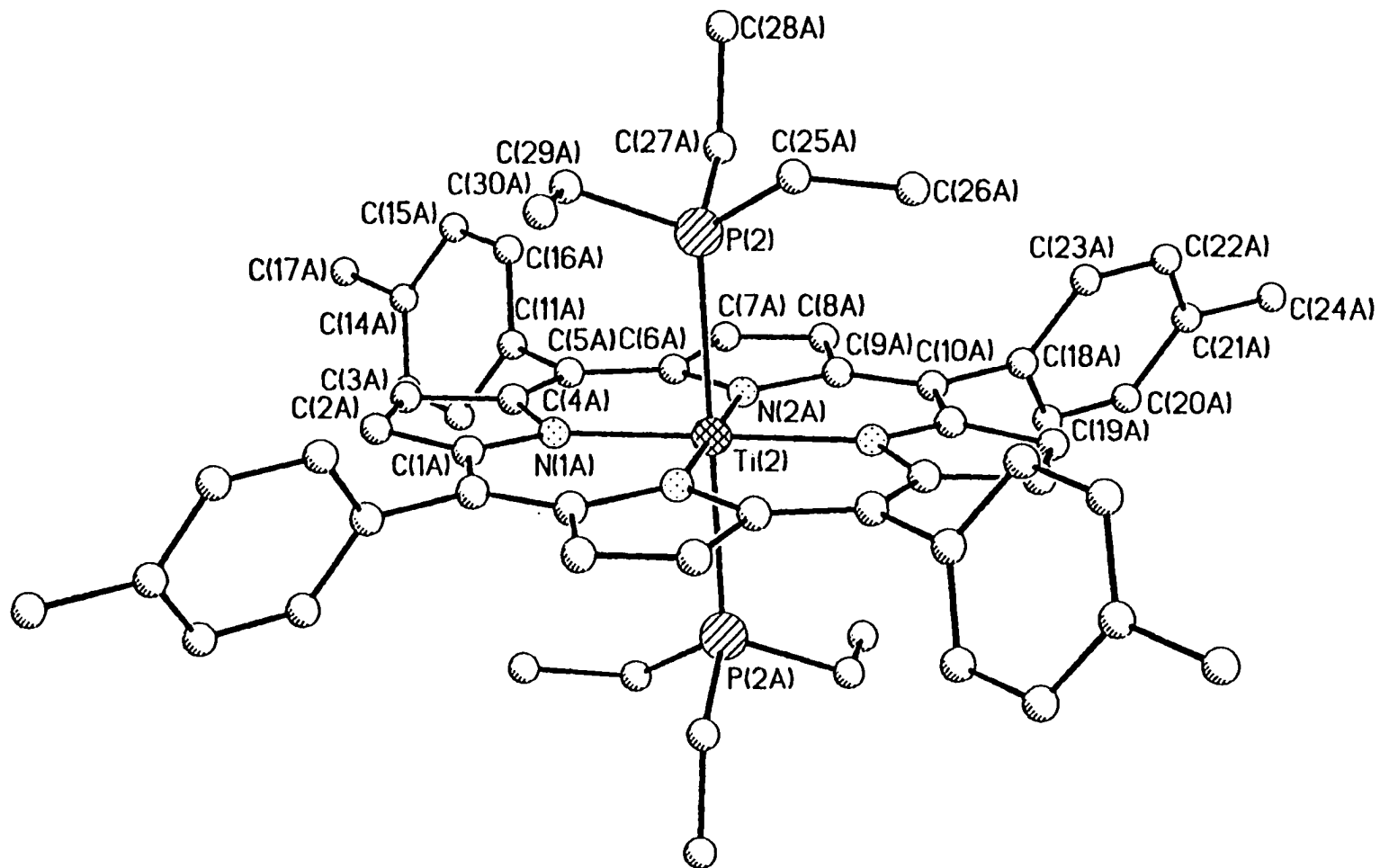
Figure 1. Ball and stick representation of (TTP)Ti(PEt$_3$)$_2$.

Table II. Atomic coordinates (x 10^4) and equivalent isotropic displacement parameters ($Å^2$x 10^3) for complex 6. U(eq) is defined as one third of the trace of the orthogonalized U_{ij} tensor.

Atom	x	y	z	U(eq)
Ti(1)	10000	10000	10000	11(1)
P(1)	12143(3)	10783(2)	9349(1)	25(1)
N(1)	9168(8)	11673(7)	10020(4)	19(2)
N(2)	9323(7)	9806(7)	9167(4)	15(2)
C(1)	9154(9)	12433(8)	10495(5)	18(2)
C(2)	8435(10)	13465(9)	10346(5)	23(2)
C(3)	8020(10)	13340(9)	9782(5)	21(2)
C(4)	8447(9)	12237(8)	9574(5)	17(2)
C(5)	8178(10)	11739(9)	9036(5)	24(2)
C(6)	8604(10)	10619(9)	8834(5)	20(2)
C(7)	8241(10)	10095(9)	8318(5)	21(2)
C(8)	8755(11)	8998(10)	8314(6)	29(3)
C(9)	9470(10)	8800(9)	8831(5)	20(2)
C(10)	10206(10)	7774(9)	8967(5)	24(2)
C(11)	7346(10)	12465(9)	8626(5)	24(2)
C(12)	6114(11)	12792(10)	8910(6)	30(3)
C(13)	5348(12)	13407(10)	8516(6)	34(3)
C(14)	5716(11)	13738(10)	7864(6)	29(3)
C(15)	6943(11)	13454(10)	7589(6)	29(3)
C(16)	7790(11)	12834(10)	7954(6)	30(3)
C(17)	4834(13)	14388(12)	7446(7)	46(3)
C(18)	10315(10)	6828(9)	8519(5)	21(2)
C(19)	10927(11)	7001(10)	7861(5)	28(3)
C(20)	11106(11)	6117(10)	7459(6)	32(3)
C(21)	10699(11)	5013(10)	7691(6)	31(3)
C(22)	10098(11)	4837(10)	8331(6)	31(3)
C(23)	9879(11)	5724(10)	8747(6)	28(3)
C(24)	10958(13)	4021(11)	7254(7)	45(3)
C(25)	13418(12)	9629(11)	9352(7)	42(3)

Table II. (continued)

C(26)	14713(14)	9878(13)	8996(7)	54(4)
C(27)	12287(13)	11364(12)	8493(6)	45(3)
C(28)	12174(15)	10470(13)	8030(8)	61(4)
C(29)	12723(12)	11947(10)	9723(6)	34(3)
C(30)	12081(12)	13151(11)	9585(6)	39(3)
Ti(2)	5000	10000	5000	13(1)
P(2)	2865(3)	10900(3)	5608(1)	26(1)
N(1A)	5778(7)	10294(7)	5788(4)	16(2)
N(2A)	4488(8)	8394(7)	5455(4)	16(2)
C(1A)	6313(10)	11281(9)	5886(5)	25(3)
C(2A)	6605(10)	11207(9)	6525(5)	25(3)
C(3A)	6243(11)	10143(10)	6832(6)	31(3)
C(4A)	5733(10)	9561(9)	6379(5)	25(3)
C(5A)	5248(10)	8459(9)	6505(5)	24(2)
C(6A)	4671(10)	7917(9)	6080(5)	23(2)
C(7A)	4092(10)	6839(10)	6228(6)	27(3)
C(8A)	3559(10)	6647(9)	5699(5)	22(2)
C(9A)	3814(9)	7622(9)	5212(5)	18(2)
C(10A)	3438(10)	7734(9)	4603(5)	20(2)
C(11A)	5326(11)	7820(10)	7166(6)	30(3)
C(12A)	6515(12)	7396(10)	7309(6)	34(3)
C(13A)	6613(14)	6848(12)	7933(7)	46(3)
C(14A)	5560(13)	6731(12)	8412(7)	47(3)
C(15A)	4387(14)	7100(12)	8279(7)	47(3)
C(16A)	4301(12)	7645(10)	7656(6)	36(3)
C(17A)	5678(16)	6174(14)	9120(8)	66(4)
C(18A)	2761(10)	6787(9)	4433(5)	25(3)
C(19A)	3315(11)	5673(9)	4323(5)	24(2)
C(20A)	2666(10)	4805(10)	4166(5)	27(3)
C(21A)	1389(11)	4999(10)	4123(6)	30(3)
C(22A)	842(12)	6081(10)	4231(6)	37(3)

Table II. (continued)

C(23A)	1494(11)	6965(11)	4380(6)	34(3)
C(24A)	690(13)	4061(12)	3935(7)	46(3)
C(25A)	1802(12)	11655(11)	5098(6)	37(3)
C(26A)	1369(13)	10884(12)	4647(7)	46(3)
C(27A)	1920(12)	9822(11)	6148(7)	43(3)
C(28A)	627(13)	10183(12)	6500(7)	50(4)
C(29A)	3017(12)	11999(10)	6155(6)	36(3)
C(30A)	3320(12)	13223(11)	5799(6)	39(3)

Table III. Bond lengths [Å] and angles [°] for complex 6.

Ti(1)-N(2)	2.050(8)	Ti(2)-N(2A)#2	2.057(8)
Ti(1)-N(2)#1	2.050(8)	Ti(2)-N(2A)	2.057(8)
Ti(1)-N(1)	2.066(8)	Ti(2)-N(1A)	2.055(8)
Ti(1)-N(1)#1	2.066(8)	Ti(2)-N(1A)#2	2.055(8)
Ti(1)-P(1)	2.644(3)	Ti(2)-P(2)#2	2.619(3)
Ti(1)-P(1)#1	2.644(3)	Ti(2)-P(2)	2.619(3)
P(1)-C(27)	1.815(13)	P(2)-C(27A)	1.826(13)
P(1)-C(29)	1.836(12)	P(2)-C(25A)	1.827(12)
P(1)-C(25)	1.845(13)	P(2)-C(29A)	1.832(12)
N(1)-C(1)	1.388(13)	N(1A)-C(1A)	1.374(13)
N(1)-C(4)	1.402(13)	N(1A)-C(4A)	1.411(13)
N(2)-C(6)	1.387(13)	N(2A)-C(9A)	1.392(12)
N(2)-C(9)	1.401(13)	N(2A)-C(6A)	1.399(13)
C(1)-C(2)	1.409(15)	C(1A)-C(2A)	1.417(15)
C(1)-C(10)#1	1.418(14)	C(1A)-C(10A)#2	1.446(15)
C(2)-C(3)	1.363(14)	C(2A)-C(3A)	1.372(16)
C(3)-C(4)	1.402(14)	C(3A)-C(4A)	1.433(15)
C(4)-C(5)	1.401(14)	C(4A)-C(5A)	1.397(15)
C(5)-C(6)	1.417(15)	C(5A)-C(6A)	1.403(14)
C(5)-C(11)	1.507(15)	C(5A)-C(11A)	1.501(15)
C(6)-C(7)	1.421(14)	C(6A)-C(7A)	1.419(15)
C(7)-C(8)	1.343(15)	C(7A)-C(8A)	1.385(15)
C(8)-C(9)	1.434(15)	C(8A)-C(9A)	1.437(15)
C(9)-C(10)	1.409(15)	C(9A)-C(10A)	1.395(14)
C(10)-C(1)#1	1.418(14)	C(10A)-C(1A)#2	1.446(15)
C(10)-C(18)	1.495(14)	C(10A)-C(18A)	1.478(14)
C(11)-C(16)	1.419(16)	C(11A)-C(16A)	1.374(17)
C(11)-C(12)	1.400(16)	C(11A)-C(12A)	1.422(17)
C(12)-C(13)	1.382(16)	C(12A)-C(13A)	1.401(18)
C(13)-C(14)	1.359(16)	C(13A)-C(14A)	1.374(19)
C(14)-C(15)	1.380(16)	C(14A)-C(15A)	1.385(19)

Table III. (continued)

C(14)-C(17)	1.518(17)	C(14A)-C(17A)	1.57(2)
C(15)-C(16)	1.408(16)	C(15A)-C(16A)	1.394(18)
C(18)-C(23)	1.399(15)	C(18A)-C(19A)	1.397(15)
C(18)-C(19)	1.403(15)	C(18A)-C(23A)	1.405(16)
C(19)-C(20)	1.366(16)	C(19A)-C(20A)	1.375(15)
C(20)-C(21)	1.390(16)	C(20A)-C(21A)	1.412(16)
C(21)-C(22)	1.367(16)	C(21A)-C(22A)	1.361(17)
C(21)-C(24)	1.514(17)	C(21A)-C(24A)	1.500(17)
C(22)-C(23)	1.388(16)	C(22A)-C(23A)	1.384(16)
C(25)-C(26)	1.499(19)	C(25A)-C(26A)	1.522(17)
C(27)-C(28)	1.513(19)	C(27A)-C(28A)	1.508(19)
C(29)-C(30)	1.527(17)	C(29A)-C(30A)	1.552(17)
N(2)-Ti(1)-N(2)#1	180.0	N(2A)#2-Ti(2)-N(2A)	180.0
N(2)-Ti(1)-N(1)	90.1(3)	N(2A)#2-Ti(2)-N(1A)	89.7(3)
N(2)#1-Ti(1)-N(1)	89.9(3)	N(2A)-Ti(2)-N(1A)	90.3(3)
N(2)-Ti(1)-N(1)#1	89.9(3)	N(2A)#2-Ti(2)-N(1A)#2	90.3(3)
N(2)#1-Ti(1)-	90.1(3)	N(2A)-Ti(2)-N(1A)#2	89.7(3)
N(1)-Ti(1)-N(1)#1	180.0	N(1A)-Ti(2)-N(1A)#2	180.0
N(2)-Ti(1)-P(1)	94.3(2)	N(2A)#2-Ti(2)-P(2)#2	88.1(2)
N(2)#1-Ti(1)-P(1)	85.7(2)	N(2A)-Ti(2)-P(2)#2	91.9(2)
N(1)-Ti(1)-P(1)	91.6(2)	N(1A)-Ti(2)-P(2)#2	91.7(2)
N(1)#1-Ti(1)-P(1)	88.4(2)	N(1A)#2-Ti(2)-P(2)#2	88.3(2)
N(2)-Ti(1)-P(1)#1	85.7(2)	N(2A)#2-Ti(2)-P(2)	91.9(2)
N(2)#1-Ti(1)-P(1)#1	94.3(2)	N(2A)-Ti(2)-P(2)	88.1(2)
N(1)-Ti(1)-P(1)#1	88.4(2)	N(1A)-Ti(2)-P(2)	88.3(2)
N(1)#1-Ti(1)-P(1)#1	91.6(2)	N(1A)#2-Ti(2)-P(2)	91.7(2)
P(1)-Ti(1)-P(1)#1	180.0	P(2)#2-Ti(2)-P(2)	180.0
C(27)-P(1)-C(29)	102.7(6)	C(27A)-P(2)-C(25A)	104.3(6)
C(27)-P(1)-C(25)	104.6(6)	C(27A)-P(2)-C(29A)	103.6(6)
C(29)-P(1)-C(25)	102.3(6)	C(25A)-P(2)-C(29A)	102.6(6)

Table III. (continued)

C(27)-P(1)-Ti(1)	120.1(5)	C(27A)-P(2)-Ti(2)	113.2(4)
C(29)-P(1)-Ti(1)	114.5(4)	C(25A)-P(2)-Ti(2)	117.3(4)
C(25)-P(1)-Ti(1)	110.7(4)	C(29A)-P(2)-Ti(2)	114.3(4)
C(1)-N(1)-C(4)	106.6(8)	C(1A)-N(1A)-C(4A)	105.5(8)
C(1)-N(1)-Ti(1)	126.9(7)	C(1A)-N(1A)-Ti(2)	128.1(7)
C(4)-N(1)-Ti(1)	126.5(6)	C(4A)-N(1A)-Ti(2)	126.0(6)
C(6)-N(2)-C(9)	106.2(8)	C(9A)-N(2A)-C(6A)	107.7(8)
C(6)-N(2)-Ti(1)	127.4(6)	C(9A)-N(2A)-Ti(2)	125.7(6)
C(9)-N(2)-Ti(1)	126.4(6)	C(6A)-N(2A)-Ti(2)	126.5(6)
N(1)-C(1)-C(2)	109.2(9)	N(1A)-C(1A)-C(2A)	111.4(9)
N(1)-C(1)-C(10)#1	125.6(9)	N(1A)-C(1A)-C(10A)#2	124.4(9)
C(2)-C(1)-C(10)#1	125.2(9)	C(2A)-C(1A)-C(10A)#2	124.2(10)
C(3)-C(2)-C(1)	107.2(9)	C(3A)-C(2A)-C(1A)	106.6(10)
C(2)-C(3)-C(4)	109.0(9)	C(2A)-C(3A)-C(4A)	107.9(10)
C(5)-C(4)-N(1)	124.6(9)	C(5A)-C(4A)-N(1A)	125.5(9)
C(5)-C(4)-C(3)	127.4(9)	C(5A)-C(4A)-C(3A)	125.8(10)
N(1)-C(4)-C(3)	108.0(8)	N(1A)-C(4A)-C(3A)	108.6(9)
C(4)-C(5)-C(6)	127.0(10)	C(4A)-C(5A)-C(6A)	126.0(10)
C(4)-C(5)-C(11)	116.9(9)	C(4A)-C(5A)-C(11A)	116.3(9)
C(6)-C(5)-C(11)	116.1(9)	C(6A)-C(5A)-C(11A)	117.7(9)
N(2)-C(6)-C(5)	124.4(9)	N(2A)-C(6A)-C(5A)	125.5(9)
N(2)-C(6)-C(7)	109.2(9)	N(2A)-C(6A)-C(7A)	108.4(9)
C(5)-C(6)-C(7)	126.0(10)	C(5A)-C(6A)-C(7A)	126.0(10)
C(8)-C(7)-C(6)	108.3(10)	C(8A)-C(7A)-C(6A)	108.3(10)
C(7)-C(8)-C(9)	107.9(10)	C(7A)-C(8A)-C(9A)	107.1(9)
N(2)-C(9)-C(10)	126.2(9)	N(2A)-C(9A)-C(10A)	127.6(9)
N(2)-C(9)-C(8)	108.3(9)	N(2A)-C(9A)-C(8A)	108.5(8)
C(10)-C(9)-C(8)	125.5(10)	C(10A)-C(9A)-C(8A)	124.0(9)
C(9)-C(10)-C(1)#1	124.7(9)	C(9A)-C(10A)-C(1A)#2	124.0(9)
C(9)-C(10)-C(18)	118.0(9)	C(9A)-C(10A)-C(18A)	118.8(9)
C(1)#1-C(10)-C(18)	117.3(9)	C(1A)#2-C(10A)-C(18A)	117.1(9)

Table III. (continued)

C(16)-C(11)-C(12)	119.0(10)	C(16A)-C(11A)-C(12A)	117.4(11)
C(16)-C(11)-C(5)	121.2(10)	C(16A)-C(11A)-C(5A)	123.2(11)
C(12)-C(11)-C(5)	119.8(10)	C(12A)-C(11A)-C(5A)	119.4(11)
C(13)-C(12)-C(11)	118.8(11)	C(13A)-C(12A)-C(11A)	120.2(12)
C(14)-C(13)-C(12)	124.3(12)	C(14A)-C(13A)-C(12A)	119.9(13)
C(13)-C(14)-C(15)	117.0(11)	C(13A)-C(14A)-C(15A)	121.0(13)
C(13)-C(14)-C(17)	122.6(11)	C(13A)-C(14A)-C(17A)	119.9(13)
C(15)-C(14)-C(17)	120.5(11)	C(15A)-C(14A)-C(17A)	119.1(13)
C(14)-C(15)-C(16)	122.6(11)	C(14A)-C(15A)-C(16A)	118.4(14)
C(15)-C(16)-C(11)	118.3(11)	C(11A)-C(16A)-C(15A)	122.9(12)
C(23)-C(18)-C(19)	117.7(10)	C(19A)-C(18A)-C(23A)	116.0(10)
C(23)-C(18)-C(10)	121.5(10)	C(19A)-C(18A)-C(10A)	123.2(10)
C(19)-C(18)-C(10)	120.7(9)	C(23A)-C(18A)-C(10A)	120.8(10)
C(20)-C(19)-C(18)	121.1(11)	C(20A)-C(19A)-C(18A)	122.2(10)
C(19)-C(20)-C(21)	121.1(11)	C(19A)-C(20A)-C(21A)	120.9(11)
C(22)-C(21)-C(20)	118.2(11)	C(22A)-C(21A)-C(20A)	117.2(11)
C(22)-C(21)-C(24)	120.9(11)	C(22A)-C(21A)-C(24A)	121.9(11)
C(20)-C(21)-C(24)	120.8(11)	C(20A)-C(21A)-C(24A)	120.8(11)
C(21)-C(22)-C(23)	122.0(11)	C(21A)-C(22A)-C(23A)	122.2(12)
C(22)-C(23)-C(18)	119.8(11)	C(22A)-C(23A)-C(18A)	121.5(11)
C(26)-C(25)-P(1)	119.7(10)	C(26A)-C(25A)-P(2)	114.2(9)
C(28)-C(27)-P(1)	114.2(10)	C(28A)-C(27A)-P(2)	119.9(10)
C(30)-C(29)-P(1)	113.8(8)	C(30A)-C(29A)-P(2)	114.5(9)

Table IV. Crystal data, data collection, and solution and refinement for complex 7, (TTP)Ti[OP(Oct)$_3$]$_2$.

Empirical formula	C$_{96}$H$_{138}$N$_4$O$_2$P$_2$Ti
Crystal habit, color	Irregular block, Dark red
Crystal size	0.25 x 0.20 x 0.18 mm
Crystal system	Monoclinic
Space group	P2$_1$/n
Unit cell dimensions	a = 10.2196(1) Å α = 90°
	b = 28.6024(5) Å β = 96.169(1)°
	c = 15.4589(2) Å γ = 90°
Volume	4492.55(11) Å^3
Z	2
Formula weight	1489.94
Density (calculated)	1.101 Mg/m^3
Absorption coefficient	0.179 mm^{-1}
F(000)	1620
Diffractometer	Siemens SMART Platform CCD
Wavelength	0.71073 Å
Temperature	173(2) K
θ range for data collection	1.42 to 25.00°
Index ranges	-12 ≤ h ≤ 12, 0 ≤ k ≤ 33, 0 ≤ ≤ 18
Reflections collected	21423
Independent reflection	7802 (R$_{int}$ = 0.0574)
System used	SHELXTL-V5.0
Solution	Direct methods
Refinement method	Full-matrix least-squares on F^2
Weighting scheme	W = [σ^2(F$_o^2$) + (AP)^2 + (BP)]$^{-1}$, where P = (F$_o^2$ + 2Fc^2))/3, A = 0.0552, and B = 0.0
Absorption correction	SADABS (Sheldrick, 1996)
Max. and min. transmission	1.000 and 0.487
Data / restraints / parameters	7800 / 0 / 475
R indices (I > 2σ(I) = 7872)	R1 = 0.0548, wR2 = 0.1138
R indices (all data)	R1 = 0.1026, wR2 = 0.1303
Goodness-of-fit on F^2	0.989
Largest diff. peak and hole	0.336 and -0.333 eÅ^{-3}

Table V. Atomic coordinates and equivalent isotropic displacement parameters for complex 7. U(eq) is defined as one third of the trace of the orthogonalized U_{ij} tensor.

Atom	x	y	z	U(eq)
Ti(1)	0.0000	0.0000	0.5000	0.0202(2)
O(1)	0.1116(2)	0.00980(5)	0.39664(10)	0.0250(4)
N(1)	-0.0277(2)	0.07137(6)	0.50583(12)	0.0214(5)
C(1)	-0.1123(2)	0.09807(8)	0.44893(15)	0.0207(6)
C(2)	-0.1000(3)	0.14541(8)	0.4733(2)	0.0262(6)
C(3)	-0.0087(3)	0.14814(8)	0.5457(2)	0.0271(6)
C(4)	0.0364(2)	0.10222(8)	0.5656(2)	0.0222(6)
C(5)	0.1365(2)	0.08951(8)	0.6339(2)	0.0232(6)
C(6)	0.1920(2)	0.04514(8)	0.6461(2)	0.0223(6)
C(7)	0.2901(3)	0.03204(9)	0.7167(2)	0.0272(6)
C(8)	0.3077(3)	-0.01442(8)	0.7135(2)	0.0269(6)
C(9)	0.2210(2)	-0.03249(8)	0.6404(2)	0.0226(6)
C(10)	0.1999(2)	-0.07942(8)	0.6212(2)	0.0225(6)
N(2)	0.1558(2)	0.00521(6)	0.59692(12)	0.0224(5)
C(11)	0.1787(3)	0.12727(8)	0.6977(2)	0.0239(6)
C(12)	0.0903(3)	0.14581(9)	0.7508(2)	0.0327(7)
C(13)	0.1275(3)	0.18073(9)	0.8111(2)	0.0377(7)
C(14)	0.2544(3)	0.19876(9)	0.8198(2)	0.0338(7)
C(15)	0.3416(3)	0.18082(9)	0.7666(2)	0.0383(7)
C(16)	0.3053(3)	0.14581(9)	0.7066(2)	0.0335(7)
C(17)	0.2946(3)	0.23692(10)	0.8856(2)	0.0547(9)
C(18)	0.2684(3)	-0.11504(8)	0.6815(2)	0.0240(6)
C(19)	0.1989(3)	-0.13879(11)	0.7393(2)	0.0510(9)
C(20)	0.2574(3)	-0.17250(11)	0.7951(2)	0.0565(10)
C(21)	0.3883(3)	-0.18435(9)	0.7952(2)	0.0356(7)
C(22)	0.4575(3)	-0.16092(10)	0.7376(2)	0.0475(8)
C(23)	0.3990(3)	-0.12703(10)	0.6813(2)	0.0419(8)
C(24)	0.4515(3)	-0.22126(11)	0.8562(2)	0.0596(10)
P(1)	0.25328(7)	0.01950(2)	0.38250(4)	0.0259(2)

Table V. (continued)

Atom	x	y	z	U(eq)
C(25)	0.3582(3)	-0.02816(8)	0.4207(2)	0.0301(7)
C(26)	0.3156(3)	-0.07425(8)	0.3753(2)	0.0357(7)
C(27)	0.3830(3)	-0.11724(8)	0.4163(2)	0.0310(7)
C(28)	0.3447(3)	-0.16195(8)	0.3673(2)	0.0340(7)
C(29)	0.4040(3)	-0.20601(8)	0.4100(2)	0.0366(7)
C(30)	0.3616(3)	-0.25090(9)	0.3622(2)	0.0388(7)
C(31)	0.4196(3)	-0.29485(9)	0.4064(2)	0.0461(8)
C(32)	0.3809(3)	-0.33957(10)	0.3580(2)	0.0578(10)
C(33)	0.2713(3)	0.02715(9)	0.2677(2)	0.0346(7)
C(34)	0.1426(3)	0.03653(9)	0.2098(2)	0.0411(8)
C(35)	0.0654(3)	-0.00738(10)	0.1834(2)	0.0440(8)
C(36)	-0.0592(3)	0.00145(10)	0.1225(2)	0.0452(8)
C(37)	-0.1297(3)	-0.04307(11)	0.0908(2)	0.0495(8)
C(38)	-0.2595(3)	-0.03569(12)	0.0355(2)	0.0567(9)
C(39)	-0.3314(4)	-0.08049(13)	0.0072(3)	0.0761(12)
C(40)	-0.4564(4)	-0.0731(2)	-0.0542(3)	0.100(2)
C(41)	0.3114(3)	0.07284(8)	0.4357(2)	0.0290(6)
C(42)	0.2427(3)	0.11665(8)	0.3955(2)	0.0304(7)
C(43)	0.2925(3)	0.16181(8)	0.4395(2)	0.0311(7)
C(44)	0.2291(3)	0.20552(8)	0.3973(2)	0.0373(7)
C(45)	0.2813(3)	0.25101(9)	0.4393(2)	0.0392(7)
C(46)	0.2202(3)	0.29477(9)	0.3972(2)	0.0478(9)
C(47)	0.2665(4)	0.34020(9)	0.4400(2)	0.0571(10)
C(48)	0.2070(4)	0.38363(10)	0.3962(3)	0.0767(12)

Table VI. Bond lengths [Å] and angles [°] for complex 7.

Ti(1)–N(1)	2.064(2)	C(18)–C(23)	1.378(4)
Ti(1)–N(1)	2.064(2)	C(18)–C(19)	1.379(4)
Ti(1)–N(2)	2.071(2)	C(19)–C(20)	1.385(4)
Ti(1)–N(2)	2.071(2)	C(20)–C(21)	1.380(4)
Ti(1)–O(1)	2.080(2)	C(21)–C(22)	1.370(4)
Ti(1)–O(1)	2.080(2)	C(21)–C(24)	1.513(4)
O(1)–P(1)	1.513(2)	C(22)–C(23)	1.394(4)
N(1)–C(4)	1.390(3)	P(1)–C(25)	1.795(3)
N(1)–C(1)	1.393(3)	P(1)–C(41)	1.803(2)
C(1)–C(2)	1.407(3)	P(1)–C(33)	1.817(3)
C(1)–C(10)	1.433(3)	C(25)–C(26)	1.534(3)
C(2)–C(3)	1.381(3)	C(26)–C(27)	1.515(3)
C(3)–C(4)	1.414(3)	C(27)–C(28)	1.516(3)
C(4)–C(5)	1.436(3)	C(28)–C(29)	1.518(3)
C(5)–C(6)	1.395(3)	C(29)–C(30)	1.521(3)
C(5)–C(11)	1.494(3)	C(30)–C(31)	1.521(4)
C(6)–N(2)	1.399(3)	C(31)–C(32)	1.513(4)
C(6)–C(7)	1.449(3)	C(33)–C(34)	1.533(4)
C(7)–C(8)	1.342(3)	C(34)–C(35)	1.516(4)
C(8)–C(9)	1.454(3)	C(35)–C(36)	1.520(4)
C(9)–C(10)	1.386(3)	C(36)–C(37)	1.519(4)
C(9)–N(2)	1.401(3)	C(37)–C(38)	1.514(4)
C(10)–(C1)	1.433(3)	C(38)–C(39)	1.518(4)
C(10)–C(18)	1.502(3)	C(39)–C(40)	1.522(5)
C(11)–C(12)	1.390(3)	C(41)–C(42)	1.534(3)
C(11)–C(16)	1.392(4)	C(42)–C(43)	1.521(3)
C(12)–C(13)	1.391(3)	C(43)–C(44)	1.522(3)
C(13)–C(14)	1.389(4)	C(44)–C(45)	1.524(3)
C(14)–C(15)	1.376(4)	C(45)–C(46)	1.514(4)
C(14)–C(17)	1.518(3)	C(46)–C(47)	1.511(4)
C(15)–C(16)	1.388(3)	C(47)–C(48)	1.511(4)

Table VI. (continued)

N(1)–Ti(1)–N(1)	180.0	C(16)–C(11)–C(5)	122.6(2)
N(1)–Ti(1)–N(2)	90.25(7)	C(13)–C(12)–C(11)	121.4(3)
N(1)–Ti(1)–N(2)	89.75(7)	C(12)–C(13)–C(14)	121.1(3)
N(1)–Ti(1)–N(2)	89.74(7)	C(15)–C(14)–C(13)	117.6(2)
N(1)–Ti(1)–N(2)	90.26(7)	C(15)–C(14)–C(17)	121.5(3)
N(2)–Ti(1)–N(2)	180.0	C(13)–C(14)–C(17)	120.9(3)
N(1)–Ti(1)–O(1)	90.61(7)	C(14)–C(15)–C(16)	121.7(3)
N(1)–Ti(1)–O(1)	89.39(7)	C(15)–C(16)–C(11)	121.3(3)
N(2)–Ti(1)–O(1)	95.95(7)	C(23)–C(18)–C(19)	116.4(2)
N(2)–Ti(1)–O(1)	84.05(7)	C(23)–C(18)–C(10)	123.7(2)
Ti(1)–O(1)	89.39(7)	C(19)–C(18)–C(10)	119.9(2)
N(1)–Ti(1)–O(1)	90.61(7)	C(18)–C(19)–C(20)	121.9(3)
N(2)–Ti(1)–O(1)	84.05(7)	C(21)–C(20)–C(19)	121.7(3)
N(2)–Ti(1)–O(1)	95.95(7)	C(22)–C(21)–C(20)	116.5(3)
O(1)–Ti(1)–O(1)	180.0	C(22)–C(21)–C(24)	122.1(3)
P(1)–O(1)–Ti(1)	138.43(10)	C(20)–C(21)–C(24)	121.4(3)
C(4)–N(1)–C(1)	106.7(2)	C(21)–C(22)–C(23)	122.0(3)
C(4)–N(1)–Ti(1)	126.9(2)	C(18)–C(23)–C(22)	121.5(3)
C(1)–N(1)–Ti(1)	26.39(15)	O(1)–P(1)–C(25)	111.14(11)
N(1)–C(1)–C(2)	109.1(2)	O(1)–P(1)–C(41)	111.26(11)
N(1)–C(1)–C(10)	124.7(2)	C(25)–P(1)–C(41)	109.69(12)
C(2)–C(1)–C(10)	126.2(2)	O(1)–P(1)–C(33)	111.23(12)
C(3)–C(2)–C(1)	107.7(2)	C(25)–P(1)–C(33)	107.04(13)
C(2)–C(3)–C(4)	107.4(2)	C(41)–P(1)–C(33)	106.27(12)
N(1)–C(4)–C(3)	109.0(2)	C(26)–C(25)–P(1)	111.8(2)
N(1)–C(4)–C(5)	125.1(2)	C(27)–C(26)–C(25)	114.3(2)
C(3)–C(4)–C(5)	125.8(2)	C(26)–C(27)–C(28)	113.2(2)
C(6)–C(5)–C(4)	125.3(2)	C(29)–C(28)–C(27)	114.4(2)
C(6)–C(5)–C(11)	119.0(2)	C(28)–C(29)–C(30)	114.2(2)
C(4)–C(5)–C(11)	115.7(2)	C(29)–C(30)–C(31)	113.7(2)
C(5)–C(6)–N(2)	126.1(2)	C(32)–C(31)–C(30)	114.1(3)

Table VI. (continued)

C(5)–C(6)–C(7)	125.1(2)	C(34)–C(33)–P(1)	114.8(2)
N(2)–C(6)–C(7)	108.6(2)	C(35)–C(34)–C(33)	113.7(2)
C(8)–C(7)–C(6)	108.2(2)	C(36)–C(35)–C(34)	114.0(2)
C(7)–C(8)–C(9)	107.9(2)	C(35)–C(36)–C(37)	113.4(2)
C(10)–C(9)–N(2)	126.0(2)	C(38)–C(37)–C(36)	115.0(3)
C(10)–C(9)–C(8)	125.3(2)	C(37)–C(38)–C(39)	114.4(3)
N(2)–C(9)–C(8)	108.5(2)	C(38)–C(39)–C(40)	114.2(3)
C(9)–C(10)–(C1)	126.3(2)	C(42)–C(41)–P(1)	113.1(2)
C(9)–C(10)–C(18)	118.2(2)	C(43)–C(42)–C(41)	113.4(2)
C(1)–C(10)–C(18)	115.4(2)	C(42)–C(43)–C(44)	113.6(2)
C(6)–N(2)–C(9)	106.4(2)	C(43)–C(44)–C(45)	114.0(2)
C(6)–N(2)–Ti(1)	126.1(2)	C(46)–C(45)–C(44)	114.4(2)
C(9)–N(2)–Ti(1)	125.51(15)	C(47)–C(46)–C(45)	115.3(3)
C(12)–C(11)–C(16)	116.9(2)	C(48)–C(47)–C(46)	114.7(3)
C(12)–C(11)–C(5)	120.4(2)		

CHAPTER 5: SYNTHESIS, STRUCTURE, AND REACTIVITY OF

ZIRCONIUM AND HAFNIUM IMIDO METALLOPORPHYRINS

A paper submitted to Inorganic Chemistry

Joseph L. Thorman, Ilia A. Guzei, Victor G. Young, Jr.[‡], and L. Keith Woo[*]

Abstract

Zirconium and hafnium porphyrin imido complexes (TTP)M=NAr^{Pr} [TTP = *meso*-

5,10,15,20-tetra-*p*-tolylporphyrinato dianion, M = Zr (1), Hf (2), Ar^{Pr} = 2,6-

diisopropylphenyl] were synthesized from (TTP)MCl$_2$ and 2 equivalents of LiNHAr^{Pr}. The

zirconium imido complex, (TTP)Zr=NAr^{Pr}, was also obtained from the preformed imido

Zr(NAr^{Pr})Cl$_2$(THF)$_2$ and (TTP)Li$_2$(THF)$_2$. Treatment of (TTP)HfCl$_2$ with excess LiNH(*p*-

MeC$_6$H$_4$) resulted in the formation of a bis(amido), (TTP)Hf(NH-*p*-MeC$_6$H$_4$)$_2$ (3), instead of

an imido complex. In the presence of excess aniline, 2 formed an equilibrium mixture of

bis(amido) compounds, (TTP)Hf(NHPh)(NHAr^{Pr}) and (TTP)Hf(NHPh)$_2$. The nucleophilic

character of the imido moiety is exhibited by its reaction with ^{t}BuNCO, producing isolable

N,O-bound ureato metallacycles. The kinetic product obtained with zirconium, (TTP)Zr(η^2-

NAr^{Pr}C(=N^{t}Bu)O) (4a), isomerized to (TTP)Zr(η^2-N^{t}BuC(=NAr^{Pr})O) (4b) in solution.

Upon heating to 80 °C, 4a produced the carbodiimide, Ar^{Pr}N=C=N^{t}Bu, and a transient

Zr(IV) oxo complex. The analogous hafnium complex (TTP)Hf(η^2-NAr^{Pr}C(=N^{t}Bu)O) (5a)

did not eject the carbodiimide upon heating to 110 °C but isomerized to (TTP)Hf(η^2-

N^{t}BuC(=NAr^{Pr})O) (**5b**). To support the formulation of **4a** and **5a** as N,O bound, the

complex (TTP)Hf(η^2-NAr^{Pr}C(=NAr^{Pr})O) (**6**) was studied by variable temperature NMR.

The corresponding thio- and seleno-ureato metallacycles were not isolable in the reaction

between **1** and **2** with ^{t}BuNCS and ^{t}BuNCSe. Concomitant formation of the metallacycle

with decomposition to the carbodiimide, Ar^{Pr}N=C=N^{t}Bu, reflects the lower C-Ch bond

strength in the proposed N,Ch-bound metallacycles. Treatment of **2** with 1,3-

diisopropylcarbodiimide resulted in the η^2-guanidino complex, (TTP)Hf(η^2-

NAr^{Pr}C(=N^{i}Pr)N^{i}Pr) (**7a**), which isomerized to the less sterically crowded isomer

(TTP)Hf(η^2-N^{i}PrC(=NAr^{Pr})N^{i}Pr) (**7b**). Complexes **1**, **2**, **4a**, **4b**, and **7a** were characterized

by X-ray crystallography. The monomeric terminal imido compounds, **1** and **2**, are

isomorphous: M-N$_{(imido)}$ distances of 1.863(2) Å (Zr) and 1.859(2) Å (Hf); M-N$_{(imido)}$-C

angles of 172.5(2)° (Zr) and 173.4(2)° (Hf). The structures of the ureato complexes **4a** and

4b and the guanidino complex **7a** exhibit typical alkoxido and amido bond distances (Zr-N:

2.1096(13) Å (**4a**), 2.137(3) Å (**4b**); Zr-O: 2.0677(12) Å (**4a**), 2.066(3) Å (**4b**); Hf-N:

2.087(2) Å, 2.151(2) Å (**7a**)).

Introduction

The discovery of C-H bond activation by zirconium imido complexes in 1988

prompted investigations of group 4 imido complexes in a variety of supporting ligand

environments.[1,2] Cyclopentadienyl, bulky amido, tetraazaannulene, alkoxo, and bis(amido-

phosphine) groups have been successfully employed as ancillary ligands for isolable terminal

Ti, Zr, and Hf imido complexes.[1,2,3,4,5,6,7,8,9,10] Titanium imido compounds rapidly became the

most studied of group 4 and have revealed novel chemistry[11] including C-H bond

activation,[12] [2+2] cycloaddition,[9] and use in titanium nitride film deposition processes.[13]

The documented reactivity associated with the M=NR moiety involving zirconium has been

more varied. The nucleophilic character of the imido nitrogen has been utilized in

hydroamination catalysis,[14] dihydrogen activation,[15] and the formation of a wide variety of

metallacycles with substrates ranging from azidotrimethylsilane and benzaldehyde

N-phenylimine[8] to ethylene.[7] Alkynes, isocyanates, and isocyanides have produced isolable

[2+2] cycloaddition products as well (Scheme 1).[1,7,9,16] Studies of hydroamination and

hydrocarbon activation involving zirconium imido complexes illustrate the need for further

investigations utilizing different ancillary ligands.[14,17] We have recently explored the

chemistry of tetravalent titanium and tin metalloporphyrin complexes containing amido and

imido ligands (Scheme 2).[18] The metals in the titanium and tin hexa-coordinate complexes

reside in the plane of the porphyrin and thus have the ancillary ligands situated in a *trans*-

configuration. In comparison, the larger congeners of group 4 have the metal displaced

substantially above the porphyrin by ~ 1 Å. This generates a *cis*-arrangement of unidentate

substituents which is slightly more sterically confined relative to metallocene analogues.[19] A

similar coordination environment is seen in the more flexible and less sterically demanding

tetramethyldibenzotetraaza[14]annulene (TMTAA) ligand. For example, the imido complex

of Zr(TMTAA) includes a bound pyridine *cis* to the nitrene group.[20] Monomeric zirconium

and hafnium metalloporphyrin chemistry has been explored with a wide variety of ligands,

though all are limited to formal single bonds between the metal and ligand.[19] Herein we

describe the first isolation and reactivity of zirconium and hafnium metalloporphyrin imido

Cp$_2$Zr=N^{t}Bu + MeC≡CPh ⟶ [structure: four-membered ring with N-^{t}Bu at top, Cp$_2$Zr at left, Me at right, Ph at bottom]

(tmtaa)Zr=NAr^{iPr} + ^{t}BuNCO ⟶ [structure: four-membered ring with N-Ar at top, (tmtaa)Zr at left, =O at right carbon, N-^{t}Bu at bottom]

[structure: Cp$_2$Zr with N^{t}Bu and THF] + 2 ^{t}BuNC ⟶ [structure: Cp$_2$Zr ring with N^{t}Bu, N-^{t}Bu, CN^{t}Bu]

Scheme 1.

(TTP)TiCl$_2$ + 2 LiNHR → (TTP)Ti=NR + 2 LiCl + H$_2$NR

(TTP)TiCl$_2$ + excess H$_2$N^{t}Bu → (TTP)Ti=N^{t}Bu + 2 [H$_3$N^{t}Bu]Cl

(TTP)Ti(η^2-EtCCEt) + ½ PhN=NPh → (TTP)Ti=NPh + EtCCEt

(TTP)Ti(η^2-EtCCEt) + N$_3$TMS → (TTP)Ti=NTMS + N$_2$

(TTP)Ti(NPh$_2$)$_2$ + H$_2$N^{t}Bu → (TTP)Ti=N^{t}Bu + 2 HNPh$_2$

(TTP)TiCl$_2$ + 2 LiNPh$_2$ → (TTP)Ti(NPh)$_2$ + 2 LiCl

(TTP)SnCl$_2$ + 2 LiNHPh → (TTP)Sn(NHPh)$_2$ + 2 LiCl

(TTP)Sn(NHPh)$_2$ + 2 H$_2$Ntolyl → (TTP)Sn(NHtolyl)$_2$ + 2 H$_2$NPh

Scheme 2.

complexes as well as the characterization of N,O-bound ureato(2-) and guanidino(2-) derivatives.

Experimental

General Procedures. All manipulations were performed under an inert atmosphere of nitrogen using a Vacuum Atmospheres glovebox equipped with a Model MO40-1 Dri-Train gas purifier. All solvents were rigorously degassed and dried prior to use. Benzene-d_6, toluene, and hexane were freshly distilled from purple solutions of sodium benzophenone and brought into the glovebox without exposure to air. The dichloro complexes $(TTP)ZrCl_2$ and $(TTP)HfCl_2$ were prepared according to published procedures,[21] but were recrystallized from CH_2Cl_2/hexane prior to use. Commercially purchased compounds, p-toluidine, 2,6-diisopropylaniline, ^tBuNCO, and ^tBuNCS (Aldrich) were dried over activated neutral alumina. The compounds $Zr(Ar^{Pr})Cl_2(THF)_2$,[5] ^tBuNCSe,[22] and $LiNHAr^{Pr}$[5] were prepared from literature procedures. ^1H NMR data were recorded at 20.0 °C, unless otherwise stated, on either Varian VXR (300 MHz) or Bruker DRX (400 MHz) spectrometers. Chemical shifts were referenced to proton solvent impurities (δ 7.15, C_6D_5H). UV-vis data were recorded on a HP8452A diode array spectrophotometer and reported as λ_{max} in nm (log ϵ). Elemental analyses (C, H, N) were performed by Iowa State University Instrument Services.

$(TTP)Zr=NAr^{Pr}$, 1. Method 1: To a toluene solution (ca. 20 mL) of $(TTP)ZrCl_2$ (352.6 mg, 0.424 mmol) at -25C was added a slurry of $LiNHAr^{Pr}$ (166.4 mg, 0.908 mmol) in toluene (ca. 6 mL). This solution slowly darkened to a red color upon warming to 25 °C. After 2 h, the solution was filtered over celite. The filtrate was concentrated *in vacuo* to a

black oil. This residue was triturated with hexanes (ca. 12 mL), filtered, and dried *in vacuo* to afford dark blue **1** (370.4 mg, 93% yield). Analytically pure crystalline samples could be obtained by layering a toluene solution with hexanes (1:2 V:V), allowing to stand at -25 °C, filtering, and drying the solid *in vacuo*. ^{1}H NMR (C_6D_6, 300 MHz): 9.17 (s, 8H, β-H), 8.26 (d, 4H, $^3J_{H-H}$ = 8 Hz, *meso*-$C_6H_4CH_3$), 7.97 (d, 4H, $^3J_{H-H}$ = 8 Hz, *meso*-$C_6H_4CH_3$), 7.28 (dd, 8H, $^3J_{H-H}$ = 8 Hz, *meso*-$C_6H_4CH_3$), 6.08 (s, 3H, *m*-, *p*-C_6H_3), 2.42 (s, 12H, *meso*-$C_6H_4CH_3$), 0.18 (m, 2H, -$CHMe_2$), 0.00 (d, 12H, $^3J_{H-H}$ = 7 Hz, -CH*Me*$_2$). ^{13}C NMR (CD_2Cl_2, 400 MHz): 153.8, 144.3, 143.6, 142.8, 139.9, 138.9, 137.9, 133.8 (*o*-tolyl), 133.0 (*o*-tolyl), 132.6, 132.4 (β-pyrrole), 130.0, 129.4 (*m*-tolyl), 124.3, 119.5 (*m*-Ar^{Pr}), 115.0 (*p*-Ar^{Pr}), 27.8 (-CHMe$_2$), 26.1 (-CH*Me*$_2$), 25.7 (*p*-MeC_6H_5). UV/vis (benzene): 544 (4.32), 439 (shoulder, 4.44), 420 (5.56), 398 (shoulder, 4.53). Anal. Calcd. for $C_{60}H_{53}N_5Zr$: C, 77.05; H, 5.71; N, 7.49. Found: C, 76.66; H, 5.97; N, 7.02. Method 2: A round bottom flask was charged with Zr(NAr^{Pr})Cl$_2$(THF)$_2$ (171.9 mg, 0.357 mmol) and (TTP)Li$_2$(THF)$_2$ (119.3 mg, 0.173 mmol). Toluene (ca. 20 mL) was added and the reaction mixture was allowed to stir at ambient temperature for 18 h. The dark red solution was filtered over celite and the filtrate reduced to dryness *in vacuo*. Recrystallization from toluene/hexanes at -25 °C afforded **1** (126 mg, 78% yield).

(TTP)Hf=NAr^{Pr}, 2. To a rapidly stirred toluene solution (ca. 15 mL) of (TTP)HfCl$_2$ (212.6 mg, 0.232 mmol) at -25 °C was added a slurry of LiNHAr^{Pr} (89.6 mg, 0.489 mmol) in toluene (ca. 6 mL). The solution became dark red upon warming to 25 °C over 2 h. The solution was then filtered over celite. The filtrate was concentrated *in vacuo* to a black oil. This residue was triturated with hexanes (ca. 12 mL), filtered, washed with hexanes (4 x 4

mL), and dried *in vacuo* to afford dark blue **2** (143 mg, 60% yield). Crystals were grown

analogously to **1**. ^{1}H NMR (C$_6$D$_6$, 300 MHz): 9.17 (s, 8H, β-H), 8.23 (dd, 4H, $^3J_{H-H}$ = 8

Hz, $^2J_{H-H}$ = 2 Hz, *meso*-C$_6H_4$CH$_3$), 7.97 (dd, 4H, $^3J_{H-H}$ = 8 Hz, $^2J_{H-H}$ = 2 Hz, *meso*-C$_6H_4$CH$_3$),

7.31 (d, 4H, $^3J_{H-H}$ = 8 Hz, *meso*-C$_6H_4$CH$_3$), 7.25 (d, 4H, $^3J_{H-H}$ = 8 Hz, *meso*-C$_6H_4$CH$_3$), 6.16

(d, 2H, $^3J_{H-H}$ = 8 Hz, *m*-C$_6H_3$), 6.04 (t, 1H, $^3J_{H-H}$ = 8 Hz, *p*-C$_6$H$_3$), 2.41 (s, 12H, *meso*-

C$_6$H$_4$C*H$_3$*), 0.17 (m, 2H, -C*H*Me$_2$), 0.00 (d, 12H, $^3J_{H-H}$ = 7 Hz, -CH*Me$_2$*). UV/vis (benzene):

542 (4.52), 419 (5.67), 397 (shoulder, 4.80). Anal. Calcd. for C$_{60}$H$_{53}$N$_5$Hf: C, 70.47; H,

5.22; N, 6.85. Found: C, 70.39; H, 5.25; N, 6.54.

(TTP)Hf(NHC$_6$H$_4$-*p*-Me)$_2$, 3. A slurry of (TTP)HfCl$_2$ (252.6 mg, 0.275 mmol) and

LiNH(*p*-MeC$_6$H$_4$) (67.7 mg, 0.60 mmol) in hexanes (ca. 15 mL) was stirred for 10 hours at

25 °C at which time the dark red suspension was filtered. The solid was transferred to a

clean fritted filter and washed through with CH$_2$Cl$_2$ (2 x 2 mL). The resulting solution was

taken to dryness to yield blue microcrystalline **3** (172 mg, 59% yield). ^{1}H NMR (C$_6$D$_6$, 300

MHz): 9.17 (s, 8H, β-H), 8.24 (d, 4H, $^3J_{H-H}$ = 7 Hz, *meso*-C$_6H_4$CH$_3$), 7.88 (d, 4H, $^3J_{H-H}$ = 7

Hz, *meso*-C$_6H_4$CH$_3$), 7.28 (br, 8H, *meso*-C$_6H_4$CH$_3$), 6.13 (d, 4H, $^3J_{H-H}$ = 8 Hz, *m*-tolyl), 4.27

(d, 4H, $^3J_{H-H}$ = 8 Hz, *o*-tolyl), 2.40 (s, 12H, *meso*-C$_6$H$_4$C*H$_3$*), 1.74 (s, 6H, *p*-*Me*C$_6$H$_4$), 0.96

(s, 2H, N*H*). UV/vis (benzene): 544 (4.44), 418 (5.56), 398 (shoulder, 4.80).

(TTP)Zr(η^2-NAr^{iPr}C(=N^{t}Bu)O), 4a. A solution of (TTP)Zr=NAr^{iPr} (313 mg, 0.334

mmol) and ^{t}BuNCO (250 L, 2.19 mol) in toluene (ca. 15 mL) was stirred for 13 h, reduced

to dryness *in vacuo* and recrystallized from a toluene solution layered with heptane at -25 °C

for 1 day to yield microcrystalline dark blue **4a** (112 mg, 32% yield). ^{1}H NMR (C$_6$D$_6$, 300

MHz): 9.13 (s, 8H, β-H), 8.13 (d, 4H, $^3J_{H-H}$ = 8 Hz, *meso*-C$_6H_4$CH$_3$), 7.87 (d, 4H, $^3J_{H-H}$ = 8

Hz, *meso*-C$_6$H$_4$CH$_3$), 7.29 (dd, 8H, $^3J_{H-H}$ = 8 Hz, *meso*-C$_6$H$_4$CH$_3$), 6.79 (t, 1H, $^3J_{H-H}$ = 8 Hz,

p-C$_6$H$_3$), 6.60 (d, 2H, $^3J_{H-H}$ = 8 Hz, *m*-C$_6$H$_3$), 2.40 (s, 12H, *meso*-C$_6$H$_4$C*H$_3$*), 0.82 (d, 6H, $^3J_{H-}$

$_H$ = 7 Hz, -CH*Me$_2$*), 0.42 (d, 6H, $^3J_{H-H}$ = 7 Hz, -CH(C*H$_3$*)$_2$), 0.35 (s, 9H, N-C*Me$_3$*), -0.51 (m,

2H, -C*H*Me$_2$). ^{13}C NMR (C$_6$D$_6$, 400 MHz): 152.5, 149.6, 142.7, 140.6, 139.0, 138.0,

135.5, 133.6, 132.8, 127-130 (C$_6$D$_6$), 125.6, 123.4, 121.6, 50.4, 30.4, 27.1, 25.2, 24.2, 21.4.

UV/vis (toluene): 550 (4.65), 439 (shoulder, 4.94), 418 (5.73). Anal. Calcd. for

C$_{65}$H$_{62}$N$_6$OZr: C, 75.47; H, 6.04; N, 8.12. Found: C, 75.24; H, 6.14; N, 7.94. Exposure to

water results in rapid decomposition to yield the urea, Ar^{Pr}NHC(O)NH^{t}Bu, as detected by

GCMS: Calcd. (found) C$_{17}$H$_{28}$N$_2$O 276.42 (277) m/z. ^{1}H NMR (C$_6$D$_6$, 300 MHz): 7.16 (m,

1H, *p*-C$_6$H$_3$), 7.08 (d, 2H, *m*-C$_6$H$_3$), 4.02 (s, 1H, N*H*), 3.57 (m, 2H, -C*H*Me$_2$), 1.23 (d, 12H,

-CH*Me$_2$*), 1.18 (s, 9H, N-C*Me$_3$*).

(TTP)Zr(η^2-N^{t}BuC(=NAr^{Pr})O), 4b. A solution of (TTP)Zr=NAr^{Pr} (330 mg, 0.353

mmol) and ^{t}BuNCO (250 L, 2.19 mol) in toluene (ca. 15 mL) was stirred for 13 h, reduced

to dryness *in vacuo* and recrystallized from toluene/heptane at -25 °C over 17 days.

Filtration yielded microcrystalline red **4b** which was washed with 12 mL of toluene (104.5

mg, 29% yield). By ^{1}H NMR one-half equivalent of toluene was observed as a solvate. ^{1}H

NMR (C$_6$D$_6$, 400 MHz): 9.09 (s, 8H, *β*-H), 8.23 (d, 4H, $^3J_{H-H}$ = 6 Hz, *meso*-C$_6$H$_4$CH$_3$), 7.83

(d, 4H, $^3J_{H-H}$ = 6 Hz, *meso*-C$_6$H$_4$CH$_3$), 7.38 (d, 4H, $^3J_{H-H}$ = 6 Hz, *meso*-C$_6$H$_4$CH$_3$), 7.25 (d,

4H, $^3J_{H-H}$ = 6 Hz, *meso*-C$_6$H$_4$CH$_3$), 6.98 (m, 1H, *p*-C$_6$H$_3$), 6.91 (d, 2H, *m*-C$_6$H$_3$), 2.41 (s,

12H, *meso*-C$_6$H$_4$C*H$_3$*), 1.84 (spt, 2H, -C*H*Me$_2$), 0.78 (d, 6H, $^3J_{H-H}$ = 7 Hz, -CH*Me$_2$*), 0.31 (d,

6H, $^3J_{H-H}$ = 7 Hz, -CH*Me$_2$*), -0.14 (s, 9H, N-C*Me$_3$*). ^{13}C NMR (C$_6$D$_6$, 400 MHz): 154.3,

150.1, 145.4, 139.6, 138.0, 137.8, 135.4 (*o*-tolyl), 133.6 (*o*-tolyl), 132.8 (*β*-pyrrole), 127-

129 solvent, 125.6 (*m*-tolyl), 121.4 (*m*-Ar^{Pr}), 120.6 (*p*-Ar^{Pr}), 53.0 (-*C*(Me)$_3$), 29.0 (C(*Me*)$_3$),

28.0 (-*C*H(Me)$_2$), 23.6 (-CH(*Me*)$_2$), 23.1 (-CH(*Me*)$_2$), 21.4 (*p*-*Me*C$_6$H$_5$). UV-vis (toluene):

551 (4.31), 4.39 (shoulder, 4.57), 417 (5.46). Anal. Calcd. for C$_{68.5}$H$_{66}$N$_6$OZr: C, 76.14; H,

6.16; N, 7.78. Found: C, 76.21; H, 6.37; N, 7.32. Exposure to water results in rapid

decomposition to yield the urea Ar^{Pr}NHC(O)NH^{t}Bu as detected by GCMS.

(TTP)Hf(η^2-NAr^{Pr}C(=N^{t}Bu)O), 5a. A solution of (TTP)Hf=NAr^{Pr} (324 mg, 0.317

mmol) and ^{t}BuNCO (54 L, 0.473 mmol) in toluene (ca. 10 mL) was stirred for 4.5 h at 25

°C. The solution was filtered and the filtrate was reduced *in vacuo* to produce an oily

residue. The residue was triturated with 10 mL of hexanes and filtered to yield blue 5a (228

mg, 64% yield). ^{1}H NMR (C$_6$D$_6$, 300MHz): 9.16 (s, 8H, β-H), 8.12 (d, 4H, $^3J_{H-H}$ = 7 Hz,

meso-C$_6$H$_4$CH$_3$), 7.86 (d, 4H, $^3J_{H-H}$ = 7 Hz, *meso*-C$_6$H$_4$CH$_3$), 7.29 (dd, 8H, $^3J_{H-H}$ = 7 Hz,

meso-C$_6$H$_4$CH$_3$), 6.77 (t, 1H, *p*-C$_6$H$_3$), 6.62 (d, 2H, *m*-C$_6$H$_3$), 2.40 (s, 12H, *meso*-C$_6$H$_4$C*H$_3$*),

0.84 (d, 6H, $^3J_{H-H}$ = 7 Hz, -CH*Me$_2$*), 0.43 (d, 6H, $^3J_{H-H}$ = 7 Hz, -CH*Me$_2$*), 0.34 (s, 9H, N-

C*Me$_3$*), -0.53 (m, 2H, -C*H*Me$_2$). ^{13}C NMR (C$_6$D$_6$, 400 MHz): 151.9, 149.7, 143.5, 140.4,

138.9, 138.0, 135.5 (*o*-tolyl), 133.6 (*o*-tolyl), 133.0 (β-pyrrole), 129-127 solvent, 125.6,

123.5 (*p*-Ar^{Pr}), 121.5 (*m*-Ar^{Pr}), 50.3 (-*C*(Me)$_3$), 30.4 (-C(*Me*)$_3$), 26.9 (-*C*H(Me)$_2$), 25.3

(-CH(*Me*)$_2$), 24.4 (-CH(*Me*)$_2$), 21.4 (*p*-*Me*C$_6$H$_5$). UV/vis (toluene): 549 (4.40), 416 (5.47).

Anal. Calcd. for C$_{65}$H$_{62}$N$_6$OHf: C, 69.60; H, 5.57; N, 7.49. Found: C, 69.20; H, 5.53; N,

7.30. Exposure to water results in rapid decomposition to yield the urea

Ar^{Pr}NHC(O)NH^{t}Bu.

(TTP)Hf(η^2-NAr^{Pr}C(=NAr^{Pr})O), 6. A solution of (TTP)Hf=NAr^{Pr} (290.7 mg,

0.284 mmol) and Ar^{Pr}NCO (47 L, 0.412 mmol) in toluene (ca. 40 mL) was stirred for 10 h

at 25 °C. The solution was filtered and the filtrate was reduced in volume (ca. 13 mL) *in vacuo*. The concentrated solution was layered with hexanes (ca. 13 mL) and placed in freezer at -25 °C overnight. This solution was filtered and the filtrate reduced to dryness *in vacuo*. The residue was recrystallized from a toluene solution layered with hexanes at -25 °C overnight. Compound 6 was collected as a dark blue powder (81 mg, 25% yield). ^{1}H NMR (C_7D_8, 400 MHz): 9.04 (s, 8H, β-H), 7.84 (d, 4H, $^3J_{H-H}$ = 7 Hz, *meso*-$C_6H_4CH_3$), 7.79 (d, 4H, $^3J_{H-H}$ = 7 Hz, *meso*-$C_6H_4CH_3$), 7.36 (d, 4H, $^3J_{H-H}$ = 7 Hz, *meso*-$C_6H_4CH_3$), 7.29 (d, 4H, $^3J_{H-H}$ = 7 Hz, *meso*-$C_6H_4CH_3$) 6.94 (t, 1H, *p*-C_6H_3), 6.84 (t, 1H, *p*-C_6H_3), 6.79 (d, 2H, *m*-C_6H_3), 6.61 (d, 2H, *m*-C_6H_3), 2.44 (s, 12H, *meso*-$C_6H_4CH_3$), 1.93 (m, 2H, -CHMe$_2$), 0.62 (d, 6H, -CHMe_2), 0.44 (d, 6H, -CHMe_2), 0.33 (bs, 12H, -CHMe_2), -0.07 (m, 2H, -CHMe$_2$). ^{13}C NMR (C_6D_6, 400 MHz). 151.5, 149.6, 148.8, 144.1, 140.7, 138.7, 138.6, 138.1, 135.5, 132.9 (β-pyrrole), 132.7, 130-126 solvent, 125.9, 123.9, 122.0, 121.7, 120.8, 26.9(-CH(Me)$_2$), 26.8(-CH(Me)$_2$), 26.5(-CH(Me)$_2$), 24.7(-CH(Me)$_2$), 23.8(-CH(Me)$_2$), 21.4(p-MeC$_6$H$_4$). UV/vis (toluene): 549 (4.27), 415 (5.45). Anal. Calcd. for $C_{73}H_{70}N_6OHf$: C, 71.52; H, 5.76; N, 6.86. Found: C, 69.20; H, 5.53; N, 7.30. This compound appeared pure by ^{1}H NMR, but elemental analyses were routinely low in carbon by 1% or more. Exposure to water results in rapid decomposition to yield the urea $Ar^{iPr}NHC(O)NHAr^{iPr}$.

(TTP)Hf(η^2-NAr^{iPr}C(=N^{i}Pr)N^{i}Pr), 7a. To a stirred solution of 2 (294.7 mg, 0.288 mmol) in toluene (ca. 12 mL) was added 1,3-diisopropylcarbodiimide (69 L, 0.441 mmol). The mixture was allowed to stir at ambient temperature for 2 hours. This dark red solution was filtered and reduced to dryness *in vacuo*. The residue was washed with hexanes (2 x 6 mL) to afford dark blue 7a (147.1 mg, 44% yield). Crystals suitable for X-ray diffraction

were obtained by recrystallization from a toluene solution layered with hexanes at -25 °C.

^{1}H NMR (C_6D_6, 400 MHz): 9.13 (s, 8H, β-H), 8.22 (d, 4H, $^3J_{H-H}$ = 8 Hz, meso-$C_6H_4CH_3$),

7.76 (d, 4H, $^3J_{H-H}$ = 8 Hz, meso-$C_6H_4CH_3$), 7.35 (d, 4H, $^3J_{H-H}$ = 8 Hz, meso-$C_6H_4CH_3$), 7.24

(d, 4H, $^3J_{H-H}$ = 8 Hz, meso-$C_6H_4CH_3$), 6.85 (t, 1H, $^3J_{H-H}$ = 8 Hz, p-C_6H_3), 6.68 (d, 2H, $^3J_{H-H}$ =

8 Hz, m-C_6H_3), 2.40 (s, 12H, meso-$C_6H_4CH_3$), 1.63 (m, 1H, $^3J_{H-H}$ = 6 Hz, N-CHMe$_2$), 0.96

(d, 6H, $^3J_{H-H}$ = 7 Hz, C_6H_3-CHMe_2), 0.46 (dd, 12H, N-CHMe_2 and C_6H_3-CHMe_2), 0.13 (bd,

7H, $^3J_{H-H}$ = 6 Hz, N-CHMe_2 and N-CHMe$_2$), -0.31 (m, 2H, $^3J_{H-H}$ = 7 Hz, C_6H_3-CHMe$_2$).

COSY was used to identify protons in overlapping signals. The 2,6-di-isopropyl resonances

on the NAr^{Pr} fragment were definitively assigned by HMBC. ^{13}C NMR (C_6D_6, 200 MHz):

152.0, 150.3, 146.1, 142.3 (o-Ar^{Pr}), 139.1, 137.9, 135.3 (o-tolyl), 133.7 (o-tolyl), 132.8

(β-pyrrole), 130-126 solvent, 125.3, 122.8 (p-Ar^{Pr}), 122.7 (m-Ar^{Pr}), 47.38, 26.8, 25.6, 24.5,

22.8, 21.4. UV/vis (toluene): 549 (4.32), 416 (5.42). ^{1}H NMR showed that one equivalent

of toluene remained after extended drying in vacuo. Anal. Calcd. for $C_{67}H_{67}N_7Hf\cdot C_7H_8$: C,

71.62; H. 6.09; N, 7.90. Found: C, 71.58; H, 6.23; N, 7.70. Exposure to water results in

rapid decomposition to yield the guanine Ar^{Pr}NHC(=N^{i}Pr)NH^{i}Pr as detected by GCMS:

calcd. (found) $C_{19}H_{33}N_3$ 303.49 (305 [M + H$^+$]).

Reaction of 2 with Aniline. An NMR tube equipped with a Teflon stopcock was

charged with 2 (10.36 mg, 10.13 mol), Ph$_3$CH (88.5 mL, 0.1397 M, 12.36 mol) as an

internal standard, H$_2$NPh (2.9 L, 31.8 mol) and C_6D_6 (ca. 0.6 mL). This solution was

allowed to equilibrate over 11 hours at 25 °C at which time there were present in solution,

H$_2$NAr^{Pr} (9.89 mol), H$_2$NPh (14.8 mol), (TTP)Hf(NHAr^{Pr})(NHPh) (1.5 mol), and

(TTP)Hf(NHPh)$_2$ (7.32 mol). K = 3.3 ± 0.3. ^{1}H NMR (C_6D_6, 400 MHz): 9.16 (s, β-H,

(TTP)Hf(NHPh)$_2$ and (TTP)Hf(NHPh)(NHAr^{Pr})), 8.22 (bd, *meso*-C$_6$*H*$_4$CH$_3$

(TTP)Hf(NHPh)$_2$ and (TTP)Hf(NHPh)(NAr^{Pr}))$_2$, 7.86 (bd, *meso*-C$_6$*H*$_4$CH$_3$

(TTP)Hf(NHPh)$_2$ and (TTP)Hf(NHPh)(NAr^{Pr})), 7.26 (b, *meso*-C$_6$*H*$_4$CH$_3$ (TTP)Hf(NHPh)$_2$

and (TTP)Hf(NHPh)(NAr^{Pr})), 6.91 (t, *p*-H$_2$N*Ar^{Pr}*), 6.71 (t, *p*-H$_2$N*Ph*), 6.52 (t, *p*-C$_6$*H*$_3$

(TTP)Hf(NHPh)(NHAr^{Pr})), 6.32 (m, *m*-H$_2$N*Ph* and *m*-NH*Ph* of (TTP)Hf(NHPh)$_2$), 6.06

(m, *p*-HN*Ph* of (TTP)Hf(NHPh)$_2$ and (TTP)Hf(NHPh)(NHAr^{Pr})), 4.24 (d, *o*-C$_6$*H*$_5$ of

(TTP)Hf(NHPh)$_2$), 4.06 (d, *o*-C$_6$*H*$_5$ of (TTP)Hf(NHPh)(NHAr^{Pr})), 3.16 (bs, *H*$_2$NAr^{Pr}), 2.73

(bs, *H*$_2$NPh), 2.62 (m, H$_2$NAr^{Pr}), 2.39 (s, *meso*-C$_6$H$_4$C*H*$_3$), 1.13 (d, H$_2$NAr^{Pr}), 0.93 (s,

(TTP)Hf(N*H*Ph)$_2$ and (TTP)Hf(N*H*Ph)(N*H*Ar^{Pr})), 0.38 (d, (TTP)Hf(NHPh)(NHAr^{Pr}), 0.14

(d, (TTP)Hf(NHPh)(NHAr^{Pr}), −0.05 (m, (TTP)Hf(NHPh)(NHAr^{Pr}).

Decomposition of 4a. An NMR tube equipped with a Teflon stopcock was charged

with **4a** (11.9 mg, 11.5 mol), Ph$_3$CH (87.5 mL, 0.1455 M, 12.73 mol) as an internal

standard, and C$_6$D$_6$ (ca. 0.6 mL). After 238 h at 80 °C, **4a** had been consumed, compounds

4b (1.24 mol), [(TTP)ZrO]$_2$ (0.42 mol), and Ar^{Pr}N=C=N'Bu (9.5 mol, 83% yield by NMR)

were detected. ^{1}H NMR (C$_6$D6, 300 MHz): Ar^{Pr}N=C=N'Bu: 7.07 (m, 3H, *m*-, *p*-C$_6$*H*$_3$),

3.64 (spt, 2H -C*H*Me$_2$), 1.24 (d, 12H, -CH*Me$_2$*), 1.18 (s, 9H, N-*'Bu*). [(TTP)ZrO]$_2$: 8.74 (s,

8H, *β*-H), 7.95 (d, 4H, *meso*-C$_6$*H*$_4$CH$_3$), 7.56 (d, 4H, *meso*-C$_6$*H*$_4$CH$_3$), 7.42 (d, 4H, *meso*-

C$_6$*H*$_4$CH$_3$), 2.45 (s, 12H, *meso*-C$_6$H$_4$C*H*$_3$).

Decomposition of 4b. An NMR tube equipped with a Teflon stopcock was charged

with **4b** (7.32 mg, 7.58 mmol), Ph$_3$CH (90.0 mL, 0.1455 M, 13.1 mmol) as an internal

standard, and C$_7$D$_8$ (ca. 0.6 mL). After 228.5 h at 110 °C, **4b** had been consumed,

[(TTP)ZrO]$_2$ and Ar^{Pr}N=C=N'Bu (6.96 mmol, 92% yield by NMR) were produced. ^{1}H

NMR: $Ar^{iPr}N=C=N^tBu$: 3.60 (m, 2H, $-CHMe_2$), 1.23 (d, 12H, $-CHMe_2$), 1.20 (s, 9H, ^tBu), all other signals obscured by solvents. $[(TTP)ZrO]_2$:[23] 8.69 (s, 16H, β-H), 7.81 (d, 8H, $meso$-$C_6H_4CH_3$), 7.61 (d, 8H, $meso$-$C_6H_4CH_3$), 7.43 (d, 8H, $meso$-$C_6H_4CH_3$), 7.18 (d, 8H, $meso$-$C_6H_4CH_3$), 2.51 (s, 24H, $meso$-$C_6H_4CH_3$).

Reaction of 1 with ^tBuNCS. An NMR tube equipped with a Teflon stopcock was charged with 1 (17.43 mg, 18.63 mol), Ph_3CH (92.0 mL, 0.1397 M, 12.85 mol) as an internal standard, ^tBuNCS (2.8 L, 23.2 mol), and C_6D_6 (ca. 0.6 mL). After 21 h at 25°C, 1 had been consumed and $(TTP)Zr(\eta^2\text{-}NAr^{iPr}C(=N^tBu)S)$ (4.33 mol), $[(TTP)ZrS]_2$ (0.92 mol), and $Ar^{iPr}N=C=N^tBu$ (12.35 mol) had been produced. After an additional 70 h at 25°C, a large amount of brown precipitate was present as well as $[(TTP)ZrS]_2$ (0.21 mol) and $Ar^{iPr}N=C=N^tBu$ (16.91 mol, 91% yield by NMR). ^1H NMR (C_6D_6, 300 MHz): $Ar^{iPr}N=C=N^tBu$: 7.07 (m, N-2,6-(^iPr)C_6H_3), 3.64 (m, N-2,6-(^iPr)C_6H_3), 1.24 (d, N-2,6-(Pr)C_6H_3), 1.18 (s, N-^tBu). $[(TTP)Zr(\eta^2\text{-}NAr^{iPr}C(=N^tBu)S)]$: 9.08 (s, 8H, β-H), 8.30 (d, 4H, $meso$-$C_6H_4CH_3$), 7.69 (d, 4H, $meso$-$C_6H_4CH_3$), 7.35 (d, 4H, $meso$-$C_6H_4CH_3$), 7.21 (d, 4H, $meso$-$C_6H_4CH_3$), 6.96 (t, 1H, p-C_6H_3), 6.76 (d, 2H, m-C_6H_3), 2.39 (s, 12H, $meso$-$C_6H_4CH_3$), 1.02 (d, 6H, $-CHMe_2$), 0.52 (s, 9H, N-CMe_3), 0.51 (d, 6H, $-CHMe_2$), -0.13 (m, 2H, $-CHMe_2$). $[(TTP)ZrS]_2$: 8.74 (s, 8H, β-H), 7.95 (d, 4H, $meso$-$C_6H_4CH_3$), 7.56 (d, 4H, $meso$-$C_6H_4CH_3$), 7.42 (d, 4H, $meso$-$C_6H_4CH_3$), 2.45 (s, 12H, $meso$-$C_6H_4CH_3$).

Reaction of 2 with ^tBuNCS. An NMR tube equipped with a Teflon stopcock was charged with 2 (13.88 mg, 13.57 mol), Ph_3CH (67 mL, 0.1397 M, 9.36 mol) as an internal standard, ^tBuNCS (1.8 L, 14.90 mol), and C_6D_6 (ca. 0.6 mL). After 191 hours at 25 °C, 2 was still present (0.44 mol), as well as $(TTP)Hf(\eta^2\text{-}NAr^{iPr}C(=N^tBu)S)$ (9.47 mol),

[(TTP)HfS]$_2$ (1.56 mol), and Ar^{Pr}N=C=N^{t}Bu (2.75 mol). The temperature was

subsequently raised to 80°C for 21 hours to yield a nearly colorless solution containing

[(TTP)HfS]$_2$ (1.36 mol) and Ar^{Pr}N=C=N^{t}Bu (12.17 mol, 90% yield by NMR). ^{1}H NMR

(C$_6$D$_6$, 300 MHz): [(TTP)Hf(η^2-NAr^{Pr}C(=N^{t}Bu)S)]: 9.12 (s, 8H, β-H), 8.29 (d, 4H, *meso-*

C$_6$*H*$_4$CH$_3$), 7.69 (d, 4H, *meso-*C$_6$*H*$_4$CH$_3$), 7.35 (d, 4H, *meso-*C$_6$*H*$_4$CH$_3$), 7.21 (d, 4H, *meso-*

C$_6$*H*$_4$CH$_3$), 6.94 (t, 1H, *p-*C$_6$*H*$_3$), 6.77 (d, 2H, *m-*C$_6$*H*$_3$), 2.39 (s, 12H, *meso-*C$_6$H$_4$C*H*$_3$), 1.04

(d, 6H, -CH*Me*$_2$), 0.52 (s, 9H, N-C*Me*$_3$), 0.51 (d, 6H, -CH*Me*$_2$), -0.15 (m, 2H, -C*H*Me$_2$).

[(TTP)HfS]$_2$: 8.75 (s, 8H, β-H), 7.97 (d, 4H, *meso-*C$_6$*H*$_4$CH$_3$), 7.55 (d, 4H, *meso-*

C$_6$*H*$_4$CH$_3$), 7.42 (d, 4H, *meso-*C$_6$*H*$_4$CH$_3$), 2.45 (s, 12H, *meso-*C$_6$H$_4$C*H*$_3$).

Reaction of 1 with ^{t}BuNCSe. An NMR tube equipped with a Teflon stopcock was

charged with 1 (19.32 mg, 20.66 mol), Ph$_3$CH (71 mL, 0.1397 M, 9.92 mol) as an internal

standard, ^{t}BuNCSe (7.5 mg, 46.27 mol), and C$_6$D$_6$ (ca. 0.6 mL). After 8 hours at 25°C, 1

had been consumed and a large amount of brown precipitate had formed. Ar^{Pr}N=C=N^{t}Bu

(17.71 mol) was produced in 86% (NMR yield). No intermediates were detected during this

reaction.

Reaction of 2 with ^{t}BuNCSe. An NMR tube equipped with a Teflon stopcock was

charged with 2 (16.64 mg, 16.27 mol), Ph$_3$CH (85 mL, 0.1455 M, 12.37 mol) as an internal

standard, ^{t}BuNCSe (10.1 mg, 62.3 mol), and C$_6$D$_6$ (ca. 0.6 mL). After 109 hours at 25°C,

Ar^{Pr}N=C=N^{t}Bu (13.59 mol, 84% yield) had formed. No intermediates were detected during

this reaction.

Isomerization of 4a to 4b. An NMR tube equipped with a Teflon stopcock was

charged with 4a (23.2 mg, 22.45 mol), Ph$_3$CH (90 mL, 0.1397 M, 12.57 mol), as an internal

standard, and C_6D_6 (ca. 0.6 mL). After 912 hours at ambient temperature the progress of the reaction had slowed markedly and only a trace of **4a** remained (0.70 mol, 97% consumption). Quantification of **4b** was precluded by its insolubility. However, X-ray diffraction quality crystals precipitated out during the reaction. No additional products or intermediates were observed throughout this reaction, $t_{1/2} \approx 670$ hours.

Isomerization of 5a. An NMR tube equipped with a Teflon stopcock was charged with **5a** (16.86 mg, 15.03 mol), Ph$_3$CH (92.5 mL, 0.1397 M, 12.92 mol), and C_6D_6 (ca. 0.6 mL). After 534 hours at 80 °C, the progress of the reaction had slowed markedly and only a trace of **5a** remained. The product, (TTP)Hf(η^2-N^{t}BuC(=NAr^{Pr})O), (14.36 mol) was present in 94% yield. No additional products or intermediates were observed throughout this reaction, $t_{1/2} \approx 250$ hours. ^{1}H NMR (C_6D_6, 300MHz): 9.12 (s, 8H, β-H), 8.24 (b, 4H, meso-C$_6$*H*$_4$CH$_3$), 7.83 (b, 4H, meso-C$_6$*H*$_4$CH$_3$), 7.38 (b, 4H, meso-C$_6$*H*$_4$CH$_3$), 7.26 (b, 4H, meso-C$_6$*H*$_4$CH$_3$), 6.93 (m, 3H, m-, p-C$_6$*H*$_3$), 2.41 (s, 12H, meso-C$_6$H$_4$C*H*$_3$), 1.83 (m, 2H, -C*H*Me$_2$), 0.78 (d, 6H, $^3J_{H-H}$ = 7 Hz, -CH*Me*$_2$), 0.32 (d, 6H, $^3J_{H-H}$ = 7 Hz, -CH*Me*$_2$), -0.14 (s, 9H, N-C*Me*$_3$).

Isomerization of 7a. Complex **7a** was synthesized *in situ* in an NMR tube equipped with a Teflon stopcock. The tube was charged with **2** (12.38 mg, 12.10 mol), ^{i}PrN=C=N^{i}Pr (6.5 L, 41.5 mol), Ph$_3$CH (89 mL, 0.1455 M, 12.95 mol), and C_6D_6 (ca. 0.6 mL). The formation of **7a** was complete in minutes. The sample was then heated at 80°C for 488 hours, $t_{1/2} \approx 108$ hours. The product, (TTP)Hf(η^2-N^{i}PrC(=NAr^{Pr})N^{i}Pr) (**7b**), (11.67 mol) was produced in 96% (NMR yield). No additional products or intermediates were observed throughout this reaction. ^{1}H NMR (C_6D_6, 300 MHz): 9.12 (s, 8H, β-H), 8.59 (d, 4H, $^3J_{H-H}$

= 7 Hz, *meso*-C$_6$*H*$_4$CH$_3$), 7.76 (d, 4H, ^{3}J$_{H-H}$ = 7 Hz, *meso*-C$_6$*H*$_4$CH$_3$), 7.36 (d, 4H, ^{3}J$_{H-H}$ = 7

Hz, *meso*-C$_6$*H*$_4$CH$_3$), 7.25 (d, 4H, ^{3}J$_{H-H}$ = 7 Hz, *meso*-C$_6$*H*$_4$CH$_3$), 6.69 (d, 2H, *m*-C$_6$*H*$_3$), 6.59

(m, 1H, *p*-C$_6$*H*$_3$), 2.40 (s, 14H, *meso*-C$_6$H$_4$C*H*$_3$ and NC*H*Me$_2$), 1.62 (spt, 2H, C$_6$H$_3$-

(C*H*Me$_2$)$_2$), 0.70 (d, 12H, ^{3}J$_{H-H}$ = 7 Hz, C$_6$H$_3$-(CH*Me*$_2$)$_2$), -0.18 (b, 12H, N-CH*Me*$_2$). The

methine proton resonance of the N'Pr group was found by COSY to overlap with the *meso*-

C$_6$H$_4$C*H*$_3$ signal at 2.40 ppm. The respective isopropyl groups were definitively assigned by

HMBC.

Structure Determinations of (TTP)Zr=NAr^{iPr} (1), (TTP)Hf=NAr^{iPr} (2),

(TTP)Zr(η^2-NAr^{iPr}C(=N(^{t}Bu)O) (4a), (TTP)Zr(η2-N^{t}BuC(=N(Ar^{iPr})O) (4b), and

(TTP)Hf(η^2-NAr^{iPr}C(=N^{i}Pr)N^{i}Pr) (7a). Crystal data is found in Table 1. Compounds **1**

and **2** were treated similarly by attachment to a glass fiber and mounting on a Siemens

SMART system for data collection at 173(2) K. An initial set of cell constants was

calculated from reflections harvested from three sets of 20 frames. These initial sets of

frames were oriented such that orthogonal wedges of reciprocal space were surveyed. This

produced orientation matrices determined from 208 and 218 reflections for compounds **1**

and **2**, respectively. Final cell constants were calculated from a set of 7055 and 8028 strong

reflections from the actual data collection, respectively, for **1** and **2**. Three major swaths of

frames were collected with 0.30° steps in ω. The data were merged into a unique set as

indicated by the data collection ranges. The space groups were determined on the basis of

systematic absences and intensity statistics, and a successful direct-methods solution was

calculated which provided most non-hydrogen atoms from the E-map. Several full-matrix

least squares/difference Fourier cycles were performed which located the remainder of non-

hydrogen atoms, which were refined with anisotropic displacement parameters. All

hydrogen atoms were placed in ideal positions and refined as riding atoms with relative

isotropic displacement parameters. Both complexes were found with one toluene and one-

half heptane in the unit cell. The heptane was disordered over an inversion center such that

three carbons lie on one side and four on the other. Therefore, the third and fourth carbon

atoms are terminal methyl groups part of the time. All calculations were performed using

SGI INDY R4400-SC or Pentium computers using the SHELXTL V5.0 program suite.[24]

Crystals of **4a**, **4b**, and **7a** were treated in an analogous manner to that of **1** and **2**.

Systematic absences in the diffraction data were uniquely consistent for space groups

denoted in Appendix A. The structures were solved using direct methods, completed by

subsequent difference Fourier synthesis and refined by full-matrix least-squares procedures.

All nonhydrogen atoms were refined with anisotropic displacement coefficients unless

otherwise specified. All hydrogen atoms were treated as idealized contributions. The

refinement of **7a** revealed the presence of several disordered solvent molecules. The

SQUEEZE filter of the program PLATON[25] was applied to identify and account for one and

a half solvent molecules of toluene present in the asymmetric unit of **7a** along with one

molecule of the complex. In the case of **4b**, there are two and one-half molecules of benzene

also present in the asymmetric unit. The half molecule is a part of a benzene molecule

residing on an inversion center. The solvent molecules were refined isotropically. The

SQUEEZE filter was also applied to **4a** to identify and account for one-half of a toluene

molecule and one-half of a heptane molecule present in the asymmetric unit.

Crystallographic data in CIF format are deposited at the Cambridge Crystallographic Data Center. Deposition numbers are 105601 (**1**), 105602 (**2**), 105603 (**4a**), 105604 (**4b**), and 105605 (**7a**).

Results

Synthesis and Characterization of Imido Complexes. Treatment of *cis*-(TTP)ZrCl$_2$ with 2 equiv of bulky lithium amide reagents, LiNHR (R = 2,4,6-Me$_3$C$_6$H$_2$, 2,4,6-^{t}Bu$_3$C$_6$H$_2$, 2,4,6-Ph$_3$C$_6$H$_2$, 2,6-^{i}PrC$_6$H$_3$), in toluene resulted in the formation of new terminal imido complexes (eq 1). Of these new imido compounds, the 2,6-diisopropylphenyl

$$(TTP)ZrCl_2 + 2\ LiNHR \rightarrow (TTP)Zr=NR + 2\ LiCl + NH_2R \tag{1}$$

derivative (TTP)Zr=NAr^{iPr}, complex **1**, was the most amenable to isolation and purification. The analogous Hf complex, (TTP)Hf=NAr^{iPr}, complex **2**, was also synthesized using the same metathesis reaction. Complex **1** alternatively could be prepared by the reaction of Zr(NAr^{iPr})Cl$_2$(THF)$_2$[5] with (TTP)Li$_2$(THF)$_2$. All of these new imido complexes are moisture sensitive. In addition, the Zr imido complexes with mesityl, 2,4,6-tris-*t*-butylphenyl and 2,4,6-triphenylphenyl substituents decomposed over time, precluding our ability to isolate analytically pure samples. The rate of this decomposition qualitatively followed the steric bulk of the substituent. However, with 2,6-diisopropylphenyl substituents, complexes **1** and **2** could be kept in the solid state at ambient temperature under a N$_2$ atmosphere for months. In solution at ambient temperature, complex **2** decomposed to uncharacterized diamagnetic

species over a matter of weeks, while 1 is stable in C_6D_6 at elevated temperatures (80°C) for several days.

The ^1H NMR spectra of imido complexes 1 and 2 share the same approximate characteristics. Particularly diagnostic is the porphyrin ring current effect on the imido ligand protons. Consequently, the *meta* and *para* aryl protons of the imido exhibit upfield shifts of ~ 0.90 ppm relative to the free amine. The *m*-, and *p*-protons of H_2NAr^{Pr} occur at 7.05 ppm (d) and 6.91 ppm (t), respectively. Thus, a well separated doublet (6.16 ppm, *m*-H) and triplet (6.04 ppm, *p*-H) for complex 2 is observed. In comparison, complex 1 exhibits a three-proton singlet at 6.08 ppm for the *m*- and *p*-ArPr protons. The aryl isopropyl groups are also shifted upfield relative to the corresponding free amine resonances at 2.63 ppm (spt) and 1.14 ppm (d). For example in complex 1, the methine multiplet appears at 0.18 ppm and the methyl doublet occurs at 0.00 ppm.

The crystal structures of compounds 1 (Fig. 1) and 2 (Fig. 2) are isomorphous. Each compound co-crystallizes with one toluene and one-half heptane per unit cell. As expected, metrical parameters are similar due to the nearly equivalent sizes of the metals. Most structurally characterized five-coordinate Zr and Hf imido complexes have been described as possessing a trigonal bipyramidal arrangement of the ligands around the metal. The geometry about the metals in complexes 1 and 2 is best described as distorted square-pyramidal. The four pyrrole nitrogens of the porphyrin form the basal plane with an average *trans*-pyrrole N_{por}-M-N_{por} angle of 140° and 142°, respectively. Metal-N_{imido} bond lengths are 1.863(2) and 1.859(2) Å for the Zr and Hf complexes, respectively. These values are well within the range of known alkyl and aryl substituted imido ligands for Zr and Hf
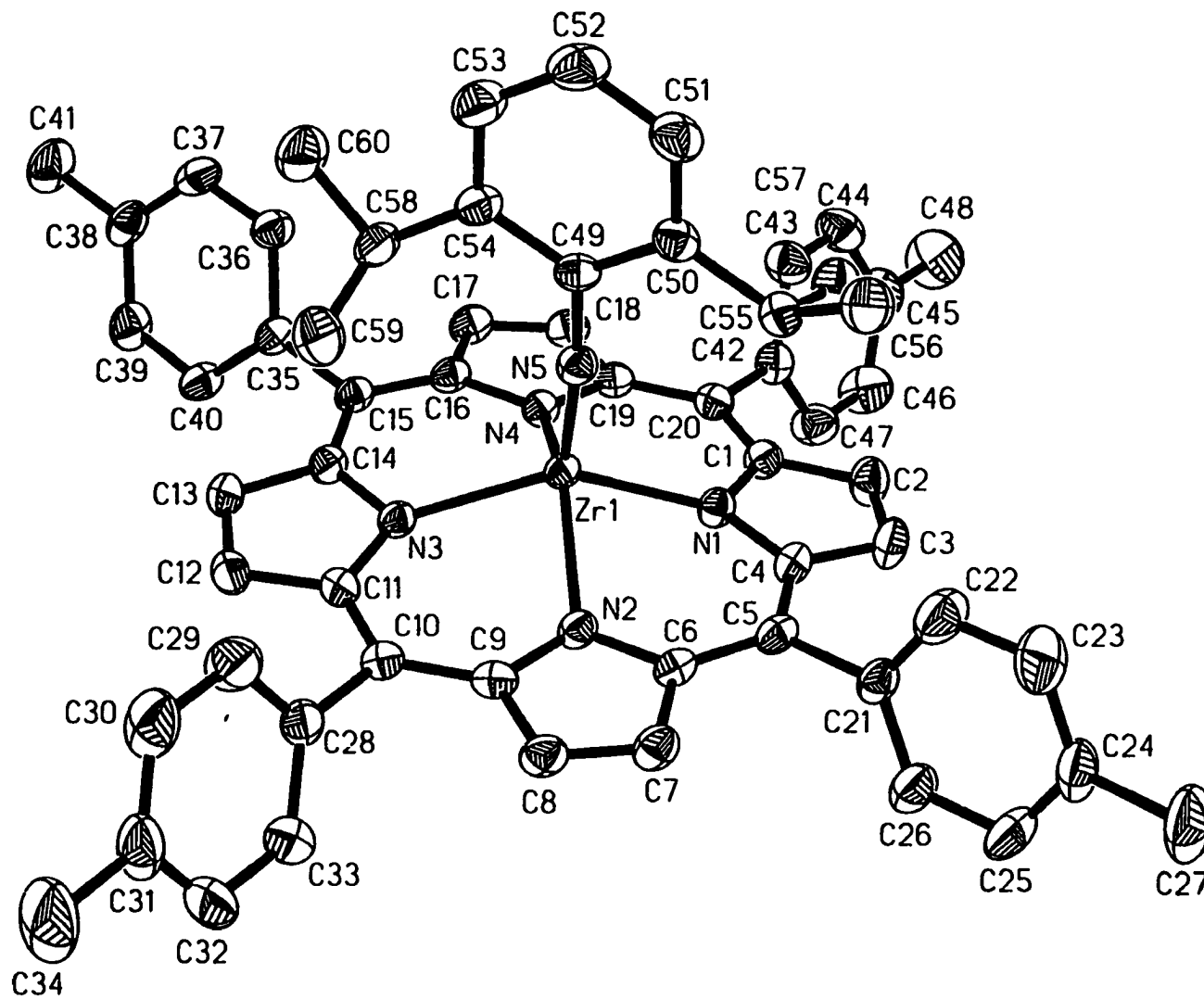
Figure 1. ORTEP representation of (TTP)Zr=NAr^{iPr}. Thermal ellipsoids drawn at 50% probability level.
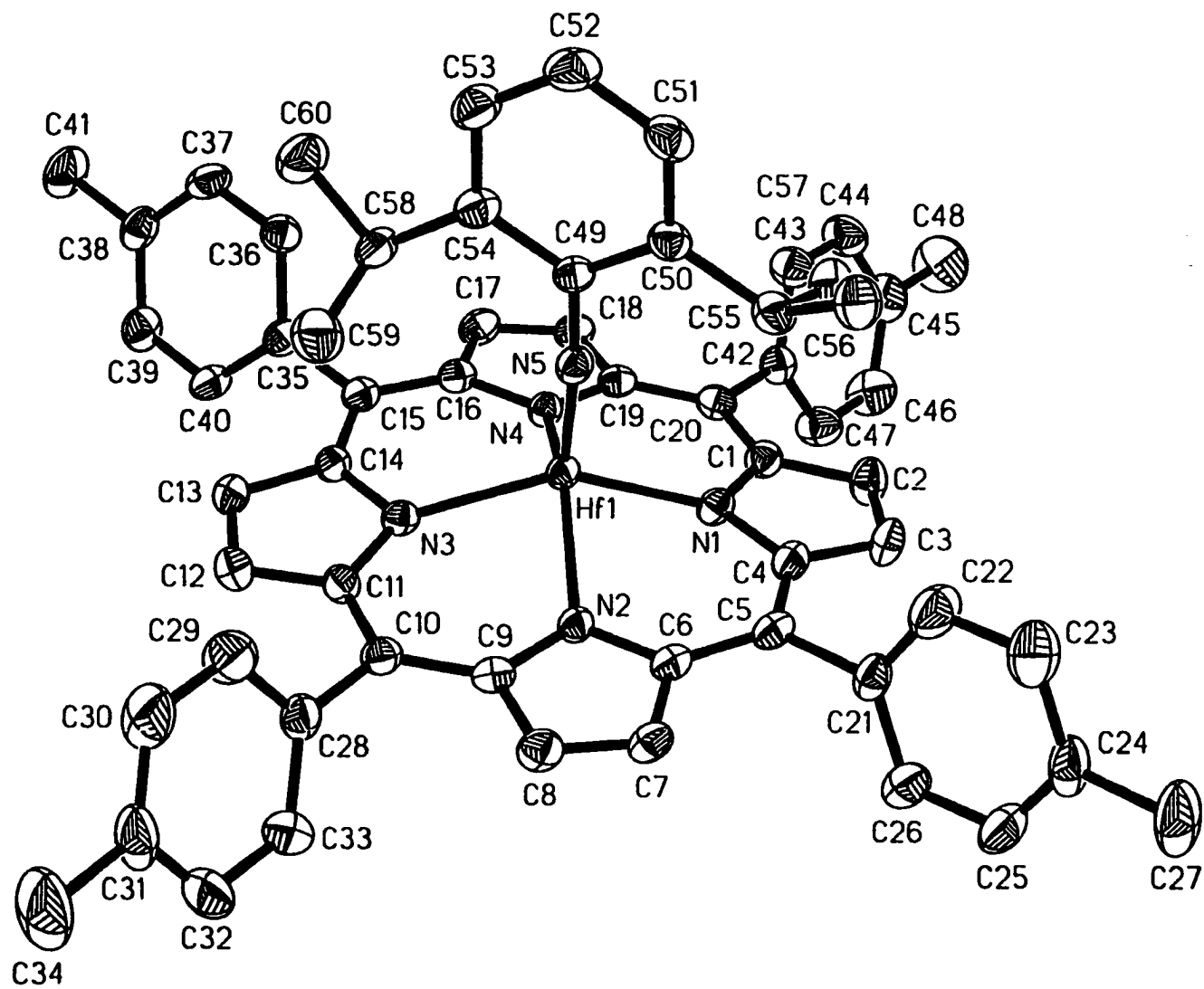
Figure 2. ORTEP representation of (TTP)Hf=NAr^{iPr}. Thermal ellipsoids drawn at 50% probability level.

complexes. Typical M-N$_{imido}$ distances range from 1.826(4) to 1.876(4) Å for zirconium[1,3-6,12] and 1.850(3) for hafnium.[6] Only a small deviation from linearity is observed in the M-N5-C49 angles, 172.5(2) complex and 173.4(2) (complex 2). Similar metrical features have been reported for the corresponding bond angles of other imido complexes (164.5 to 179.5 for Zr and 174.4 for Hf). The metal centers in other structurally characterized Zr and Hf metalloporphyrin complexes exhibit coordination numbers from six to eight. The range of out-of-plane distances for hexa-coordinated Zr(IV) and Hf(IV) porphyrin complexes is 0.84 to 1.06 Å.[26] In comparison to these examples, the metals in the five coordinate complexes 1 and 2 reside closer to the plane defined by the four pyrrole nitrogens. The metal atoms in complexes 1 and 2 are located 0.75 and 0.71 Å above the N1-N2-N3-N4 plane, respectively. The smaller value observed for complex 2 is consistent with corresponding values in the congeners, [(TPP)Zr(OH)$_2$(O)]$_2$; [(TPP)Hf(OH)$_2$(O)]$_2$ (1.057; 1.048 Å) and (TPP)Zr(O$_2$CCH$_3$)$_2$; (TPP)Hf(O$_2$CCH$_3$)$_2$ (1.036; 1.012 Å).[21,27]

A domed ruffling[28] deformation of the porphyrin macrocycle, a common phenomenon with relatively large metals, is observed in both imido compounds, although to a lesser extent in complex 2. Deviations from the 24-atom porphyrin plane due to ruffling in complex 1 are 11 (C5), -8 (C10), 19 (C15), and -10 (C20) pm. The resultant dihedral angles in complex 1 of the pyrrole rings containing N1, N2, N3, and N4 relative to the mean 24-atom porphyrin plane are 5.0, -2.6, 5.5, and -8.5°, respectively.

Formation of Bis(Amido) Complexes. Treatment of complex 2 with excess aniline results in the complete disappearance of the starting imido complex. Two new bis(amido) complexes, (TTP)Hf(NHPh)$_2$ and (TTP)Hf(NHPh)(NHAr^{Pr}), are produced as observed by

^{1}H NMR. These two bis(amido) complexes are in equilibrium with the free amines as shown in eq 2 (K = 3.3 ± 0.3). The proton resonances of the coordinated aryl amido ligands are shifted upfield. For example, the o-C_6H_5 doublet of aniline appears at 6.34 ppm whereas the corresponding o-protons of the amide in (TTP)Hf(NHPh)$_2$ appear at 4.24 ppm. The amide

$$(TTP)Hf(NHAr^{iPr})(NHPh) + H_2NPh \rightleftharpoons (TTP)Hf(NHPh)_2 + H_2NAr^{iPr} \qquad (2)$$
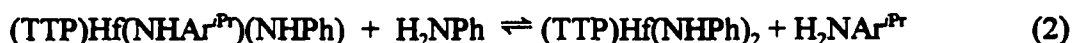
NH protons are found at 0.93 ppm. Thus, in the presence of the less sterically demanding aniline, a bis(amido) is produced with concomitant loss of the bulkier 2,6-diisopropylphenyl amine. Although no new imido complexes were detected by ^{1}H NMR during this reaction, decomposition of the bis(amido) complexes to intractable products was observed over days at ambient temperature. Bulky amines, H_2NR (R = 2,4,6-Me$_3$C$_6$H$_2$, 2,4,6-^{t}Bu$_3$C$_6$H$_2$, or 2,4,6-Ph$_3$C$_6$H$_2$), do not react with complexes 1 or 2. Treatment of (TTP)HfCl$_2$ with 2 equivalents of LiNH(C$_6$H$_4$-p-CH$_3$) in hexanes affords the bis(amido), (TTP)Hf(NH-C$_6$H$_4$-p-CH$_3$)$_2$ (3). The amide NH protons are readily distinguishable in the ^{1}H NMR at 0.96 ppm as a sharp singlet integrating as 2 protons. In free p-toluidine the NH protons appear at 2.74 ppm (bs).

[2+2] Condensation Products of Complexes 1 and 2 with R-NCO. Treatment of imido complex 1 with ^{t}Bu-NCO at ambient temperature resulted in the rapid appearance of a new species, **4a**, which was formulated as an addition product as monitored by ^{1}H NMR. The new compound retains the 2,6-diisopropylphenyl fragment. It also exhibits a new nine-

proton singlet at 0.35 ppm consistent with a bound t-butyl group. Moreover, the isopropyl methyl substituents give rise to two new doublets at 0.82 (6H) and 0.42 (6H) ppm. Heating a C_6D_6 solution of **4a** in an NMR probe to 323 K resulted in no broadening of the isopropyl signals. This observation suggested that the isopropyl methyl groups are diastereotopic. Further heating of compound **4a** to 353 K in C_6D_6 for 238 h resulted in the production of 1 equiv of the carbodiimide, $^tBuN=C=NAr^{iPr}$. The production of carbodiimide suggests that compound **4a** can be formulated as an η^2-N,O-ureato complex (eq 3). The remaining metal

$$\text{(3)}$$
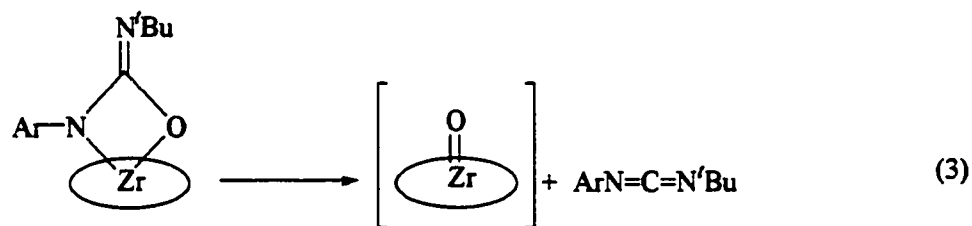
complex was observed transiently by ^{1}H NMR, but eventually precipitated out of solution. Initially this complex was formulated as a terminal oxo species, (TTP)Zr=O. However, this putative (TTP)Zr=O complex did not react with excess ^tBuNCO to form (TTP)Zr=N^tBu (eq 4).[29] The metal byproduct has been identified as the dimeric species $[(TTP)Zr]_2(\mu-O)_2$.[23,30]

$$\text{(4)}$$
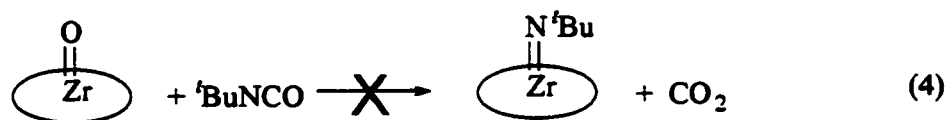
Over days at 298 K in C_6D_6, complex **4a** isomerizes to a new complex, **4b**. The ureato ligand is still retained as indicated by the presence of *t*-butyl and isopropyl resonances in the ^1H NMR spectrum. However, all proton signals of complex **4b** have shifted relative to those of complex **4a**. For example, the *t*-butyl resonance of complex **4b** has shifted upfield by 0.49 ppm to -0.14 ppm (s, 9H). The relative change on the isopropyl methyl protons is less drastic. These now appear at 0.31 (d, 6H) and 0.78 ppm (d, 6H). However, a much stronger shift is observed for the methine protons of the isopropyl groups. In complex **4a**, this signal appeared at -0.51 ppm. The corresponding resonance for complex **4b** is shifted substantially downfield to 1.84 ppm.

Two candidates serve as possible structures for complex **4b**. These are η^2-N,O- and η^2-N,N-bound ureatos **I** and **II** shown below in Scheme 3. The strong downfield shift of the isopropyl methine signal suggests that the N-bound aryl group in complex **4b** is further from the porphyrin ring than is its counterpart in complex **4a**. Thus, structure **I** is most likely the correct formulation for complex **4b**. Moreover, heating **4b** at 383 K for 228.5 h resulted in the production of $^tBuN=C=NAr^{iPr}$ (92% by NMR). This reactivity is also consistent with the
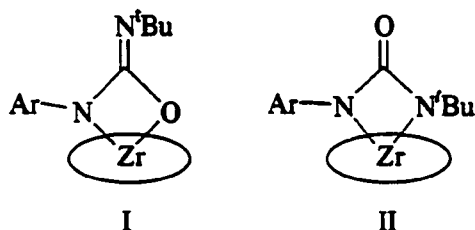
Scheme 3.

N,O-bound isomer I. Final confirmation of the correct structure for complex **4b** was derived from synthesis of an analogue and by X-ray diffraction analysis (*vide infra*).

Whereas complex **4a** is formed within minutes at ambient temperature from the reaction of **1** and *t*-butyl isocyanate, the isomerization of **4a** to **4b** (eq 5) requires ≈ 38 days at 298 K in C_6D_6. The production of carbodiimide was not observed during this transformation.

$$M = \begin{array}{c} Zr \ \ \mathbf{4a} \\ Hf \ \ \mathbf{6} \end{array}$$

(5)
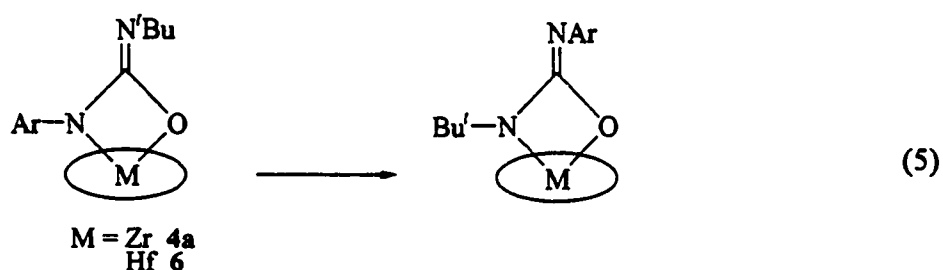
The analogous Hf imido complex **2** also forms a kinetic η^2-N,O-ureato complex, **5a**, on treatment with 'BuNCO. The Hf reaction is much slower than that of Zr and takes several hours at 298 K. In addition, **5a** isomerizes to a thermodynamic product, **5b**, after heating at 353 K for 534 h in C_6D_6. Conversion of **5a** to **5b** occurs cleanly with no formation of carbodiimide even at 383 K. The kinetic isomers **4a** and **5a** both share similar spectroscopic characteristics, as do the thermodynamic products **4b** and **5b**. All four complexes, **4a**, **4b**, **5a**, and **5b**, yield the urea, 'BuNH-C(O)-NHAr^{Pr}, upon hydrolysis.

Treatment of complex **2**, (TTP)Hf=NAr^{Pr}, with Ar^{Pr}NCO produced a new adduct, **6**, containing two inequivalent Ar^{Pr} fragments. Diagnostic of the two different Ar^{Pr} groups are the two unique isopropyl methine signals at 1.93 (m, 2H) and -0.07 ppm (m, 2H). Clearly, complex **6** must be an η^2-N,O-bound ureato. An η^2-N,N-bound ureato ligand would have

equivalent Ar^{iPr} fragments. Heating complex **6** does not result in conversion to a new isomer. This observation is consistent with all observed isomers of **4** and **5** having N,O-bound ligands.

The two Ar^{iPr} groups of complex **6** exhibit different variable temperature behavior. The methyl groups of one Ar^{iPr} unit give rise to a broad 12-proton signal at 0.33 ppm at 293 K in toluene-d$_8$. Upon cooling, this broad signal begins to decoalesce at 245 K and eventually sharpens into two new doublets (0.85 and −0.03 ppm) at 234 K as expected for diastereotopic isopropyl methyl moieties. On warming to 323 K, the methyl signals for this Ar^{iPr} fragment sharpen into a single slightly broadened doublet (12H) at 0.31 ppm. The other Ar^{iPr} fragment exhibits diastereotopic isopropyl methyl groups with doublets at 0.61 and 0.44 ppm throughout the temperature range from 234 K to 323 K. These latter signals are assigned to the Ar^{iPr} fragment which is proximal to the porphyrin ligand. The distal Ar^{iPr} group is not sterically constrained by the porphyrin macrocycle and can rotate about the N-C$_{ipso}$ bond. The free energy of activation for this rotational process is 12 ± 0.3 kcal/mol.

Synthesis and Isomerization of (TTP)Hf(η^2-NAr^{iPr}C(=N^{i}Pr)N^{i}Pr). Reaction of complex **2** with a slight excess of 1,3-diisopropylcarbodiimide results in the formation of a new guanidino complex, **7a**. The two N-isopropyl groups of **7a** are inequivalent as indicated by ^{1}H NMR. The proton assignments for this complex were confirmed by HMBC experiments. For example, the methyl proton signal at 0.96 is coupled to an aromatic ^{13}C resonance at 142.3 ppm. Thus, the 0.96 ppm peak must be associated with an isopropyl fragment of the Ar^{iPr} group. The methine protons of these fragments appear at 1.63 (spt, 1H) and 0.13 (spt, 1H) ppm. The upfield methine proton overlaps with one of the methyl

signals of the N-^{i}Pr group at 0.13 ppm, but was identified by COSY. The N-^{i}Pr groups

remain inequivalent as the temperature is raised to 323 K. Complex 7a is clearly an

unsymmetrical N,N-bound guanidino species. Over a period of approximately three weeks

at 353 K in C$_6$D$_6$, a new product, 7b, was formed with the concomitant loss of 7a. At 323

K, the ^{1}H NMR spectrum (toluene-d$_8$ solution) of 7b exhibits a broad peak at −0.17 ppm for

the methyl groups of both proximal N^{i}Pr moieties. The distal NAr^{iPr} displays its isopropyl

resonances at 0.70 (d, 12H) and 1.62 (spt, 2H) ppm. Unambiguous assignments for proton

resonances were derived from HMBC experiments. The proton peaks at 0.70 and 1.62 ppm

are both coupled to an aromatic carbon signal at 137.2 ppm. These two proton resonances

correspond to the isopropyl groups of the Ar^{iPr} fragment. Consequently, complex 7b is

formulated as the symmetric guanidino, (TTP)Hf(η^2-N^{i}PrC(=Ar^{iPr})N^{i}Pr).

7a   7b
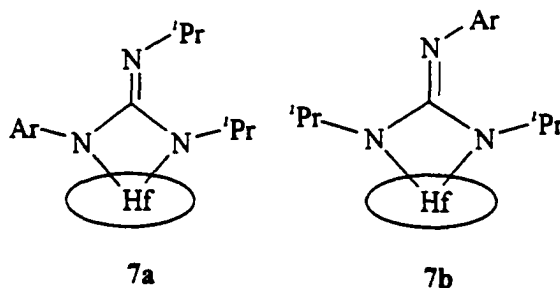
Reaction of complexes 1 and 2 with ^{t}BuNCS and ^{t}BuNCSe. Imido complexes 1

and 2 undergo reactions with ^{t}BuNCS and ^{t}BuNCSe at a slower rate than the analogous

reactions with ^{t}BuNCO. This reflects the greater electrophilic nature of the carbon atom in

^{t}BuNCO relative to ^{t}BuNCS and ^{t}BuNCSe. In the reaction with ^{t}BuNCS, the loss of 1

occurred over 21 hours. In the reaction of ^{t}BuNCS with 2, the presence of the starting

imido Hf complex was detected even after 191 hours. In both cases, a transient complex

assigned as the [2+2] cycloaddition product was observable, but it decomposed simultaneously to the carbodiimide, $^tBu-N=C=NAr^{Pr}$ and sparingly soluble $[(TTP)Zr(\mu-S)]_2$. Formulation of the zirconium product as a μ-sulfido bridged dimer was based on the similarity of its ^1H NMR spectrum to that of the oxygen analogue $[(TTP)Zr(\mu-O)]_2$. The transient metallacycles were assigned by the similarity of the ^1H, NAr^{Pr} and ^tBu NMR chemical shifts to those of the oxygen containing analogues, 4a and 5a (Table 2). In the presence of excess ^tBuNCSe, 1 and 2 are consumed without the observation of intermediates during the formation of carbodiimide, $^tBu-N=C=NAr^{Pr}$. Once again, the loss of the zirconium imido (8 hrs) is faster than in the hafnium case (109 hrs).

Table 2. Chemical shifts of the NAr^{Pr} and ^tBu protons in the N,Ch-bound ureato derivatives.

Reactant	$^tBuN=C=E$	CHMe$_2$, NAr^{Pr} (ppm)^a from metallacycle complex	^tBu (ppm)
(TTP)Zr=NAr^{Pr} (1)	^tBuNCO	0.82 (d), 0.42 (d) (4a)	0.35 (s)
(TTP)Hf=NAr^{Pr} (2)	^tBuNCO	0.84 (d), 0.43 (d) (5a)	0.34 (s)
(TTP)Zr=NAr^{Pr} (1)	^tBuNCS	1.02 (d), 0.51 (d)	0.52 (s)
(TTP)Hf=NAr^{Pr} (2)	^tBuNCS	1.04 (d), 0.51 (d)	0.52 (s)

^{a} C_6D_6, 20 °C

Structures of (TTP)Zr(η^2-NAr^{Pr}C(=N^tBu)O), 4a, (TTP)Zr(η^2-N^tBuC(=NAr^{Pr})O), 4b, and (TTP)Hf(η^2-NAr^{Pr}C(=NPr^i)NPr^i), 7a. The ureato ligand is bound to the zirconium in both 4a (Fig. 3) and 4b (Fig. 4) through nitrogen and oxygen. Both complexes 4a and 4b possess a slightly puckered ureato metallacycle. This four-membered ring is nearly perpendicular to the mean 24-atom porphyrin core, with dihedral angles between planes of 91.1 (4a) and 101.2 (4b). The ureato fragment is staggered with respect to the pyrrole nitrogens. Representative torsional angles are 30.3° (N2-Zr-N6-C49)
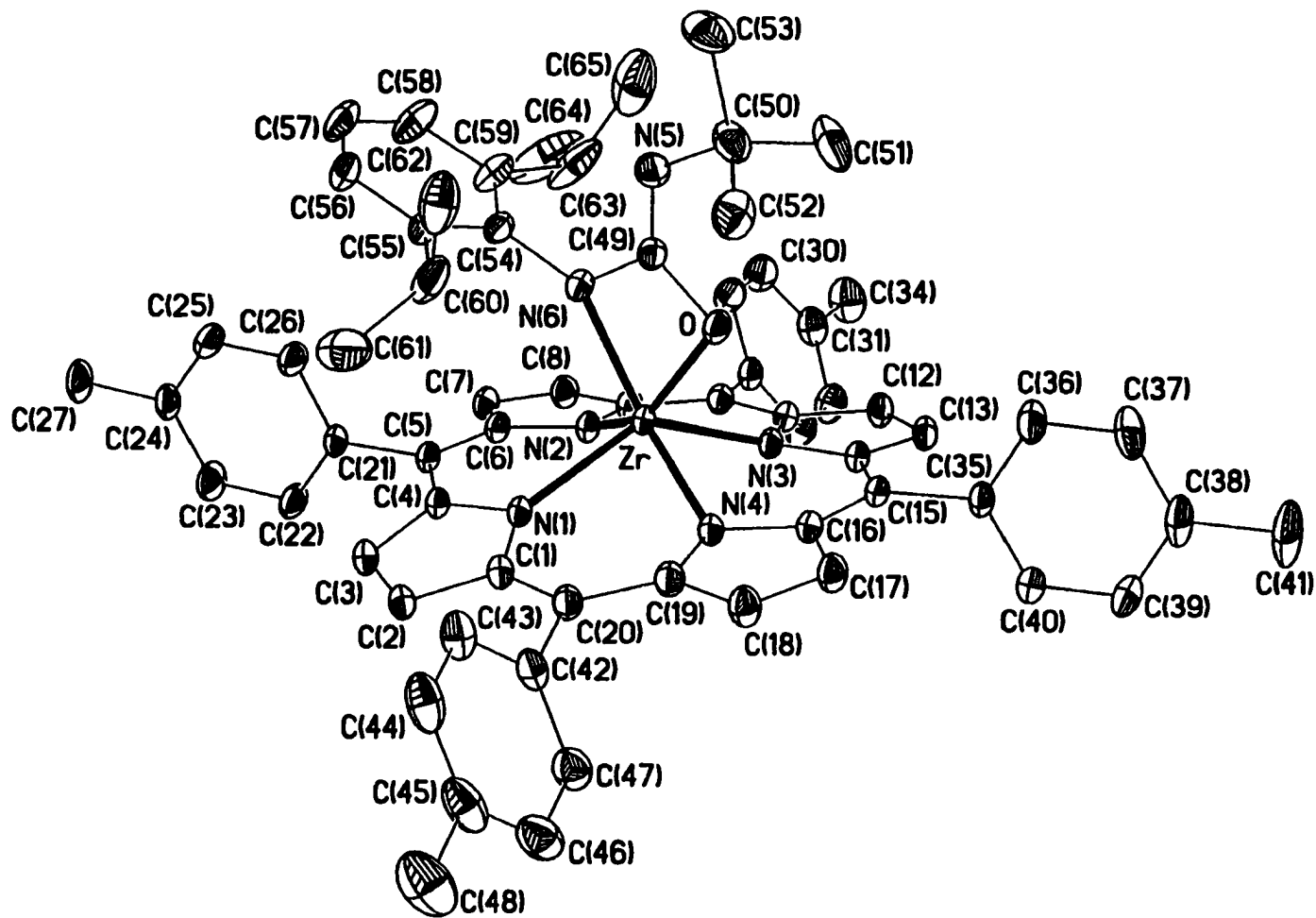
Figure 3. ORTEP representation of (TTP)Zr(η^2-NAr^{iPr}C(=N^{t}Bu)O). Thermal ellipsoids drawn at 30% probability level.
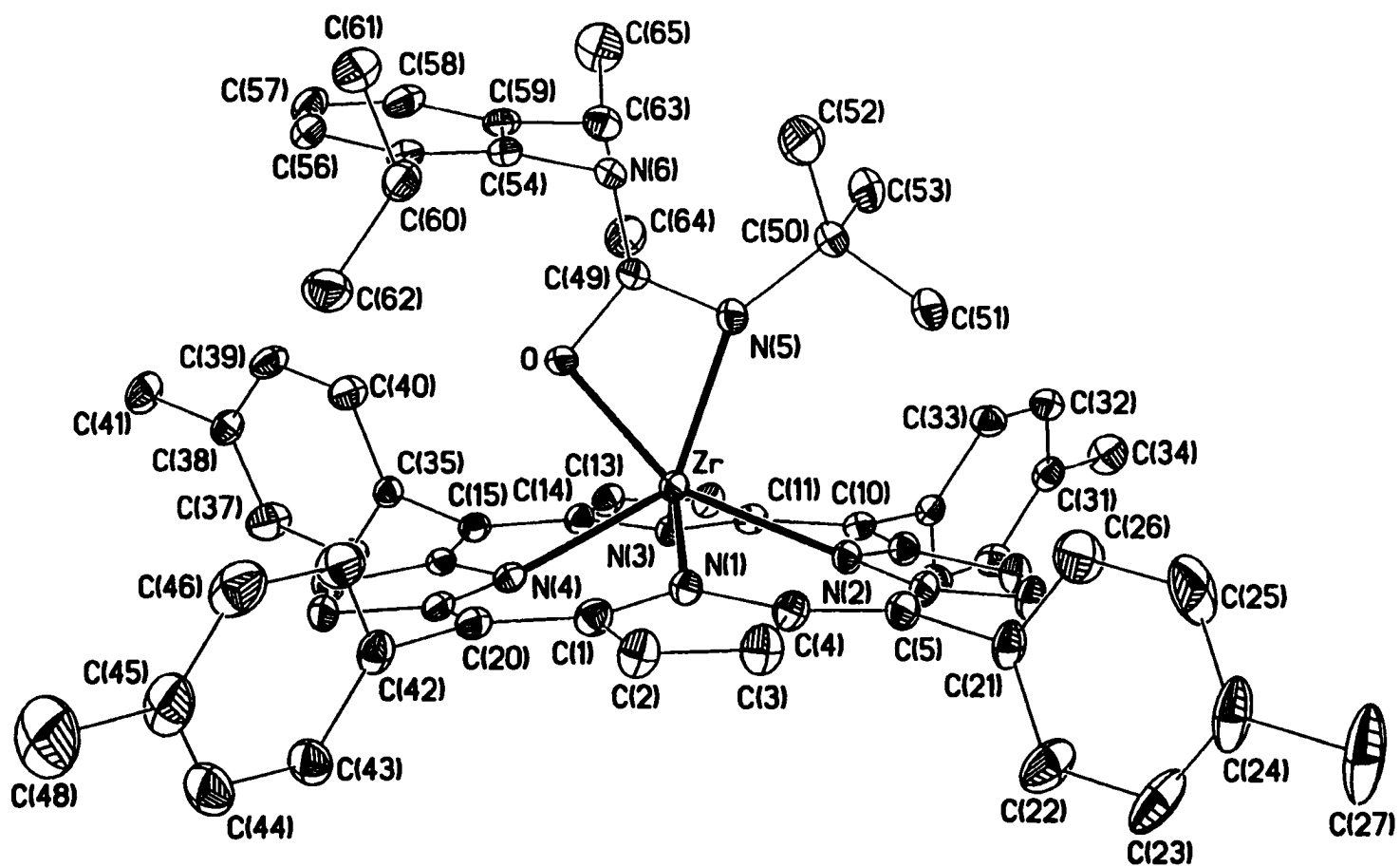
Figure 4. ORTEP representation of (TTP)Zr(η^2-N^{t}BuC(=NAr^{iPr})O). Thermal ellipsoids drawn at 30% probability level.

and 34° (N4-Zr-O-C49) for **4a** and 24.7° (N2-Zr-N5-C49) and 7.7° (N4-Zr-O-C49) for **4b**.

The displacement of the Zr from the four-nitrogen pyrrole plane, 0.8891 Å (**4a**) and 0.9069

Å (**4b**), is comparable to related six-coordinate compounds (*vide supra*). For **4a**, the 24-

atom porphyrin core exhibits a higher degree of ruffling and doming in comparison to the

imido complex **1**. Unexpectedly, very little ruffling is observed in **4b**. Instead, marked

doming and an appreciable saddle deformation is seen in the deviations of the -pyrrole

carbon atoms from the 24-atom porphyrin core [2 (C2), 3 (C3), -27 (C7), -26 (C8), 4 (C12),

8 (C13), -20 (C17), -25 (C18) pm]. The metallacycle fragments contain obtuse N-C-O

angles 106.16(14) and 107.1(3), as well as acute N-Zr-O angles 63.62(5) and 63.13(11), in

4a and **4b** respectively.[29] In comparison to Zr-N amide bond lengths ranging from 2.027(7)-

2.159(3) Å[31] the Zr-N6 distance in **4a** and the Zr-N5 bond length in **4b** are somewhat

elongated with distances of 2.1096(13) and 2.137(3), respectively (Table 2). These bond

lengths are slightly shorter than those found for the N,N-bound ureato ligand in

[Zr(tmtaa)(η^2-NAr^{Pr}C(=O)N^{i}Bu)]; Zr-N^{i}Pr (2.168(4) Å) and Zr-N^{i}Bu (2.155(4) Å).[9] No π-

bonding between Zr-O is suggested by the rather long bond lengths, 2.0677(12) Å in **4a** and

2.066(3) Å in **4b**, and the acute C49-O-Zr angles of 96.76(10) in **4a** and 96.7(2) in **4b**.[31]

Other intramolecular metallacycle distances are normal.

The kinetic product from the treatment of complex **2** with 1,3-

diisopropylcarbodiimide yields the unsymmetric guanidino(2-) complex (TTP)Hf(η^2-

NAr^{Pr}C(=N^{i}Pr)N^{i}Pr) **7a**. The slightly puckered Hf(η^2-NAr^{Pr}C(=N^{i}Pr)N^{i}Pr) metallacyle (Fig.

5) is perpendicular to the mean 24-atom porphyrin core, with a dihedral angle between

planes of 89.9. The metallacycle is staggered in relation to the pyrrole nitrogens to a lesser
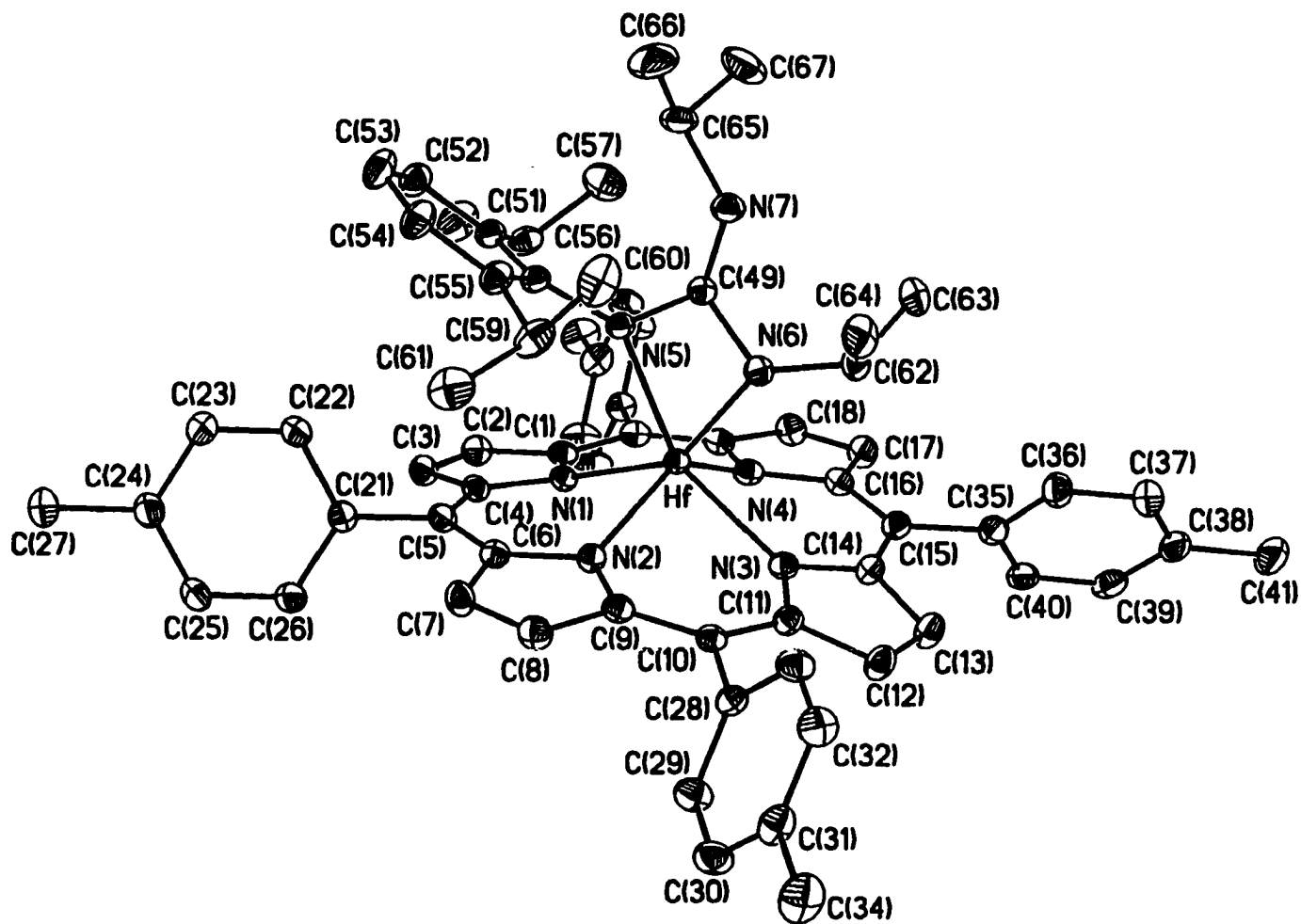
Figure 5. ORTEP representation of (TTP)Hf(η²-NAr^iPrC(=N^iPr)N^iPr). Thermal ellipsoids drawn at 30% probability level.

degree than that of the ureato complexes. The torsional angles are 15.9 (N1-Hf-N5-C49)

and 5.4° (N3-Hf-N6-C49). The Hf-N'Pr distance (2.087(6) Å) is within known Hf amido

bond distances (2.03-2.12 Å).[32] However, the notably longer Hf-NAr^{Pr} distance (2.151(2)

Å) may be due to the steric bulk of the Ar^{Pr} group. Consequently, there is an irregularity in

the Hf-N$_{pyrrole}$ distances: Hf-N1, 2.251(2); Hf-N2, 2.184(2); Hf-N3, 2.238(2); and Hf-N4,

2.207(2) Å. The two longer distances correspond to the nearly eclipsed nitrogens.

Intrametallacycle C-N single and double bond distances are typical and are summarized in

Table 3. As in complexes 4a and 4b, the porphyrin macrocycle of 7a shows ruffling and

Table 3.   Selected intramolecular metallacycle bond (Å) distances and angles (°) of 4a, 4b, and 7a.

Complex	Zr-O	M-N$_{amide}$	N$_{amide}$-C(49)	N$_{imine}$=C(49)	O-C(49)
4a	2.0677(12)	2.1096(13)	1.401(2)	1.269(2)	1.349(5)
4b	2.066(3)	2.137(3)	1.387(5)	1.277(5)	1.3530(19)
7a		2.087(2) Hf-N(6)	1.391(3) N(6)-C(49)	1.282(4)	
		2.151(2) Hf-N(5)	1.428(3) N(5)-C(49)		

Complex	O-Zr-N	N-Hf-N	E-C(49)-N$_{amide}$
4a	63.62(5)		106.16(14) E = O
4b	63.13(11)		107.1(3) E = O
7a		63.21(8)	104.0(2) E = N

doming distortions. However, a somewhat more pronounced saddle deformation is

observed, possibly due to the more sterically demanding metallacycle. As expected, the

hexa-coordinate hafnium center is further out of the N$_4$-pyrrole plane (0.9111 Å) compared

to the five-coordinate imido complex 2 (out-of-plane distance of 0.7092 Å). The

coordination environments most closely resemble a distorted trigonal prism with the metal

ion displaced towards one of the rectangular faces.[33]

Discussion

In continuing our work with titanium amido and imido chemistry, we have expanded

our efforts to zirconium and hafnium. For hexacoordinate complexes, the large displacement

of Zr and Hf from the porphyrin plane confines the two ligands to a *cis*-geometry. This

places further restrictions on the sizes of the two mutually *cis* ligands. Thus, it is possible to

prepare *cis*-(TTP)M(NHC$_6$H$_4$-*p*-CH$_3$)$_2$ (M = Zr, Hf) by simple metathesis reactions of *cis*-

(TTP)MCl$_2$ with LiNHAr. However, when *o*-substituents are present on the amide reagent,

formation of a bis(amido) complex is not observed. Instead, a terminal imido complex is

produced. Presumably, *o*-substituted aryl amides are too bulky to form a *cis*-bis(amido)

species. Moreover, the kinetic stability of the final terminal imido complexes is also a

function of the size of the *o*-substituent. Varying the amide aryl group in the reaction of

LiNHR (R = 2,4,6-Me$_3$C$_6$H$_2$, 2,4,6-'BuC$_6$H$_2$ or 2,4,6-Ph$_3$C$_6$H$_2$) with (TTP)MCl$_2$ led to

thermally unstable imido complexes as observed by ^{1}H NMR. In these cases, analytically

pure samples could not be isolated.[34] The 2,4,6-triphenyl derivative, (TTP)Hf=NC$_6$H$_2$Ph$_3$,

was isolated as poorly diffracting crystals. A low resolution molecular structure confirms

the presence of an imido ligand, but the complex was thermally unstable in solution and in

the solid state.[35] The steric constraints in the related tetraazaanulene complexes are less

demanding. Thus, the formation of a secondary bis(amido), Zr(tmtaa)(HNAr^{iPr})$_2$,[9] is possible.

Examples of isolated N,N-bound ureato complexes formed from imido complexes have been thoroughly studied.[29] In addition, the similar N,O-bound carbamates are well known reaction products from [2+2] cycloaddition of isocyantes to oxo species.[29] To the best of our knowledge, there are no examples in the literature of an isolated transition metal N,O-bound ureato(2-).[36] This is somewhat of an anomaly since early transition metal M–O bonds are generally stronger than M–N bonds.[37] Nonetheless, the importance of N,O-bound forms has been implicated in the catalytic condensation of phenyl isocyanate to N,N-diphenylcarbodiimide via a proposed vanadium N,O-bound ureato intermediate.[38] There are two interesting examples that illustrate the reactivity of zirconium imido complexes with 'BuNCO. The first case involves the implication of a N,O-bound ureato(2-) as an intermediate in the reaction of $Cp_2Zr(N^tBu)$ with 'Bu-NCO. The final products are 1,3-di-t-butylcarbodiimide and $(Cp_2ZrO)_n$.[7] In the second example, treatment of the tetraazaanulene derivative, $(tmtaa)Zr=NAr^{Pr}$, with 'Bu-NCO yields the N,N-bound ureato.[9] The latter demonstrates the smaller steric demands of the tetraazaannulene ligand in comparison to those of the porphyrin ureato complexes 4a and 5a. Mean bond dissociation enthalpy data collected for amido $M(NR_2)_4$ (M = Zr, Hf; R = Me, Et) compounds indicate that Hf-NR_2 bonds are generally stronger than Zr bonds by $\approx$ 5%.[39] We propose that the stronger bonds of Hf explain the distinct conditions under which isomerization and decomposition of the ureato complexes 4a and 5a occur.

Specifically, higher temperatures are required for the isomerization of hafnium complex 5a (80°C) versus the zirconium analogue 4a (25°C). Similarly, the ejection of carbodiimide occurs for 4a at 80°C but does not for 5a at 110°C.

The anomalous preference of the N,O-binding motif of complexes **4b** and **5b** is presumably a manifestation of steric factors. The N,N-form is likely to have unfavorable steric interactions between the bulky Ar^{iPr} group and the porphyrin. The known N,N-bound ureato complexes, where steric factors appear not to be as critical, may be dictated by the resultant stronger C=O bond versus the weaker C=N bond required in a N,O-bound ureato.[40] Kinetic products with the bulky NAr^{iPr} group proximal to the porphyrin are converted to thermodynamic complexes with the smaller proximal ^tBuN group. This steric influence also appears to occur in the isomerization of the guanidino complex **7a**. These isomerizations are readily detected by ^1H NMR spectroscopy since the substituents of the metallacycle are strongly affected by the porphyrin ring current as a function of proximity. Under identical reaction conditions, the consumption of imido complexes **1** and **2** by ^tBuNCO was found to be complete within minutes for Zr but required $\approx$ 90 minutes for Hf. This difference may be attributed to the slightly more confined coordination sphere due to a smaller out-of-plane distance in **2** relative to the Zr imido analogue. Parallel behavior is seen in the reactions of imido complexes **1** and **2** with ^tBuNCS and ^tBuNCSe. For the [2+2] metallacycle products from reaction of complexes **1** or **2** with $^tBuNC=Ch$, the hafnium complexes were found to be more stable towards elimination of carbodiimide. The loss of carbodiimide from **4a** involves the cleavage of M-N and C-O σ-bonds and the formation of a metal-oxygen σ-bond and a carbon-nitrogen π-bond. Since the C-O cleavage and C=N formation processes are equivalent for both Zr and Hf, the difference in reactivity lies in the M-N and M=O bonds. Since Hf forms stronger σ-bonds than Zr,[41] **5a** does not eject

carbodiimide. The weaker C-S and C-Se bonds in 'BuNCS and 'BuNCSe are manifested in progressively more reactive N,Ch-bound metallacycles with respect to loss of carbodiimide.

In the reaction of 1 and 2 with 'BuNCS and 'BuNCSe the simultaneous presence of Ar^{iPr}N=C=N'Bu and the imido complexes does not lead to a guanidino derivative, presumably due to the steric bulk of the carbodiimide. In the presence of the less sterically demanding 'PrN=C=N'Pr, a kinetic [2+2] condensation product, (TTP)Hf(η^2-NAr^{iPr}C(=N'Pr)N'Pr) 7a, is formed.[42] As seen with the isocyanate [2+2] analogues, an isomerization slowly occurs which leads to a thermodynamic isomer with the bulky NAr^{iPr} moiety at the 3 position of the metallacycle.

The variable temperature ^{1}H NMR spectra of the guanidino complex 7b in toluene-d_8 reveal the dynamic aspects involving the imine nitrogen. At 223 K, two doublets for the diastereotopic isopropyl methyl groups are observed for NAr^{iPr} at 0.79 and 0.73 ppm. In addition, a doublet is observed for the methyl groups of each N'Pr unit at 0.60 (d, 6H) and -0.82 (d, 6H) ppm. The fact that a single doublet is present for the methyl protons of each N'Pr group indicates that the HfNCN four-membered metallacyclic ring must, on the NMR time scale, have a time-averaged mirror plane of symmetry which bisects the N'Pr groups. Warming the sample to 243 K results in coalescence of the NAr^{iPr} isopropyl groups (G‡ = 11.8 ± 0.3 kcal/mol). This resonance subsequently sharpens to a single doublet at temperatures above 253 K. At 283 K, the N'Pr methyl signals have coalesced (G‡ = 12.1 ± 0.3 kcal/mol) and reappear as a sharp doublet (-0.17 ppm) at 363 K. These two coalescence phenomena have equivalent activation barriers and are consistent with an inversion process at the imine nitrogen. The transition state for this process has C$_{2v}$ symmetry which results in

equivalent N^{i}Pr groups and NAr^{iPr} isopropyl groups which are no longer diastereotopic on the NMR time scale. Although rotation about the C_{ipso}-N_{imino} bond could also rationalize the coalescence behavior of the NAr^{iPr} isopropyl resonances, it is likely to be a higher energy process than inversion at the imine nitrogen. The observation of two coalescence temperatures for complex **7b** is presumably a result of a larger frequency difference for the N^{i}Pr resonances at the low-temperature limit relative to that for the NAr^{iPr} isopropyl signals.

In a similar manner, the η^2-N,O-ureato complex **6** also exhibits dynamic ^{1}H NMR features. However, only one of the NAr^{iPr} groups exhibits fluxional behavior. Since the NAr^{iPr} fragments proximal to the porphyrin in complexes **4a** and **5a** exhibit no fluxionality, the distal NAr^{iPr} group in complex **6** must be involved in the dynamic process. Moreover, the only motion that would collapse the diastereotopic ^{i}Pr methyl signals into a single resonance is rotation about the C_{ipso}-N_{imino} bond. The absence of an observable syn-anti isomerization for complex **6** suggests two possibilities: 1) rapid inversion which is not restricted at the lowest temperature observed (223 K) or 2) existence of only one isomer. However, syn-anti inversion barriers of imine units are relatively high, typically on the order of 10-20 kcal/mol.[43] Also, it is unlikely that the imine inversion barrier in complex **7** is significantly lower than normal. Consequently, the imine fragment in complex **6** must exist in one geometric form. This is not unreasonable as the two large Ar^{iPr} substituents should prefer to occupy mutually anti sites.

syn-   anti-
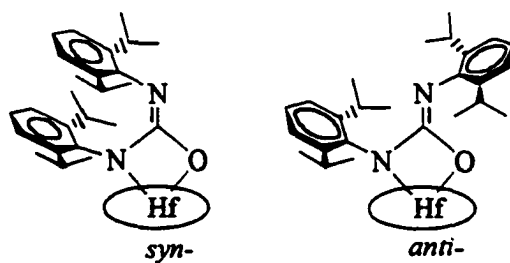
Conclusion

In summary we have found the rigid basil plane formed by the porphyrin results in novel zirconium and hafnium imido reaction products in comparison to known $L_nM=NR$ (M = Zr, Hf) complexes with other supporting ligand systems. Kinetic products from the reaction of RNCO and $^iPrN=C=N^iPr$ with imido complexes 1 and 2 are formed with the NAr^{iPr} moiety remaining bonded to the metal and the heterocumulene derived nitrene in the distal (3-position) of the metallacycle. Distinct isomerization conditions found for **4a** and **5a** illustrate the steric interactions of the porphyrin macrocycle with substituents in the a position of the metallacycle ligand as well as bonding characteristics between Zr–N and Hf–N. Steric factors appear to be manifested in the conversion of the kinetic isomers to the thermodynamic complexes. Difference in bond strengths between the $M-N_{amide}$ bond (M = Zr, Hf) are exhibited in the requirement of more forcing conditions for isomerization of **5a** relative to **4a**.

The imido complexes also exhibit reactivity with a variety of other heterocumulenes, aldehydes, and ketones. The chemistry of an interesting pinacolone coupling product, $(TTP)Zr(\eta^2-OC(^tBu)(Me)CH=C(^tBu)O)$, is currently under investigation.[23]

References

‡   University of Minnesota, X-ray Crystallographic Laboratory.

1.   Walsh, P. J.; Hollander, F. J.; Bergman, R. G. *J. Am. Chem. Soc.* **1988**, *110*, 8729.

2.   Cummins, C. C.; Baxter, S. M.; Wolczanski, P. T. *J. Am. Chem. Soc.* **1988**, *110*, 8731.

3.   Profilet, R. D.; Zambrano, C. H.; Fanwick, P. E.; Nash, J. J.; Rothwell, I. P. *Inorg. Chem.* **1990**, *29*, 4362.

4.   Bai, Y.; Roesky, H. W.; Noltemeyer, M.; Witt, M. *Chem. Ber.* **1992**, *125*, 825.

5.   Arney, D. J.; Bruck, M. A.; Huber, S. R.; Wigley, D. E. *Inorg. Chem.* **1992**, *31*, 3749.

6.   Zambrano, C. H.; Profilet, R. D.; Hill, J. E.; Fanwick, P. E.; Rothwell, I. P. *Polyhedron* **1993**, *12*, 689.

7.   Walsh, P. J.; Hollander, F. J.; Bergman, R. G. *Organometallics* **1993**, *12*, 3705.

8.   Meyer, K. E.; Walsh, P. J.; Bergman, R. G. *J. Am. Chem. Soc.* **1995**, *117*, 974.

9.   Blake, A. J.; Mountford, P.; Nikonov, G. I.; Swallow, D. *J. Chem. Soc., Chem. Commun.* **1996**, 1835.

10.   Fryzuk, M. D.; Love, J. B.; Rettig, S. J. *Organometallics* **1998**, *17*, 846.

11.   (a) Wigley, D. E. *Progress in Inorganic Chemistry* **1994**, *42*, 239. (b) Mountford, P. *J. Chem. Soc., Chem. Commun.* **1997**, 2127.

12.   Bennett, J. L.; Wolczanski, P. T. *J. Am. Chem. Soc.* **1994**, *116*, 2179 and references therein.

13.   Winter, C. H.; Lewkebandara, T. S.; Prosica, J. W.; Rheingold, A. L. *Inorg. Chem.* **1994**, *33*, 1227.

14.   (a) Walsh, P. J.; Baranger, A. M.; Bergman, R. G. *J. Am. Chem. Soc.* **1992**, *114*, 1708. (b) Baranger, A. M.; Walsh, P. J.; Bergman, R. G. *J. Am. Chem. Soc.* **1993**, *115*, 2753.

15.   Cummins, C. C.; Van Duyne, G. D.; Schaller, C. P.; Wolczanski, P. T. *Organometallics* **1991**, *10*, 164.

16. Meyer, K. E.; Walsh, P. J.; Bergman, R. G. *J. Am. Chem. Soc.* **1994**, *116*, 2669.

17. Schaller, C. P.; Cummins, C. C.; Wolczanski, P. T. *J. Am. Chem. Soc.* **1996**, *118*, 591.

18. (a) Berreau, L. M.; Young, V. G., Jr.; Woo, L. K. *Inorg. Chem.* **1995**, *34*, 527. (b) Gray, S. D.; Thorman, J. L.; Berreau, L. M.; Woo, L. K. *Inorg. Chem.* **1997**, *36*, 278. (c) Gray, S. D., Thorman, J. L.; Adamian, V. A.; Kadish, K. M.; Woo, L. K. *Inorg. Chem.* **1998**, *37*, 1. (d) Chen, J.; Woo, L. K. *Inorg. Chem.* **1998**, *37*, 3269.

19. Brand, H.; Arnold, J. *Coord. Chem. Rev.* **1995**, *140*, 137.

20. Blake, A. J.; McInnes, J. M.; Mountford, P.; Nikonov, G. I.; Swallow, D.; Watkin, D. J. *J. Chem. Soc., Dalton Trans.* **1999**, 379.

21. (a) Kim, H.; Whang, D.; Kim, K.; Do, Y. *Inorg. Chem.* **1993**, *32*, 360. (b) Ryu, S.; Whang, D.; Kim, J.; Yeo, W.; Kim, K. *J. Chem. Soc., Dalton Trans.* **1993**, 205.

22. Sonoda, N.; Yamamoto, G.; Tsutsum, S. *Bull. Chem. Soc. Japan*, **1972**, *45*, 2937.

23. Thorman, J. L.; Guzei, I. A.; Young, V. G., Jr.; Woo, L. K. Manuscript in preparation.

24. SHELXTL-Plus V5.0, Siemens Industrial Automation, Inc., Madison, WI.

25. All software and sources of the scattering factors are contained in the SHELXTL V5.10 program library. Sheldrick, G., Siemens XRD, Madison, WI.

26. (a) (OEP)ZrCl$_2$, (OEP)Zr(OBu^i)$_2$, and (OEP)ZrMe$_2$ Brand, H.; Arnold, J. *Organometallics* **1993**, *12*, 3655. (b) (OEP)Zr(CH$_2$SiMe$_3$)$_2$ Brand, H.; Arnold, J. *J. Am. Chem. Soc.* **1992**, *114*, 2266. (c) (TPP)Hf(benzenedithiolato) Ryu, S.; Whang, D.; Yeo, H.; Kim, K. *Inorg. Chim. Acta* **1994**, *221*, 51.

27. Shannon, R. D. *Acta Cryst.* **1976**, *A32*, 751.

28. Jentzen, W.; Simpson, M. C.; Hobbs, J. D.; Song, X.; Ema, T.; Nelson, N. Y.; Medforth, C. J.; Smith, K. M.; Veyrat, M.; Mazzanti, M.; Ramasseul, R.; Marchon, J.-C.; Takeuchi, T.; Goddard, W. A., III.; Shelnutt, J. A. *J. Am. Chem. Soc.* **1995**, *117*, 11085.

29. (a) Bryan, J. C.; Burrell, A. K.; Miller, M. M.; Smith, W. H.; Burns, C. J.; Sattelberger, A. P. *Polyhedron* **1993**, *12*, 1769. (b) Legzdins, P.; Phillips, E. C.; Rettig, S. J.; Trotter, J.; Veltheer, J. E.; Yee, V. C. *Organometallics* **1992**, *11*, 3104. (c) Jolly, M.; Mitchell, J. P.; Gibson, V. C. *J. Chem. Soc., Dalton Trans.* **1992**, 1329. (d) Michelman, R. I.; Anderson, R. A.; Bergman, R. G. *J. Am. Chem. Soc.* **1991**, *113*,

5100. (e) Leung, W. H.; Wilkinson, G.; Hussain-Bates, B.; Hursthouse, M. B. *J. Chem. Soc., Dalton Trans.* **1991**, 2791. (f) Herrmann, W. A.; Weichselbaumer, G.; Paciello, R. A.; Fischer, R. A.; Herdtweck, E.; Okuda, J.; Marz, D. W. *Organometallics* **1990**, *9*, 489. (g) Pilato, R. S.; Housemekerides, C. E.; Jernakoff, P.; Rubin, D.; Geoffroy, G. L.; Rheingold, A. L. *Organometallics* **1990**, *8*, 2333. For reviews of RNCO: (h) Bruanstein, P.; Nobel, D. *Chem. Rev.* **1989**, *89*, 1927. (i) Cenini, S.; LaMonica, G. *Inorg. Chim. Acta* **1976**, *18*, 279.

30. Protonolysis of $(OEP)Zr(CH_2SiMe_3)_2$ by 1 equivalent of H_2O in $CDCl_3$ generates 2 equivalents of $SiMe_4$ and an unisolated complex formulated by ^1H NMR as $[(OEP)Zr]_2(\mu-O)_2$.[26a]

31. (a) Hagen, K.; Holwill, C. J.; Rice, D. A; Runnacles, J. D. *Inorg. Chem.* **1988**, *27*, 2032. (b) Cardin, D. J.; Lappert, M. F.; Raston, C. L. *Chemistry of Organ-Zirconium and -Hafnium Compounds*; Ellis Horwood Limited: West Sussex, 1986; p 101.

32. (a) 2.12 Å average: $Hf(=NAr^{iPr})(NH(Ar^{iPr})_2$(4-pyrrolidinpyridine)$_2$, ref. 6. (b) 2.03 Å: $Cp^*_2Hf(H)(NHMe)$, Hillhouse, G. L.; Bulls, A. R.; Santarsiero, B. D.; Bercaw, J. E. *Organometallics* **1988**, *7*, 1309. (c) 2.092 Å average: $(Me_4taen)Hf(NMe_2)_2$, Black, D. G.; Jordan, R. F.; Rogers, R. D. *Inorg. Chem.* **1997**, *36*, 103. (d) Covalent radii estimates: O = 0.66, N = 0.70 Å; Jolly, W. L. *Modern Inorganic Chemistry*; McGraw-Hill: New York, 1984; p 52. Zr = 1.48, Hf = 1.49, O = 0.73, N = 0.75 Å. Porterfield, W. W. *Inorganic Chemistry*, 2nd ed.; Academic Press: San Deigo, CA, 1998; p 214.

33. For a leading reference pertaining to geometries of d^0 ML_6 complexes, see ref. 32c.

34. For example, during a recrystallization attempt of (TTP)Zr(=NMes*) from toluene/hexanes at –25 °C, approximately 30% decomposed to uncharacterized paramagnetic species.

35. Thorman, J. L.; Woo, L. K. Unpublished results. R value ≈13%. At ambient temperature $(TTP)Hf(NPh(Ph)_3)$ crystals decomposed within hours.

36. (a) Examples of molybdenum and chromium N,O-bound ureato(1-): Lam, H. W.; Wilkinson, G.; Hussain-Bates, B.; Hursthouse, M. B. *J. Chem. Soc., Dalton Trans.* **1993**, 781. (b) Synthesis of $((Me_3Si)_2N)_2Sn(NAr^{iPr}C(=NAr^{iPr})O)$ from $((Me_3Si)_2N)_2Sn(=NAr^{iPr})$ and $Ar^{iPr}NCO$: Ossig, G.; Meller, A.; Freitag, S. Herbst-Irmer, R.; Sheldrick, G. M. *Chem. Ber.* **1993**, *126*, 2247.

37. (a) Ziegler, T.; Tschinke, V.; Versluis, L.; Baerends, E. J.; Ravenek, W. *Polyhedron* **1988**, *7*, 1625. (b) Lappert, M. F.; Patil, D. S.; Pedley, J. B. *J. Chem. Soc., Chem. Commun.* **1975**, 830. (c) Schock, L. E.; Marks, T. J. *J. Am. Chem. Soc.* **1988**, *110*, 7701.

38. Birdwhistell, K. R.; Boucher, T.; Ensminger, M.; Harris, S.; Johnson, M.; Toporek, S. *Organometallics* **1993**, *12*, 1023.

39. (Zr-NMe$_2$) = 83.6 kcal/mol, (Hf-NMe$_2$) = 88.4 kcal/mol. Cardin, D. J.; Lappert, M. F.; Raston, C. L. *Chemistry of Organ-Zirconium and -Hafnium Compounds*; Ellis Horwood Limited: West Sussex, 1986; pp 16-22.

40. March, J. *Advanced Organic Chemistry: Reactions, Mechanisms, and Structure*, 4th ed.; Wiley: New York, 1992; p 24.

41. (a) Ziegler, T.; Tschinke, V.; Versluis, L.; Baerends, E. J.; Ravenek, W. *Polyhedron* **1988**, *7*, 1625. (b) Lappert, M. F.; Patil, D. S.; Pedley, J. B. *J. Chem. Soc., Chem. Commun.* **1975**, 830. (c) Schock, L. E.; Marks, T. J. *J. Am. Chem. Soc.* **1988**, *110*, 7701.

42. Guanidino(2-): Tin, M. K. T.; Yap, G. P. A.; Richeson, D. S. *Inorg. Chem.* **1998**, *37*, 6728. Guanidino(1-): Gazard, P. A.; Melvyn, K.; Batsanov, A. S.; Howard, J. A. K. *J. Chem. Soc., Dalton Trans.* **1997**, 4625.

43. (a) Patai, S. *The Chemistry of the Carbon-Nitrogen Double Bond*; Interscience Publishers: London, 1970; Chapter 9. (b) Hartwig, J. F.; Bergman, R. G.; Andersen, R. A. *Organometallics* **1991**, *10*, 3344. (c) Knorr, R.; Ruhdorfer, J.; Mehlstaeubl, J.; Boehrer, P.; Stephenson, D. S. *Chem. Ber.* **1993**, *126*, 747.

APPENDIX A

Table I. Crystal data, data collection, and solution and refinement for complex 1, (TTP)Zr=NAr^{iPr}

Empirical formula	$C_{70.50}H_{69}N_5Zr$
Crystal habit, color	Block, Purple
Crystal size	0.28 x 0.26 x 0.22 mm
Crystal system	Monoclinic
Space group	P2$_1$/n
	$a = 16.6358(2)$ Å $\alpha = 90°$
	$b = 18.7583(1)$ Å $\beta = 103.970(1)°$
	$c = 19.4375(2)$ Å $\gamma = 90°$
Volume	5886.24(10) Å^3
Z	4
Formula weight	1077.53
Density (calculated)	1.216 Mg/m^3
Absorption coefficient	0.233 mm^{-1}
F(000)	2268
Diffractometer	Siemens SMART Platform CCD
Wavelength	0.71073 Å
Temperature	172(2) K
θ range for data collection	1.45 to 25.00°
Index ranges	$-19 \leq h \leq 19, 0 \leq k \leq 22, 0 \leq l \leq 23$
Reflections collected	29098
Independent reflection	10237 ($R_{int} = 0.0313$)
System used	SHELXTL-V5.0
Solution	Direct methods
Refinement method	Full-matrix least-squares on F^2
Weighting scheme	$W = [\sigma^2(F_o^2) + (AP)^2 + (BP)]^{-1}$, where P = $(F_o^2 + 2Fc^2))/3$, A = 0.0610, and B = 1.8549p]
Absorption correction	SADABS (Sheldrick, 1996)
Max. and min. transmission	1.000 and 0.774
Data / restraints / parameters	10232 / 0 / 694
R indices (I > 2σ(I) = 7872)	R1 = 0.0403, wR2 = 0.0984
R indices (all data)	R1 = 0.0620, wR2 = 0.1093
Goodness-of-fit on F^2	0.977
Largest diff. peak and hole	0.305 and -0.509 eÅ^{-3}

Table II. Atomic coordinates and equivalent isotropic displacement parameters for (TTP)Zr=NAr^{Pr}. U(eq) is defined as one third of the trace of the orthogonalized U_{ij} tensor.

Atom	x	y	z	U(eq)	SOF
Zr(1)	-0.088226(14)	0.850698(12)	0.366714(12)	0.02126(8)	1
N(1)	-0.05427(12)	0.89076(10)	0.27073(10)	0.0248(5)	1
N(2)	-0.21346(12)	0.88735(10)	0.31222(10)	0.0253(5)	1
N(3)	-0.12386(12)	0.89068(10)	0.46278(10)	0.0238(4)	1
N(4)	0.03461(12)	0.89471(10)	0.42093(10)	0.0241(5)	1
C(1)	0.0249(2)	0.90287(13)	0.26186(13)	0.0275(6)	1
C(2)	0.0209(2)	0.90520(15)	0.18713(14)	0.0357(6)	1
C(3)	-0.0590(2)	0.89473(14)	0.15167(14)	0.0345(6)	1
C(4)	-0.1069(2)	0.88683(13)	0.20378(13)	0.0264(6)	1
C(5)	-0.1937(2)	0.87927(13)	0.18944(13)	0.0272(6)	1
C(6)	-0.24299(15)	0.88094(13)	0.23957(13)	0.0252(5)	1
C(7)	-0.3318(2)	0.87456(14)	0.22401(14)	0.0311(6)	1
C(8)	-0.3549(2)	0.87672(14)	0.28604(13)	0.0306(6)	1
C(9)	-0.28105(15)	0.88459(13)	0.34209(13)	0.0263(6)	1
C(10)	-0.27707(15)	0.88695(13)	0.41546(13)	0.0272(6)	1
C(11)	-0.20454(15)	0.89168(12)	0.47124(13)	0.0257(5)	1
C(12)	-0.2018(2)	0.89672(13)	0.54540(13)	0.0302(6)	1
C(13)	-0.1205(2)	0.89614(13)	0.58156(13)	0.0296(6)	1
C(14)	-0.0714(2)	0.89337(12)	0.53007(13)	0.0261(6)	1
C(15)	0.01589(15)	0.89382(12)	0.54483(13)	0.0253(5)	1
C(16)	0.06418(15)	0.89928(12)	0.49382(13)	0.0255(5)	1
C(17)	0.15097(15)	0.91619(13)	0.50962(14)	0.0296(6)	1
C(18)	0.17299(15)	0.92237(13)	0.44717(13)	0.0292(6)	1
C(19)	0.10076(14)	0.90870(12)	0.39072(13)	0.0250(5)	1
C(20)	0.09688(15)	0.91151(12)	0.31760(13)	0.0264(5)	1
C(21)	-0.23799(15)	0.86779(14)	0.11293(13)	0.0289(6)	1
C(22)	-0.2362(2)	0.8011(2)	0.0829(2)	0.0488(8)	1
C(23)	-0.2784(2)	0.7880(2)	0.0128(2)	0.0530(8)	1
C(24)	-0.3223(2)	0.8405(2)	-0.02917(15)	0.0445(8)	1
C(25)	-0.3231(2)	0.9078(2)	0.0010(2)	0.0539(9)	1

Table II. (continued)

Atom	x	y	z	U(eq)	SOF
C(26)	-0.2818(2)	0.9211(2)	0.07111(15)	0.0422(7)	1
C(27)	-0.3700(2)	0.8262(2)	-0.1046(2)	0.0727(12)	1
C(28)	-0.3576(2)	0.88031(15)	0.43707(14)	0.0325(6)	1
C(29)	-0.3737(2)	0.8201(2)	0.4738(2)	0.0458(7)	1
C(30)	-0.4487(2)	0.8126(2)	0.4930(2)	0.0569(9)	1
C(31)	-0.5095(2)	0.8641(2)	0.4761(2)	0.0549(9)	1
C(32)	-0.4938(2)	0.9237(2)	0.4402(2)	0.0578(9)	1
C(33)	-0.4184(2)	0.9325(2)	0.4212(2)	0.0451(7)	1
C(34)	-0.5926(2)	0.8545(3)	0.4952(2)	0.0868(14)	1
C(35)	0.06324(15)	0.88746(13)	0.62060(13)	0.0258(6)	1
C(36)	0.1149(2)	0.82850(14)	0.64228(14)	0.0319(6)	1
C(37)	0.1575(2)	0.82102(15)	0.71253(15)	0.0369(7)	1
C(38)	0.1517(2)	0.8712(2)	0.76362(14)	0.0362(7)	1
C(39)	0.1012(2)	0.93047(15)	0.74168(14)	0.0380(7)	1
C(40)	0.0577(2)	0.93848(13)	0.67145(13)	0.0323(6)	1
C(41)	0.1990(2)	0.8624(2)	0.8404(2)	0.0532(9)	1
C(42)	0.1765(2)	0.92737(13)	0.29691(13)	0.0290(6)	1
C(43)	0.2416(2)	0.8790(2)	0.3115(2)	0.0390(7)	1
C(44)	0.3159(2)	0.8938(2)	0.2931(2)	0.0443(7)	1
C(45)	0.3264(2)	0.9566(2)	0.2588(2)	0.0453(7)	1
C(46)	0.2613(2)	1.0052(2)	0.2451(2)	0.0496(8)	1
C(48)	0.4069(2)	0.9721(2)	0.2372(2)	0.0696(11)	1
N(5)	-0.08884(12)	0.75144(10)	0.36319(10)	0.0262(5)	1
C(49)	-0.08283(14)	0.67806(13)	0.36953(13)	0.0252(5)	1
C(50)	-0.0901(2)	0.63417(13)	0.30838(14)	0.0293(6)	1
C(51)	-0.0809(2)	0.56045(14)	0.31730(15)	0.0365(7)	1
C(52)	-0.0649(2)	0.52955(15)	0.3840(2)	0.0428(7)	1
C(53)	-0.0597(2)	0.57214(14)	0.4434(2)	0.0382(7)	1
C(54)	-0.0689(2)	0.64579(13)	0.43763(14)	0.0297(6)	1
C(55)	-0.1070(2)	0.66805(14)	0.23524(13)	0.0324(6)	1

Table II. (continued)

C(56)	-0.1509(2)	0.6181(2)	0.1755(2)	0.0453(7)	1
C(57)	-0.0267(2)	0.6976(2)	0.2203(2)	0.0457(7)	1
C(58)	-0.0670(2)	0.69282(14)	0.50188(14)	0.0346(6)	1
C(59)	-0.1548(2)	0.7095(2)	0.5064(2)	0.0485(8)	1
C(60)	-0.0158(2)	0.6631(2)	0.5713(2)	0.0494(8)	1
C(61)	0.3054(3)	0.7086(2)	0.2490(2)	0.0733(11)	1
C(62)	0.3698(3)	0.7264(2)	0.2179(2)	0.0839(13)	1
C(63)	0.4493(3)	0.7250(3)	0.2557(3)	0.0925(14)	1
C(64)	0.4690(3)	0.7076(3)	0.3248(3)	0.109(2)	1
C(65)	0.4097(3)	0.6899(3)	0.3579(3)	0.099(2)	1
C(66)	0.3281(3)	0.6897(2)	0.3218(2)	0.0789(12)	1
C(67)	0.2158(3)	0.7093(3)	0.2073(3)	0.123(2)	1
C(68)	-0.0353(3)	1.0273(2)	-0.0005(2)	0.0865(13)	1
C(69)	-0.1193(3)	1.0033(3)	-0.0436(2)	0.0927(14)	1
C(70)	-0.1879(4)	1.0582(3)	-0.0478(3)	0.116(2)	0.50
C(70')	-0.1879(4)	1.0582(3)	-0.0478(3)	0.116(2)	0.50
C(71')	-0.1845(7)	1.1249(5)	-0.0867(6)	0.108(3)	0.50

Table III. Bond lengths [Å] and angles [°] for (TTP)Zr=NAr^{Pr}

Zr1–N5	1.863(2)	C28–C29	1.395(4)
Zr1–N2	2.207(2)	C29–C30	1.395(4)
Zr1–N1	2.208(2)	C30–C31	1.379(5)
Zr1–N4	2.220(2)	C31–C32	1.377(5)
Zr1–N3	2.221(2)	C31–C34	1.526(4)
N1–C4	1.384(3)	C32–C33	1.399(4)
N1–C1	1.388(3)	C35–C40	1.395(3)
N2–C6	1.384(3)	C35–C36	1.401(4)
N2–C9	1.385(3)	C36–C37	1.386(4)
N3–C14	1.387(3)	C37–C38	1.388(4)
N3–C11	1.391(3)	C38–C39	1.398(4)
N4–C16	1.386(3)	C38–C41	1.518(4)
N4–C19	1.392(3)	C39–C40	1.390(4)
C1–C20	1.416(3)	C42–C43	1.388(4)
C1–C2	1.439(3)	C42–C47	1.390(4)
C2–C3	1.356(4)	C43–C44	1.396(4)
C3–C4	1.440(3)	C44–C45	1.386(4)
C4–C5	1.411(3)	C45–C46	1.392(4)
C5–C6	1.417(3)	C45–C48	1.524(4)
C5–C21	1.507(3)	C46–C47	1.390(4)
C6–C7	1.439(3)	N5–C49	1.383(3)
C7–C8	1.352(3)	C49–C54	1.423(3)
C8–C9	1.439(3)	C49–C50	1.427(3)
C9–C10	1.412(3)	C50–C51	1.397(3)
C10–C11	1.417(3)	C50–C55	1.520(4)
C10–C28	1.502(3)	C51–C52	1.386(4)
C11–C12	1.434(3)	C52–C53	1.388(4)
C12–C13	1.365(4)	C53–C54	1.391(4)
C13–C14	1.437(3)	C54–C58	1.523(4)
C14–C15	1.411(3)	C55–C56	1.533(4)
C15–C16	1.422(3)	C55–C57	1.537(4)
C15–C35	1.498(3)	C58–C60	1.517(4)

Table III. (continued)

C16–C17	1.437(3)	C58–C59	1.518(4)
C17–C18	1.355(3)	C61–C62	1.392(6)
C18–C19	1.441(3)	C61–C66	1.418(6)
C19–C20	1.408(3)	C61–C67	1.515(6)
C20–C42	1.504(3)	C62–C63	1.349(6)
C21–C26	1.380(4)	C63–C64	1.344(7)
C21–C22	1.384(4)	C64–C65	1.344(6)
C22–C23	1.397(4)	C65–C66	1.370(6)
C23–C24	1.372(4)	C68–C69	1.514(6)
C24–C25	1.392(4)	C68–C68–#1	1.553(8)
C24–C27	1.514(4)	C69–C70'	1.525(6)
C25–C26	1.393(4)	C69–C70	1.525(6)
C28–C33	1.388(4)	C70'–C71'	1.470(10)
N5–Zr1–N2	107.31(8)	C21–C22–C23	120.9(3)
N5–Zr1–N1	108.02(8)	C24–C23–C22	121.6(3)
N2–Zr1–N1	83.85(7)	C23–C24–C25	117.3(3)
N5–Zr1–N4	112.67(8)	C23–C24–C27	121.8(3)
N2–Zr1–N4	140.01(7)	C25–C24–C27	120.9(3)
N1–Zr1–N4	83.14(7)	C24–C25–C26	121.5(3)
N5–Zr1–N3	111.60(8)	C21–C26–C25	120.8(3)
N2–Zr1–N3	83.44(7)	C33–C28–C29	117.7(2)
N1–Zr1–N3	140.36(7)	C33–C28–C10	122.1(2)
N4–Zr1–N3	82.95(7)	C29–C28–C10	120.3(2)
C4–N1–C1	107.2(2)	C28–C29–C30	120.9(3)
C4–N1–Zr1	122.94(15)	C31–C30–C29	121.1(3)
C1–N1–Zr1	127.2(2)	C32–C31–C30	118.2(3)
C6–N2–C9	107.5(2)	C32–C31–C34	120.9(3)
C6–N2–Zr1	121.6(2)	C30–C31–C34	121.0(3)
C9–N2–Zr1	123.7(2)	C31–C32–C33	121.4(3)
C14–N3–C11	107.0(2)	C28–C33–C32	120.7(3)

Table III. (continued)

C14–N3–Zr1	124.8(2)	C40–C35–C36	118.0(2)
C11–N3–Zr1	124.4(2)	C40–C35–C15	122.2(2)
C16–N4–C19	107.3(2)	C36–C35–C15	119.8(2)
C16–N4–Zr1	124.6(2)	C37–C36–C35	120.5(3)
C19–N4–Zr1	126.9(2)	C36–C37–C38	121.9(3)
N1–C1–C20	125.2(2)	C37–C38–C39	117.5(2)
N1–C1–C2	108.4(2)	C37–C38–C41	121.3(3)
C20–C1–C2	126.4(2)	C39–C38–C41	121.2(3)
C3–C2–C1	108.1(2)	C40–C39–C38	121.2(3)
C2–C3–C4	107.4(2)	C39–C40–C35	120.9(2)
N1–C4–C5	125.2(2)	C43–C42–C47	118.3(2)
N1–C4–C3	108.9(2)	C43–C42–C20	120.6(2)
C5–C4–C3	125.9(2)	C47–C42–C20	121.0(2)
C4–C5–C6	126.6(2)	C42–C43–C44	120.9(3)
C4–C5–C21	116.3(2)	C45–C44–C43	121.0(3)
C6–C5–C21	117.1(2)	C44–C45–C46	117.8(3)
N2–C6–C5	125.6(2)	C44–C45–C48	121.1(3)
N2–C6–C7	108.4(2)	C46–C45–C48	121.1(3)
C5–C6–C7	126.0(2)	C47–C46–C45	121.6(3)
C8–C7–C6	108.0(2)	C46–C47–C42	120.4(3)
C7–C8–C9	107.7(2)	C49–N5–Zr1	172.5(2)
N2–C9–C10	125.2(2)	N5–C49–C54	119.9(2)
N2–C9–C8	108.5(2)	N5–C49–C50	120.7(2)
C10–C9–C8	126.2(2)	C54–C49–C50	119.4(2)
C9–C10–C11	126.7(2)	C51–C50–C49	118.9(2)
C9–C10–C28	116.9(2)	C51–C50–C55	121.3(2)
C11–C10–C28	116.3(2)	C49–C50–C55	119.8(2)
N3–C11–C10	125.2(2)	C52–C51–C50	121.3(2)
N3–C11–C12	108.8(2)	C51–C52–C53	119.7(3)
C10–C11–C12	126.0(2)	C52–C53–C54	121.4(3)
C13–C12–C11	107.7(2)	C53–C54–C49	119.1(2)

Table III. (continued)

C12–C13–C14	107.5(2)	C53–C54–C58	122.0(2)
N3–C14–C15	125.0(2)	C49–C54–C58	118.9(2)
N3–C14–C13	108.9(2)	C50–C55–C56	113.6(2)
C15–C14–C13	126.0(2)	C50–C55–C57	110.8(2)
C14–C15–C16	125.8(2)	C56–C55–C57	110.7(2)
C14–C15–C35	118.1(2)	C60–C58–C59	111.5(2)
C16–C15–C35	116.1(2)	C60–C58–C54	114.4(2)
N4–C16–C15	126.0(2)	C59–C58–C54	109.7(2)
N4–C16–C17	108.8(2)	C62–C61–C66	116.5(4)
C15–C16–C17	125.1(2)	C62–C61–C67	121.7(5)
C18–C17–C16	107.6(2)	C66–C61–C67	121.8(4)
C17–C18–C19	108.1(2)	C63–C62–C61	121.0(4)
N4–C19–C20	125.8(2)	C64–C63–C62	121.2(5)
N4–C19–C18	108.1(2)	C63–C64–C65	120.7(5)
C20–C19–C18	126.0(2)	C64–C65–C66	120.4(5)
C19–C20–C1	126.3(2)	C65–C66–C61	120.2(4)
C19–C20–C42	116.7(2)	C69–C68–C68 #1	114.0(5)
C1–C20–C42	117.0(2)	C68–C69–C70'	114.1(4)
C26–C21–C22	117.9(3)	C68–C69–C70	114.1(4)
C26–C21–C5	122.7(2)	C71'–C70'–C69	118.7(5)
C22–C21–C5	119.3(2)		

Table IV. Crystal data, data collection, and solution and refinement for complex 2, (TTP)Hf=NAr^{iPr}

Crystal Data	
Empirical formula	$C_{70.50}H_{69}HfN_5$
Crystal habit, color	Block, Purple
Crystal size	0.28 x 0.24 x 0.12 mm
Crystal system	Monoclinic
Space group	$P2_1/n$
	$a = 16.6081(2)$ Å $\alpha = 90°$
	$b = 18.6360(3)$ Å $\beta = 104.029(1)°$
	$c = 19.3910(1)$ Å $\gamma = 90°$
Volume	$5822.67(12)$ Å^3
Z	4
Formula weight	1164.80
Density (calculated)	1.329 Mg/m^3
Absorption coefficient	1.838 mm^{-1}
F(000)	2396
Diffractometer	Siemens SMART Platform CCD
Wavelength	0.71073 Å
Temperature	173(2) K
θ range for data collection	1.45 to 25.06°
Index ranges	$-19 \le h \le 19, 0 \le k \le 22, 0 \le \ell \le 23$
Reflections collected	32323
Independent reflection	10215 ($R_{int} = 0.0270$)
System used	SHELXTL-V5.0
Solution	Direct methods
Refinement method	Full-matrix least-squares on F^2
Weighting scheme	$W = [\sigma^2(F_o^2) + (AP)^2 + (BP)]^{-1}$, where $P = (F_o^2 + 2Fc^2))/3$, A = 0.0208, and B = 6.0854
Absorption correction	SADABS (Sheldrick, 1996)
Max. and min. transmission	1.000 and 0.860
Data / restraints / parameters	10215 / 0 / 694
R indices (I > 2σ(I) = 7872)	R1 = 0.0263, wR2 = 0.0573
R indices (all data)	R1 = 0.0343, wR2 = 0.0602
Goodness-of-fit on F^2	1.055
Largest diff. peak and hole	0.444 and -1.079 eÅ^{-3}

Table V. Atomic coordinates and equivalent isotropic displacement parameters for (TTP)Hf=NAr^{iPr}. U(eq) is defined as one third of the trace of the orthogonalized U_{ij} tensor.

Atom	x	y	z	U(eq)	SOF
Hf(1)	-0.087843(7)	0.852927(6)	0.366437(6)	0.01930(4)	1
N(1)	-0.05394(14)	0.89105(12)	0.27095(12)	0.0225(5)	1
N(2)	-0.21251(14)	0.88714(12)	0.31219(12)	0.0220(5)	1
N(3)	-0.12337(14)	0.89067(12)	0.46204(12)	0.0223(5)	1
N(4)	0.03442(14)	0.89506(12)	0.42062(12)	0.0219(5)	1
C(1)	0.0252(2)	0.9030(2)	0.2622(2)	0.0255(6)	1
C(2)	0.0209(2)	0.9055(2)	0.1872(2)	0.0324(7)	1
C(3)	-0.0589(2)	0.8953(2)	0.1522(2)	0.0317(7)	1
C(4)	-0.1068(2)	0.8870(2)	0.20389(15)	0.0254(6)	1
C(5)	-0.1935(2)	0.8796(2)	0.18916(15)	0.0254(6)	1
C(6)	-0.2423(2)	0.88091(15)	0.23918(15)	0.0234(6)	1
C(7)	-0.3309(2)	0.8750(2)	0.2235(2)	0.0285(7)	1
C(8)	-0.3544(2)	0.8767(2)	0.2856(2)	0.0293(7)	1
C(9)	-0.2801(2)	0.88477(15)	0.3420(2)	0.0237(6)	1
C(10)	-0.2768(2)	0.8870(2)	0.4152(2)	0.0253(6)	1
C(11)	-0.2040(2)	0.8919(2)	0.4706(2)	0.0244(6)	1
C(12)	-0.2011(2)	0.8966(2)	0.5448(2)	0.0281(7)	1
C(13)	-0.1204(2)	0.8962(2)	0.5806(2)	0.0268(7)	1
C(14)	-0.0710(2)	0.89306(14)	0.52940(15)	0.0226(6)	1
C(15)	0.0166(2)	0.89329(14)	0.54436(15)	0.0240(6)	1
C(16)	0.0642(2)	0.89888(14)	0.49349(15)	0.0231(6)	1
C(17)	0.1513(2)	0.9152(2)	0.5093(2)	0.0278(7)	1
C(18)	0.1734(2)	0.9218(2)	0.4470(2)	0.0273(7)	1
C(19)	0.1004(2)	0.90850(15)	0.39064(15)	0.0233(6)	1
C(20)	0.0969(2)	0.91180(15)	0.3176(2)	0.0243(6)	1
C(21)	-0.2378(2)	0.8682(2)	0.11271(15)	0.0275(7)	1
C(22)	-0.2348(2)	0.8019(2)	0.0820(2)	0.0449(9)	1
C(23)	-0.2764(2)	0.7890(2)	0.0120(2)	0.0514(10)	1
C(24)	-0.3220(2)	0.8416(2)	-0.0294(2)	0.0431(9)	1

Table V. (continued)

Atom	x	y	z	U(eq)	SOF
C(25)	-0.3241(2)	0.9083(2)	0.0013(2)	0.0493(10)	1
C(26)	-0.2828(2)	0.9223(2)	0.0715(2)	0.0402(8)	1
C(27)	-0.3696(2)	0.8273(3)	-0.1046(2)	0.0710(14)	1
C(28)	-0.3567(2)	0.8806(2)	0.4367(2)	0.0300(7)	1
C(29)	-0.3727(2)	0.8203(2)	0.4737(2)	0.0425(8)	1
C(30)	-0.4478(2)	0.8131(2)	0.4926(2)	0.0518(10)	1
C(31)	-0.5084(2)	0.8648(3)	0.4755(2)	0.0519(11)	1
C(32)	-0.4924(2)	0.9245(2)	0.4397(2)	0.0509(10)	1
C(33)	-0.4178(2)	0.9330(2)	0.4204(2)	0.0421(8)	1
C(34)	-0.5913(2)	0.8553(3)	0.4949(2)	0.081(2)	1
C(35)	0.0636(2)	0.8870(2)	0.62033(15)	0.0252(6)	1
C(36)	0.1159(2)	0.8281(2)	0.6417(2)	0.0288(7)	1
C(37)	0.1588(2)	0.8202(2)	0.7118(2)	0.0339(7)	1
C(38)	0.1528(2)	0.8705(2)	0.7630(2)	0.0329(7)	1
C(39)	0.1017(2)	0.9296(2)	0.7415(2)	0.0352(7)	1
C(40)	0.0578(2)	0.9379(2)	0.6713(2)	0.0292(7)	1
C(41)	0.2001(2)	0.8615(2)	0.8399(2)	0.0497(10)	1
C(42)	0.1766(2)	0.9273(2)	0.2970(2)	0.0264(6)	1
C(43)	0.2417(2)	0.8789(2)	0.3113(2)	0.0353(7)	1
C(44)	0.3157(2)	0.8934(2)	0.2928(2)	0.0399(8)	1
C(45)	0.3265(2)	0.9563(2)	0.2589(2)	0.0422(8)	1
C(46)	0.2614(2)	1.0055(2)	0.2449(2)	0.0450(9)	1
C(47)	0.1875(2)	0.9915(2)	0.2636(2)	0.0380(8)	1
C(48)	0.4070(2)	0.9713(3)	0.2373(2)	0.0649(12)	1
N(5)	-0.08781(14)	0.75321(12)	0.36357(12)	0.0240(5)	1
C(49)	-0.0823(2)	0.67981(15)	0.36943(15)	0.0224(6)	1
C(50)	-0.0890(2)	0.6357(2)	0.3082(2)	0.0262(6)	1
C(51)	-0.0794(2)	0.5620(2)	0.3169(2)	0.0319(7)	1
C(52)	-0.0634(2)	0.5305(2)	0.3839(2)	0.0384(8)	1
C(53) .	-0.0589(2)	0.5730(2)	0.4431(2)	0.0338(7)	1

Table V. (continued)

Atom	x	y	z	U(eq)	SOF
C(54)	-0.0680(2)	0.6472(2)	0.4373(2)	0.0272(6)	1
C(55)	-0.1054(2)	0.6699(2)	0.2354(2)	0.0307(7)	1
C(56)	-0.1493(2)	0.6192(2)	0.1756(2)	0.0422(8)	1
C(57)	-0.0250(2)	0.6992(2)	0.2207(2)	0.0435(8)	1
C(58)	-0.0670(2)	0.6937(2)	0.5015(2)	0.0296(7)	1
C(59)	-0.1551(2)	0.7095(2)	0.5060(2)	0.0447(9)	1
C(60)	-0.0160(2)	0.6641(2)	0.5714(2)	0.0455(9)	1
C(61)	0.3061(3)	0.7084(2)	0.2487(3)	0.0677(13)	1
C(62)	0.3707(3)	0.7262(3)	0.2178(3)	0.0740(14)	1
C(63)	0.4509(3)	0.7246(3)	0.2559(3)	0.085(2)	1
C(64)	0.4702(3)	0.7074(3)	0.3249(3)	0.096(2)	1
C(65)	0.4101(3)	0.6895(3)	0.3581(3)	0.088(2)	1
C(66)	0.3290(3)	0.6895(3)	0.3208(3)	0.0728(13)	1
C(67)	0.2172(4)	0.7097(4)	0.2071(3)	0.114(2)	1
C(68)	-0.0346(3)	1.0276(3)	-0.0006(3)	0.0801(15)	1
C(69)	-0.1189(3)	1.0030(3)	-0.0434(3)	0.085(2)	1
C(70)	-0.1876(4)	1.0581(4)	-0.0474(3)	0.107(2)	0.50
C(70')	-0.1876(4)	1.0581(4)	-0.0474(3)	0.107(2)	0.50
C(71')	-0.1859(7)	1.1241(6)	-0.0872(6)	0.091(3)	0.50

Table VI. Bond lengths [Å] and angles [°] for (TTP)Hf=NAr^Pr.

Hf(1)–N(5)	1.859(2)	C(28)–C(29)	1.393(5)
Hf(1)–N(2)	2.178(2)	C(29)–C(30)	1.389(5)
Hf(1)–N(1)	2.181(2)	C(30)–C(31)	1.374(5)
Hf(1)–N(4)	2.193(2)	C(31)–C(32)	1.372(6)
Hf(1)–N(3)	2.193(2)	C(31)–C(34)	1.523(5)
N(1)–C(4)	1.384(3)	C(32)–C(33)	1.388(5)
N(1)–C(1)	1.383(4)	C(35)–C(40)	1.390(4)
N(2)–C(9)	1.382(4)	C(35)–C(36)	1.398(4)
N(2)–C(6)	1.387(3)	C(36)–C(37)	1.381(4)
N(3)–C(14)	1.383(3)	C(37)–C(38)	1.385(5)
N(3)–C(11)	1.388(4)	C(38)–C(39)	1.391(4)
N(4)–C(16)	1.381(3)	C(38)–C(41)	1.518(4)
N(4)–C(19)	1.382(4)	C(39)–C(40)	1.389(4)
C(1)–C(20)	1.407(4)	C(42)–C(43)	1.384(4)
C(1)–C(2)	1.439(4)	C(42)–C(47)	1.393(4)
C(2)–C(3)	1.348(4)	C(43)–C(44)	1.388(4)
C(3)–C(4)	1.432(4)	C(44)–C(45)	1.377(5)
C(4)–C(5)	1.405(4)	C(45)–C(46)	1.392(5)
C(5)–C(6)	1.406(4)	C(45)–C(48)	1.522(5)
C(5)–C(21)	1.502(4)	C(46)–C(47)	1.388(5)
C(6)–C(7)	1.432(4)	N(5)–C(49)	1.374(4)
C(7)–C(8)	1.353(4)	C(49)–C(54)	1.416(4)
C(8)–C(9)	1.444(4)	C(49)–C(50)	1.426(4)
C(9)–C(10)	1.407(4)	C(50)–C(51)	1.388(4)
C(10)–C(11)	1.413(4)	C(50)–C(55)	1.513(4)
C(10)–C(28)	1.489(4)	C(51)–C(52)	1.391(4)
C(11)–C(12)	1.431(4)	C(52)–C(53)	1.382(4)
C(12)–C(13)	1.353(4)	C(53)–C(54)	1.393(4)
C(13)–C(14)	1.433(4)	C(54)–C(58)	1.514(4)
C(14)–C(15)	1.413(4)	C(55)–C(57)	1.532(5)
C(15)–C(16)	1.409(4)	C(55)–C(56)	1.537(4)

Table VI. (continued)

C(15)–C(35)	1.495(4)	C(58)–C(60)	1.516(4)
C(16)–C(17)	1.437(4)	C(58)–C(59)	1.517(5)
C(17)–C(18)	1.351(4)	C(61)–C(62)	1.389(7)
C(18)–C(19)	1.444(4)	C(61)–C(66)	1.402(7)
C(19)–C(20)	1.404(4)	C(61)–C(67)	1.501(7)
C(20)–C(42)	1.499(4)	C(62)–C(63)	1.358(7)
C(21)–C(22)	1.377(4)	C(63)–C(64)	1.337(7)
C(21)–C(26)	1.387(4)	C(64)–C(65)	1.354(7)
C(22)–C(23)	1.388(5)	C(65)–C(66)	1.366(7)
C(23)–C(24)	1.372(5)	C(68)–C(69)	1.515(7)
C(24)–C(25)	1.383(5)	C(68)–C(68) #1	1.539(9)
C(24)–C(27)	1.504(5)	C(69)–C(70')	1.523(7)
C(25)–C(26)	1.393(5)	C(69)–C(70)	1.523(7)
C(28)–C(33)	1.388(4)	C(70')–C(71')	1.458(12)

N(5)–Hf(1)–N(2)	106.57(9)	C(21)–C(22)–C(23)	121.1(3)
N(5)–Hf(1)–N(1)	107.35(9)	C(24)–C(23)–C(22)	121.5(4)
N(2)–Hf(1)–N(1)	84.58(8)	C(23)–C(24)–C(25)	117.3(3)
N(5)–Hf(1)–N(4)	111.42(9)	C(23)–C(24)–C(27)	121.8(4)
N(2)–Hf(1)–N(4)	142.00(8)	C(25)–C(24)–C(27)	120.9(4)
N(1)–Hf(1)–N(4)	83.71(8)	C(24)–C(25)–C(26)	122.1(3)
N(5)–Hf(1)–N(3)	110.36(9)	C(21)–C(26)–C(25)	119.7(3)
N(2)–Hf(1)–N(3)	83.99(8)	C(33)–C(28)–C(29)	117.7(3)
N(1)–Hf(1)–N(3)	142.27(8)	C(33)–C(28)–C(10)	122.1(3)
N(4)–Hf(1)–N(3)	83.56(8)	C(29)–C(28)–C(10)	120.2(3)
C(4)–N(1)–C(1)	107.4(2)	C(30)–C(29)–C(28)	120.6(3)
C(4)–N(1)–Hf(1)	123.0(2)	C(31)–C(30)–C(29)	121.4(4)
C(1)–N(1)–Hf(1)	127.2(2)	C(32)–C(31)–C(30)	118.0(3)
C(9)–N(2)–C(6)	107.4(2)	C(32)–C(31)–C(34)	121.1(4)
C(9)–N(2)–Hf(1)	124.2(2)	C(30)–C(31)–C(34)	120.8(4)
C(6)–N(2)–Hf(1)	122.0(2)	C(31)–C(32)–C(33)	121.6(3)

Table VI. (continued)

C(14)–N(3)–C(11)	106.9(2)		C(28)–C(33)–C(32)	120.6(3)
C(14)–N(3)–Hf(1)	124.9(2)		C(40)–C(35)–C(36)	118.0(3)
C(11)–N(3)–Hf(1)	124.8(2)		C(40)–C(35)–C(15)	122.5(3)
C(16)–N(4)–C(19)	107.3(2)		C(36)–C(35)–C(15)	119.4(3)
C(16)–N(4)–Hf(1)	124.7(2)		C(37)–C(36)–C(35)	120.7(3)
C(19)–N(4)–Hf(1)	126.8(2)		C(36)–C(37)–C(38)	121.6(3)
N(1)–C(1)–C(20)	125.3(3)		C(37)–C(38)–C(39)	117.8(3)
N(1)–C(1)–C(2)	108.2(2)		C(37)–C(38)–C(41)	121.3(3)
C(20)–C(1)–C(2)	126.4(3)		C(39)–C(38)–C(41)	120.9(3)
C(3)–C(2)–C(1)	107.9(3)		C(40)–C(39)–C(38)	121.2(3)
C(2)–C(3)–C(4)	107.9(3)		C(39)–C(40)–C(35)	120.7(3)
N(1)–C(4)–C(5)	125.6(3)		C(43)–C(42)–C(47)	118.0(3)
N(1)–C(4)–C(3)	108.5(2)		C(43)–C(42)–C(20)	121.3(3)
C(5)–C(4)–C(3)	125.8(3)		C(47)–C(42)–C(20)	120.8(3)
C(4)–C(5)–C(6)	126.2(3)		C(42)–C(43)–C(44)	121.3(3)
C(4)–C(5)–C(21)	116.6(3)		C(45)–C(44)–C(43)	121.0(3)
C(6)–C(5)–C(21)	117.2(2)		C(44)–C(45)–C(46)	118.0(3)
N(2)–C(6)–C(5)	125.7(2)		C(44)–C(45)–C(48)	120.8(3)
N(2)–C(6)–C(7)	108.5(2)		C(46)–C(45)–C(48)	121.2(3)
C(5)–C(6)–C(7)	125.9(3)		C(47)–C(46)–C(45)	121.2(3)
C(8)–C(7)–C(6)	108.2(3)		C(46)–C(47)–C(42)	120.5(3)
C(7)–C(8)–C(9)	107.4(3)		C(49)–N(5)–Hf(1)	173.4(2)
N(2)–C(9)–C(10)	125.7(2)		N(5)–C(49)–C(54)	119.8(3)
N(2)–C(9)–C(8)	108.5(2)		N(5)–C(49)–C(50)	121.0(3)
C(10)–C(9)–C(8)	125.7(3)		C(54)–C(49)–C(50)	119.2(3)
C(9)–C(10)–C(11)	125.9(3)		C(51)–C(50)–C(49)	119.1(3)
C(9)–C(10)–C(28)	117.4(2)		C(51)–C(50)–C(55)	121.3(3)
C(11)–C(10)–C(28)	116.6(3)		C(49)–C(50)–C(55)	119.6(3)
N(3)–C(11)–C(10)	125.4(3)		C(50)–C(51)–C(52)	121.4(3)
N(3)–C(11)–C(12)	108.9(2)		C(53)–C(52)–C(51)	119.6(3)
C(10)–C(11)–C(12)	125.6(3)		C(52)–C(53)–C(54)	121.2(3)
C(13)–C(12)–C(11)	107.6(3)		C(53)–C(54)–C(49)	119.5(3)
C(12)–C(13)–C(14)	107.9(3)		C(53)–C(54)–C(58)	121.4(3)
N(3)–C(14)–C(15)	125.1(3)		C(49)–C(54)–C(58)	119.0(3)

Table VI. (continued)

N(3)—C(14)—C(13)	108.7(2)	C(50)—C(55)—C(57)	110.8(3)
C(15)—C(14)—C(13)	126.2(3)	C(50)—C(55)—C(56)	113.0(3)
C(16)—C(15)—C(14)	125.5(3)	C(57)—C(55)—C(56)	110.7(3)
C(16)—C(15)—C(35)	116.6(2)	C(54)—C(58)—C(60)	114.9(3)
C(14)—C(15)—C(35)	117.9(3)	C(54)—C(58)—C(59)	109.8(3)
N(4)—C(16)—C(15)	126.2(3)	C(60)—C(58)—C(59)	110.9(3)
N(4)—C(16)—C(17)	108.8(2)	C(62)—C(61)—C(66)	116.0(4)
C(15)—C(16)—C(17)	124.9(3)	C(62)—C(61)—C(67)	121.7(5)
C(18)—C(17)—C(16)	107.8(3)	C(66)—C(61)—C(67)	122.3(5)
C(17)—C(18)—C(19)	107.5(3)	C(63)—C(62)—C(61)	121.2(5)
N(4)—C(19)—C(20)	126.1(2)	C(64)—C(63)—C(62)	121.0(5)
N(4)—C(19)—C(18)	108.6(2)	C(63)—C(64)—C(65)	120.6(5)
C(20)—C(19)—C(18)	125.3(3)	C(64)—C(65)—C(66)	119.6(5)
C(19)—C(20)—C(1)	125.8(3)	C(65)—C(66)—C(61)	121.5(5)
C(19)—C(20)—C(42)	117.0(2)	C(69)—C(68)—C(68) #1	113.1(6)
C(1)—C(20)—C(42)	117.2(3)	C(68)—C(69)—C(70')	113.9(5)
C(22)—C(21)—C(26)	118.4(3)	C(68)—C(69)—C(70)	113.9(5)
C(22)—C(21)—C(5)	119.5(3)	C(71')—C(70')—C(69)	119.0(6)
C(26)—C(21)—C(5)	122.1(3)		

Table VII. Crystal data and structure refinement for complex **4a**, (TTP)Zr(N'ArC(=N'Bu)O).

Empirical formula	$C_{72}H_{74}N_6OZr$
Formula weight	1226.76
Temperature	173(2) K
Wavelength	0.71073 Å
Crystal system	Triclinic
Space group	P$\bar{1}$
Unit cell dimensions	a = 13.5421(10) Å α = 98.0192(14)°
	b = 15.4623(11) Å β = 100.8337(14)°
	c = 16.7239(12) Å γ = 113.9894(11)°
Volume, Z	3050.0(4) Å^3, 2
Density (calculated)	1.337 Mg/m^3
Absorption coefficient	0.229 mm^{-1}
F(000)	1300
Crystal size	0.40 x 0.30 x 0.30 mm
θ range for data collection	1.69 to 28.86°
Limiting indices	$-17 \leq h \leq 18, -20 \leq k \leq 20, -19 \leq l \leq 21$
Reflections collected	19079
Independent reflections	13540 (R_{int} = 0.0122)
Refinement method	Full-matrix least-squares on F^2
Data / restraints / parameters	13540 / 0 / 658
Goodness-of-fit on F^2	0.999
Final R indices [I > 2σ(I)]	R1 = 0.0340, wR2 = 0.0910
R indices (all data)	R1 = 0.0418, wR2 = 0.0954
Largest diff. peak and hole	0.491 and −0.378 eÅ^{-3}

Table VIII. Atomic coordinates [x 10^4] and equivalent isotropic displacement parameters [$\mathring{A}^2$ x 10^3] for complex 4a. U(eq) is defined as one third of the trace of the orthogonalized U_{ij} tensor.

Atom	x	y	z	U(eq)
Zr	7509(1)	1532(1)	2127(1)	25(1)
O	8737(1)	2627(1)	3119(1)	39(1)
N(1)	6456(1)	1671(1)	1013(1)	30(1)
N(2)	7161(1)	144(1)	1260(1)	29(1)
N(3)	7135(1)	508(1)	2960(1)	29(1)
N(4)	6429(1)	2028(1)	2718(1)	29(1)
N(5)	10533(1)	3614(1)	2974(1)	38(1)
N(6)	9088(1)	2291(1)	1910(1)	31(1)
C(1)	5921(1)	2269(1)	971(1)	33(1)
C(2)	5556(2)	2283(1)	109(1)	36(1)
C(3)	5888(2)	1726(1)	-359(1)	37(1)
C(4)	6442(1)	1331(1)	196(1)	31(1)
C(5)	6829(1)	657(1)	-65(1)	32(1)
C(6)	7098(1)	71(1)	415(1)	31(1)
C(7)	7228(2)	-768(1)	80(1)	37(1)
C(8)	7333(2)	-1222(1)	704(1)	36(1)
C(9)	7306(1)	-649(1)	1444(1)	31(1)
C(10)	7389(1)	-867(1)	2235(1)	31(1)
C(11)	7311(1)	-315(1)	2941(1)	30(1)
C(12)	7399(2)	-519(1)	3757(1)	34(1)
C(13)	7266(2)	167(1)	4260(1)	34(1)
C(14)	7086(1)	804(1)	3770(1)	30(1)
C(15)	6848(1)	1570(1)	4060(1)	30(1)
C(16)	6535(1)	2133(1)	3571(1)	30(1)
C(17)	6217(2)	2868(1)	3872(1)	37(1)
C(18)	5902(2)	3196(1)	3204(1)	40(1)
C(19)	6025(1)	2669(1)	2486(1)	34(1)
C(20)	5750(2)	2766(1)	1656(1)	34(1)

Table VIII. (continued)

Atom	x	y	z	U(eq)
C(21)	6943(1)	528(1)	-945(1)	32(1)
C(22)	6092(2)	-149(2)	-1616(1)	50(1)
C(23)	6257(2)	-269(2)	-2411(1)	53(1)
C(24)	7261(2)	285(2)	-2556(1)	39(1)
C(25)	8104(2)	977(2)	-1886(1)	54(1)
C(26)	7953(2)	1095(2)	-1087(1)	52(1)
C(27)	7442(2)	143(2)	-3421(1)	53(1)
C(28)	7569(2)	-1743(1)	2333(1)	35(1)
C(29)	8519(2)	-1819(2)	2212(1)	45(1)
C(30)	8714(2)	-2605(2)	2355(1)	52(1)
C(31)	7969(2)	-3344(2)	2635(1)	48(1)
C(32)	6999(2)	-3292(2)	2725(1)	50(1)
C(33)	6796(2)	-2509(1)	2577(1)	42(1)
C(34)	8219(3)	-4167(2)	2841(2)	68(1)
C(35)	6848(2)	1774(1)	4965(1)	33(1)
C(36)	7821(2)	2396(1)	5584(1)	45(1)
C(37)	7789(2)	2620(2)	6412(1)	55(1)
C(38)	6808(2)	2225(2)	6640(1)	52(1)
C(39)	5851(2)	1586(2)	6027(1)	67(1)
C(40)	5867(2)	1367(2)	5199(1)	57(1)
C(41)	6781(3)	2497(2)	7543(2)	82(1)
C(42)	5202(2)	3417(1)	1500(1)	40(1)
C(43)	5702(2)	4221(2)	1174(1)	50(1)
C(44)	5187(2)	4831(2)	1052(1)	60(1)
C(45)	4190(2)	4657(2)	1233(1)	61(1)
C(46)	3688(2)	3858(2)	1554(2)	60(1)
C(47)	4195(2)	3244(2)	1687(1)	49(1)
C(48)	3650(3)	5338(2)	1101(2)	91(1)
C(49)	9549(1)	2916(1)	2714(1)	31(1)
C(50)	10924(2)	4270(2)	3812(1)	49(1)
C(51)	10903(2)	3726(2)	4515(2)	73(1)

Table VIII. (continued)

Atom	x	y	z	U(eq)
C(52)	10208(2)	4823(2)	3883(2)	58(1)
C(53)	12136(2)	4998(2)	3899(2)	70(1)
C(54)	9721(1)	2472(1)	1310(1)	34(1)
C(55)	9778(2)	3203(2)	882(1)	43(1)
C(56)	10373(2)	3332(2)	274(1)	50(1)
C(57)	10893(2)	2764(2)	94(1)	55(1)
C(58)	10857(2)	2064(2)	531(2)	61(1)
C(59)	10284(2)	1909(2)	1146(2)	49(1)
C(60)	9290(2)	3908(2)	1114(2)	64(1)
C(61)	8511(2)	3947(2)	346(2)	91(1)
C(62)	10228(3)	4927(2)	1560(2)	73(1)
C(63)	10357(3)	1211(2)	1686(2)	87(1)
C(64)	10350(3)	291(2)	1186(3)	128(2)
C(65)	11373(4)	1734(3)	2431(2)	114(2)

Table IX. Bond lengths [Å] and angles [°] for complex 4a.

Zr-O	2.0677(12)	C(9)-C(10)	1.405(2)
Zr-N(6)	2.1096(13)	C(10)-C(11)	1.405(2)
Zr-N(1)	2.2163(13)	C(10)-C(28)	1.497(2)
Zr-N(3)	2.2216(13)	C(11)-C(12)	1.436(2)
Zr-N(4)	2.2254(13)	C(12)-C(13)	1.352(2)
Zr-N(2)	2.2314(14)	C(13)-C(14)	1.432(2)
Zr-C(49)	2.6008(17)	C(14)-C(15)	1.396(2)
O-C(49)	1.3530(19)	C(15)-C(16)	1.404(2)
N(1)-C(1)	1.387(2)	C(15)-C(35)	1.503(2)
N(1)-C(4)	1.388(2)	C(16)-C(17)	1.432(2)
N(2)-C(9)	1.384(2)	C(17)-C(18)	1.359(2)
N(2)-C(6)	1.3848(19)	C(18)-C(19)	1.430(2)
N(3)-C(11)	1.384(2)	C(19)-C(20)	1.413(2)
N(3)-C(14)	1.3902(19)	C(20)-C(42)	1.497(2)
N(4)-C(19)	1.379(2)	C(21)-C(22)	1.375(3)
N(4)-C(16)	1.3861(19)	C(21)-C(26)	1.380(3)
N(5)-C(49)	1.269(2)	C(22)-C(23)	1.389(3)
N(5)-C(50)	1.471(3)	C(23)-C(24)	1.368(3)
N(6)-C(49)	1.401(2)	C(24)-C(25)	1.377(3)
N(6)-C(54)	1.424(2)	C(24)-C(27)	1.513(2)
C(1)-C(20)	1.399(2)	C(25)-C(26)	1.387(3)
C(1)-C(2)	1.440(2)	C(28)-C(29)	1.387(3)
C(2)-C(3)	1.348(3)	C(28)-C(33)	1.397(3)
C(3)-C(4)	1.436(2)	C(29)-C(30)	1.386(3)
C(4)-C(5)	1.398(2)	C(30)-C(31)	1.391(3)
C(5)-C(6)	1.401(2)	C(31)-C(32)	1.383(3)
C(5)-C(21)	1.501(2)	C(31)-C(34)	1.511(3)
C(6)-C(7)	1.432(2)	C(32)-C(33)	1.390(3)
C(7)-C(8)	1.353(2)		
C(8)-C(9)	1.434(2)		

Table IX. (continued)

C(35)-C(40)	1.377(3)	C(50)-C(51)	1.536(3)
C(35)-C(36)	1.383(3)	C(50)-C(52)	1.541(3)
C(36)-C(37)	1.393(3)	C(54)-C(59)	1.403(3)
C(37)-C(38)	1.371(3)	C(54)-C(55)	1.404(3)
C(38)-C(39)	1.373(4)	C(55)-C(56)	1.399(3)
C(38)-C(41)	1.521(3)	C(55)-C(60)	1.529(3)
C(39)-C(40)	1.385(3)	C(56)-C(57)	1.366(3)
C(42)-C(47)	1.383(3)	C(57)-C(58)	1.377(3)
C(42)-C(43)	1.395(3)	C(58)-C(59)	1.392(3)
C(43)-C(44)	1.397(3)	C(59)-C(63)	1.522(3)
C(44)-C(45)	1.367(4)	C(60)-C(61)	1.527(4)
C(45)-C(46)	1.384(4)	C(60)-C(62)	1.531(4)
C(45)-C(48)	1.524(3)	C(63)-C(65)	1.506(5)
C(46)-C(47)	1.398(3)	C(63)-C(64)	1.541(4)
C(50)-C(53)	1.532(3)		

O-Zr-N(6)	63.62(5)	O-Zr-C(49)	31.11(5)
O-Zr-N(1)	128.36(5)	N(6)-Zr-C(49)	32.53(5)
N(6)-Zr-N(1)	98.15(5)	N(1)-Zr-C(49)	116.28(5)
O-Zr-N(3)	90.39(5)	N(3)-Zr-C(49)	110.55(5)
N(6)-Zr-N(3)	125.61(5)	N(4)-Zr-C(49)	106.66(5)
N(1)-Zr-N(3)	132.82(5)	N(2)-Zr-C(49)	120.33(5)
O-Zr-N(4)	80.85(5)	C(49)-O-Zr	96.76(10)
N(6)-Zr-N(4)	132.57(5)	C(1)-N(1)-C(4)	106.28(13)
N(1)-Zr-N(4)	79.44(5)	C(1)-N(1)-Zr	128.87(11)
N(3)-Zr-N(4)	82.23(5)	C(4)-N(1)-Zr	123.28(11)
O-Zr-N(2)	141.42(5)	C(9)-N(2)-C(6)	105.92(13)
N(6)-Zr-N(2)	92.80(5)	C(9)-N(2)-Zr	129.27(10)
N(1)-Zr-N(2)	82.58(5)	C(6)-N(2)-Zr	122.05(11)
N(3)-Zr-N(2)	78.93(5)	C(11)-N(3)-C(14)	106.30(13)
N(4)-Zr-N(2)	132.90(5)	C(11)-N(3)-Zr	128.57(10)

Table IX. (continued)

C(14)-N(3)-Zr	121.27(11)	C(19)-N(4)-Zr	126.74(10)
C(19)-N(4)-C(16)	105.96(13)	C(16)-N(4)-Zr	120.54(10)
C(49)-N(5)-C(50)	120.92(16)	C(10)-C(11)-C(12)	125.32(15)
C(49)-N(6)-C(54)	119.01(14)	C(13)-C(12)-C(11)	107.47(15)
C(49)-N(6)-Zr	93.40(9)	C(12)-C(13)-C(14)	107.78(14)
C(54)-N(6)-Zr	146.76(12)	N(3)-C(14)-C(15)	126.20(14)
N(1)-C(1)-C(20)	125.46(14)	N(3)-C(14)-C(13)	109.11(14)
N(1)-C(1)-C(2)	109.12(14)	C(15)-C(14)-C(13)	124.63(14)
C(20)-C(1)-C(2)	125.41(16)	C(14)-C(15)-C(16)	126.05(14)
C(3)-C(2)-C(1)	107.62(15)	C(14)-C(15)-C(35)	117.49(14)
C(2)-C(3)-C(4)	107.70(15)	C(16)-C(15)-C(35)	116.32(14)
N(1)-C(4)-C(5)	126.02(14)	N(4)-C(16)-C(15)	125.37(15)
N(1)-C(4)-C(3)	109.25(15)	N(4)-C(16)-C(17)	109.65(14)
C(5)-C(4)-C(3)	124.59(15)	C(15)-C(16)-C(17)	124.90(15)
C(4)-C(5)-C(6)	125.73(14)	C(18)-C(17)-C(16)	107.19(15)
C(4)-C(5)-C(21)	117.52(14)	C(17)-C(18)-C(19)	107.31(16)
C(6)-C(5)-C(21)	116.73(15)	N(4)-C(19)-C(20)	124.59(15)
N(2)-C(6)-C(5)	125.83(15)	N(4)-C(19)-C(18)	109.88(14)
N(2)-C(6)-C(7)	109.46(14)	C(20)-C(19)-C(18)	125.52(16)
C(5)-C(6)-C(7)	124.38(15)	C(1)-C(20)-C(19)	124.22(16)
C(8)-C(7)-C(6)	107.72(15)	C(1)-C(20)-C(42)	118.28(15)
C(7)-C(8)-C(9)	107.05(16)	C(19)-C(20)-C(42)	117.46(15)
N(2)-C(9)-C(10)	124.82(15)	C(22)-C(21)-C(26)	118.12(16)
N(2)-C(9)-C(8)	109.81(14)	C(22)-C(21)-C(5)	122.98(15)
C(10)-C(9)-C(8)	125.36(16)	C(26)-C(21)-C(5)	118.88(16)
C(9)-C(10)-C(11)	124.20(15)	C(21)-C(22)-C(23)	120.63(18)
C(9)-C(10)-C(28)	118.12(15)	C(24)-C(23)-C(22)	121.56(18)
C(11)-C(10)-C(28)	117.68(14)	C(23)-C(24)-C(25)	117.72(16)
N(3)-C(11)-C(10)	125.36(14)	C(23)-C(24)-C(27)	121.35(19)
N(3)-C(11)-C(12)	109.32(14)	C(25)-C(24)-C(27)	120.93(18)

Table IX. (continued)

C(24)-C(25)-C(26)	121.25(18)	N(5)-C(49)-N(6)	124.69(15)
C(21)-C(26)-C(25)	120.69(19)	O-C(49)-N(6)	106.16(14)
C(29)-C(28)-C(33)	117.26(17)	N(5)-C(49)-Zr	177.14(13)
C(29)-C(28)-C(10)	121.82(16)	O-C(49)-Zr	52.14(8)
C(33)-C(28)-C(10)	120.89(16)	N(6)-C(49)-Zr	54.07(8)
C(28)-C(29)-C(30)	121.49(19)	N(5)-C(50)-C(53)	105.63(19)
C(29)-C(30)-C(31)	121.16(19)	N(5)-C(50)-C(51)	112.40(18)
C(32)-C(31)-C(30)	117.59(18)	C(53)-C(50)-C(51)	109.3(2)
C(32)-C(31)-C(34)	121.4(2)	N(5)-C(50)-C(52)	110.60(17)
C(30)-C(31)-C(34)	121.0(2)	C(53)-C(50)-C(52)	109.42(19)
C(31)-C(32)-C(33)	121.38(19)	C(51)-C(50)-C(52)	109.4(2)
C(32)-C(33)-C(28)	121.00(18)	C(59)-C(54)-C(55)	120.17(16)
C(40)-C(35)-C(36)	117.99(17)	C(59)-C(54)-N(6)	119.28(16)
C(40)-C(35)-C(15)	120.76(16)	C(55)-C(54)-N(6)	120.55(16)
C(36)-C(35)-C(15)	121.22(15)	C(56)-C(55)-C(54)	118.66(19)
C(35)-C(36)-C(37)	120.24(19)	C(56)-C(55)-C(60)	119.57(18)
C(38)-C(37)-C(36)	121.6(2)	C(54)-C(55)-C(60)	121.59(16)
C(39)-C(38)-C(37)	117.81(18)	C(57)-C(56)-C(55)	121.3(2)
C(39)-C(38)-C(41)	121.2(2)	C(56)-C(57)-C(58)	119.79(18)
C(37)-C(38)-C(41)	120.9(2)	C(57)-C(58)-C(59)	121.3(2)
C(38)-C(39)-C(40)	121.2(2)	C(58)-C(59)-C(54)	118.68(19)
C(35)-C(40)-C(39)	121.1(2)	C(58)-C(59)-C(63)	120.61(19)
C(47)-C(42)-C(43)	118.43(18)	C(54)-C(59)-C(63)	120.46(17)
C(47)-C(42)-C(20)	120.86(17)	C(61)-C(60)-C(55)	111.6(2)
C(43)-C(42)-C(20)	120.71(18)	C(61)-C(60)-C(62)	110.7(2)
C(42)-C(43)-C(44)	119.7(2)	C(55)-C(60)-C(62)	110.8(2)
C(45)-C(44)-C(43)	121.9(2)	C(65)-C(63)-C(59)	110.1(2)
C(44)-C(45)-C(46)	118.7(2)	C(65)-C(63)-C(64)	111.4(3)
C(44)-C(45)-C(48)	120.9(3)	C(59)-C(63)-C(64)	112.6(3)
C(46)-C(45)-C(48)	120.4(3)		
C(45)-C(46)-C(47)	120.3(2)		
C(42)-C(47)-C(46)	121.1(2)		
N(5)-C(49)-O	129.14(16)		

Table X. Crystal data and structure refinement for complex **4b**, (TTP)Zr(N^{r}BuC(=N^{r}Pr)O).

Empirical formula	$C_{80}H_{77}N_6OZr$
Formula weight	1229.70
Temperature	173(2) K
Wavelength	0.71073 Å
Crystal system	Triclinic
Space group	P$\bar{1}$
Unit cell dimensions	a = 12.9237(8) Å α = 97.1370(10)°
	b = 16.3912(10) Å β = 105.1960(10)°
	c = 16.6590(10) Å γ = 100.5320(10)°
Volume, Z	3292.6(3) Å^3, 2
Density (calculated)	1.240 Mg/m^3
Absorption coefficient	0.218 mm^{-1}
F(000)	1294
Crystal size	0.20 x 0.10 x 0.05 mm
θ range for data collection	1.28 to 23.35°
Limiting indices	$-13 \le h \le 14, -17 \le k \le 18, -18 \le l \le 17$
Reflections collected	15220
Independent reflections	9395 (R_{int} = 0.0396)
Completeness to θ = 23.35°	98.1%
Refinement method	Full-matrix least-squares on F^2
Data / restraints / parameters	9395 / 37 / 729
Goodness-of-fit on F^2	0.995
Final R indices [I > 2σ(I)]	R1 = 0.0547, wR2 = 0.1457
R indices (all data)	R1 = 0.0785, wR2 = 0.1580
Largest diff. peak and hole	1.032 and -0.658 eÅ^{-3}

Table XI. Atomic coordinates [x 10⁴] and equivalent isotropic displacement parameters [Å² x 10³] for complex **4b**. U(eq) is defined as one third of the trace of the orthogonalized U_{ij} tensor.

Atom	x	y	z	U(eq)
Zr	1187(1)	-1536(1)	1446(1)	22(1)
O	2275(2)	-1710(2)	761(2)	27(1)
N(1)	1686(3)	-729(2)	2716(2)	27(1)
N(2)	-271(3)	-2054(2)	1868(2)	24(1)
N(3)	-153(3)	-1672(2)	269(2)	23(1)
N(4)	1687(3)	-265(2)	1117(2)	23(1)
N(5)	1780(3)	-2670(2)	1484(2)	28(1)
N(6)	2807(3)	-2977(2)	521(2)	28(1)
C(1)	2533(4)	-9(3)	3010(3)	29(1)
C(2)	2841(4)	170(3)	3911(3)	35(1)
C(3)	2167(4)	-407(3)	4162(3)	36(1)
C(4)	1431(4)	-961(3)	3428(2)	29(1)
C(5)	528(4)	-1578(3)	3420(3)	30(1)
C(6)	-283(3)	-2061(3)	2692(2)	26(1)
C(7)	-1249(4)	-2646(3)	2702(3)	35(1)
C(8)	-1831(4)	-2987(3)	1893(3)	32(1)
C(9)	-1222(3)	-2618(3)	1370(2)	26(1)
C(10)	-1582(3)	-2780(2)	476(2)	26(1)
C(11)	-1080(3)	-2326(3)	-28(2)	26(1)
C(12)	-1441(4)	-2462(3)	-936(3)	29(1)
C(13)	-747(4)	-1899(3)	-1185(3)	29(1)
C(14)	55(3)	-1401(3)	-449(2)	24(1)
C(15)	913(3)	-731(2)	-433(2)	24(1)
C(16)	1607(3)	-175(2)	290(2)	24(1)
C(17)	2386(4)	569(3)	282(3)	30(1)
C(18)	2942(4)	917(3)	1089(3)	29(1)
C(19)	2531(3)	393(2)	1617(2)	24(1)
C(20)	2949(3)	506(3)	2499(3)	27(1)
C(21)	339(4)	-1721(3)	4253(3)	34(1)
C(22)	-289(5)	-1279(4)	4601(3)	59(2)
C(23)	-537(5)	-1440(5)	5331(3)	68(2)
C(24)	-157(5)	-2047(4)	5740(3)	59(2)

Table XI. (continued)

Atom	x	y	z	U(eq)
C(25)	489(6)	-2484(4)	5412(3)	76(2)
C(26)	741(5)	-2321(4)	4668(3)	59(2)
C(27)	-422(6)	-2245(5)	6546(4)	95(3)
C(28)	-2571(3)	-3473(2)	44(2)	25(1)
C(29)	-3559(4)	-3315(3)	-401(3)	32(1)
C(30)	-4449(4)	-3974(3)	-824(3)	36(1)
C(31)	-4379(4)	-4808(3)	-837(3)	32(1)
C(32)	-3397(4)	-4966(3)	-379(3)	34(1)
C(33)	-2503(4)	-4311(3)	53(3)	32(1)
C(34)	-5328(4)	-5528(3)	-1308(3)	44(1)
C(35)	1168(3)	-619(2)	-1243(2)	25(1)
C(36)	636(4)	-180(3)	-1809(3)	46(1)
C(37)	967(5)	-49(3)	-2520(3)	51(2)
C(38)	1818(4)	-352(3)	-2685(3)	33(1)
C(39)	2323(4)	-818(3)	-2130(3)	37(1)
C(40)	2015(4)	-943(3)	-1418(3)	36(1)
C(41)	2194(4)	-203(3)	-3455(3)	46(1)
C(42)	3898(4)	1237(3)	2920(3)	32(1)
C(43)	3784(4)	2061(3)	2917(3)	41(1)
C(44)	4679(5)	2734(3)	3268(3)	56(2)
C(45)	5714(5)	2611(4)	3629(3)	58(2)
C(46)	5829(5)	1794(4)	3628(4)	58(2)
C(47)	4943(4)	1115(3)	3286(3)	43(1)
C(48)	6691(6)	3364(4)	4009(5)	94(2)
C(49)	2339(3)	-2496(3)	898(3)	26(1)
C(50)	1740(4)	-3481(3)	1798(3)	39(1)
C(51)	1174(5)	-3453(3)	2490(4)	58(2)
C(52)	2909(5)	-3593(4)	2180(4)	60(2)
C(53)	1087(5)	-4215(3)	1082(4)	56(2)
C(54)	3281(4)	-2665(3)	-96(3)	29(1)
C(55)	4219(4)	-2002(3)	120(3)	32(1)
C(56)	4638(4)	-1749(3)	-519(3)	37(1)
C(57)	4176(4)	-2145(3)	-1349(3)	38(1)

Table XI. (continued)

Atom	x	y	z	U(eq)
C(58)	3272(4)	-2807(3)	-1557(3)	38(1)
C(59)	2812(4)	-3087(3)	-941(3)	31(1)
C(60)	4804(4)	-1566(3)	1032(3)	37(1)
C(61)	5968(4)	-1721(3)	1317(3)	46(1)
C(62)	4831(5)	-618(3)	1142(4)	54(1)
C(63)	1785(4)	-3792(3)	-1168(3)	36(1)
C(64)	767(4)	-3420(3)	-1279(4)	53(1)
C(65)	1664(5)	-4451(3)	-1939(3)	61(2)
C(100)	-2680(8)	-4124(8)	-3834(9)	398(15)
C(101)	-3643(9)	-4645(7)	-4392(14)	407(16)
C(102)	-4513(15)	-5101(9)	-4166(8)	252(8)
C(103)	-4199(9)	-4916(6)	-3283(7)	164(4)
C(104)	-3256(8)	-4404(6)	-2692(7)	141(4)
C(105)	-2408(11)	-3962(7)	-2952(9)	194(5)
C(200)	5445(7)	1508(5)	-3742(5)	137(3)
C(201)	5431(8)	1936(4)	-4382(5)	148(4)
C(202)	4645(7)	2364(5)	-4632(6)	127(3)
C(203)	3850(8)	2378(6)	-4250(5)	149(4)
C(204)	3891(8)	1944(5)	-3612(5)	146(4)
C(205)	4663(6)	1508(5)	-3344(6)	131(3)
C(300)	1029(19)	-5219(12)	5263(14)	273(9)
C(301)	701(14)	-4930(9)	4538(10)	200(6)
C(302)	-284(12)	-4728(8)	4300(8)	165(4)

Table XII. Bond lengths [Å] and angles [°] for complex 4b.

Zr-O	2.066(3)	C(14)-C(15)	1.402(6)
Zr-N(5)	2.137(3)	C(15)-C(16)	1.395(6)
Zr-N(3)	2.206(3)	C(15)-C(35)	1.495(5)
Zr-N(1)	2.217(3)	C(16)-C(17)	1.437(6)
Zr-N(2)	2.241(3)	C(17)-C(18)	1.343(6)
Zr-N(4)	2.244(3)	C(18)-C(19)	1.434(5)
Zr-C(49)	2.596(4)	C(19)-C(20)	1.403(6)
O-C(49)	1.349(5)	C(20)-C(42)	1.494(6)
N(1)-C(4)	1.390(5)	C(21)-C(26)	1.371(7)
N(1)-C(1)	1.391(5)	C(21)-C(22)	1.371(7)
N(2)-C(6)	1.377(5)	C(22)-C(23)	1.379(7)
N(2)-C(9)	1.384(5)	C(23)-C(24)	1.366(8)
N(3)-C(11)	1.385(5)	C(24)-C(25)	1.368(9)
N(3)-C(14)	1.399(5)	C(24)-C(27)	1.528(7)
N(4)-C(16)	1.384(5)	C(25)-C(26)	1.405(7)
N(4)-C(19)	1.384(5)	C(28)-C(29)	1.385(6)
N(5)-C(49)	1.387(5)	C(28)-C(33)	1.394(6)
N(5)-C(50)	1.485(5)	C(29)-C(30)	1.386(6)
N(6)-C(49)	1.277(5)	C(30)-C(31)	1.384(6)
N(6)-C(54)	1.428(5)	C(31)-C(32)	1.387(6)
C(1)-C(20)	1.406(6)	C(31)-C(34)	1.500(6)
C(1)-C(2)	1.425(6)	C(32)-C(33)	1.387(6)
C(2)-C(3)	1.349(6)	C(35)-C(36)	1.376(6)
C(3)-C(4)	1.422(6)	C(35)-C(40)	1.381(6)
C(4)-C(5)	1.394(6)	C(36)-C(37)	1.388(6)
C(5)-C(6)	1.410(6)	C(37)-C(38)	1.364(6)
C(5)-C(21)	1.510(5)	C(38)-C(39)	1.380(6)
C(6)-C(7)	1.434(6)	C(38)-C(41)	1.517(6)
C(7)-C(8)	1.350(6)	C(39)-C(40)	1.374(6)
C(8)-C(9)	1.436(6)	C(42)-C(43)	1.386(6)
C(9)-C(10)	1.413(6)	C(42)-C(47)	1.391(6)
C(10)-C(11)	1.394(6)	C(43)-C(44)	1.384(7)
C(10)-C(28)	1.493(6)	C(44)-C(45)	1.378(8)
C(11)-C(12)	1.436(5)	C(45)-C(46)	1.375(8)
C(12)-C(13)	1.347(6)	C(45)-C(48)	1.528(8)
C(13)-C(14)	1.422(6)	C(46)-C(47)	1.381(7)

Table XII. (continued)

C(50)-C(51)	1.519(6)	N(5)-Zr-N(1)	111.73(12)
C(50)-C(53)	1.525(7)	N(3)-Zr-N(1)	134.72(11)
C(50)-C(52)	1.532(7)	O-Zr-N(2)	149.98(11)
C(54)-C(55)	1.404(6)	N(5)-Zr-N(2)	93.40(12)
C(54)-C(59)	1.409(6)	N(3)-Zr-N(2)	79.62(11)
C(55)-C(56)	1.389(6)	N(1)-Zr-N(2)	81.47(12)
C(55)-C(60)	1.524(6)	O-Zr-N(4)	76.15(10)
C(56)-C(57)	1.375(7)	N(5)-Zr-N(4)	137.36(12)
C(57)-C(58)	1.376(7)	N(3)-Zr-N(4)	81.23(12)
C(58)-C(59)	1.398(6)	N(1)-Zr-N(4)	79.70(11)
C(59)-C(63)	1.519(6)	N(2)-Zr-N(4)	129.24(11)
C(60)-C(61)	1.533(6)	O-Zr-C(49)	31.08(11)
C(60)-C(62)	1.535(6)	N(5)-Zr-C(49)	32.26(12)
C(63)-C(64)	1.527(6)	N(3)-Zr-C(49)	99.36(12)
C(63)-C(65)	1.527(6)	N(1)-Zr-C(49)	125.42(12)
C(100)-C(101)	1.397(5)	N(2)-Zr-C(49)	122.30(12)
C(100)-C(105)	1.397(5)	N(4)-Zr-C(49)	106.95(12)
C(101)-C(102)	1.397(5)	C(49)-O-Zr	96.7(2)
C(102)-C(103)	1.397(5)	C(4)-N(1)-C(1)	105.9(3)
C(103)-C(104)	1.396(5)	C(4)-N(1)-Zr	125.8(3)
C(104)-C(105)	1.396(5)	C(1)-N(1)-Zr	126.2(3)
C(200)-C(201)	1.345(4)	C(6)-N(2)-C(9)	105.8(3)
C(200)-C(205)	1.346(4)	C(6)-N(2)-Zr	126.2(3)
C(201)-C(202)	1.345(4)	C(9)-N(2)-Zr	125.9(2)
C(202)-C(203)	1.345(4)	C(11)-N(3)-C(14)	105.9(3)
C(203)-C(204)	1.346(4)	C(11)-N(3)-Zr	125.6(2)
C(204)-C(205)	1.345(4)	C(14)-N(3)-Zr	121.3(3)
C(300)-C(301)	1.346(11)	C(16)-N(4)-C(19)	105.8(3)
C(300)-C(302)#1	1.35(2)	C(16)-N(4)-Zr	121.1(3)
C(301)-C(302)	1.345(11)	C(19)-N(4)-Zr	126.0(2)
C(302)-C(300)#1	1.35(2)	C(49)-N(5)-C(50)	120.4(3)
		C(49)-N(5)-Zr	92.4(2)
O-Zr-N(5)	63.13(11)	C(50)-N(5)-Zr	147.0(3)
O-Zr-N(3)	90.79(11)	C(49)-N(6)-C(54)	117.7(3)
N(5)-Zr-N(3)	110.13(12)	N(1)-C(1)-C(20)	125.4(4)
O-Zr-N(1)	123.28(12)	N(1)-C(1)-C(2)	109.2(4)

Table XII. (continued)

Angle	(deg)	Angle	(deg)
C(20)-C(1)-C(2)	125.1(4)	N(4)-C(19)-C(20)	125.0(4)
C(3)-C(2)-C(1)	107.5(4)	N(4)-C(19)-C(18)	109.5(3)
C(2)-C(3)-C(4)	108.1(4)	C(20)-C(19)-C(18)	125.4(4)
N(1)-C(4)-C(5)	125.3(4)	C(19)-C(20)-C(1)	124.8(4)
N(1)-C(4)-C(3)	109.1(4)	C(1)-C(20)-C(42)	116.9(4)
C(5)-C(4)-C(3)	125.2(4)	C(19)-C(20)-C(42)	118.3(4)
C(4)-C(5)-C(6)	125.8(4)	C(26)-C(21)-C(22)	117.7(4)
C(4)-C(5)-C(21)	118.5(4)	C(26)-C(21)-C(5)	121.7(4)
C(6)-C(5)-C(21)	115.5(4)	C(22)-C(21)-C(5)	120.6(4)
N(2)-C(6)-C(5)	125.9(4)	C(21)-C(22)-C(23)	119.5(6)
N(2)-C(6)-C(7)	109.6(4)	C(24)-C(23)-C(22)	121.6(5)
C(5)-C(6)-C(7)	124.6(4)	C(23)-C(24)-C(25)	121.2(5)
C(8)-C(7)-C(6)	108.0(4)	C(24)-C(25)-C(26)	120.8(6)
C(7)-C(8)-C(9)	106.6(4)	C(21)-C(26)-C(25)	120.7(5)
C(9)-C(10)-C(28)	117.9(4)	C(29)-C(28)-C(33)	118.1(4)
N(2)-C(9)-C(10)	125.5(4)	C(29)-C(28)-C(10)	122.0(4)
N(2)-C(9)-C(8)	110.1(3)	C(33)-C(28)-C(10)	119.9(4)
C(10)-C(9)-C(8)	124.4(4)	C(28)-C(29)-C(30)	122.4(6)
C(11)-C(10)-C(9)	124.2(4)	C(31)-C(30)-C(29)	118.0(5)
C(11)-C(10)-C(28)	117.9(3)	C(30)-C(31)-C(32)	122.2(4)
C(10)-C(11)-C(12)	125.5(4)	C(32)-C(31)-C(34)	120.0(4)
C(13)-C(12)-C(11)	107.6(4)	C(31)-C(32)-C(33)	117.7(4)
C(12)-C(13)-C(14)	108.0(4)	C(32)-C(33)-C(28)	121.7(4)
N(3)-C(11)-C(10)	125.3(3)	C(36)-C(35)-C(40)	120.6(4)
N(3)-C(11)-C(12)	109.2(3)	C(36)-C(35)-C(15)	121.1(4)
N(3)-C(14)-C(15)	124.7(4)	C(40)-C(35)-C(15)	120.6(4)
N(3)-C(14)-C(13)	109.2(3)	C(35)-C(36)-C(37)	118.4(4)
C(14)-C(15)-C(35)	118.4(4)	C(36)-C(37)-C(38)	123.6(4)
C(16)-C(15)-C(35)	115.8(4)	C(37)-C(38)-C(41)	117.9(4)
C(16)-C(15)-C(14)	125.6(4)	C(37)-C(38)-C(39)	117.4(4)
C(15)-C(16)-C(17)	126.1(4)	C(39)-C(38)-C(41)	122.0(4)
N(4)-C(16)-C(17)	109.5(4)	C(38)-C(39)-C(40)	120.6(4)
N(4)-C(16)-C(15)	126.0(4)	C(39)-C(40)-C(35)	121.6(4)
C(18)-C(17)-C(16)	124.5(4)	C(40)-C(39)-C(38)	120.8(4)
C(17)-C(18)-C(19)	107.6(4)		

Table XII. (continued)

C(43)-C(42)-C(47)	117.5(4)	C(56)-C(57)-C(58)	119.5(4)
C(43)-C(42)-C(20)	121.3(4)	C(57)-C(58)-C(59)	121.3(4)
C(47)-C(42)-C(20)	121.2(4)	C(58)-C(59)-C(54)	118.6(4)
C(44)-C(43)-C(42)	121.0(5)	C(58)-C(59)-C(63)	121.8(4)
C(45)-C(44)-C(43)	121.4(5)	C(54)-C(59)-C(63)	119.5(4)
C(46)-C(45)-C(44)	117.6(5)	C(55)-C(60)-C(61)	110.8(4)
C(46)-C(45)-C(48)	121.9(6)	C(55)-C(60)-C(62)	111.0(4)
C(44)-C(45)-C(48)	120.5(6)	C(61)-C(60)-C(62)	111.0(4)
C(45)-C(46)-C(47)	121.8(5)	C(59)-C(63)-C(64)	109.9(4)
C(46)-C(47)-C(42)	120.8(5)	C(59)-C(63)-C(65)	114.2(4)
N(6)-C(49)-O	124.6(4)	C(64)-C(63)-C(65)	111.0(4)
N(6)-C(49)-N(5)	128.3(4)	C(101)-C(100)-C(105)	126.6(17)
O-C(49)-N(5)	107.1(3)	C(102)-C(101)-C(100)	126(2)
N(6)-C(49)-Zr	171.6(3)	C(101)-C(102)-C(103)	105.0(18)
O-C(49)-Zr	52.23(17)	C(104)-C(103)-C(102)	131.9(14)
N(5)-C(49)-Zr	55.35(18)	C(105)-C(104)-C(103)	120.9(12)
N(5)-C(50)-C(51)	108.2(3)	C(104)-C(105)-C(100)	109.7(13)
N(5)-C(50)-C(53)	110.2(4)	C(201)-C(200)-C(205)	119.7(10)
C(51)-C(50)-C(53)	109.1(4)	C(202)-C(201)-C(200)	120.9(10)
N(5)-C(50)-C(52)	110.2(4)	C(203)-C(202)-C(201)	121.0(10)
C(51)-C(50)-C(52)	108.2(4)	C(202)-C(203)-C(204)	116.4(11)
C(53)-C(50)-C(52)	110.8(4)	C(205)-C(204)-C(203)	124.3(11)
C(55)-C(54)-C(59)	120.1(4)	C(204)-C(205)-C(200)	117.7(10)
C(55)-C(54)-N(6)	122.5(4)	C(301)-C(300)-C(302)#1	113.3(18)
C(59)-C(54)-N(6)	117.2(4)	C(302)-C(301)-C(300)	121.2(18)
C(56)-C(55)-C(54)	118.8(4)	C(301)-C(302)-C(300)#1	
C(56)-C(55)-C(60)	119.0(4)	125.6(14)	
C(54)-C(55)-C(60)	122.2(4)		
C(57)-C(56)-C(55)	121.7(5)		

Table XIII. Crystal data and structure refinement for complex 7a, (TTP)Hf(NAr^{iPr}C(=N^{i}Pr)N^{i}Pr).

Empirical formula	$C_{67}H_{67}HfN_7$ • 3/2 toluene
Formula weight	1274.96
Temperature	173(2) K
Wavelength	0.71073 Å
Crystal system	Monoclinic
Space group	P2$_1$/c
Unit cell dimensions	a = 14.8756(8) Å α = 90°
	b = 16.7514(9) Å β = 91.7960(10)°
	c = 26.1874(15) Å γ = 90°
Volume, Z	6522.4(6) Å^3, 4
Density (calculated)	1.298 Mg/m^3
Absorption coefficient	1.646 mm^{-1}
F(000)	2636
Crystal size	0.30 x 0.20 x 0.20 mm
θ range for data collection	1.37 to 28.34°
Limiting indices	$-15 \le h \le 19, -21 \le k \le 21, -33 \le l \le 34$
Reflections collected	40118
Independent reflections	15118 (R$_{int}$ = 0.0352)
Completeness to θ = 28.34°	92.8%
Refinement method	Full-matrix least-squares on F^2
Data / restraints / parameters	15118 / 0 / 676
Goodness-of-fit on F^2	1.027
Final R indices [I > 2σ(I)]	R1 = 0.0316, wR2 = 0.0814
R indices (all data)	R1 = 0.0401, wR2 = 0.0850
Largest diff. peak and hole	1.414 and −1.744 eÅ^{-3}

Table XIV. Atomic coordinates [x 10⁴] and equivalent isotropic displacement parameters [Å² x 10³] for complex 7a. U(eq) is defined as one third of the trace of the orthogonalized U_{ij} tensor.

Atom	x	y	z	U(eq)
Hf	2993(1)	5101(1)	3448(1)	22(1)
N(1)	2141(1)	4106(1)	3749(1)	24(1)
N(2)	1774(1)	5779(1)	3593(1)	26(1)
N(3)	3595(2)	6141(1)	3871(1)	27(1)
N(4)	4000(2)	4472(1)	3936(1)	27(1)
N(5)	2721(2)	4610(1)	2700(1)	26(1)
N(6)	3738(2)	5559(1)	2853(1)	27(1)
N(7)	3784(2)	5004(1)	2030(1)	35(1)
C(1)	2418(2)	3352(1)	3903(1)	27(1)
C(2)	1654(2)	2830(2)	3918(1)	33(1)
C(3)	922(2)	3253(2)	3765(1)	33(1)
C(4)	1223(2)	4053(2)	3659(1)	28(1)
C(5)	652(2)	4683(2)	3513(1)	29(1)
C(6)	902(2)	5491(2)	3501(1)	28(1)
C(7)	305(2)	6147(2)	3419(1)	35(1)
C(8)	787(2)	6826(2)	3471(1)	36(1)
C(9)	1698(2)	6608(1)	3587(1)	28(1)
C(10)	2397(2)	7138(1)	3713(1)	27(1)
C(11)	3270(2)	6913(1)	3865(1)	29(1)
C(12)	3946(2)	7451(2)	4065(1)	37(1)
C(13)	4685(2)	7017(2)	4182(1)	38(1)
C(14)	4481(2)	6198(2)	4052(1)	29(1)
C(15)	5086(2)	5570(2)	4108(1)	30(1)
C(16)	4858(2)	4759(2)	4062(1)	29(1)
C(17)	5442(2)	4109(2)	4200(1)	36(1)
C(18)	4944(2)	3438(2)	4188(1)	36(1)
C(19)	4042(2)	3648(2)	4026(1)	29(1)
C(20)	3311(2)	3132(1)	4014(1)	29(1)
C(21)	-309(2)	4475(2)	3392(1)	30(1)
C(22)	-522(2)	3995(2)	2971(1)	37(1)
C(23)	-1401(2)	3757(2)	2868(1)	41(1)

Table XIV. (continued)

Atom	x	y	z	U(eq)
C(24)	-2098(2)	4002(2)	3173(1)	40(1)
C(25)	-1884(2)	4489(2)	3588(1)	46(1)
C(26)	-1001(2)	4719(2)	3698(1)	41(1)
C(27)	-3054(2)	3732(2)	3067(2)	57(1)
C(28)	2197(2)	8014(1)	3711(1)	28(1)
C(29)	1611(2)	8343(2)	4050(1)	39(1)
C(30)	1439(2)	9159(2)	4049(1)	42(1)
C(31)	1849(2)	9659(2)	3710(1)	38(1)
C(32)	2443(2)	9335(2)	3378(1)	41(1)
C(33)	2624(2)	8522(2)	3375(1)	36(1)
C(34)	1654(2)	10550(2)	3711(2)	55(1)
C(35)	6039(2)	5796(2)	4246(1)	32(1)
C(36)	6522(2)	6247(2)	3905(1)	42(1)
C(37)	7383(2)	6513(2)	4029(1)	52(1)
C(38)	7788(2)	6335(2)	4502(1)	47(1)
C(39)	7302(2)	5878(2)	4840(1)	45(1)
C(40)	6448(2)	5614(2)	4716(1)	37(1)
C(41)	8719(2)	6639(3)	4636(2)	75(1)
C(42)	3497(2)	2273(2)	4156(1)	31(1)
C(43)	3208(2)	1965(2)	4616(1)	44(1)
C(44)	3382(3)	1174(2)	4743(1)	49(1)
C(45)	3840(2)	673(2)	4425(1)	40(1)
C(46)	4137(2)	985(2)	3971(1)	40(1)
C(47)	3964(2)	1777(2)	3840(1)	36(1)
C(48)	3981(3)	-200(2)	4563(2)	53(1)
C(49)	3431(2)	5041(1)	2470(1)	26(1)
C(50)	2009(2)	4311(2)	2372(1)	29(1)
C(51)	1875(2)	3476(2)	2320(1)	31(1)
C(52)	1243(2)	3202(2)	1957(1)	41(1)
C(53)	747(2)	3724(2)	1655(1)	48(1)
C(54)	833(2)	4536(2)	1731(1)	44(1)
C(55)	1449(2)	4846(2)	2095(1)	36(1)
C(56)	2425(2)	2887(2)	2642(1)	36(1)

Table XIV. (continued)

Atom	x	y	z	U(eq)
C(57)	3372(2)	2780(2)	2459(1)	56(1)
C(58)	1980(3)	2069(2)	2686(1)	58(1)
C(59)	1457(2)	5750(2)	2176(1)	43(1)
C(60)	1977(3)	6209(2)	1782(2)	57(1)
C(61)	497(3)	6087(2)	2181(1)	57(1)
C(62)	4502(2)	6093(2)	2769(1)	33(1)
C(63)	5372(2)	5644(2)	2660(1)	45(1)
C(64)	4272(2)	6721(2)	2357(1)	46(1)
C(65)	3613(2)	4365(2)	1657(1)	47(1)
C(66)	3271(4)	4711(3)	1155(1)	81(1)
C(67)	4512(3)	3929(2)	1593(2)	73(1)

Table XV. Bond lengths [Å] and angles [°] for complex 7a.

Bond	Length	Bond	Length
Hf-N(6)	2.087(2)	C(17)-C(18)	1.346(4)
Hf-N(5)	2.151(2)	C(18)-C(19)	1.437(4)
Hf-N(2)	2.184(2)	C(19)-C(20)	1.389(4)
Hf-N(4)	2.207(2)	C(20)-C(42)	1.509(3)
Hf-N(3)	2.238(2)	C(21)-C(26)	1.510(4)
Hf-N(1)	2.251(2)	C(21)-C(22)	1.386(4)
Hf-C(49)	2.664(3)	C(22)-C(23)	1.393(4)
N(1)-C(4)	1.381(3)	C(23)-C(24)	1.384(4)
N(1)-C(1)	1.385(3)	C(24)-C(25)	1.391(4)
N(2)-C(9)	1.393(3)	C(24)-C(27)	1.389(4)
N(2)-C(6)	1.397(3)	C(25)-C(26)	1.392(4)
N(3)-C(11)	1.381(3)	C(28)-C(29)	1.377(4)
N(3)-C(14)	1.389(3)	C(28)-C(33)	1.390(4)
N(4)-C(16)	1.393(3)	C(29)-C(30)	1.377(4)
N(4)-C(19)	1.401(3)	C(30)-C(31)	1.371(4)
N(5)-C(49)	1.428(3)	C(31)-C(32)	1.393(5)
N(5)-C(50)	1.432(3)	C(31)-C(34)	1.520(4)
N(6)-C(49)	1.391(3)	C(32)-C(33)	1.388(4)
N(6)-C(62)	1.470(3)	C(35)-C(36)	1.390(5)
N(7)-C(49)	1.282(4)	C(35)-C(40)	1.391(4)
N(7)-C(65)	1.466(4)	C(36)-C(37)	1.378(4)
C(1)-C(20)	1.400(4)	C(37)-C(38)	1.374(4)
C(1)-C(2)	1.405(4)	C(38)-C(39)	1.505(4)
C(2)-C(3)	1.435(4)	C(38)-C(41)	1.390(5)
C(3)-C(4)	1.444(3)	C(39)-C(40)	1.376(4)
C(4)-C(5)	1.400(4)	C(42)-C(47)	1.388(4)
C(5)-C(6)	1.405(4)	C(42)-C(43)	1.391(4)
C(5)-C(21)	1.497(4)	C(43)-C(44)	1.394(4)
C(6)-C(7)	1.425(3)	C(44)-C(45)	1.520(4)
C(7)-C(8)	1.349(4)	C(45)-C(46)	1.385(4)
C(8)-C(9)	1.427(4)	C(45)-C(48)	1.420(4)
C(9)-C(10)	1.398(4)	C(46)-C(47)	1.409(4)
C(10)-C(11)	1.399(4)	C(50)-C(55)	1.381(4)
C(10)-C(28)	1.498(3)	C(50)-C(51)	1.379(4)
C(11)-C(12)	1.436(4)	C(51)-C(52)	1.519(4)
C(12)-C(13)	1.345(4)	C(51)-C(56)	1.393(4)
C(13)-C(14)	1.443(4)	C(52)-C(53)	1.420(4)
C(14)-C(15)	1.390(4)	C(53)-C(54)	1.402(4)
C(15)-C(16)	1.404(4)	C(54)-C(55)	1.381(4)
C(15)-C(35)	1.500(4)	C(55)-C(59)	1.530(4)
C(16)-C(17)	1.432(4)	C(56)-C(57)	1.513(4)

Table XV. (continued)

C(56)-C(58)	1.527(4)	C(62)-C(64)	1.537(4)
C(59)-C(60)	1.517(5)	C(65)-C(66)	1.512(5)
C(59)-C(61)	1.535(5)	C(65)-C(67)	1.538(5)
C(62)-C(63)	1.531(4)		
N(6)-Hf-N(5)	63.21(8)	C(49)-N(5)-Hf	94.01(15)
N(6)-Hf-N(2)	113.66(8)	C(50)-N(5)-Hf	142.54(17)
N(5)-Hf-N(2)	102.89(8)	C(49)-N(6)-C(62)	120.7(2)
N(6)-Hf-N(4)	104.02(8)	C(49)-N(6)-Hf	98.01(15)
N(5)-Hf-N(4)	116.76(8)	C(62)-N(6)-Hf	140.07(17)
N(2)-Hf-N(4)	134.46(8)	C(49)-N(7)-C(65)	124.5(2)
N(6)-Hf-N(3)	82.56(8)	N(1)-C(1)-C(20)	124.9(2)
N(5)-Hf-N(3)	144.09(8)	N(1)-C(1)-C(2)	109.5(2)
N(2)-Hf-N(3)	80.23(8)	C(20)-C(1)-C(2)	125.5(2)
N(4)-Hf-N(3)	80.27(7)	C(3)-C(2)-C(1)	107.8(2)
N(6)-Hf-N(1)	148.38(8)	C(2)-C(3)-C(4)	106.9(2)
N(5)-Hf-N(1)	86.77(8)	N(1)-C(4)-C(5)	125.9(2)
N(2)-Hf-N(1)	81.05(8)	N(1)-C(4)-C(3)	109.8(2)
N(4)-Hf-N(1)	79.82(8)	C(5)-C(4)-C(3)	124.2(3)
N(3)-Hf-N(1)	128.63(7)	C(4)-C(5)-C(6)	125.0(2)
N(6)-Hf-C(49)	31.13(8)	C(4)-C(5)-C(21)	116.8(2)
N(5)-Hf-C(49)	32.33(8)	C(6)-C(5)-C(21)	118.1(2)
N(2)-Hf-C(49)	114.55(8)	N(2)-C(6)-C(5)	125.0(2)
N(4)-Hf-C(49)	110.95(8)	N(2)-C(6)-C(7)	109.3(2)
N(3)-Hf-C(49)	113.54(8)	C(5)-C(6)-C(7)	125.6(2)
N(1)-Hf-C(49)	117.77(7)	C(8)-C(7)-C(6)	108.0(3)
C(4)-N(1)-C(1)	106.0(2)	C(7)-C(8)-C(9)	107.7(2)
C(4)-N(1)-Hf	123.54(16)	N(2)-C(9)-C(10)	124.8(2)
C(1)-N(1)-Hf	127.71(17)	N(2)-C(9)-C(8)	109.5(2)
C(9)-N(2)-C(6)	105.5(2)	C(10)-C(9)-C(8)	125.6(2)
C(9)-N(2)-Hf	125.79(17)	C(9)-C(10)-C(11)	125.0(2)
C(6)-N(2)-Hf	124.19(16)	C(9)-C(10)-C(28)	118.4(2)
C(11)-N(3)-C(14)	105.5(2)	C(11)-C(10)-C(28)	116.5(2)
C(11)-N(3)-Hf	126.14(17)	N(3)-C(11)-C(10)	125.2(2)
C(14)-N(3)-Hf	125.62(16)	N(3)-C(11)-C(12)	110.0(2)
C(16)-N(4)-C(19)	105.4(2)	C(10)-C(11)-C(12)	124.7(2)
C(16)-N(4)-Hf	124.84(16)	C(13)-C(12)-C(11)	107.5(2)
C(19)-N(4)-Hf	126.38(17)	C(12)-C(13)-C(14)	107.2(2)
C(49)-N(5)-C(50)	117.8(2)	N(3)-C(14)-C(15)	126.1(2)

Table XV. (continued)

N(3)-C(14)-C(13)	109.6(2)	C(36)-C(37)-C(38)	120.6(3)
C(15)-C(14)-C(13)	124.3(3)	C(39)-C(38)-C(37)	117.7(3)
C(14)-C(15)-C(16)	124.7(2)	C(39)-C(38)-C(41)	122.0(3)
C(14)-C(15)-C(35)	116.1(2)	C(37)-C(38)-C(41)	120.3(4)
C(16)-C(15)-C(35)	119.3(2)	C(40)-C(39)-C(38)	121.6(3)
N(4)-C(16)-C(15)	124.9(2)	C(39)-C(40)-C(35)	120.9(3)
N(4)-C(16)-C(17)	109.8(2)	C(47)-C(42)-C(43)	118.2(2)
C(15)-C(16)-C(17)	124.8(3)	C(47)-C(42)-C(20)	121.2(2)
C(18)-C(17)-C(16)	107.5(3)	C(43)-C(42)-C(20)	120.6(2)
C(17)-C(18)-C(19)	108.1(2)	C(44)-C(43)-C(42)	120.1(3)
C(20)-C(19)-N(4)	125.4(2)	C(45)-C(44)-C(43)	122.0(3)
C(20)-C(19)-C(18)	125.3(2)	C(44)-C(45)-C(46)	117.9(3)
N(4)-C(19)-C(18)	109.0(2)	C(44)-C(45)-C(48)	120.7(3)
C(19)-C(20)-C(1)	125.3(2)	C(46)-C(45)-C(48)	121.4(3)
C(19)-C(20)-C(42)	116.8(2)	C(45)-C(46)-C(47)	120.6(3)
C(1)-C(20)-C(42)	117.8(2)	C(42)-C(47)-C(46)	121.2(3)
C(26)-C(21)-C(22)	118.3(3)	N(7)-C(49)-N(6)	122.8(2)
C(26)-C(21)-C(5)	122.0(2)	N(7)-C(49)-N(5)	133.2(2)
C(22)-C(21)-C(5)	119.6(2)	N(6)-C(49)-N(5)	104.0(2)
C(23)-C(22)-C(21)	120.6(3)	N(7)-C(49)-Hf	169.9(2)
C(22)-C(23)-C(24)	121.3(3)	N(6)-C(49)-Hf	50.86(12)
C(25)-C(24)-C(23)	117.8(3)	N(5)-C(49)-Hf	53.66(12)
C(25)-C(24)-C(27)	120.8(3)	C(55)-C(50)-C(51)	119.9(2)
C(23)-C(24)-C(27)	121.4(3)	C(55)-C(50)-N(5)	120.1(2)
C(24)-C(25)-C(26)	121.1(3)	C(51)-C(50)-N(5)	120.0(2)
C(21)-C(26)-C(25)	120.8(3)	C(52)-C(51)-C(50)	118.6(3)
C(29)-C(28)-C(33)	118.2(2)	C(52)-C(51)-C(56)	120.3(2)
C(29)-C(28)-C(10)	121.3(2)	C(50)-C(51)-C(56)	121.0(2)
C(33)-C(28)-C(10)	120.4(2)	C(53)-C(52)-C(51)	121.5(3)
C(28)-C(29)-C(30)	120.9(3)	C(52)-C(53)-C(54)	119.7(3)
C(31)-C(30)-C(29)	120.9(3)	C(53)-C(54)-C(55)	121.3(3)
C(32)-C(31)-C(30)	118.4(3)	C(54)-C(55)-C(50)	118.6(3)
C(32)-C(31)-C(34)	121.1(3)	C(54)-C(55)-C(59)	117.5(3)
C(30)-C(31)-C(34)	120.5(3)	C(50)-C(55)-C(59)	123.8(3)
C(31)-C(32)-C(33)	121.4(3)	C(57)-C(56)-C(51)	113.0(2)
C(32)-C(33)-C(28)	120.3(3)	C(57)-C(56)-C(58)	109.1(3)
C(36)-C(35)-C(40)	117.9(3)	C(51)-C(56)-C(58)	113.4(3)
C(36)-C(35)-C(15)	119.2(3)	C(60)-C(59)-C(55)	114.1(3)
C(40)-C(35)-C(15)	122.8(3)	C(60)-C(59)-C(61)	108.3(3)
C(37)-C(36)-C(35)	121.3(3)	C(55)-C(59)-C(61)	111.2(3)

Table XV. (continued)

N(6)-C(62)-C(63)	113.0(2)	N(7)-C(65)-C(66)	110.3(3)
N(6)-C(62)-C(64)	111.4(2)	N(7)-C(65)-C(67)	106.7(3)
C(63)-C(62)-C(64)	112.2(3)	C(66)-C(65)-C(67)	110.9(3)

CHAPTER 6. NEW CHEMISTRY OF ZIRCONIUM AND HAFNIUM IMIDO

COMPLEXES: CONDENSATION AND METATHESIS REACTIONS

A paper to be submitted to Inorganic Chemistry

Joseph L. Thorman, Ilia A. Guzei, Victor G. Young, Jr.[‡], and L. Keith Woo[*]

Abstract

The zirconium and hafnium imido metalloporphyrin complexes, $(TTP)M=NAr^{iPr}$, $(TTP = meso\text{-}5,10,15,20\text{-tetra-}p\text{-tolylporphyrinato dianion}; M = Zr$ (**1**), Hf; $Ar^{iPr} = 2,6$-diisopropylphenyl) have been utilized as reagents in the preparation of complexes containing metal-oxygen bonds. The imido complexes react in a step-wise manner in the presence of two equivalents of pinacolone to form the endiolate products $(TTP)M[OC(^tBu)CHC(^tBu)(Me)O]$ (M = Zr, **2**; Hf, **3**), with elimination of H_2NAr^{iPr}. The bis(μ-oxo) complex $[(TTP)ZrO]_2$, **4**, is formed upon reaction of $(TTP)Zr=NAr^{iPr}$ with PhNO. Treatment of compound **4** with water or compound **2** with acetone, produced the bis(μ-hydroxo)(μ-oxo) bridged dimer $[(TTP)Zr]_2(\mu\text{-}O)(\mu\text{-}OH)_2$, **5**. Compounds **2**, **4**, and **5** were structurally characterized by single-crystal X-ray diffraction.

Introduction

The preparation of group 4 chalcogenido complexes is an attractive goal in light of the demonstrated reactivity of metallocene and tetraazaannulene analogues described in a

number of surveys.[1,2,3] Notable examples include C-H bond activation, cycloaddition, and enolate formation. Toward this end, we have developed nitrene group and chalcogenido atom transfer routes with titanium metalloporphyrin complexes. Efforts to extend this methodology to the heavier congeners has now become an area of attention. Kim and coworkers have investigated the persulfido- and perselenido-bridged complexes of zirconium and hafnium [(TPP)M]$_2$(μ-η^2-Ch$_2$)$_2$ complexes. These are the only known dimeric group 4 metalloporphyrin chalcogenido complexes.[4]

In an ongoing investigation of group 4 metalloporphyrin imido complexes, we have found a number of novel reactivity properties.[5,6,7] We demonstrated previously that the imido complexes, (TTP)M=NAr^{Pr} (M = Zr, Hf), exhibit reactivity with heterocumulenes to form [2 + 2] cycloaddition products.[8] Further reactivity has been explored with other unsaturated substrates. Among these, we now describe results found from the reactions of the zirconium and hafnium imido complexes with pinacolone and PhNO.

Experimental

General Procedures. All manipulations were performed under a nitrogen atmosphere using a Vacuum Atmospheres glovebox equipped with a Model MO40-1 Dri-Train gas purifier. Benzene, benzene-d_6, toluene, THF, and hexane were freshly distilled from purple solutions of sodium benzophenone and brought into the drybox without exposure to air. Methylene chloride was dried by passage through a column of activated neutral alumina. The dichloro, (TTP)MCl$_2$, imido, (TTP)M=NAr^{Pr} (M = Zr, Hf), and (TTP)Zr(η^2-NAr^{Pr}C(=N^{t}Bu)O) compounds were prepared according to literature

procedures.[8] Pinacolone was purchased from Aldrich, vacuum transferred and dried by passage through a plug of activated neutral alumina. Pinacolone-d_{12} was prepared according to a literature procedure.[9] ^{1}H and ^{13}C NMR data were acquired on Varian VXR (300 MHz, 20°C) or Bruker DRX (400 MHz, 25°C) spectrometers. Chemical shifts are referenced to proton solvent impurities (δ 7.15, C_6D_5H). UV-vis data were recorded on a HP8452A diode array spectrophotometer and reported as λ_{max} in nm (log ϵ). Elemental analyses (C, H, N) were performed by Iowa State Universi.. Instrument Services. GCMS studies were performed on a Varian gas chromatograph coupled to an ITS 40 ion trap mass spectrometer (capillary column DB-5MS).

(TTP)Zr(NHAr^{iPr})[OC(^{t}Bu)(=CH$_2$)], 2a. This complex is formed within minutes from treatment of the imido complex, 1, with one equivalent of pinacolone in toluene or benzene. Although complex **2a** is stable in its mother liquor for days at ambient temperature and at 80°C, it could not be isolated in an analytically pure form. ^{1}H NMR (C_6D_6, 400 MHz): 9.18 (s, 8H, β-H), 8.55 (d, 4H, $^3J_{H-H}$ = 7 Hz, meso-C_6H_4CH$_3$), 7.85 (d, 4H, $^3J_{H-H}$ = 7 Hz, meso-C_6H_4CH$_3$), 7.33 (d, 4H, $^3J_{H-H}$ = 8 Hz, meso-C_6H_4CH$_3$), 7.23 (d, 4H, $^3J_{H-H}$ = 8 Hz, meso-C_6H_4CH$_3$), 6.22 (m, 3H, m-, p-NHAr^{iPr}), 3.02 (s, 1H, OC(=CH$_2$)^{t}Bu), 2.40 (s, 12H, meso-C_6H_4CH$_3$), 1.35 (s, 1H, OC(=CH$_2$)^{t}Bu), 0.96 (s, 1H, NHAr^{iPr}), 0.46 (d, 6H, 2,6-(^{i}Pr)$_2$-C_6H_4), 0.32 (d, 6H, 2,6-(^{i}Pr)$_2$-C_6H_4), -0.22 (m, 2H, NHAr^{iPr}), -0.50 (s, 9H, OC(=CH$_2$)^{t}Bu). ^{13}C NMR (C_6D_6): 170.7 (OC(=CH$_2$)^{t}Bu), 150.6, 148.6, 139.8, 137.1, 135.2 (o-tolyl), 134.2 (o-tolyl), 132.5 (β-pyrrole), 128.5 (m-tolyl), 125.6, 125.4, 121.2 (m,p-Ar^{iPr}), 119.7 (m,p-Ar^{iPr}), 83.3 (OC(=CH$_2$)^{t}Bu), 34.1, 29.0 (CH(Me)$_2$), 27.3 (OC(=CH$_2$)(C(CH$_3$)$_3$), 24.6 (CH(Me)$_2$), 22.0 (CH(Me)$_2$), 21.4 (CH$_3$-tolyl).

(TTP)Zr[OC('Bu)CHC('Bu)(Me)O], 2. A solution of (TTP)Zr=NAr^{Pr} (237 mg,

0.253 mmol) and pinacolone (200 μL, 1.60 mmol) in benzene (ca. 15 mL) was stirred at

25°C for 40 h. This dark blue solution was filtered and the filtrate solution evaporated to

dryness *in vacuo* to yield blue **2** (204 mg, 84 % yield). UV/vis (toluene): 548 (4.55), 425

(5.66), 405 (shoulder, 3.23). ^{1}H NMR (C$_6$D$_6$, 300MHz): 9.21 (m, 8H, β-H), 8.47 (d, 4H,

^{3}J$_{H-H}$ = 7 Hz, *meso*-C$_6$H$_4$CH$_3$), 7.93 (d, 4H, ^{3}J$_{H-H}$ = 7 Hz, *meso*-C$_6$H$_4$CH$_3$), 7.36 (d, 4H, ^{3}J$_{H-H}$

= 8 Hz, *meso*-C$_6$H$_4$CH$_3$), 7.25 (d, 4H, ^{3}J$_{H-H}$ = 8 Hz, *meso*-C$_6$H$_4$CH$_3$), 3.00 (s, 1H,

OC('Bu)C*H*C('Bu)(Me)O), 2.40 (s, 12H, *meso*-C$_6$H$_4$C*H$_3$*), 0.04 (s, 9H,

OC(*'Bu*)CHC('Bu)(Me)O), -0.46 (s, 9H, OC('Bu)CHC(*'Bu*)(Me)O), -0.69 (s, 3H,

OC('Bu)CHC('Bu)(*Me*)O. ^{13}C NMR (C$_6$D$_6$): 159.5 (O*C*(=CH)('Bu)), 150.4 (α-pyrrole),

150.1 (α-pyrrole), 140.0, 137.4, 135.2 (*o*-tolyl), 134.5 (*o*-tolyl), 132.61 (β-pyrrole), 132.56

(β-pyrrole), 127.9 (*m*-tolyl, obscured by solvent), 127.8 (*m*-tolyl, obscured by solvent),

124.7, 97.6 (OC(=*C*H)('Bu)), 80.0 (O*C*(Me)('Bu)), 37.2, 34.8, 27.4 (OC(=CH)C*Me$_3$*), 24.3

(OC(Me)C*Me$_3$*), 23.7 (OC(*Me*)('Bu)), 21.4 (*C*H$_3$-tolyl). Anal. Calcd. (Found) for

C$_{60}$H$_{58}$N$_4$O$_2$Zr: C, 75.20 (75.35); H, 6.10 (6.19); N, 5.85 (5.59).

(TTP)Hf(NHAr^{iPr})[OC('Bu)(=CH$_2$)], 3a. The formation of complex **3a** was

observed in a NMR tube experiment. An NMR tube equipped with a teflon stopcock was

charged with (TTP)Hf=NAr^{Pr} (11.7 mg, 11.5 μmol), Ph$_3$CH (91.0 μL, 0.1439 M in C$_6$D$_6$,

13.0 μmol), pinacolone (6.7 μL, 53.6 μmol) and C$_6$D$_6$ (ca. 0.6 mL). Complex **3a** (11.5

μmol, 100% NMR yield) was formed after 17 h at 25 °C. Complex **3** (11.4 μmol, 99 %

NMR yield) is formed after heating this solution for 25 h at 85 °C. ^{1}H NMR (C$_6$D$_6$, 400

MHz): 9.20 (s, 8H, β-H), 8.55 (d, 4H, ^{3}J$_{H-H}$ = 7 Hz, *meso*-C$_6$H$_4$CH$_3$), 7.85 (d, 4H, ^{3}J$_{H-H}$ = 7

Hz, *meso*-C$_6$*H*$_4$CH$_3$), 7.33 (d, 4H, $^3J_{H-H}$ = 8 Hz, *meso*-C$_6$*H*$_4$CH$_3$), 7.23 (d, 4H, $^3J_{H-H}$ = 8 Hz,

meso-C$_6$*H*$_4$CH$_3$), 6.22 (m, 3H, *m*-, *p*-NHAr^{iPr}), 2.91 (s, 1H, OC(=C*H*$_2$)^{t}Bu), 2.40 (s, 12H,

meso-C$_6$H$_4$C*H*$_3$), 1.18 (s, 1H, OC(=C*H*$_2$)^{t}Bu), 0.88 (s, N*H*Ar^{iPr}, obscured by pinacolone),

0.48 (d, 6H, 2,6-(CH(C*H*$_3$)$_2$)$_2$-C$_6$H$_4$), 0.31 (d, 6H, 2,6-(CH(C*H*$_3$)$_2$)$_2$-C$_6$H$_4$), -0.17 (m, 2H,

2,6-(C*H*(CH$_3$)$_2$)$_2$-C$_6$H$_4$), -0.50 (s, 9H, OC(=CH$_2$)^t*Bu*).

(TTP)Hf[OC(^{t}Bu)CHC(^{t}Bu)(Me)O], 3. A solution of (TTP)Hf=NAr^{iPr} (128 mg,

0.125 mmol) and pinacolone (90 μL, 0.72 mmol) in toluene (ca. 10 mL) was stirred at 25 °C

for 140 h. The reaction had not reached completion at this time and was subsequently

heated for 26 h at 80 °C. This dark blue solution was filtered and the filtrate solution

evaporated to dryness *in vacuo* and recrystallized from a toluene solution layered with

hexanes at -25 °C overnight to yield blue 3 (79 mg, 61 % yield). ^{1}H NMR (C$_6$D$_6$, 300MHz):

9.23 (m, 8H, *β*-H), 8.47 (d, 4H, $^3J_{H-H}$ = 7 Hz, *meso*-C$_6$*H*$_4$CH$_3$), 7.91 (d, 4H, $^3J_{H-H}$ = 7 Hz,

meso-C$_6$*H*$_4$CH$_3$), 7.35 (d, 4H, $^3J_{H-H}$ = 8 Hz, *meso*-C$_6$*H*$_4$CH$_3$), 7.24 (d, 4H, $^3J_{H-H}$ = 8 Hz,

meso-C$_6$*H*$_4$CH$_3$), 2.92 (s, 1H, OC(^{t}Bu)C*H*C(^{t}Bu)(Me)O), 2.40 (s, 12H, *meso*-C$_6$H$_4$C*H*$_3$),

0.04 (s, 9H, OC(^{t}*Bu*)CHC(^{t}Bu)(Me)O), -0.43 (s, 9H, OC(^{t}Bu)CHC(^{t}*Bu*)(Me)O), -0.72 (s,

3H, OC(^{t}Bu)CHC(^{t}Bu)(*Me*)O.

[(TTP)ZrO]$_2$, 4. A solution of (TTP)Zr=NAr^{iPr} (214 mg, 0.228 mmol) and PhNO

(28.2 mg, 0.263 mmol) in toluene (ca. 15 mL) was stirred at 25°C for 1.5 h. This dark blue

solution was filtered and the filtrate solution evaporated to dryness *in vacuo* to yield blue 4

(99 mg, 56 % yield). UV/vis (toluene): 548 (4.38), 511 (4.51), 473 (4.40), 420 (5.56). 364

(4.41). ^{1}H NMR (CDCl$_3$, 300MHz): 8.44 (s, 8H, *β*-H), 7.58 (m, 8H, *meso*-C$_6$*H*$_4$CH$_3$), 7.40

(m, 8H, *meso*-C$_6$*H*$_4$CH$_3$), 2.71 (s, 12H, *meso*-C$_6$H$_4$C*H*$_3$). ^{13}C NMR (CDCl$_3$): 148.0, 139.3,

136.8, 135.7 (*meso-C₆H₄CH₃*), 132.9 (*meso-C₆H₄CH₃*), 130.6 (*β*-pyrrole), 127.0 (*meso-C₆H₄CH₃*), 122.5, 21.5 (*meso-C₆H₄CH₃*). GCMS (Ar^{Pr}N=NPh) Calcd(found): 266.39(266) m/z. Anal. Calcd. (Found) for C₉₆H₇₂N₈O₂Zr₂: C, 74.29 (74.38); H, 4.68 (5.29); N, 7.22 (6.60).

[(TTP)Zr]₂(μ-O)(μ-OH)₂, 5. A solution of **2** (129 mg, 0.135 mmol) and acetone (150 μL, 2.04 mmol) in toluene (ca. 10 mL) was refluxed for 36 h. This dark blue solution was filtered and the solid washed with toluene (3 x 2 mL) to yield blue **5** (92 mg, 43 % yield). UV/vis (CH₂Cl₂): 541 (4.64), 416 (5.75). ¹H NMR (CDCl₃, 300MHz): 8.41 (s, 16H, *β*-H), 7.62 (bd, *meso-C₆H₄CH₃*), 7.46 (bd, *meso-C₆H₄CH₃*), 7.41 (bd, *meso-C₆H₄CH₃*), 2.71 (s, 24H, *meso-C₆H₄CH₃*), -8.27 (s, 2H, μ-O*H*). ¹³C NMR (CDCl₃): 148.1, 139.2, 136.8, 130.4 (*β*-pyrrole), 129.0 (*meso-C₆H₄CH₃*), 128.2, 127.0, 125.3, 21.5 (*meso-C₆H₄CH₃*). Anal. Calcd. (Found) for C₉₆H₇₄N₈O₃Zr₂: C, 73.44 (73.99); H, 4.75 (4.91); N, 7.14 (6.48).

Reaction of complex 2a with *p*-toluidine. Complex **2a** was generated *in situ* in a NMR tube equipped with a teflon stopcock. Within minutes of adding approximately 6 eq of H₂Ntolyl all NHAr^{Pr} in **2a** had been replaced by NHtolyl to form (TTP)Zr(NHtolyl)(OC('Bu)(=CH₂)), **2b**. ¹H NMR (C₆D₆, 300 MHz): 9.14 (s, 8H, *β*-H), 8.46 (d, 4H, *meso-C₆H₄CH₃*), 7.85 (d, 4H, *meso-C₆H₄CH₃*), 7.35 (d, 4H, *meso-C₆H₄CH₃*), 7.22 (d, 4H, *meso-C₆H₄CH₃*), 6.29 (d, *m*-tolyl, obscured by H₂Ntolyl), 4.20 (d, 2H, *o*-tolyl), 3.00 (s, 1H, OC(=C*H₂*)'Bu), 2.39 (s, 12H, *meso-C₆H₄CH₃*), 1.87 (s, 6H, *p*-*Me*C₆H₄), (OC(=C*H₂*)'Bu and N*H*Ar^{iPr} signals not observed, obscured by pinacolone and H₂NAr^{Pr}), -0.26 (s, 9H, OC(=CH₂)'*Bu*). Addition of 2 eq of pinacolone lead to the formation of complex **2** within 15 minutes.

Reaction of complex 2a with 2-octanone. A NMR tube equipped with a teflon

stopcock was charged with (TTP)Zr=NAr^{Pr} (15.6 mg, 16.7 µmol), Ph$_3$CH (93.0 µL, 0.1397

M in C$_6$D$_6$, 13.0 µmol), pinacolone (2.3 µL, 18.4 µmol) and C$_6$D$_6$ (ca. 0.6 mL). Allowing

the tube to stand at 20 °C for 16 h afforded 2a in quantitative yield at which time 2-

octanone (7.0 µL, 44.7 µmol) was added. Allowing this reaction mixture to stand at 20 °C

for 23 h afforded (TTP)Zr(OC(^{t}Bu)CHC(hexyl)(Me)O) (15.0 µmol, 90 % NMR yield).

Complex 2 was not observed at any time during this reaction. Treatment of the final

reaction mixture with water produced the enone as one of the many decomposition products.

^{1}H NMR (C$_6$D$_6$, 300MHz): 9.21 (s, 8H, β-H), 8.41 (d, 4H, $^3J_{H-H}$ = 7 Hz, *meso*-C$_6$$H_4CH_3$),

7.91 (d, 4H, $^3J_{H-H}$ = 7 Hz, *meso*-C$_6$$H_4CH_3$), 7.37 (d, 4H, $^3J_{H-H}$ = 8 Hz, *meso*-C$_6$$H_4CH_3$), 7.24

(d, 4H, $^3J_{H-H}$ = 8 Hz, *meso*-C$_6$$H_4CH_3$), 2.84 (s, 1H, OC(^{t}Bu)CHC(hexyl)(Me)O), 2.40 (s,

12H, *meso*-C$_6$H$_4$CH_3), 1.2-0.6 (m, OC(^{t}Bu)CHC(*hexyl*)(Me)O, obscured by H$_2$NAr^{Pr},

pinacolone, and 2-octanone), 0.05 (s, 9H, OC(^{t}Bu)CHC(hexyl)(Me)O), -0.29 (m, 2H,

OC(^{t}Bu)CHC(CH_2(CH$_2$)$_4$CH$_3$)(Me)O), -0.72 (s, 3H, OC(^{t}Bu)CHC(hexyl)(*Me*)O. GCMS

(2,2,5-trimethyl-4-undecen-3-one, C$_{14}$H$_{26}$O): Calcd. (found): [M$^+$] 210.36(211) m/z.

Reaction of (TTP)Zr(η^2-NAr^{Pr}C(=N^{t}Bu)O) with pinacolone. A NMR tube

equipped with a teflon stopcock was charged with (TTP)Zr(η^2-NAr^{Pr}C(=N^{t}Bu)O) (13.1 mg,

12.68 µmol), Ph$_3$CH (91.5 µL, 0.1455 M in C$_6$D$_6$, 13.3 µmol), pinacolone (7.0 µL, 56.0

µmol) and C$_6$D$_6$ (ca. 0.6 mL). Allowing the tube to stand at 20 °C for 15 h afforded 2 (11.5

µmol, 90 % NMR yield) and Ar^{Pr}NHC(O)NH^{t}Bu (9.2 µmol, 72 % NMR yield). GCMS

C$_{17}$H$_{28}$N$_2$O: Calcd. (found): [M$^+$] 276.42 (277) m/z. ^{1}H NMR (C$_6$D$_6$, 300 MHz): 7.16 (m, *p*-

C$_6$$H_3$, obscured by H$_2$NAr^{Pr}), 7.08 (d, 2H, *m*-C$_6$$H_3$, obscured by H$_2$NAr^{Pr}), 4.02 (s, 1H,

NH), 3.57 (m, 2H, -CHMe$_2$), 1.23 (d, 12H, -CHMe_2), 1.18 (s, 9H, N-CMe_3).

Structure Determinations of (TTP)Zr[OC(^{t}Bu)CHC(^{t}Bu)(Me)O] (2),

[(TTP)ZrO]$_2$ (4), and [(TTP)Zr]$_2$(μ-O)(μ-OH)$_2$ (5). Crystal data is found in Appendix A.

Compound 5 was treated by attachment to a glass fiber and mounting on a Siemens SMART

system for data collection at 173(2) K. An initial set of cell constants was calculated from

reflections harvested from three sets of 20 frames. These initial sets of frames were oriented

such that orthogonal wedges of reciprocal space were surveyed. This produced orientation

matrices determined from 154 reflections for compound 5. Final cell constants were

calculated from a set of 4170 strong reflections from the actual data collection. Three major

swaths of frames were collected with 0.30° steps in ω. The space group was determined on

the basis of systematic absences and intensity statistics, and a successful direct-methods

solution was calculated which provided most non-hydrogen atoms from the E-map. Several

full-matrix least squares/difference Fourier cycles were performed which located the

remainder of non-hydrogen atoms, which were refined with anisotropic displacement

parameters. Atom O1 is located on the crystallographic two-fold axis. Its longer metal

bond lengths suggest it is a hydroxide. Its proton is assumed to be in sp^3 geometry and

disordered over the two possible, partially occupied sites. The other two oxygens, bridging

hydroxide (O3) and oxo (O2), were equally disordered over the crystallographic two-fold

axis and were refined with restrained metal-oxygen distances. All hydrogen atoms were

placed in ideal positions and refined as riding atoms with relative isotropic displacement

parameters. There were 1.5 solvent molecules of benzene per asymmetric unit. SHLEXTL

DELU and SAME restraints were employed here to keep reasonable C-C distances and

approximate rigid-body anisotropic displacement parameters. There were 48 restraints used altogether. Three bad reflections were omitted from the final least-squares refinement. All calculations were performed using SGI INDY R4400-SC or Pentium computers using the SHELXTL V5.0 program suite.[10]

Crystals of 2 and 4 were treated in an analogous manner to that of 5. Systematic absences in the diffraction data were uniquely consistent for space groups denoted in Appendix A. The structures were solved using direct methods, completed by subsequent difference Fourier synthesis and refined by full-matrix least-squares procedures. For complex 2, all porphyrin non-hydrogen atoms and zirconium were refined with anisotropic displacement coefficients. All other non-hydrogens were refined isotropically. The enediolate ligand exhibited high thermal activity and was refined with an idealized geometry. The crystal was refined as a twin with a 52:48 ratio contribution from the two components. There were three severely disordered solvent molecules also present in the asymmetric unit, which were identified and refined as a hexane, toluene, and a half of a toluene molecule using the SQUEEZE option in the PLATON[11] program. PLATON calculated the upper limit of volume that can be occupied by the solvent to be 2028.3 Å^3 or 30.8 % of the unit volume. The program calculated 512 electrons, four hexane and six toluene molecules, in the unit cell for the diffuse species. Similar treatment was addressed to two severely disordered toluene molecules that were identified and refined in the asymmetric unit of complex 4. PLATON calculated the upper limit of volume that can be occupied by the solvent to be 2016.5 Å^3 or 22.5 % of the unit volume. The program calculated 812 electrons, eight toluene molecules, in the unit cell for the diffuse species. Note that all

derived data in the following tables are based on known contents. No data is given for the diffusely scattering solvent molecules. Crystallographic data in CIF format are deposited at the Cambridge Crystallographic Data Center.

Results

Pinacolone coupling from (TTP)Zr=NAr^{iPr}, 1. Upon treatment of (TTP)Zr=NAr^{iPr}, 1, with one equivalent of pinacolone a new species is observed within 5 minutes. Product analysis was achieved by ^{1}H NMR spectroscopy.[12] The observation of a 3-proton multiplet at 6.22 ppm, due to the *meta-* and *para*-Ar^{iPr} protons, indicate that the NAr^{iPr} moiety has been retained in the product. This chemical shift is close to the upfield signals found for the corresponding aryl protons of the imido complex, 1, at 6.08 ppm. Additionally, the new Ar^{iPr} isopropyl proton chemical shifts, 0.46 (d, 6H), 0.32 (d, 6H), -0.23 (m, 2H) ppm, remain significantly upfield of the free amine [2.63 (spt, 2H), 1.14 (d, 12H)] and only slightly downfield from those found in complex 1 [0.18 (m, 2H), 0.00 (d, 12H)]. The N-*H* amido proton is observed at 0.95 ppm, similar to the chemical shifts reported for (TTP)Hf(N*H*Ph)(N*H*Ar^{iPr}).[8] Signals at 3.02 (s, 1H), 1.35 (s, 1H), and -0.50 (s, 9H) ppm signify the presence of a single bound pinacolone fragment. The large variation in chemical shifts for the two geminal protons is unusual, but must arise due to differences in position relative to the porphyrin ring current.

Three possible limiting isomers for this product consistent with the ^{1}H NMR data, are shown in Figure 1. Distinctive ^{13}C NMR resonances attributed to the bound pinacolone fragment, but not due to the *t*-butyl group, are found at 170.7 and 83.3 ppm. A HETCOR
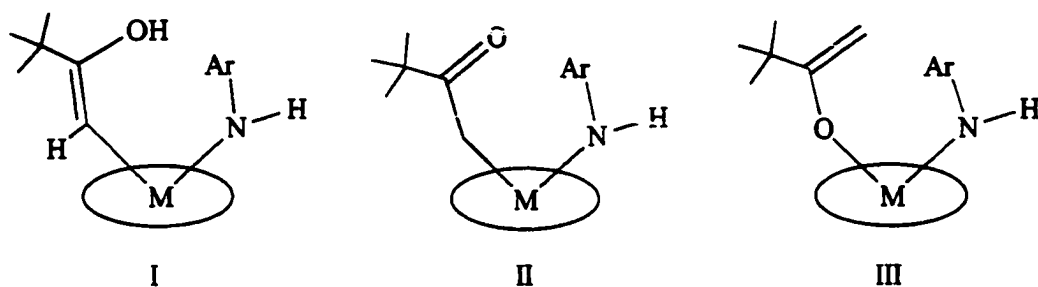
Figure 1. Possible isomers from condensation reaction between 1 and pinacolone.

experiment revealed that the protons resonating at 3.02 and 1.35 ppm are both bound to the

same carbon atom (83.3 ppm), precluding isomer I. The proton resonating at 3.02 ppm

displays a through-space interaction with the t-butyl group (-0.50 ppm) in a NOESY

experiment. Consequently, this proton must be cisoid to the t-butyl group. The ^{13}C NMR is

incompatible with isomer II as the peak at 83.3 ppm is too far downfield for a C-bound

enolate.[13] A metallocene enolate complex, Cp_2*$Zr(OH)[\eta^1$-$OC(=CH_2)(Bu^t)]$, possesses

similar ^{13}C NMR chemical shifts, 84.1 [$OC(Bu^t)=CH_2$] and 172.8 ppm [$OC(=CH_2)(Bu^t)$].

The NMR data for the condensation product is most consistent with an O-bound enolate,

isomer III. The enolato complex, $(TTP)Zr(NHAr^{Pr})[OC(=CH_2)(^tBu)]$, 2a, could not be

isolated in pure form due to decomposition to intractable products during purification

attempts.

Treatment of complex 2a with one equivalent of pinacolone results in the elimination

of H_2NAr^{Pr} and formation of a metalloporphyrin product containing two pinacolone

fragments. The ^{1}H NMR integrations of the double condensation product are consistent

with the overall loss of 2 hydrogens from the two pinacolone molecules. A singlet at 3.00

ppm is assigned to an olefinic proton that has been shifted upfield by the porphryin ring

current. The two 'Bu groups are observed as singlets at 0.04 (9H) and -0.46 (9H) ppm and the remaining methyl singlet appears at -0.69 (3H) ppm. Upon cooling a toluene-d_8 solution of complex 2, broadening of the t-butyl singlet at -0.46 ppm is observed in the ^{1}H NMR. At 234 K this singlet has nearly broadened into the baseline while the geminal methyl signal (-0.69 ppm) remains sharp.[14] An unusual feature of complex 2 is the β-pyrrole proton resonance. This signal appears as an AB quartet (9.21 ppm, $^3J_{H-H}$ = 4.6 Hz, δv = 4.8 Hz) due to the stereogenic center in the endiolate ligand. Two isomers are consistent with the 1-D ^{1}H NMR data for the two coupled pinacolone molecules (Figure 2).
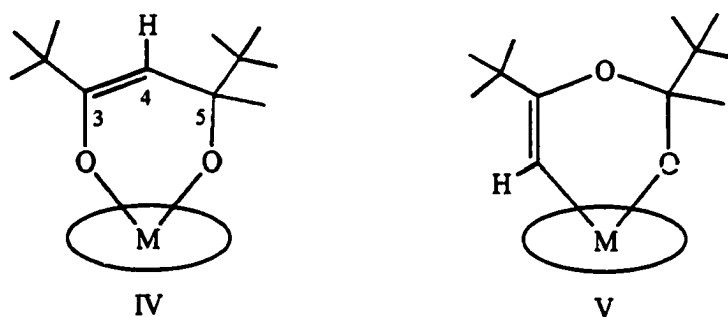
Figure 2. Possible isomers of coupled pinacolone derivatives consistent with ^{1}H NMR.

The position of the olefinic proton was established by a NOESY experiment which shows through-space interactions of this hydrogen to both t-butyl groups and to the methyl group. Furthermore, the methyl group which resonates at -0.69 ppm is also close, spatially, to the t-butyl unit with the signal at -0.46 ppm. Isomer IV is consistent with the NOESY experiment while isomer V would exhibit a NOE interaction of the olefinic proton with only one 'Bu group. The connectivity of the hydrocarbon backbone is definitively established by a HMBC experiment that shows two-bond coupling interactions between the olefinic proton

and both carbon 3 and carbon 5 (see Figure 2 for numbering). Isomer V would contain a

two-bond coupling of the olefinic proton to only one carbon atom. The chemical shifts of

carbon 3 (160.0 ppm), carbon 4 (97.6 ppm), and carbon 5 (80.0 ppm) of the metallacycle

backbone were assigned by HETCOR and HMBC NMR experiments.

In addition to 2-D NMR results, support for the assignment of the two t-butyl groups

in complex **2** was facilitated by deuterium labeling. Treatment of the imido **1** with 1 eq of

pinacolone followed by excess pinacolone-d_{12} produced complex **2** with a 9-proton singlet in

the ^{1}H NMR spectrum at 0.04 ppm. Conversely, treatment of **1** with 1 eq of pinacolone-d_{12}

and then with excess proteo-pinacolone produced metallacycle **2** with a 9-proton singlet at

-0.46 ppm and a 3-proton singlet at -0.69 ppm. These experiments also reveal that the

source of the protons transferred to the imido group is the methyl group of the first

pinacolone consumed. Based on the NMR structural analysis, the reaction sequence for

pinacolone condensation with complex **1** is shown in equations 1-2.

Complex **2** could also be synthesized by alternate routes. Formation of the

metallacycle **2** occurs on treatment of the ureato complex, $(TTP)Zr(\eta^2-NAr^{Pr}C(=N^tBu)O)$,

with excess pinacolone. The urea, $NHAr^{Pr}C(=O)NH^tBu$, is a by-product of this process.

Treatment of $(TTP)ZrCl_2$ with excess pinacolone in the presence of piperidine also results in

the formation of complex **2**. Although this is a more direct synthetic approach, it yields

impure product. A one-pot synthesis which involves adding excess pinacolone to *in situ*

generated **1**, produced complex **2** in comparable yield and purity to that found for the

reaction with isolated imido complex **1**. Whereas the formation of complex **2** from enolate

species **2a** requires hours to reach completion, treatment of complex **2b** with pinacolone

$$(1)$$

$$(2)$$
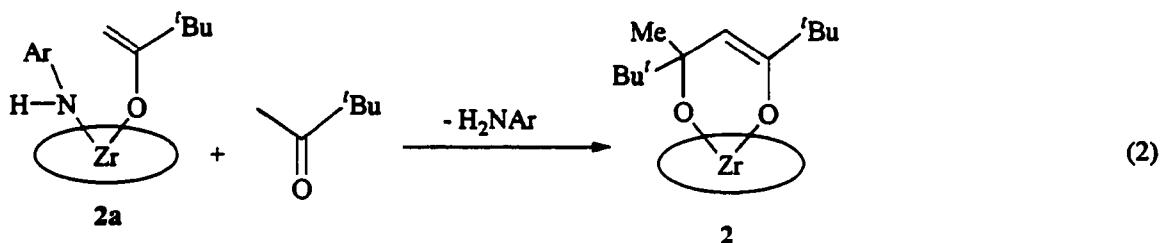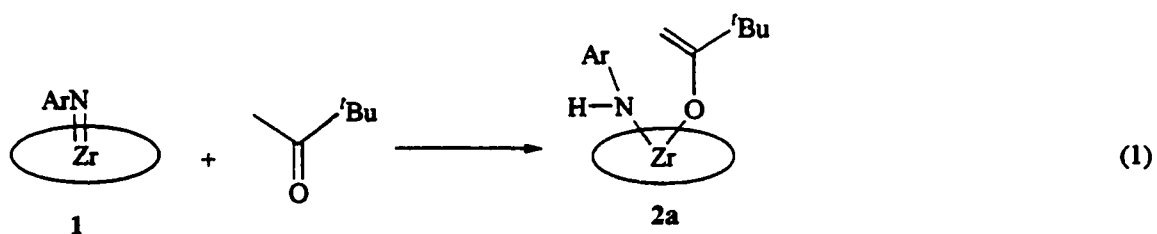
results in the rapid formation of the endiolate.

The preceding investigation also employed hafnium in place of zirconium, but due to similar characteristics only the latter was addressed. The largest discrepancy in the ^{1}H NMR of the amido/enolato congeners was found for the methylene resonances. Those for **3a** (2.91, 1.18 ppm) are slightly upfield of those in **2a** (3.02, 1.35 ppm). Similarly, the olefinic resonance in the endiolate complex is upfield for the hafnium derivative (2.92 ppm) relative to that for the zirconium complex (3.00 ppm). Reaction times were observed to be somewhat longer for Hf as observed previously in other chemistry of Hf and Zr metalloporphyrin complexes.[8] Under identical reaction conditions treatment of the respective imido, (TTP)M=NAr^{Pr} (M = Zr, Hf), with excess pinacolone produced the amide/enolate complex within minutes for zirconium and 1 h for hafnium.

Formation of oxygen bridged dimers 4 and 5. The bis(μ-oxo) complex, [(TTP)ZrO]$_2$, **4**, was initially observed in the thermal decomposition of the N,O-bound

ureato complexes, $(TTP)Zr(\eta^2\text{-}NAr^{iPr}C(=N^tBu)O)$ and $(TTP)Zr(\eta^2\text{-}N^tBuC(=NAr^{iPr})O)$.[8,15] A

more facile route to complex **4** was found from the metathesis reaction between complex **1**

and PhNO (eq 3). The dimer was formed in moderate yield along with the diazene,

$PhN=NAr^{iPr}$. The ^1H NMR spectrum of the bis(μ-oxo) species exhibits signals typical of

$$(3)$$
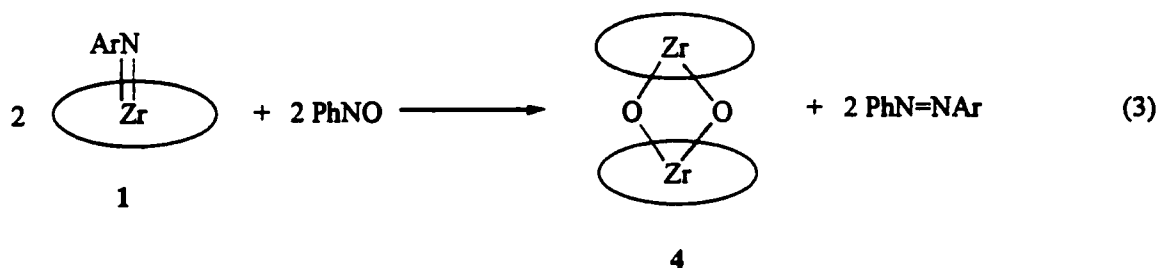
zirconium metalloporphyrin complexes. The exception is an upfield shift of the β-pyrrole

signal to 8.44 ppm due to the face-to-face orientation of the two porphyrin rings. The β-

pyrrole signal remains as a singlet at 223 K in $CDCl_3$, indicating fast rotation of the

porphyrin rings relative to one another. Complex **4** readily undergoes hydrolysis upon

exposure to water to produce the (μ-oxo)bis(μ-hydroxo) dimer, complex **5** (eq 4).

$$(4)$$
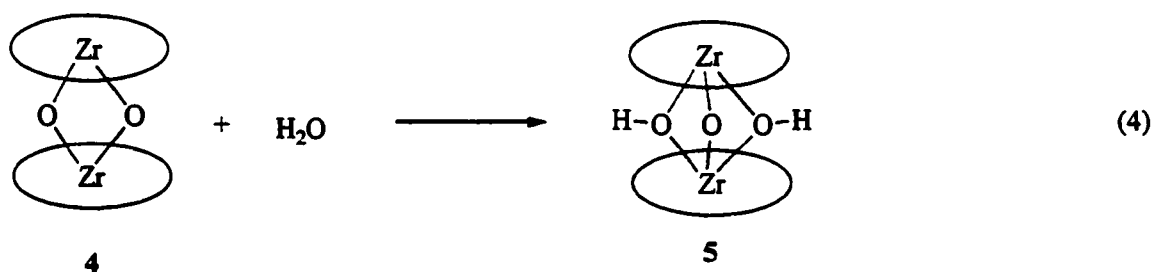
The most facile preparation of compound **5** was found from heating a toluene solution of **2**

in the presence of excess acetone. The hydroxyl protons at -8.27 ppm (s, 2H) were found to

be upfield from those reported for the tetraphenylporphyrin analogue (-6.73 ppm, s, 2H).[16b]

Crystal structures of (TTP)Zr(OC('Bu)CHC('Bu)(Me)O) (2), [(TTP)ZrO]₂ (4),

and [(TTP)Zr]₂(μ-O)(μ-OH)₂ (5). The crystallographic data for complexes 2, 4, and 5 are

presented in Appendix A and selected metrical parameters are collected in Tables 1-2. All of

the molecules exhibit typical out-of-plane distance of the zirconium from the mean 4-N$_{pyrrole}$

plane for six- and seven-coordinate metals. In the case of complex 2, acquisition of high

quality crystals was not possible despite numerous recrystallizations. We attribute these

difficulties to the solvent dependent nature of the crystals and volatile solvent molecules

packed in the voids of the lattice. While extensive disorder in the enediolate ligand

precluded anisotropic refinement of the carbon backbone, the oxygen atom identities were

unequivocally established and are consistent with the results of spectroscopic experiments.

A representation of complex 2 is given in Figure 3. The Zr-O bond distances of 1.963(6)

[Zr-O1] and 1.945(7) Å [Zr-O2] compare well with those in alkoxido compounds,[17] but are

considerably shorter than the single bonds observed in the four-atom metallacycles

(TTP)Zr(η^2-NAr^{Pr}C(=N'Bu)O) [2.0677(12) Å] and (TTP)Zr(η^2-N'BuC(=NAr^{Pr})O)

[2.066(3) Å].[1] Atom O1 eclipses the Zr-N2 bond within 2.0° while atom O2 is staggered in

relation to the Zr-N3 and Zr-N4 bonds by 62.5° and 26.5°, respectively. The Zr-N2

[2.290(10) Å] and Zr-N4 [2.295(9) Å] bonds are long compared to Zr-N3 [2.177(9) Å] and

Zr-N4 [2.295(9) Å] distances. These differences are likely due to contributions from

nitrogen-oxygen repulsions [N2-O1: 2.717(2) Å; N4-O2: 2.721(2) Å].[18]

Compound 4 (Figure 4) results from the formal dimerization of two (TTP)Zr=O

units. The metal-oxygen bond distances, 1.9719(16) and 1.9791(16)Å [Zr1-O1 and Zr1-

O2], are elongated compared to known oxo-bridged analogues but still suggest the presence

Table 1. Selected bond distances Zr-E (Å) of complexes 2, 4, 5.

Complex	2		4		5	
	Zr-O1	1.963(6)	Zr1-O1	1.9719(16)	Zr1-O1	2.166(3)
	Zr-O2	1.945(7)	Zr1-O2	1.9791(16)	Zr1-O2	1.988(4)
					Zr1-O3	2.171(5)
	Zr-N1	2.254(8)	Zr1-N1	2.246(2)	Zr1-N1	2.291(3)
	Zr-N2	2.290(10)	Zr1-N2	2.280(2)	Zr1-N2	2.279(3)
	Zr-N3	2.177(9)	Zr1-N3	2.241(2)	Zr1-N3	2.266(3)
	Zr-N4	2.295(9)	Zr1-N4	2.280(2)	Zr1-N4	2.286(3)
Zr-N$_4$ plane	0.98		0.97		1.04	

Table 2. Selected bond angles (°) of complexes 2, 4, 5.

Complex	2		4		5	
	O1-Zr-O2	76.9(3)	O1-Zr1-O2	78.56(8)	O1-Zr1-O2	76.1(2)
					O1-Zr1-O3	66.6(2)
					O2-Zr1-O3	74.0(2)
			Zr-O-Zr	101.64(12) av.	Zr-O1-Zr	89.91(14)
					Zr-O2-Zr	100.6(3)
					Zr-O3-Zr	89.7(2)
	N1-Zr-N3	131.97(18)	N1-Zr1-N3	130.35(8)	N1-Zr1-N3	125.83(11)
	N2-Zr-N4	124.85(19)	N2-Zr1-N4	127.86(7)	N2-Zr1-N4	125.60(11)

of multiple bonding.[19] The oxygen atoms in complex 4 are staggered with respect to the Zr-N$_{pyrrole}$ bonds. The O2-Zr1-Zr1A-N4A torsion angle is 33.8° and that of O2-Zr1-Zr1A-N3A is 57.3°. The positions of the bridging oxygen atoms lying closer to the N2 and N4 atoms may explain the variation in the Zr-N$_{pyrrole}$ bond distances resulting from O-N interactions. The Zr1-Zr1A (3.0584(5) Å) and the O-O distances (2.5014 Å) are similar to previously described bridging zirconium porphyrin complexes.[16a-b] Three common distortions from planarity of the porphyrin macrocycle are observed in complex 4.[20] The doming effect is
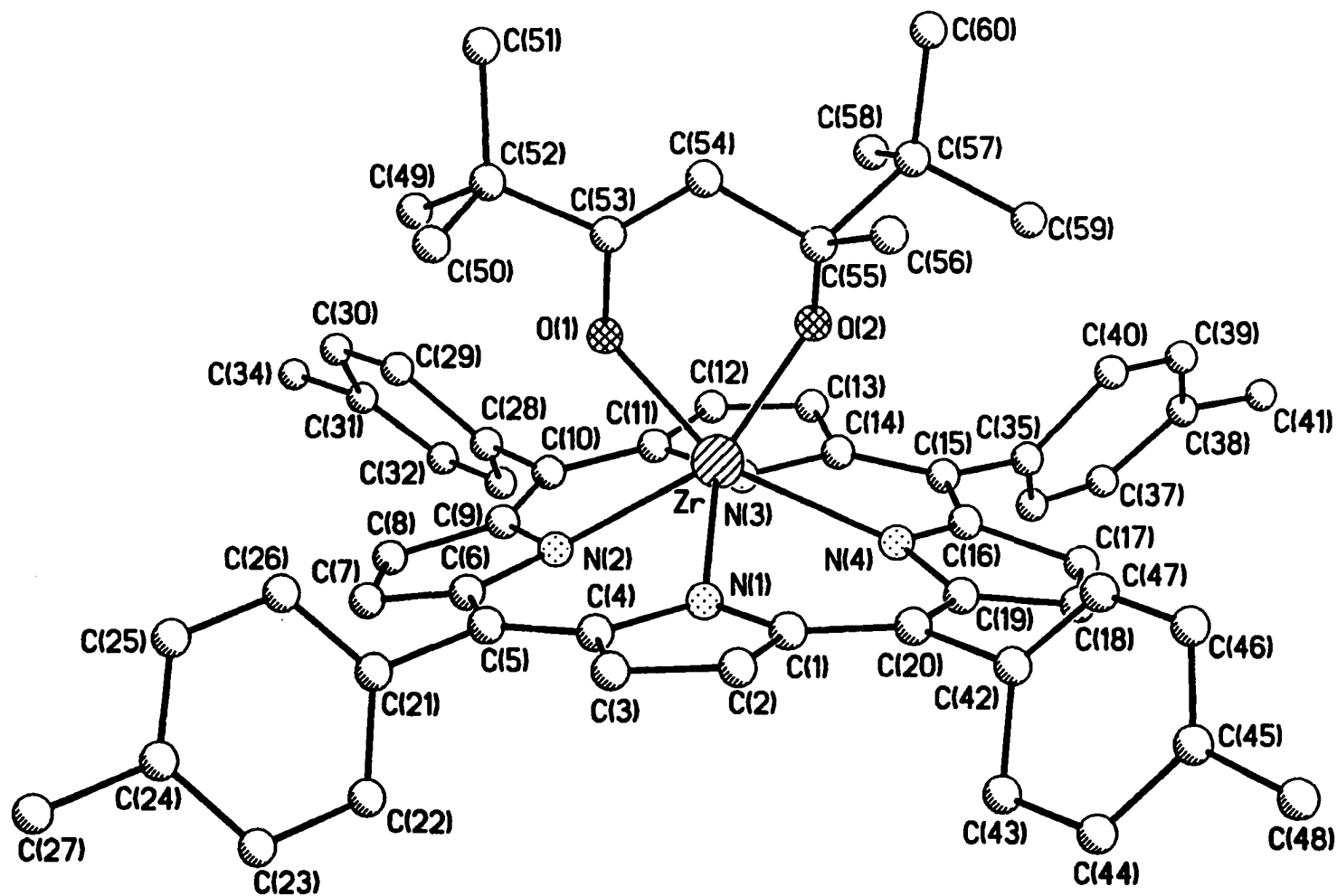
Figure 3. Ball and stick representation of complex 2, (TTP)Zr[OC('Bu)CHC('Bu)(Me)O].
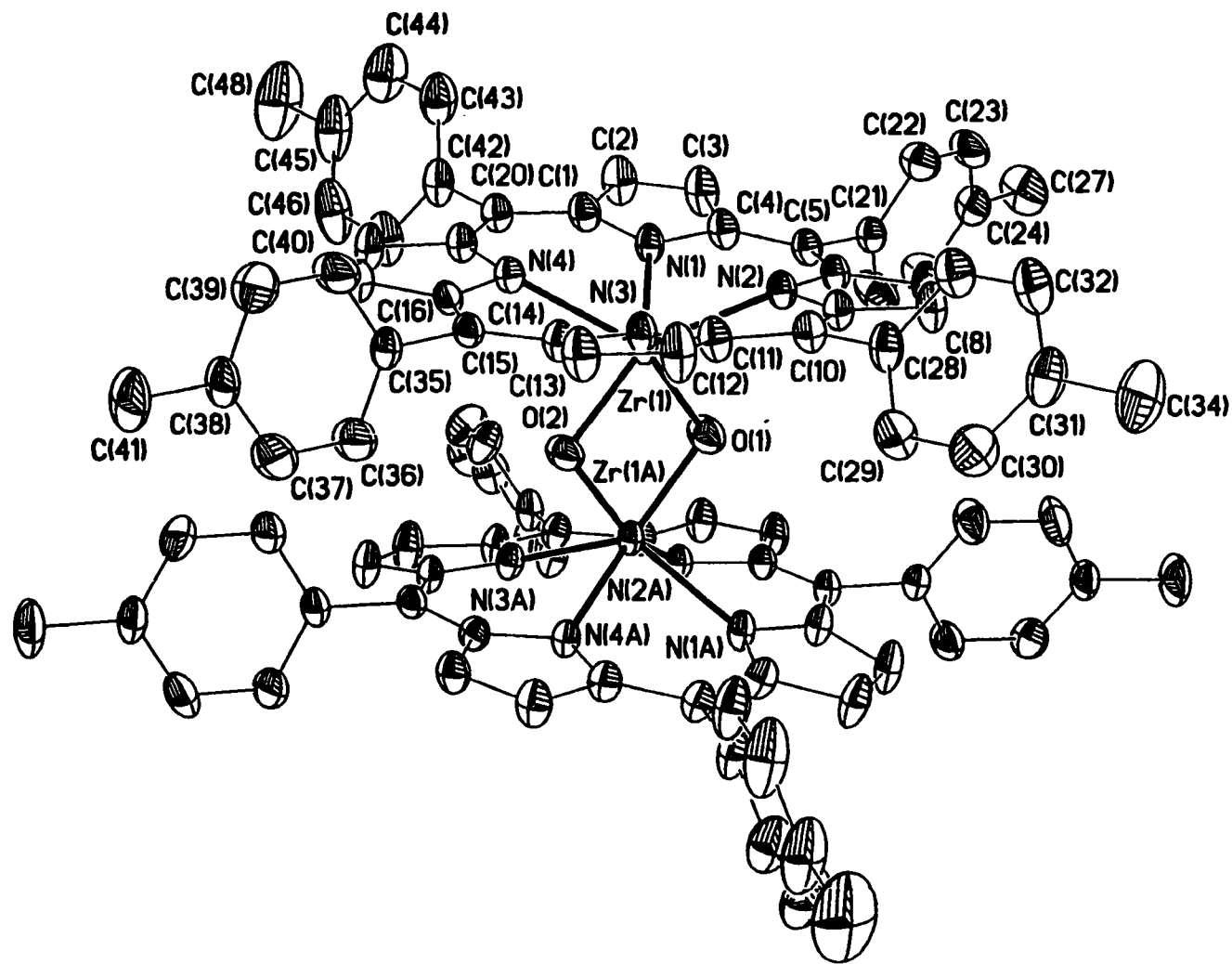
Figure 4. Molecular stucture of [(TTP)ZrO]$_2$ (4). Thermal ellipsoids are drawn at the 30% probability level.

readily perceived in the deviations of the four pyrrole nitrogens from the 24-atom porphyrin

plane [11 (N1), 7 (N2), 17 (N3), and 9 (N4) pm]. The *meso* carbon atoms alternate above

and below the mean 24-atom plane [15 (C5), -12 (C10), 16 (C15), and -12 (C20) pm] in a

ruffling deformation. Although the saddling of the porphyrin ring is perturbed by the

presence of the other two distortions, it is observed in the β-pyrrole atoms [-24 (C2), -15

(C3), 10 (C7), 1 (C8), -29 (C12), -19 (C13), 8 (C17), 2 (C18) pm].

The samples of [(TTP)Zr]$_2$(μ-O)(μ-OH)$_2$, 5, produced in this work are closely

related to the previously described phenyl derivatives [(TPP)Zr(μ-OH)$_2$]$_2$[16a] and

[(TPP)Zr]$_2$(μ-O)(μ-OH)$_2$[16b]. However, the OH proton resonance in complex 5 (-8.27 ppm)

was significantly shifted from those of the tetrahydroxy (-6.79 ppm) and the tetraphenyl

porphyrin dihydroxy analogue (-6.73 ppm). Consequently, compound 5 was subjected to a

single-crystal X-ray diffraction study. The zirconium coordination environment and metrical

parameters are unremarkable from that previously described by Kim and co-workers for

[(TPP)Zr]$_2$(μ-O)(μ-OH)$_2$. However, the presence of staggered porphyrin rings in complex 5

(Figure 5) is of marked contrast to the other structurally characterized oxygen bridged Zr

and Hf metalloporphyrin species.[16] The most acute torsion angle present in complex 5

concerning Zr-N$_{pyrrole}$ bond overlap is 22.2° [N3-Zr1-Zr1A-N2A], whereas the

corresponding angle in the TPP species is only 7.8°. The distance between the two 20-

carbon atom mean planes of the twenty carbon atoms of the porphyrins is equivalent for

complexes 4 and 5 [5.3(2) Å].
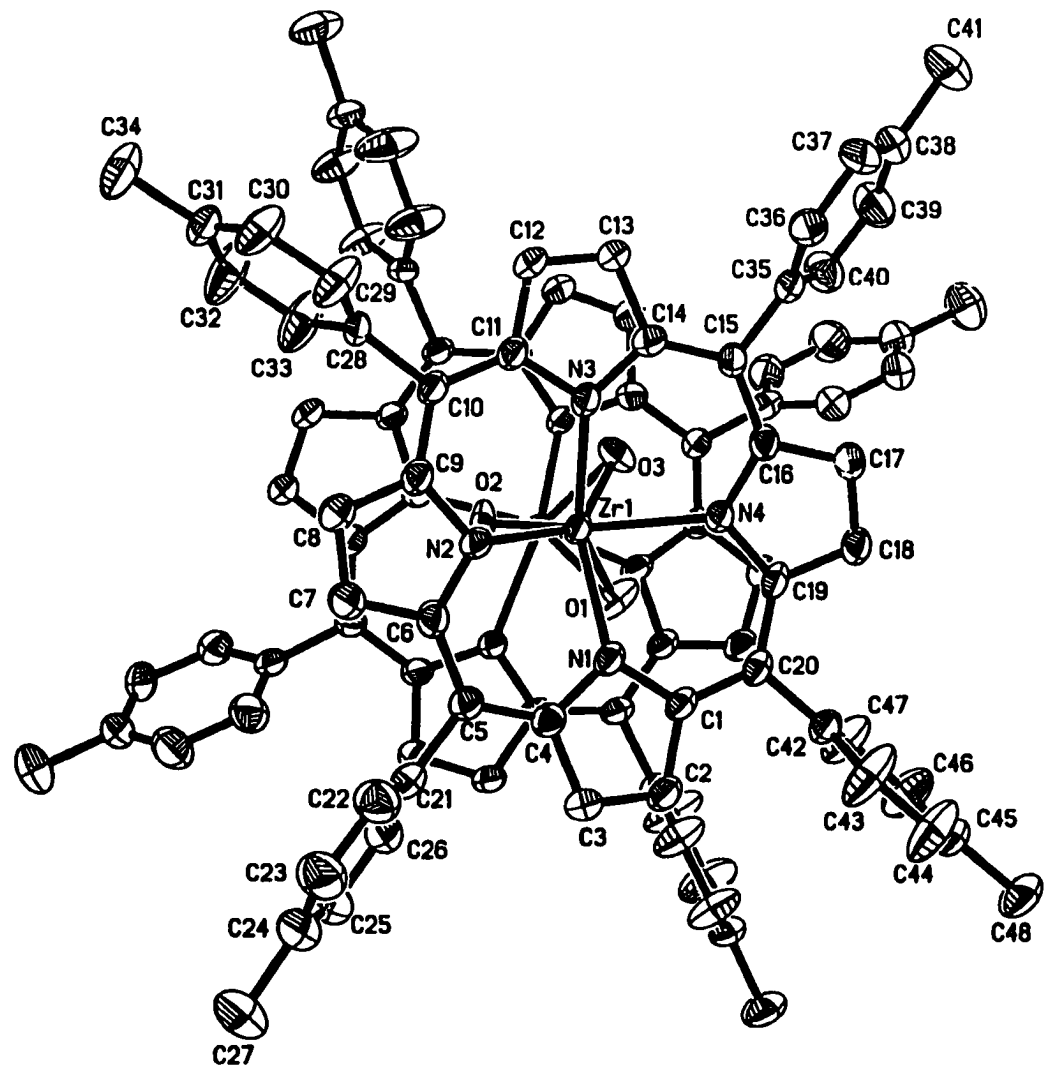
Figure 5. Top view of complex 5, [(TTP)Zr]$_2$(μ-O)(μ-OH)$_2$. Thermal ellipsoids are drawn at the 50% probability level.

Discussion

Coupling of pinacolone by (TTP)Zr=NAr^{iPr}. The basicity of the nitrene group in

terminal zirconium imido complexes has been documented in a number of studies.[8,21] A

comparable reaction of a Zr=X moiety abstracting a proton from a ketone occurs with

Cp$_2$*Zr(=O)(py) and acetophenone, producing the hydroxo/enolato derivative.[18a] An

amido/O-bound enolato species, **2a**, was found upon treatment of the imido complex, **1**,

with one equivalent of pinacolone. This enolate complex, **2a**, was inert in the presence of

PhC≡CH, acetophenone, TMSCl, or MeI at 80°C in C$_6$D$_6$. The zirconium coordination

sphere in **2a** appears to be sterically congested as indicated by two observations. The *ortho*

isopropyl groups of the NAr^{iPr} moiety are diastereotopic as a result of hindered rotation

around the N-C$_{ipso}$ bond. Secondly, the bulky H$_2$NAr^{iPr} group is readily ejected on treatment

with H$_2$Ntolyl to form (TTP)Zr(NHtolyl)[OC(=CH$_2$)(^{t}Bu)], **2b**. As expected, the reduced

steric congestion of the tolyl amido/enolate species facilitates the formation of complex **2** in

a substantially shorter time period (Scheme 1).

The formation of complex **2** presumably involves a variation of the generally

accepted aldol reaction mechanism (Scheme 2).[22] Presence of the strong nucleophile, NHAr,

causes a deviation from normal aldol condensation to form the unique chelated endiolate

product.[23]

Intractable mixtures were obtained from the addition of acetone to **1** or **2a**.

However, the reaction between (TTP)Zr(NHAr^{iPr})[OC(=CH$_2$)(^{t}Bu)] **2a** and 2-octanone

resulted in a new enediolate complex, (TTP)Zr[OC(^{t}Bu)CHC(hexyl)(Me)O]. Thus, this

synthetic methodology may be extended to other α-ketones.
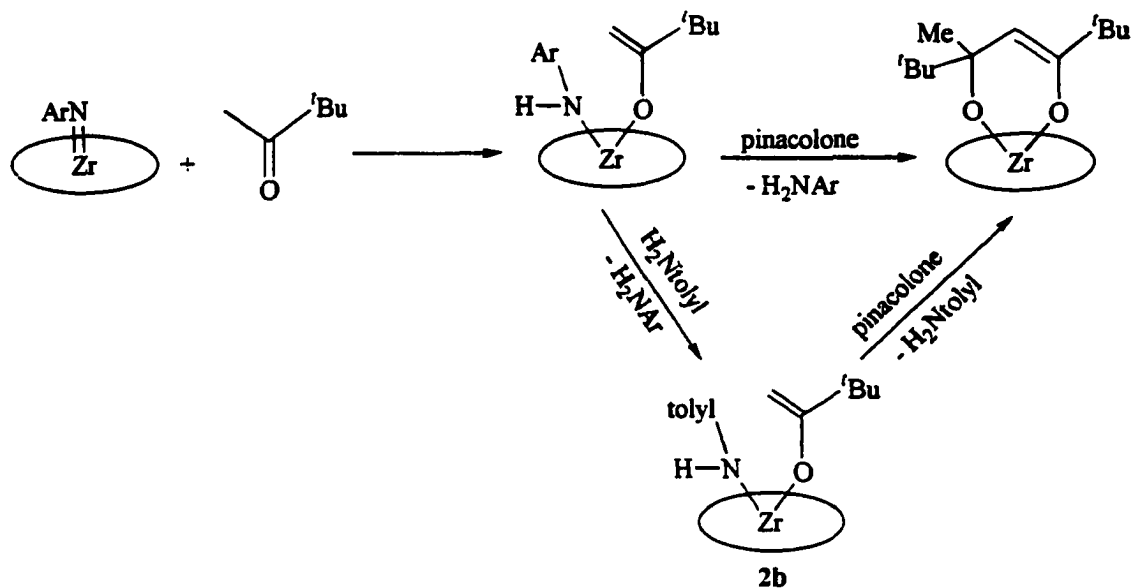
Scheme 1.
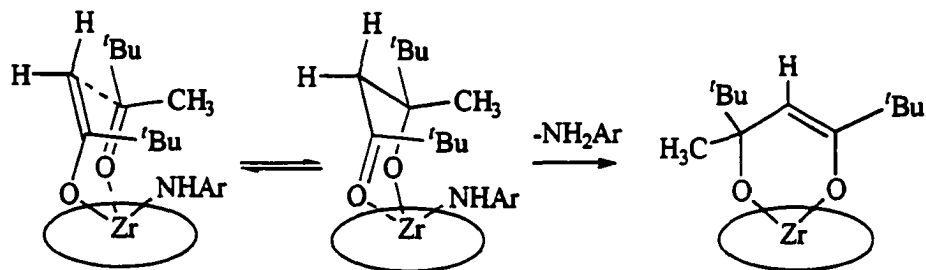
Scheme 2.

Complexes 4 and 5. An atom transfer route for the preparation of terminal oxo

species for titanium porphyrin complexes was extended to Zr for the production of complex

$4.^{24}$ Thus, the metathesis reaction between $(TTP)Zr=NAr^{Pr}$ and nitrosobenzene cleanly

produced the μ-oxo dimer, 4. The postulated transient monomeric oxo species, $(TTP)Zr=O$,

could not be trapped in the presence of THF or pyridine. Compound 4 is unreactive towards

'BuNCO, ketones, amines, and alcohols. This lack of reactivity appears to be based, in part, on steric factors since compound **4** is quickly hydrolyzed to compound **5**. Further reactivity of complex **5** was not observed in the presence of phenol, *t*-butyl amine, aniline, or $ZnEt_2$. A comparison of the structurally characterized oxygen bridged complexes $[(TPP)Hf]_2(\mu\text{-}OH)_2(\mu\text{-}O)$,[16c] $[(TPP)Zr]_2(\mu\text{-}OH)_2(\mu\text{-}O)$,[16b] and $\{[(OEP)Zr]_2(\mu\text{-}OH)_3\}(7,8\text{-}C_2B_9H_{12})$[16b] shows near eclipsing of a M-O bond with a M-N bond and the presence of eclipsed porphyrin rings. This has been attributed to $p\pi\text{-}/d\pi$-orbital interaction between the oxygen and the metal. Complex **5** does not possess eclipsed porphyrin rings. As the intramolecular steric properties of the tetraphenylporphyrin are expected to be equivalent to that of tetratolylporphyrin, $d\pi\text{-}p\pi$ interactions between the Zr and the O and N atoms are not readily apparent.[25]

It is interesting to note the structure of the only other known six-coordinate zirconium metalloporphyrin complex containing two O-bound ligands, $(OEP)Zr(O'Bu)_2$.[18e] First, the O-Zr-O angle of 90.08(9)° is rather large for this class of molecules.[26] Secondly, the zirconium atom lies remarkably far above the porphyrin plane (1.06 Å), which is in fact the furthest out of plane distance reported for six-coordinate zirconium metalloporphyrin complexes. Although these features were attributed primarily to the steric bulk of the O'Bu ligands, Zr-O π-bonding would most likely be enhanced by such an arrangement.[27] Zirconium lies further into the porphyrin plane and contains a O1-Zr1-O2 angle of 78.56(8)° in complex **4**. The presence of $d\pi\text{-}p\pi$ interactions are expected in complex **4** albeit somewhat diminished as evident in the relatively long Zr-O bonds, the acute O-Zr-O angle, and the staggered M-O/M-N bonds.

Conclusion

New examples of the novel reactivity possessed by zirconium and hafnium imido metalloporphyrin complexes have been demonstrated. These complexes mediate the stepwise coupling of pinacolone in the formation of an endiolate compound. Mixed ketone condensation products are also possible. Moreover, we have developed direct synthetic routes to zirconium metalloporphyrin complexes containing bridging oxygen ligands. (TTP)Zr=NAr^{Pr} undergoes metathesis with nitrosobenzene to produce the μ-oxo bridged dimer, [(TTP)ZrO]$_2$, **4**. The bis(μ-hydroxo)(μ-oxo) dimer, [(TTP)Zr]$_2$(μ-OH)$_2$(μ-O), **5**, is a hydrolysis product of complex **4**. Also of interest is the unique structural characteristic of staggered porphyrin rings found for complexes **4** and **5**. This is in marked contrast to the eclipsed conformers known for other Zr and Hf analogues.

References

1. Carney, M. J.; Walsh, P. J.; Hollander, F. J.; Bergman, R. G. *Organometallics* **1992**, *11*, 761 and references therein.

2. Howard, W. A; Trnka, T. M.; Waters, M.; Parkin, G. *J. Organomet. Chem.* **1997**, *528*, 95 and references therein.

3. Housmekerides, C. E.; Ramage, D. L.; Kretz, C. M.; Shontz, J. T.; Pilato, R. S.; Geoffroy, G. L.; Rheingold, A. L.; Haggerty, B. S. *Inorg. Chem.* **1992**, *31*, 4453.

4. Ryu, S. Whang, D.; Kim, H. J.; Kim, K.; Yoshida, M.; Hashimoto, K.; Tatsumi, K. *Inorg. Chem.* **1997**, *36*, 4607.

5. Berreau, L. M.; Young, V. G., Jr.; Woo, L. K. *Inorg. Chem.* **1995**, *34*, 527.

6. Gray, S. D.; Thorman, J. L.; Berreau, L. M.; Woo, L. K. *Inorg. Chem.* **1997**, *36*, 278.

7. Gray, S. D.; Thorman, J. L.; Adamian, V.; Kadish, K. M.; Woo, L. K. *Inorg. Chem.* **1998**, *37*, 1.

8. Thorman, J. L.; Guzei, I. A.; Young, V. G. Jr.; Woo, L. K. *Inorg. Chem.*, in press.

9. Gilman, H. *Organic Synthesis: Collective Volume I*; John Wiley & Sons: New York, 1932; pp. 448-452.

10. SHELXTL-Plus V5.0, Siemens Industrial Automation, Inc., Madison, WI.

11. All software and sources of the scattering factors are contained in the SHELXTL V5.10 program library. Sheldrick, G., Siemens XRD, Madison, WI.

12. The large ring current of the aromatic porphyrin macrocycle provides a useful means for identifying metal bound ligands through ^{1}H NMR. Upfield shifts of bound ligand protons are commonly 1 - 4 ppm from those of the free ligand. The ring current effects on the ^{13}C nuclei of metal bound ligands of metalloporphyrin complexes are shifted to a smaller degree which allows comparison of these resonances to those found in nonporphyrin metal analogues.

13. (a) Stack, J. G.; Doney, J. J.; Bergman, R. G.; Heathcock, C. H. *Organometallics* **1990**, *9*, 453 and references therein. (b) Wanat, R. A.; Collum, D. B. *Organometallics* **1986**, *5*, 120.

14. Conformational changes of the six-membered ring may serve as a possible source of disorder in the metallacycle as observed in the X-ray structure analysis.

15. (a) The bis(μ-oxo) complex was reported, but no details on characterization were provided: Sewchok, M. G.; Haushalter, R. C.; Merola, J. S. *Inorganica Chimica Acta*, **1988**, *144*, 47. (b) The unisolated octaethylporphyrin analogue of complex **4** has been characterized by ^{1}H NMR: Brand, H.; Arnold, J. *Organometallics* **1993**, *12*, 3655.

16. (a) Huhmann, J. L.; Corey, J. Y.; Rath, N. P.; Campana, C. F. *J. Organomet. Chem.* **1996**, *513*, 17. (b) Kim, H. J.; Whang, D.; Do, Y.; Kim, K. *Chem. Lett.* **1993**, 807. (c) Kim, H.; Whang, D.; Kim, K.; Do, Y. *Inorg. Chem.* **1993**, *32*, 360. (d) Ryu, S.; Whang, D.; Kim, J.; Yeo, W.; Kim, K. *J. Chem. Soc., Dalton Trans.* **1993**, 205. (e) Ryu, S.; Kim, J.; Yeo, H.; Kim, K. *Inorg. Chim. Acta* **1995**, *228*, 233.

17. Pertinent complexes with Zr-O bonds (Zr-O bond distance (Å), Zr-O-Zr bond angle (°)): (a) Cp$_2$Zr(OC(Me)$_2$C(TMS)C(TMS)] (1.936(2)) Rosenthal, U.; Ohff, A.; Baumann, W.; Tillack, A.; Gorls, H.; Burlakov, V. V.; Shur, V. B. *J. Organomet. Chem.* **1994**, *484*, 203. (b) Cp$_2$*Zr(OCH$_2$CH$_2$CH$_2$) (2.008(13)) Mashima, K.; Yamakawa, M.; Takaya, H. *J. Chem. Soc. Dalton Trans.* **1991**, 2851. (c) (Me$_4$taen)Zr(O'Bu)$_2$ (1.947 average) Black, D. G.; Jordan, R. F.; Rogers, R. D. *Inorg. Chem.* **1997**, *36*, 103. (d) Cp$_2$Zr(OPh)$_2$ (Zr-O = 2.008(14) average) Howard, W. A.; Trnka, T. M.; Parkin, G. *Inorg. Chem.* **1995**, *34*, 5900. (e) (OEP)Zr(O'Bu)$_2$ (1.948 average) Brand, H.; Arnold, J. *Organometallics* **1993**, *12*, 3655. (f)

Cp$_2$*Zr(OH)(OC('Bu)(CH$_2$)) (2.001(6) for OH, 2.006(5) for enolate) Ref. 2. (g) Cp$_2$*Zr(OH)(OC(Ph)(CH$_2$)) (2.010(2) for OH, 1.993(2) for enolate) Howard, W. A.; Parkin, G. *J. Am. Chem. Soc.* **1994**, *116*, 606. (h) Cp$_2$'Zr(O)(py) (1.804(4)) Howard, W. A; Waters, M.; Parkin, G. *J. Am. Chem. Soc.* **1993**, *115*, 4917. (i) [Cp$_2$ZrO]$_3$ (1.959(3), 142.5(2)) Fachinetti, G.; Floriani, C.; Chiesta-Villa, A.; Guastini, C. *J. Am. Chem. Soc.* **1979**, *101*, 1767. (j) [Cp$_2$ZrMe]$_2$O (1.948(1), 174.1) Hunter, W. E.; Hrncir, D. C.; Vann Bynum, R.; Penttila, R. A.; Atwood, J. L. *Organometallics* **1983**, *2*, 750. (k) [Cp$_2$ZrCl]$_2$O (1.94(5), 168.9(8)) Clarke, J. F.; Drew, M. G. B. *Acta. Crystallogr. B* **1974**, *30*, 2267. (l) [((TMS)$_2$N)$_2$ZrMe]$_2$O (1.950, 180.0) Planalp, R. P.; Andersen, R. A. *J. Am. Chem. Soc.* **1983**, *105*, 7774. (m) [Cp$_2$Zr(C(TMS)CH(TMS))]$_2$O (1.973(1)) Rosenthal, U.; Ohff, A.; Michalik, M.; Gorls, H.; Burlakov, V. V.; Shur, V. B. *Organometallics* **1993**, *12*, 5016. (n) [Cp$_2$Zr(triflate)]$_2$O (1.946(1), 175.6(5)) Calderazzo, F.; Englert, U.; Pampaloni, G.; Tripepi, G. *J. Organomet. Chem.* **1998**, *555*, 49. (o) [Cp$_2$Zr(SPh)]$_2$O (1.968(3), 165.8(2)) Petersen, J. L. *J. Organomet. Chem.* **1979**, *166*, 179. (p) [Cp$_2$Zr(NCO)]$_2$O (1.946(3), 165.7(2)) Klouras, N.; Tzavellas, N.; Raptopoulou, C. P. *Z. Anorg. Allg. Chem.* **1997**, *623*, 1027.

18. van der Waals radii: O (1.52 Å), N (1.55 Å); Porterfield, W. W. *Inorganic Chemistry*, 2nd ed.; Academic Press: San Deigo, CA, 1998; p 214.

19. Covalent radii estimates (Å): (a) O = 0.66; Jolly, W. L. *Modern Inorganic Chemistry*; McGraw-Hill: New York, 1984; p 52. (b) Zr = 1.48, O = 0.73; Ref. 19.

20. Jentzen, W.; Simpson, M. C.; Hobbs, J. D.; Song, X.; Ema, T.; Nelson, N. Y.; Medforth, C. J.; Smith, K. M.; Veyrat, M.; Mazzanti, M.; Ramasseul, R.; Marchon, J.-C.; Takeuchi, T.; Goddard, W. A., III.; Shelnutt, J. A. *J. Am. Chem. Soc.* **1995**, *117*, 11085.

21. (a) Walsh, P. J.; Hollander, F. J.; Bergman, R. G. *J. Am. Chem. Soc.* **1988**, *110*, 8729. (b) Cummins, C. C; Baxter, S. M.; Wolczanski, P. T. *J. Am. Chem. Soc.* **1988**, *110*, 8731. (c) Walsh, P. J.; Hollander, F. J.; Bergman, R. G. *Organometallics* **1993**, *12*, 3705. (d) Blake, A. J.; Mountford, P.; Nikonov, G. I.; Swallow, D. *J. Chem. Soc., Chem. Commun.* **1996**, 1835.

22. Yamago, S.; Machii, D.; Nakamura, E. *J. Org. Chem.* **1991**, *56*, 2098.

23. Aldol condensation reactions utilizing zirconium enolates have been well studied: Cozzi, P. G.; Veya, P.; Floriani, C.; Rotzinger, F. P.; Chiesi-Villa, A.; Rizzoli, C. *Organometallics*, **1995**, *14*, 4092 and references therein.

24. Thorman, J. L.; Woo, L. K. Manuscript in preparation.

25. Bottomley, F.; Sutin, L. *Adv. Organomet. Chem.* **1988**, *28*, 339.

26. Brand, H.; Arnold, J. *Coord. Chem. Rev.* **1995**, *140*, 137.

27. Tatsumi, K.; Hoffmann, R. *J. Am. Chem. Soc.* **1981**, *103*, 3328.

APPENDIX A

Table I. Crystal data and structure refinement for complex 2, (TTP)Zr[OC(^{t}Bu)CHC(^{t}Bu)(Me)O].

Empirical formula	$C_{76.50}H_{84}N_4O_2Zr$
Formula weight	1182.70
Temperature	173(2) K
Wavelength	0.71073 Å
Crystal system	Monoclinic
Space group	Cc
Unit cell dimensions	a = 21.8318(8) Å α = 90°.
	b = 20.7139(8) Å β = 112.624(1)°
	c = 15.7878(8) Å γ = 90°.
Volume	6590.2(5) Å^3
Z	4
Density (calculated)	1.192 Mg/m^3
Absorption coefficient	0.215 mm^{-1}
F(000)	2508
Crystal size	0.30 x 0.30 x 0.30 mm^3
Theta range for data collection	1.41 to 21.97°.
Index ranges	-22 ≤ h ≤ 22, 0 ≤ k ≤ 21, -16 ≤ l ≤ 16
Reflections collected	20673
Independent reflections	7601 [R(int) = 0.0337]
Completeness to θ = 21.97°	99.9 %
Absorption correction	Empirical with SADABS
Max. and min. transmission	0.9383 and 0.9383
Refinement method	Full-matrix least-squares on F^2
Data / restraints / parameters	7601 / 233 / 544
Goodness-of-fit on F^2	1.065
Final R indices [I>2σ(I)]	R1 = 0.0691, wR2 = 0.1909
R indices (all data)	R1 = 0.0828, wR2 = 0.2084
Largest diff. peak and hole	1.292 and -0.690 e.Å^{-3}

Table II. Atomic coordinates [x 10^4] and equivalent isotropic displacement parameters (Å^2x 10^3) for complex 2. U(eq) is defined as one third of the trace of the orthogonalized U_{ij} tensor.

Atom	x	y	z	U(eq)
Zr	1961(2)	6512(1)	4106(3)	26(1)
C(1)	1867(6)	6073(5)	5987(8)	25(2)
C(2)	1410(7)	6147(7)	6421(8)	39(3)
C(3)	793(7)	6118(7)	5723(8)	41(3)
C(4)	890(7)	6063(6)	4930(8)	29(3)
C(5)	388(7)	6007(7)	4039(8)	39(3)
C(6)	448(7)	5925(7)	3153(8)	36(3)
C(7)	-63(6)	5802(5)	2350(8)	29(3)
C(8)	216(7)	5795(6)	1694(8)	36(3)
C(9)	908(6)	5945(5)	2170(8)	25(2)
C(10)	1340(6)	6015(6)	1733(8)	30(3)
C(11)	2009(7)	6108(6)	2184(7)	30(3)
C(12)	2537(7)	6115(7)	1799(9)	37(3)
C(13)	3128(7)	6122(6)	2455(8)	38(3)
C(14)	3048(7)	6073(6)	3352(8)	30(3)
C(15)	3572(6)	5990(5)	4201(8)	23(2)
C(16)	3459(6)	5943(5)	4992(8)	20(2)
C(17)	4000(7)	5784(7)	5924(8)	44(4)
C(18)	3729(6)	5796(6)	6537(8)	32(3)
C(19)	3033(7)	5931(6)	6081(8)	35(3)
C(20)	2552(7)	6024(6)	6484(8)	29(3)
C(21)	-320(6)	5963(6)	4027(8)	33(3)
C(22)	-483(8)	5429(7)	4423(11)	52(3)
C(23)	-1142(8)	5378(7)	4403(13)	78(5)
C(24)	-1595(8)	5876(9)	3950(13)	72(5)
C(25)	-1421(7)	6368(7)	3548(11)	55(4)
C(26)	-760(7)	6414(7)	3576(10)	38(3)
C(27)	-2297(9)	5849(8)	3997(13)	82(5)
C(28)	1112(6)	6009(6)	732(8)	32(3)

Table II. (continued)

C(29)	615(8)	6490(5)	195(9)	31(3)
C(30)	349(7)	6466(5)	-778(9)	32(3)
C(31)	581(7)	5972(7)	-1228(8)	39(3)
C(32)	1055(6)	5565(6)	-705(8)	34(3)
C(33)	1295(6)	5572(6)	230(8)	36(3)
C(34)	250(8)	5975(7)	-2266(8)	55(4)
C(35)	4238(7)	5917(7)	4229(7)	40(3)
C(36)	4431(8)	5454(8)	3799(11)	59(4)
C(37)	5035(7)	5431(8)	3778(9)	69(4)
C(38)	5550(7)	5861(8)	4209(11)	59(4)
C(39)	5352(8)	6359(8)	4639(10)	63(4)
C(40)	4763(8)	6421(7)	4645(10)	42(3)
C(41)	6240(9)	5787(11)	4256(16)	122(8)
C(42)	2868(6)	6015(5)	7542(8)	27(3)
C(43)	2617(7)	5531(5)	7988(8)	31(3)
C(44)	2889(7)	5538(6)	8943(8)	36(3)
C(45)	3346(7)	6013(6)	9421(9)	39(3)
C(46)	3538(8)	6431(7)	8940(10)	52(4)
C(47)	3296(8)	6421(6)	8013(10)	43(4)
C(48)	3585(7)	5987(7)	10465(8)	50(4)
N(1)	1563(5)	6080(4)	5102(6)	24(2)
N(2)	1068(5)	5973(5)	3078(7)	31(2)
N(3)	2374(6)	6075(5)	3189(6)	31(2)
N(4)	2897(5)	6028(4)	5134(6)	22(2)
O(1)	1405(4)	7236(3)	3434(5)	56(2)
O(2)	2582(4)	7230(3)	4400(6)	66(2)
C(49)	492(12)	7895(8)	2046(8)	216(11)
C(50)	322(9)	8039(8)	3490(12)	197(10)
C(51)	830(6)	8910(4)	2917(8)	74(3)
C(52)	793(3)	8181(3)	3007(5)	41(2)
C(53)	1414(4)	7870(3)	3662(5)	47(2)

Table II. (continued)

C(54)	1908(4)	8194(4)	4291(5)	54(3)
C(55)	2502(5)	7808(5)	4870(10)	163(9)
C(56)	2673(13)	8021(12)	5859(10)	196(10)
C(57)	3164(4)	8147(5)	4909(7)	107(5)
C(58)	3180(11)	8005(8)	3972(8)	185(9)
C(59)	3752(7)	7808(6)	5633(8)	104(4)
C(60)	3249(8)	8871(5)	5076(9)	106(5)

Table III. Bond lengths [Å] and angles [°] for complex 2.

Zr-O(2)	1.945(7)	C(22)-C(23)	1.430(19)
Zr-O(1)	1.963(6)	C(23)-C(24)	1.42(2)
Zr-N(3)	2.177(9)	C(24)-C(25)	1.33(2)
Zr-N(1)	2.254(8)	C(24)-C(27)	1.563(18)
Zr-N(2)	2.290(10)	C(25)-C(26)	1.430(17)
Zr-N(4)	2.295(9)	C(28)-C(33)	1.361(14)
C(1)-N(1)	1.297(14)	C(28)-C(29)	1.477(17)
C(1)-C(20)	1.401(17)	C(29)-C(30)	1.420(16)
C(1)-C(2)	1.419(14)	C(30)-C(31)	1.444(16)
C(2)-C(3)	1.375(18)	C(31)-C(32)	1.343(17)
C(3)-C(4)	1.354(14)	C(31)-C(34)	1.516(16)
C(4)-N(1)	1.386(14)	C(32)-C(33)	1.362(16)
C(4)-C(5)	1.417(17)	C(35)-C(36)	1.333(18)
C(5)-C(6)	1.465(15)	C(35)-C(40)	1.503(19)
C(5)-C(21)	1.543(16)	C(36)-C(37)	1.331(18)
C(6)-C(7)	1.353(17)	C(37)-C(38)	1.39(2)
C(6)-N(2)	1.407(15)	C(38)-C(39)	1.39(2)
C(7)-C(8)	1.388(14)	C(38)-C(41)	1.49(2)
C(8)-C(9)	1.438(17)	C(39)-C(40)	1.297(19)
C(9)-N(2)	1.339(13)	C(42)-C(47)	1.266(17)
C(9)-C(10)	1.375(14)	C(42)-C(43)	1.448(14)
C(10)-C(11)	1.369(16)	C(43)-C(44)	1.392(15)
C(10)-C(28)	1.464(15)	C(44)-C(45)	1.397(18)
C(11)-N(3)	1.477(14)	C(45)-C(46)	1.322(18)
C(11)-C(12)	1.496(14)	C(45)-C(48)	1.527(15)
C(12)-C(13)	1.306(17)	C(46)-C(47)	1.351(18)
C(13)-C(14)	1.495(14)	O(1)-C(53)	1.360(2)
C(14)-N(3)	1.392(15)	O(2)-C(55)	1.454(2)
C(14)-C(15)	1.398(17)	C(49)-C(52)	1.523(7)
C(15)-C(16)	1.367(13)	C(50)-C(52)	1.524(7)
C(15)-C(35)	1.445(16)	C(51)-C(52)	1.523(7)

Table III. (continued)

C(16)-N(4)	1.342(13)	C(52)-C(53)	1.499(10)
C(16)-C(17)	1.527(16)	C(53)-C(54)	1.334(2)
C(17)-C(18)	1.314(15)	C(54)-C(55)	1.498(10)
C(18)-C(19)	1.435(17)	C(55)-C(56)	1.524(7)
C(19)-N(4)	1.422(13)	C(55)-C(57)	1.586(2)
C(19)-C(20)	1.434(14)	C(57)-C(60)	1.522(7)
C(20)-C(42)	1.543(15)	C(57)-C(59)	1.523(7)
C(21)-C(26)	1.332(18)	C(57)-C(58)	1.523(7)
C(21)-C(22)	1.382(18)		

O(2)-Zr-O(1)	76.9(3)	C(21)-C(26)-C(25)	118.7(13)
O(2)-Zr-N(3)	92.7(3)	C(33)-C(28)-C(10)	125.5(12)
O(1)-Zr-N(3)	106.6(3)	C(33)-C(28)-C(29)	115.5(10)
O(2)-Zr-N(1)	123.9(3)	C(10)-C(28)-C(29)	119.0(10)
O(1)-Zr-N(1)	110.9(3)	C(30)-C(29)-C(28)	120.1(10)
N(3)-Zr-N(1)	131.97(18)	C(29)-C(30)-C(31)	118.8(12)
O(2)-Zr-N(2)	150.1(3)	C(32)-C(31)-C(30)	118.4(11)
O(1)-Zr-N(2)	79.0(3)	C(32)-C(31)-C(34)	127.0(11)
N(3)-Zr-N(2)	77.5(3)	C(30)-C(31)-C(34)	114.6(12)
N(1)-Zr-N(2)	81.3(3)	C(31)-C(32)-C(33)	123.0(11)
O(2)-Zr-N(4)	79.4(3)	C(28)-C(33)-C(32)	124.1(12)
O(1)-Zr-N(4)	155.9(3)	C(36)-C(35)-C(15)	124.9(12)
N(3)-Zr-N(4)	78.7(3)	C(36)-C(35)-C(40)	112.6(12)
N(1)-Zr-N(4)	79.1(3)	C(15)-C(35)-C(40)	122.0(11)
N(2)-Zr-N(4)	124.85(19)	C(37)-C(36)-C(35)	123.2(15)
N(1)-C(1)-C(20)	126.8(10)	C(36)-C(37)-C(38)	125.9(14)
N(1)-C(1)-C(2)	110.8(11)	C(37)-C(38)-C(39)	111.7(13)
C(20)-C(1)-C(2)	122.4(10)	C(37)-C(38)-C(41)	124.8(16)
C(3)-C(2)-C(1)	105.3(10)	C(39)-C(38)-C(41)	123.4(16)
C(4)-C(3)-C(2)	106.9(10)	C(40)-C(39)-C(38)	124.9(16)

Table III. (continued)

C(3)-C(4)-N(1)	110.4(10)	C(39)-C(40)-C(35)	121.3(14)
C(3)-C(4)-C(5)	126.0(11)	C(47)-C(42)-C(43)	120.5(11)
N(1)-C(4)-C(5)	123.6(9)	C(47)-C(42)-C(20)	123.3(11)
C(4)-C(5)-C(6)	129.7(11)	C(43)-C(42)-C(20)	116.2(10)
C(4)-C(5)-C(21)	114.0(10)	C(44)-C(43)-C(42)	115.8(11)
C(6)-C(5)-C(21)	116.0(11)	C(43)-C(44)-C(45)	120.8(11)
C(7)-C(6)-N(2)	114.1(9)	C(46)-C(45)-C(44)	117.9(11)
C(7)-C(6)-C(5)	124.9(11)	C(46)-C(45)-C(48)	126.3(13)
N(2)-C(6)-C(5)	121.0(11)	C(44)-C(45)-C(48)	115.8(12)
C(6)-C(7)-C(8)	105.0(10)	C(45)-C(46)-C(47)	122.4(13)
C(7)-C(8)-C(9)	106.4(10)	C(42)-C(47)-C(46)	122.6(13)
N(2)-C(9)-C(10)	125.8(11)	C(1)-N(1)-C(4)	106.0(8)
N(2)-C(9)-C(8)	111.0(9)	C(1)-N(1)-Zr	125.5(8)
C(10)-C(9)-C(8)	123.1(10)	C(4)-N(1)-Zr	122.5(7)
C(11)-C(10)-C(9)	123.7(10)	C(9)-N(2)-C(6)	102.8(10)
C(11)-C(10)-C(28)	114.5(9)	C(9)-N(2)-Zr	125.5(7)
C(9)-C(10)-C(28)	121.8(11)	C(6)-N(2)-Zr	124.0(7)
C(10)-C(11)-N(3)	125.3(9)	C(14)-N(3)-C(11)	107.1(8)
C(10)-C(11)-C(12)	128.7(10)	C(14)-N(3)-Zr	123.8(7)
N(3)-C(11)-C(12)	104.7(10)	C(11)-N(3)-Zr	120.3(8)
C(13)-C(12)-C(11)	110.9(10)	C(16)-N(4)-C(19)	108.8(9)
C(12)-C(13)-C(14)	108.1(10)	C(16)-N(4)-Zr	124.2(6)
N(3)-C(14)-C(15)	126.5(10)	C(19)-N(4)-Zr	125.1(7)
N(3)-C(14)-C(13)	108.9(10)	C(53)-O(1)-Zr	130.7(6)
C(15)-C(14)-C(13)	124.4(11)	C(55)-O(2)-Zr	122.8(7)
C(16)-C(15)-C(14)	121.0(11)	C(53)-C(52)-C(51)	115.1(7)
C(16)-C(15)-C(35)	119.8(10)	C(53)-C(52)-C(49)	116.6(11)
C(14)-C(15)-C(35)	119.0(9)	C(51)-C(52)-C(49)	108.1(5)
N(4)-C(16)-C(15)	130.0(11)	C(53)-C(52)-C(50)	100.2(10)
N(4)-C(16)-C(17)	106.6(8)	C(51)-C(52)-C(50)	108.0(5)
C(15)-C(16)-C(17)	123.5(10)	C(49)-C(52)-C(50)	108.0(5)

Table III. (continued)

C(18)-C(17)-C(16)	107.7(11)	C(54)-C(53)-O(1)	127.5(8)
C(17)-C(18)-C(19)	108.9(10)	C(54)-C(53)-C(52)	123.7(7)
N(4)-C(19)-C(20)	123.6(11)	O(1)-C(53)-C(52)	108.4(6)
N(4)-C(19)-C(18)	107.9(9)	C(53)-C(54)-C(55)	116.6(8)
C(20)-C(19)-C(18)	128.2(10)	O(2)-C(55)-C(54)	112.0(10)
C(1)-C(20)-C(19)	124.6(10)	O(2)-C(55)-C(56)	137.0(16)
C(1)-C(20)-C(42)	122.9(9)	C(54)-C(55)-C(56)	106.5(12)
C(19)-C(20)-C(42)	112.4(10)	O(2)-C(55)-C(57)	95.6(7)
C(26)-C(21)-C(22)	123.1(12)	C(54)-C(55)-C(57)	110.4(10)
C(26)-C(21)-C(5)	118.5(11)	C(56)-C(55)-C(57)	88.3(13)
C(22)-C(21)-C(5)	118.2(11)	C(60)-C(57)-C(59)	108.2(5)
C(21)-C(22)-C(23)	118.7(14)	C(60)-C(57)-C(58)	108.2(5)
C(24)-C(23)-C(22)	117.3(13)	C(59)-C(57)-C(58)	108.2(5)
C(25)-C(24)-C(23)	121.7(13)	C(60)-C(57)-C(55)	119.5(9)
C(25)-C(24)-C(27)	121.0(15)	C(59)-C(57)-C(55)	108.6(10)
C(23)-C(24)-C(27)	117.2(13)	C(58)-C(57)-C(55)	103.8(12)
C(24)-C(25)-C(26)	120.4(14)		

Table IV. Crystal data and structure refinement for complex 4, [(TTP)ZrO]$_2$.

Empirical formula	$C_{110}H_{88}N_8O_2Zr_2$
Formula weight	1736.32
Temperature	173(2) K
Wavelength	0.71073 Å
Crystal system	Monoclinic
Space group	C2/c
Unit cell dimensions	$a = 31.8540(16)$ Å, $\alpha = 90°$.
	$b = 16.7937(8)$ Å, $\beta = 117.2540(10)°$.
	$c = 18.8770(9)$ Å, $\gamma = 90°$.
Volume	8977.1(8) Å^3
Z	4
Density (calculated)	1.285 Mg/m^3
Absorption coefficient	0.289 mm^{-1}
F(000)	3600
Crystal size	0.21 x 0.40 x 0.42 mm^3
Theta range for data collection	2.48 to 28.32°.
Index ranges	$-42 \le h \le 37, 0 \le k \le 22, 0 \le l \le 25$
Reflections collected	53684
Independent reflections	10734 [R(int) = 0.0687]
Completeness to theta = 28.32°	96.0%
Refinement method	Full-matrix least-squares on F^2
Data / restraints / parameters	10734 / 0 / 488
Goodness-of-fit on F^2	1.007
Final R indices [I>2σ(I)]	R1 = 0.0461, wR2 = 0.1068
R indices (all data)	R1 = 0.0848, wR2 = 0.1133
Largest diff. peak and hole	0.587 and -0.435 eÅ^3

Table V. Atomic coordinates (x 10^4) and equivalent isotropic displacement parameters (Å^2 x 10^3) for complex **4**. U(eq) is defined as one third of the trace of the orthogonalized U_{ij} tensor.

Atom	x	y	z	U(eq)
Zr(1)	49(1)	8424(1)	3345(1)	21(1)
O(1)	0	9165(2)	2500	40(1)
O(2)	0	7676(2)	2500	40(1)
N(1)	-521(1)	9041(1)	3525(1)	26(1)
N(2)	493(1)	9406(1)	4191(1)	24(1)
N(3)	689(1)	7759(1)	4211(1)	25(1)
N(4)	-327(1)	7396(1)	3607(1)	23(1)
C(1)	-969(1)	8776(2)	3340(2)	30(1)
C(2)	-1269(1)	9445(2)	3251(2)	41(1)
C(3)	-1004(1)	10106(2)	3388(2)	40(1)
C(4)	-537(1)	9866(2)	3567(2)	28(1)
C(5)	-154(1)	10386(1)	3776(2)	25(1)
C(6)	320(1)	10172(1)	4080(2)	24(1)
C(7)	704(1)	10725(2)	4344(2)	32(1)
C(8)	1109(1)	10298(2)	4634(2)	34(1)
C(9)	978(1)	9464(2)	4545(2)	26(1)
C(10)	1291(1)	8819(2)	4774(2)	27(1)
C(11)	1151(1)	8019(2)	4637(2)	28(1)
C(12)	1457(1)	7341(2)	4930(2)	40(1)
C(13)	1188(1)	6679(2)	4685(2)	36(1)
C(14)	706(1)	6932(2)	4239(2)	25(1)
C(15)	317(1)	6412(1)	3948(2)	23(1)
C(16)	-159(1)	6628(1)	3666(2)	23(1)
C(17)	-543(1)	6078(2)	3439(2)	29(1)
C(18)	-939(1)	6508(2)	3261(2)	33(1)
C(19)	-804(1)	7332(2)	3366(2)	28(1)
C(20)	-1108(1)	7976(2)	3245(2)	29(1)
C(21)	-282(1)	11253(2)	3681(2)	25(1)
C(22)	-223(1)	11715(2)	4323(2)	39(1)

Table V. (continued)

C(23)	-386(1)	12494(2)	4210(2)	43(1)
C(24)	-607(1)	12834(2)	3473(2)	35(1)
C(25)	-663(1)	12371(2)	2837(2)	53(1)
C(26)	-500(1)	11593(2)	2938(2)	47(1)
C(27)	-784(1)	13681(2)	3365(2)	58(1)
C(28)	1807(1)	9003(2)	5199(2)	31(1)
C(29)	2116(1)	8766(2)	4905(2)	40(1)
C(30)	2587(1)	8977(2)	5295(2)	46(1)
C(31)	2768(1)	9429(2)	5987(2)	43(1)
C(32)	2463(1)	9651(2)	6288(2)	42(1)
C(33)	1993(1)	9444(2)	5905(2)	36(1)
C(34)	3285(1)	9668(2)	6395(2)	66(1)
C(35)	425(1)	5537(1)	4007(2)	25(1)
C(36)	525(1)	5157(2)	3465(2)	45(1)
C(37)	623(1)	4347(2)	3527(2)	55(1)
C(38)	615(1)	3891(2)	4122(2)	34(1)
C(39)	507(1)	4274(2)	4654(2)	55(1)
C(40)	418(1)	5083(2)	4602(2)	50(1)
C(41)	721(1)	3005(2)	4196(2)	53(1)
C(42)	-1617(1)	7799(2)	2993(2)	35(1)
C(43)	-1820(1)	7970(2)	3483(2)	50(1)
C(44)	-2299(1)	7807(2)	3244(3)	64(1)
C(45)	-2576(1)	7468(2)	2508(3)	65(1)
C(46)	-2376(1)	7302(2)	2008(2)	61(1)
C(47)	-1902(1)	7471(2)	2246(2)	46(1)
C(48)	-3095(1)	7273(3)	2252(3)	97(2)

Table VI. Bond lengths [Å] and angles [°] for complex 4.

Zr(1)-O(1)	1.9719(16)	C(15)-C(35)	1.501(3)
Zr(1)-O(2)	1.9791(16)	C(16)-C(17)	1.433(3)
Zr(1)-N(3)	2.241(2)	C(17)-C(18)	1.354(4)
Zr(1)-N(1)	2.246(2)	C(18)-C(19)	1.436(3)
Zr(1)-N(2)	2.280(2)	C(19)-C(20)	1.399(3)
Zr(1)-N(4)	2.280(2)	C(20)-C(42)	1.495(4)
Zr(1)-Zr(1)#1	3.0584(5)	C(21)-C(26)	1.372(4)
O(1)-Zr(1)#1	1.9719(16)	C(21)-C(22)	1.378(4)
O(2)-Zr(1)#1	1.9791(16)	C(22)-C(23)	1.388(4)
N(1)-C(1)	1.379(3)	C(23)-C(24)	1.364(4)
N(1)-C(4)	1.390(3)	C(24)-C(25)	1.371(4)
N(2)-C(6)	1.377(3)	C(24)-C(27)	1.509(4)
N(2)-C(9)	1.379(3)	C(25)-C(26)	1.386(4)
N(3)-C(11)	1.386(3)	C(28)-C(29)	1.392(4)
N(3)-C(14)	1.390(3)	C(28)-C(33)	1.397(4)
N(4)-C(19)	1.378(3)	C(29)-C(30)	1.382(4)
N(4)-C(16)	1.382(3)	C(30)-C(31)	1.387(4)
C(1)-C(20)	1.400(4)	C(31)-C(32)	1.382(4)
C(1)-C(2)	1.436(4)	C(31)-C(34)	1.517(4)
C(2)-C(3)	1.347(4)	C(32)-C(33)	1.377(4)
C(3)-C(4)	1.423(4)	C(35)-C(36)	1.361(4)
C(4)-C(5)	1.402(3)	C(35)-C(40)	1.367(4)
C(5)-C(6)	1.397(3)	C(36)-C(37)	1.389(4)
C(5)-C(21)	1.500(3)	C(37)-C(38)	1.370(4)
C(6)-C(7)	1.432(3)	C(38)-C(39)	1.363(4)
C(7)-C(8)	1.352(4)	C(38)-C(41)	1.517(4)
C(8)-C(9)	1.449(3)	C(39)-C(40)	1.381(4)
C(9)-C(10)	1.400(3)	C(42)-C(43)	1.380(4)
C(10)-C(11)	1.402(3)	C(42)-C(47)	1.394(4)
C(10)-C(28)	1.492(3)	C(43)-C(44)	1.406(4)
C(11)-C(12)	1.435(3)	C(44)-C(45)	1.383(5)

Table VI. (continued)

C(12)-C(13)	1.350(4)	C(45)-C(46)	1.389(5)
C(13)-C(14)	1.435(4)	C(45)-C(48)	1.530(4)
C(14)-C(15)	1.405(3)	C(46)-C(47)	1.393(4)
C(15)-C(16)	1.407(3)		
O(1)-Zr(1)-O(2)	78.56(8)	C(13)-C(12)-C(11)	108.0(2)
O(1)-Zr(1)-N(3)	127.83(6)	C(12)-C(13)-C(14)	107.3(2)
O(2)-Zr(1)-N(3)	88.92(6)	N(3)-C(14)-C(15)	126.4(2)
O(1)-Zr(1)-N(1)	93.46(7)	N(3)-C(14)-C(13)	109.3(2)
O(2)-Zr(1)-N(1)	130.06(6)	C(15)-C(14)-C(13)	124.0(2)
N(3)-Zr(1)-N(1)	130.35(8)	C(14)-C(15)-C(16)	126.4(2)
O(1)-Zr(1)-N(2)	84.48(7)	C(14)-C(15)-C(35)	116.7(2)
O(2)-Zr(1)-N(2)	144.90(6)	C(16)-C(15)-C(35)	116.8(2)
N(3)-Zr(1)-N(2)	77.56(7)	N(4)-C(16)-C(15)	125.5(2)
N(1)-Zr(1)-N(2)	81.08(7)	N(4)-C(16)-C(17)	109.4(2)
O(1)-Zr(1)-N(4)	142.98(6)	C(15)-C(16)-C(17)	124.9(2)
O(2)-Zr(1)-N(4)	80.74(7)	C(18)-C(17)-C(16)	107.5(2)
N(3)-Zr(1)-N(4)	81.78(7)	C(17)-C(18)-C(19)	107.2(2)
N(1)-Zr(1)-N(4)	77.03(7)	N(4)-C(19)-C(20)	124.8(2)
N(2)-Zr(1)-N(4)	127.86(7)	N(4)-C(19)-C(18)	109.5(2)
O(1)-Zr(1)-Zr(1)#1	39.15(6)	C(20)-C(19)-C(18)	125.7(2)
O(2)-Zr(1)-Zr(1)#1	39.41(6)	C(19)-C(20)-C(1)	124.4(2)
N(3)-Zr(1)-Zr(1)#1	112.65(6)	C(19)-C(20)-C(42)	117.8(2)
N(1)-Zr(1)-Zr(1)#1	116.98(6)	C(1)-C(20)-C(42)	117.8(2)
N(2)-Zr(1)-Zr(1)#1	117.70(5)	C(26)-C(21)-C(22)	117.8(2)
N(4)-Zr(1)-Zr(1)#1	114.42(5)	C(26)-C(21)-C(5)	120.6(2)
Zr(1)#1-O(1)-Zr(1)	101.70(12)	C(22)-C(21)-C(5)	121.4(2)
Zr(1)#1-O(2)-Zr(1)	101.19(11)	C(21)-C(22)-C(23)	120.3(3)
C(1)-N(1)-C(4)	105.9(2)	C(24)-C(23)-C(22)	122.2(3)
C(1)-N(1)-Zr(1)	128.80(17)	C(23)-C(24)-C(25)	117.1(3)
C(4)-N(1)-Zr(1)	121.58(17)	C(23)-C(24)-C(27)	121.2(3)

Table VI. (continued)

C(6)-N(2)-C(9)	106.7(2)	C(25)-C(24)-C(27)	121.7(3)
C(6)-N(2)-Zr(1)	119.57(16)	C(24)-C(25)-C(26)	121.6(3)
C(9)-N(2)-Zr(1)	126.09(16)	C(21)-C(26)-C(25)	121.0(3)
C(11)-N(3)-C(14)	106.3(2)	C(29)-C(28)-C(33)	117.6(3)
C(11)-N(3)-Zr(1)	129.48(16)	C(29)-C(28)-C(10)	122.0(3)
C(14)-N(3)-Zr(1)	122.21(16)	C(33)-C(28)-C(10)	120.4(2)
C(19)-N(4)-C(16)	106.3(2)	C(30)-C(29)-C(28)	120.6(3)
C(19)-N(4)-Zr(1)	126.68(16)	C(29)-C(30)-C(31)	121.5(3)
C(16)-N(4)-Zr(1)	120.17(15)	C(32)-C(31)-C(30)	117.9(3)
N(1)-C(1)-C(20)	125.0(2)	C(32)-C(31)-C(34)	121.5(3)
N(1)-C(1)-C(2)	109.6(2)	C(30)-C(31)-C(34)	120.6(3)
C(20)-C(1)-C(2)	125.4(2)	C(33)-C(32)-C(31)	121.0(3)
C(3)-C(2)-C(1)	107.2(2)	C(32)-C(33)-C(28)	121.3(3)
C(2)-C(3)-C(4)	108.0(2)	C(36)-C(35)-C(40)	117.0(3)
N(1)-C(4)-C(5)	125.8(2)	C(36)-C(35)-C(15)	121.8(2)
N(1)-C(4)-C(3)	109.4(2)	C(40)-C(35)-C(15)	121.2(2)
C(5)-C(4)-C(3)	124.8(2)	C(35)-C(36)-C(37)	121.1(3)
C(6)-C(5)-C(4)	126.4(2)	C(38)-C(37)-C(36)	122.0(3)
C(6)-C(5)-C(21)	118.9(2)	C(39)-C(38)-C(37)	116.5(3)
C(4)-C(5)-C(21)	114.7(2)	C(39)-C(38)-C(41)	121.1(3)
N(2)-C(6)-C(5)	125.8(2)	C(37)-C(38)-C(41)	122.5(3)
N(2)-C(6)-C(7)	109.6(2)	C(38)-C(39)-C(40)	121.6(3)
C(5)-C(6)-C(7)	124.6(2)	C(35)-C(40)-C(39)	121.8(3)
C(8)-C(7)-C(6)	107.4(2)	C(43)-C(42)-C(47)	118.1(3)
C(7)-C(8)-C(9)	107.3(2)	C(43)-C(42)-C(20)	121.1(3)
N(2)-C(9)-C(10)	125.2(2)	C(47)-C(42)-C(20)	120.7(3)
N(2)-C(9)-C(8)	108.8(2)	C(42)-C(43)-C(44)	121.2(3)
C(10)-C(9)-C(8)	125.9(2)	C(45)-C(44)-C(43)	120.1(4)
C(9)-C(10)-C(11)	124.2(2)	C(44)-C(45)-C(46)	119.1(3)
C(9)-C(10)-C(28)	117.3(2)	C(44)-C(45)-C(48)	120.4(4)
C(11)-C(10)-C(28)	118.5(2)	C(46)-C(45)-C(48)	120.5(4)

Table VI. (continued)

N(3)-C(11)-C(10)	125.0(2)	C(45)-C(46)-C(47)	120.4(3)
N(3)-C(11)-C(12)	109.1(2)	C(46)-C(47)-C(42)	121.0(3)
C(10)-C(11)-C(12)	125.9(2)		

Table VII. Crystal data, data collection, and solution and refinement for complex 5, $[(TTP)Zr]_2(\mu\text{-}O)(\mu\text{-}OH)_2$.

Empirical formula	$C_{57}H_{46}N_4O_{1.50}Zr$
Crystal Habit, color	Plate, Red
Crystal size	0.35 x 0.26 x 0.13 mm
Crystal system	Monoclinic
Space group	C2/c
	$a = 32.0930(7)$ Å $\qquad \alpha = 90°$
	$b = 16.8621(3)$ Å $\qquad \beta = 118.930(1)°$
	$c = 19.0706(4)$ Å $\qquad \gamma = 90°$
Volume	9032.3(3) Å^3
Z	8
Formula weight	902.20
Density (calculated)	1.327 Mg/m^3
Absorption coefficient	0.291 mm
F(000)	3744
Diffractometer	Siemens SMART Platform CCD
Wavelength	0.71073 Å
Temperature	173(2) K
θ range for data collection	1.41 to 25.07°
Index ranges	$-38 \le h \le 33, 0 \le k \le 20, 0 \le l \le 22$
Reflections collected	22019
Independent reflections	7894 ($R_{int} = 0.0434$)
System used	SHELXTL-V5.0
Solution	Direct methods
Refinement method	Full-matrix least-squares on F^2
Weighting scheme	$W = [\sigma^2(F_o^2) + (AP)^2 + (BP)]^{-1}$, where $P = (F_o^2 + 2Fc^2))/3$, A = 0.0793, and B = 12.7127.
Absorption correction	SADABS (Sheldrick, 1996)
Max. and min. transmission	1.0000 and 0.716
Data / restraints / parameters	7891 / 48 / 583
R indices (I>2σ(I) = 5875)	R1 = 0.0553, wR2 = 0.1348
R indices (all data)	R1 = 0.0840, wR2 = 0.1526
Goodness-of-fit on F^2	1.030
Largest diff. peak and hole	0.855 and -0.828 eÅ^{-3}

Table VIII. Atomic coordinates [x 10^4] and equivalent isotropic displacement parameters [$Å^2$ x 10^3] for complex 5.

Atom	x	y	z	U(eq)	SOF
Zr(1)	33(1)	8483(1)	8328(1)	24(1)	1
O(1)	0	7574(2)	7500	48(1)	1
O(2)	-335(2)	8988(4)	7258(2)	39(2)	0.50
O(3)	536(2)	8668(4)	7888(2)	36(2)	0.50
N(1)	-316(1)	7434(2)	8607(2)	28(1)	1
N(2)	-514(1)	9086(2)	8585(2)	28(1)	1
N(3)	471(1)	9450(2)	9198(2)	30(1)	1
N(4)	683(1)	7788(2)	9235(2)	27(1)	1
C(1)	-150(1)	6660(2)	8682(2)	28(1)	1
C(2)	-538(1)	6120(2)	8440(2)	34(1)	1
C(3)	-935(2)	6547(2)	8241(2)	35(1)	1
C(4)	-799(1)	7373(2)	8348(2)	30(1)	1
C(5)	-1107(1)	8005(2)	8227(2)	31(1)	1
C(6)	-964(1)	8807(2)	8361(2)	32(1)	1
C(7)	-1277(2)	9455(2)	8247(3)	46(1)	1
C(8)	-1020(2)	10129(2)	8397(3)	45(1)	1
C(9)	-546(1)	9904(2)	8605(2)	31(1)	1
C(10)	-172(1)	10438(2)	8801(2)	28(1)	1
C(11)	303(1)	10222(2)	9100(2)	30(1)	1
C(12)	695(2)	10765(2)	9375(3)	42(1)	1
C(13)	1095(2)	10337(2)	9645(3)	42(1)	1
C(14)	961(1)	9509(2)	9546(2)	33(1)	1
C(15)	1277(1)	8868(2)	9756(2)	32(1)	1
C(16)	1141(1)	8059(2)	9626(2)	30(1)	1
C(17)	1467(2)	7404(2)	9909(3)	41(1)	1
C(18)	1203(2)	6736(2)	9686(3)	38(1)	1
C(19)	715(1)	6968(2)	9269(2)	30(1)	1
C(20)	329(1)	6442(2)	8981(2)	28(1)	1
C(21)	-1619(2)	7821(2)	7953(3)	37(1)	1
C(22)	-1822(2)	7976(3)	8438(3)	49(1)	1

Table VIII. (continued)

C(23)	-2295(2)	7793(3)	8177(3)	57(1)	1
C(24)	-2576(2)	7441(3)	7431(3)	53(1)	1
C(25)	-2370(2)	7290(3)	6957(3)	48(1)	1
C(26)	-1903(2)	7477(2)	7203(3)	41(1)	1
C(27)	-3090(2)	7217(4)	7168(4)	74(2)	1
C(28)	-304(1)	11298(2)	8681(2)	29(1)	1
C(29)	-267(2)	11765(2)	9294(3)	49(1)	1
C(30)	-421(2)	12549(2)	9159(3)	51(1)	1
C(31)	-610(2)	12885(2)	8418(3)	40(1)	1
C(32)	-644(2)	12408(3)	7804(3)	73(2)	1
C(33)	-493(2)	11632(3)	7931(3)	65(2)	1
C(34)	-783(2)	13734(3)	8272(3)	62(2)	1
C(35)	1798(1)	9064(2)	10173(2)	34(1)	1
C(36)	2006(2)	9460(2)	10903(3)	41(1)	1
C(37)	2482(2)	9669(3)	11276(3)	48(1)	1
C(38)	2765(2)	9490(3)	10941(3)	48(1)	1
C(39)	2559(2)	9082(3)	10219(3)	52(1)	1
C(40)	2085(2)	8878(3)	9840(3)	44(1)	1
C(41)	3290(2)	9721(3)	11349(4)	72(2)	1
C(42)	435(1)	5570(2)	9042(2)	32(1)	1
C(43)	412(2)	5110(3)	9627(3)	68(2)	1
C(44)	509(2)	4302(3)	9685(3)	73(2)	1
C(45)	630(2)	3931(2)	9183(3)	41(1)	1
C(46)	635(2)	4375(3)	8600(3)	62(2)	1
C(47)	536(2)	5182(2)	8522(3)	54(1)	1
C(48)	742(2)	3049(3)	9271(4)	62(2)	1
C(49)	-3169(2)	9269(4)	11175(5)	93(2)	1
C(50)	-2705(2)	9215(4)	11308(4)	87(2)	1
C(51)	-2412(2)	9869(4)	11566(4)	84(2)	1
C(52)	-2583(2)	10569(4)	11696(4)	81(2)	1
C(53)	-3048(2)	10617(3)	11550(4)	79(2)	1

Table VIII. (continued)

C(54)	-3338(2)	9965(4)	11292(4)	89(2)	1
C(55)	-2048(5)	7825(10)	10425(8)	200(6)	1
C(56)	-2427(6)	8300(9)	9964(9)	187(6)	1
C(57)	-2882(6)	7979(10)	9555(9)	195(7)	1

Table IX. Bond lengths [Å] and angles [°] for complex 5.

Zr(1)-O(2)	1.988(4)	C(5)-C(21)	1.497(6)
Zr(1)-O(2)#1	1.990(4)	C(6)-C(7)	1.426(5)
Zr(1)-O(1)	2.166(3)	C(7)-C(8)	1.350(6)
Zr(1)-O(3)#1	2.169(5)	C(8)-C(9)	1.427(6)
Zr(1)-O(3)	2.171(5)	C(9)-C(10)	1.400(5)
Zr(1)-N(3)	2.266(3)	C(10)-C(11)	1.392(5)
Zr(1)-N(2)	2.279(3)	C(10)-C(28)	1.498(5)
Zr(1)-N(4)	2.286(3)	C(11)-C(12)	1.435(6)
Zr(1)-N(1)	2.291(3)	C(12)-C(13)	1.339(6)
Zr(1)-Zr(1)#1	3.0600(7)	C(13)-C(14)	1.446(5)
O(1)-Zr(1)#1	2.166(3)	C(14)-C(15)	1.402(5)
O(2)-O(3)#1	0.782(7)	C(15)-C(16)	1.417(5)
O(2)-Zr(1)#1	1.990(4)	C(15)-C(35)	1.501(5)
O(3)-O(2)#1	0.781(7)	C(16)-C(17)	1.434(5)
O(3)-Zr(1)#1	2.169(5)	C(17)-C(18)	1.349(6)
N(1)-C(4)	1.383(5)	C(18)-C(19)	1.427(5)
N(1)-C(1)	1.390(4)	C(19)-C(20)	1.402(5)
N(2)-C(6)	1.376(5)	C(20)-C(42)	1.502(5)
N(2)-C(9)	1.384(5)	C(21)-C(22)	1.389(6)
N(3)-C(14)	1.383(5)	C(21)-C(26)	1.397(6)
N(3)-C(11)	1.386(4)	C(22)-C(23)	1.384(7)
N(4)-C(16)	1.367(5)	C(23)-C(24)	1.396(7)
N(4)-C(19)	1.385(4)	C(24)-C(25)	1.379(7)
C(1)-C(20)	1.404(5)	C(24)-C(27)	1.521(7)
C(1)-C(2)	1.428(5)	C(25)-C(26)	1.373(6)
C(2)-C(3)	1.350(6)	C(28)-C(29)	1.367(6)
C(3)-C(4)	1.445(5)	C(28)-C(33)	1.375(6)
C(4)-C(5)	1.394(5)	C(29)-C(30)	1.390(6)
C(5)-C(6)	1.411(5)		

Table IX. (continued)

C(30)-C(31)	1.363(6)	C(45)-C(46)	1.347(6)
C(31)-C(32)	1.380(6)	C(45)-C(48)	1.520(6)
C(31)-C(34)	1.511(6)	C(46)-C(47)	1.389(6)
C(32)-C(33)	1.376(6)	C(49)-C(54)	1.357(8)
C(35)-C(40)	1.382(6)	C(49)-C(50)	1.386(8)
C(35)-C(36)	1.391(6)	C(50)-C(51)	1.375(8)
C(36)-C(37)	1.383(6)	C(51)-C(52)	1.373(8)
C(37)-C(38)	1.372(6)	C(52)-C(53)	1.381(8)
C(38)-C(39)	1.387(7)	C(53)-C(54)	1.370(8)
C(38)-C(41)	1.525(6)	C(55)-C(56)	1.363(13)
C(39)-C(40)	1.375(6)	C(55)-C(57)#2	1.38(2)
C(42)-C(47)	1.352(6)	C(56)-C(57)	1.39(2)
C(42)-C(43)	1.390(6)	C(57)-C(55)#2	1.38(2)
C(43)-C(44)	1.390(6)		
C(44)-C(45)	1.350(6)		

O(2)-Zr(1)-O(2)#1	56.6(4)	O(2)#1-Zr(1)-N(3)	78.7(2)
O(2)-Zr(1)-O(1)	76.1(2)	O(1)-Zr(1)-N(3)	146.90(8)
O(2)#1-Zr(1)-O(1)	76.1(2)	O(3)#1-Zr(1)-N(3)	125.6(2)
O(2)-Zr(1)-O(3)#1	21.1(2)	O(3)-Zr(1)-N(3)	82.3(2)
O(2)#1-Zr(1)-O(3)#1	74.0(3)	O(2)-Zr(1)-N(2)	83.8(2)
O(1)-Zr(1)-O(3)#1	66.7(2)	O(2)#1-Zr(1)-N(2)	124.4(2)
O(2)-Zr(1)-O(3)	74.0(3)	O(1)-Zr(1)-N(2)	134.57(8)
O(2)#1-Zr(1)-O(3)	21.1(2)	O(3)#1-Zr(1)-N(2)	80.1(2)
O(1)-Zr(1)-O(3)	66.6(2)	O(3)-Zr(1)-N(2)	144.4(2)
O(3)#1-Zr(1)-O(3)	88.0(3)	N(3)-Zr(1)-N(2)	77.89(11)
O(2)-Zr(1)-N(3)	107.0(2)	O(2)-Zr(1)-N(4)	150.2(2)

Table IX. (continued)

O(2)#1-Zr(1)-N(4)	97.5(2)	Zr(1)#1-O(3)-Zr(1)	89.7(2)
O(1)-Zr(1)-N(4)	83.90(8)	C(4)-N(1)-C(1)	106.0(3)
O(3)#1-Zr(1)-N(4)	150.5(2)	C(4)-N(1)-Zr(1)	124.3(2)
O(3)-Zr(1)-N(4)	77.9(2)	C(1)-N(1)-Zr(1)	122.8(2)
N(3)-Zr(1)-N(4)	78.42(10)	C(6)-N(2)-C(9)	105.6(3)
N(2)-Zr(1)-N(4)	125.60(11)	C(6)-N(2)-Zr(1)	125.7(2)
O(2)-Zr(1)-N(1)	117.1(2)	C(9)-N(2)-Zr(1)	121.7(3)
O(2)#1-Zr(1)-N(1)	152.5(2)	C(14)-N(3)-C(11)	105.9(3)
O(1)-Zr(1)-N(1)	76.48(10)	C(14)-N(3)-Zr(1)	124.1(2)
O(3)#1-Zr(1)-N(1)	96.1(2)	C(11)-N(3)-Zr(1)	121.0(2)
O(3)-Zr(1)-N(1)	137.7(2)	C(16)-N(4)-C(19)	105.8(3)
N(3)-Zr(1)-N(1)	125.83(11)	C(16)-N(4)-Zr(1)	126.1(2)
N(2)-Zr(1)-N(1)	77.29(10)	C(19)-N(4)-Zr(1)	124.5(2)
N(4)-Zr(1)-N(1)	78.36(11)	N(1)-C(1)-C(20)	125.3(3)
O(2)-Zr(1)-Zr(1)#1	39.73(14)	N(1)-C(1)-C(2)	109.5(3)
O(2)#1-Zr(1)-Zr(1)#1	39.7(2)	C(20)-C(1)-C(2)	125.1(3)
O(1)-Zr(1)-Zr(1)#1	45.05(7)	C(3)-C(2)-C(1)	108.0(3)
O(3)#1-Zr(1)-Zr(1)#1	45.19(12)	C(2)-C(3)-C(4)	107.1(4)
O(3)-Zr(1)-Zr(1)#1	45.15(12)	N(1)-C(4)-C(5)	125.6(3)
N(3)-Zr(1)-Zr(1)#1	117.69(8)	N(1)-C(4)-C(3)	109.4(3)
N(2)-Zr(1)-Zr(1)#1	123.10(8)	C(5)-C(4)-C(3)	124.9(4)
N(4)-Zr(1)-Zr(1)#1	111.29(8)	C(4)-C(5)-C(6)	124.2(4)
N(1)-Zr(1)-Zr(1)#1	116.27(8)	C(4)-C(5)-C(21)	117.9(3)
Zr(1)-O(1)-Zr(1)#1	89.91(14)	C(6)-C(5)-C(21)	117.9(3)
O(3)#1-O(2)-Zr(1)	92.6(6)	N(2)-C(6)-C(5)	125.7(3)
O(3)#1-O(2)-Zr(1)#1	92.7(6)	N(2)-C(6)-C(7)	109.9(3)
Zr(1)-O(2)-Zr(1)#1	100.6(3)	C(5)-C(6)-C(7)	124.4(4)
O(2)#1-O(3)-Zr(1)#1	66.3(5)	C(8)-C(7)-C(6)	107.6(4)
O(2)#1-O(3)-Zr(1)	66.3(5)		

Table IX. (continued)

C(7)-C(8)-C(9)	107.0(4)	C(1)-C(20)-C(42)	116.8(3)
N(2)-C(9)-C(10)	125.6(3)	C(22)-C(21)-C(26)	118.4(4)
N(2)-C(9)-C(8)	109.9(3)	C(22)-C(21)-C(5)	121.2(4)
C(10)-C(9)-C(8)	124.4(3)	C(26)-C(21)-C(5)	120.4(4)
C(11)-C(10)-C(9)	124.7(3)	C(23)-C(22)-C(21)	120.3(5)
C(11)-C(10)-C(28)	119.2(3)	C(22)-C(23)-C(24)	121.2(5)
C(9)-C(10)-C(28)	116.1(3)	C(25)-C(24)-C(23)	117.9(4)
N(3)-C(11)-C(10)	125.3(3)	C(25)-C(24)-C(27)	121.7(5)
N(3)-C(11)-C(12)	109.6(3)	C(23)-C(24)-C(27)	120.4(5)
C(10)-C(11)-C(12)	125.2(3)	C(26)-C(25)-C(24)	121.6(5)
C(13)-C(12)-C(11)	107.7(3)	C(25)-C(26)-C(21)	120.6(4)
C(12)-C(13)-C(14)	107.5(4)	C(29)-C(28)-C(33)	117.8(4)
N(3)-C(14)-C(15)	125.4(3)	C(29)-C(28)-C(10)	121.7(4)
N(3)-C(14)-C(13)	109.3(3)	C(33)-C(28)-C(10)	120.4(4)
C(15)-C(14)-C(13)	125.4(4)	C(28)-C(29)-C(30)	120.8(4)
C(14)-C(15)-C(16)	125.0(4)	C(31)-C(30)-C(29)	121.9(4)
C(14)-C(15)-C(35)	116.7(3)	C(30)-C(31)-C(32)	116.7(4)
C(16)-C(15)-C(35)	118.3(3)	C(30)-C(31)-C(34)	121.7(4)
N(4)-C(16)-C(15)	125.1(3)	C(32)-C(31)-C(34)	121.6(4)
N(4)-C(16)-C(17)	110.1(3)	C(33)-C(32)-C(31)	121.9(4)
C(15)-C(16)-C(17)	124.7(3)	C(28)-C(33)-C(32)	120.9(4)
C(18)-C(17)-C(16)	107.0(4)	C(40)-C(35)-C(36)	117.7(4)
C(17)-C(18)-C(19)	107.4(3)	C(40)-C(35)-C(15)	121.7(4)
N(4)-C(19)-C(20)	125.6(3)	C(36)-C(35)-C(15)	120.5(4)
N(4)-C(19)-C(18)	109.7(3)	C(37)-C(36)-C(35)	120.8(4)
C(20)-C(19)-C(18)	124.7(3)	C(38)-C(37)-C(36)	121.3(4)
C(19)-C(20)-C(1)	125.4(3)	C(37)-C(38)-C(39)	117.7(4)
C(19)-C(20)-C(42)	117.7(3)	C(37)-C(38)-C(41)	121.5(5)

Table IX. (continued)

C(39)-C(38)-C(41)	120.8(5)	C(42)-C(47)-C(46)	121.2(4)
C(40)-C(39)-C(38)	121.4(5)	C(54)-C(49)-C(50)	120.5(6)
C(39)-C(40)-C(35)	121.0(4)	C(51)-C(50)-C(49)	120.0(6)
C(47)-C(42)-C(43)	116.4(4)	C(52)-C(51)-C(50)	119.3(6)
C(47)-C(42)-C(20)	122.9(4)	C(51)-C(52)-C(53)	120.1(6)
C(43)-C(42)-C(20)	120.7(4)	C(54)-C(53)-C(52)	120.3(6)
C(44)-C(43)-C(42)	121.0(4)	C(49)-C(54)-C(53)	119.7(6)
C(45)-C(44)-C(43)	121.8(5)	C(56)-C(55)-C(57)#2	119(2)
C(46)-C(45)-C(44)	116.8(4)	C(55)-C(56)-C(57)	120(2)
C(46)-C(45)-C(48)	122.6(4)	C(55)#2-C(57)-C(56)	121(2)
C(44)-C(45)-C(48)	120.6(4)		
C(45)-C(46)-C(47)	122.7(4)		

GENERAL CONCLUSIONS

Prior to this work, few group 4 metalloporphyrin complexes had been synthesized. The extent of reactivity that could be explored with these preceding examples was drastically confined as they contained only monodentate ligands. We have prepared useful group 4 metalloporphyrin complexes that contain metal bound monoanionic and dianionic ligands through a number of synthetic strategies.

The bis(amido), $(TTP)Ti(NR_2)_2$, and monoamido, $(TTP)Ti(NR_2)Cl$, complexes were prepared to investigate the formation of titanium imido metalloporphyrin complexes. Through their reactivity characteristics it was concluded that the synthesis of titanium imido complexes by the lithiated amide route is most likely through an intermolecular pathway. An additional synthetic pathway to $(TTP)Ti=NR$ complexes was found from treatment of the low-valent precursor, $(TTP)Ti(\eta^2$-alkyne), with nitrene group donors in a formal 2-electron group transfer reaction. This route proved invaluable in the production of $(TTP)Ti=N^iPr$ which allowed an assessment of the Ti=N bond reactivity in a reduced steric environment. Additional insight into the titanium-nitrogen multiple bond was gained through investigation of the rare hydrazido(2-) derivatives. It was found that the Ti=N moiety in imido and hydrazido complexes exhibits moderate nucleophilic reactivity. Furthermore, the first examples of titanium porphyrin alkoxido complexes were realized with the isolation of $(TTP)Ti(OR)_2$ and $(TTP)Ti(OR)Cl$.

The novel characteristics of the d^2 titanium metalloporphyrin complexes, $(TTP)Ti(L)_2$, were utilized in a range of ligand exchange and group and atom transfer

reactions. The interesting magnetic behavior of the bis(phosphine oxide) species has pointed to the cause of difficulty in chalcogenide atom transfer from titanium metalloporphryin complexes. We have also been able to derive estimates of the Ti=Ch bond strengths, which may prove valuable in extending the chemistry of titanium metalloporphyrin complexes.

The exploration of zirconium and hafnium imido complexes has pointed to a diverse cache of reactivity. The steric environment of the porphyrin, although a limitation in the synthesis of zirconium and hafnium imido complexes, has facilitated the isolation of unique ureato(2-) and guanidino(2-) derivatives. The zirconium imido compound was essential in the production and investigation of a number of complexes containing Zr-O bonds. The unique aldol-type condensation of pinacolone was found to go through a reactive zirconium enolato species.

ACKNOWLEDGMENTS